INFORMATION TO USERS

This manuscript has been reproduced from the microfilm master. UMI films the text directly from the original or copy submitted. Thus, some thesis and dissertation copies are in typewriter face, while others may be from any type of computer printer.

The quality of this reproduction is dependent upon the quality of the copy submitted. Broken or indistinct print, colored or poor quality illustrations and photographs, print bleedthrough, substandard margins, and improper alignment can adversely affect reproduction.

In the unlikely event that the author did not send UMI a complete manuscript and there are missing pages, these will be noted. Also, if unauthorized copyright material had to be removed, a note will indicate the deletion.

Oversize materials (e.g., maps, drawings, charts) are reproduced by sectioning the original, beginning at the upper left-hand corner and continuing from left to right in equal sections with small overlaps. Each original is also photographed in one exposure and is included in reduced form at the back of the book.

Photographs included in the original manuscript have been reproduced xerographically in this copy. Higher quality 6" x 9" black and white photographic prints are available for any photographs or illustrations appearing in this copy for an additional charge. Contact UMI directly to order.

UMI

A Bell & Howell Information Company
300 North Zeeb Road, Ann Arbor MI 48106-1346 USA
313/761-4700 800/521-0600

Université d'Ottawa • University of Ottawa

BROWN ADIPOSE TISSUE ATROPHY: EFFECTS ON ENERGY EXPENDITURE AND BODY COMPOSITION

by

Anna Melnyk

A thesis submitted to the School of Graduate Studies

in partial fulfilment of the requirement

for the degree of

Doctor of Philosophy

Department of Biochemistry

Faculty of Medicine

University of Ottawa

Ottawa, Canada

Abstract

The objective of this work was to examine the influence of brown adipose tissue (BAT) on energy expenditure and body composition. Insights were gained from rodent models with BAT disruption, which is expected to contribute to obesity due to a deficit in energy expenditure for thermogenesis (Himms-Hagen 1989b).

The capsaicin-desensitized (Cap-Des) rat has atrophied BAT with impaired thermogenesis, contradictorily leading to a decrease in body fat. Indeed, aging-associated obesity and hyperplasia of retroperitoneal white adipose tissue was prevented in 13.5 month old Cap-Des rats. The loss of function of Cap-sensitive afferent autonomic nerves (destroyed in Cap-Des rats) results in an alteration in energy balance conducive to leanness. It was suggested that the attenuated aging-associated increase in circulating calcitonin gene-related peptide (derived mainly from Cap-sensitive nerves) in the Cap-Des rat results in a lower degree of aging-associated insulin-resistance, hence in a lesser degree of obesity.

Rats with a lesion in the nucleus of the solitary tract (NTS) are known to have an impaired capacity to increase their oxygen uptake and the temperature of their interscapular (I) BAT after administration of catecholamines. A similar impairment was seen in the Cap-Des rat, known also to sustain a lesion in the NTS, and associated with marked atrophy of IBAT. The disruption of the NTS did not cause BAT atrophy by the parameters measured; atrophy of BAT in Cap-Des rats is not due to the NTS-lesion that they sustain.

UCP-DTA transgenic mice have a partial ablation of BAT, accomplished by linking DTA (diphtheria toxin A chain) to the uncoupling protein1 (UCP1) promoter. UCP1-

expressing brown adipocytes are destroyed in the UCP-DTA transgenic mouse when the tissue is stimulated. As expected, these mice develop massive obesity: also present are hyperphagia, insulin resistance, hyperglycemia, hyperinsulinemia, and hyperlipidemia characteristic of noninsulin-dependent diabetes mellitus (Lowell *et al.* 1993).

UCP-DTA and control mice were raised at thermoneutrality (35°C) in order to suppress BAT thermogenesis. As predicted, eliminating the deficit in BAT thermogenesis present in the UCP-DTA mice corrected their obesity and hyperphagia.

UCP is not totally eliminated in the UCP-DTA mice, as measured by an antibody that detects UCP1, UCP2 (and probably UCP3), and these mice are not sensitive to cold (Lowell *et al.* 1993). Mice were acclimated to mild cold (14°C) to determine the nature of compensation for the lack of UCP1-expressing brown adipocytes in UCP-DTA mice. BAT does grow in cold-adapted UCP-DTA mice, perhaps by substitution of brown adipocytes expressing a different UCP isoform for brown adipocytes that would normally express UCP1.

Adjustment of food intake in accordance with environmental temperature was shown to occur independent of changes in serum leptin concentration. Intact BAT was shown to be necessary for the control of food intake at temperatures below thermoneutrality. Because the lack of UCP1-mediated thermogenesis in BAT of knockout mice is known not to induce hyperphagia, we propose the deficiency of UCP1-expressing brown adipocytes, specifically the absence of a postulated satiety factor normally secreted from them, is responsible for the hyperphagia of the UCP-DTA mice at 24°C.

Dedication

This work is dedicated to my daughter Anita, and to my Mother who made it all possible.

Acknowledgments

First and foremost, I would like to thank my supervisor, Dr Jean Himms-Hagen. All of her help and support during my research are very much appreciated.

I would like to express my gratitude to Dr B.B. Lowell; initially for developing the UCP-DTA transgenic mice, for supplying us with probe for Southern blotting, and for supplying us with the founder mice to establish a colony.

My appreciation to Dr Sue Ritter, who collaborated with us on the NTS- lesioned rat study, and to her technician, Thu Dinh, who came to Ottawa to perform the lesioning.

I would like to thank everyone that I have worked with in Dr Himms-Hagen's lab. Dr Anna-Lisa Kates, Dr Joan Triandafillou, Dr JingYing Cui, Masoud Ghorbani, and Dr Matthew White for their friendship. Thank you to Gisèle Larose and Stefanie Foster for their technical assistance with the animals and carcass analysis assays. Thank you to Dr Swapan Banerjee who genotyped the transgenic mice used in Chapter 7. I would like to express my gratitude to Linda Jui, who worked tirelessly to produce the histological work shown in Chapters 7 and 8 of this thesis.

Thank you to everyone in Dr Martin Tenniswood's lab, for making my first few years here so memorable. To Marilyn, Kim, Sean, Jon, and Dan. Thank you for the advice and for the good times.

My appreciation to Julie Aubé, and Joanne Barlow; for their willingness in helping me meet any deadline and for being able to fix all emergencies.

I would like to thank Dr Mary-Ellen Harper, for her friendship, advice, and support, and for working with me on the thermoneutrality experiment. Thank you Shadi for helping process tissue for the thermoneutrality experiment, and for being a friend.

Finally, I would like to thank Steve for his support and encouragement, and for helping me to make it through the home stretch.

Table of Contents

Chapter 5: Brown adipose tissue in rats with lesions in the nucleus of the solitary tract

Chapter 7: Acclimation to mild cold in transgenic mice with partial ablation of BAT

List of Tables

List of Figures

List of Abbreviations

ADP	adenosine diphosphate
AMP	adenosine monophosphate
AP	area postrema
aP2	adipocyte P2
ARs	adrenergic receptors
ATP	adenosine triphosphate
A^{vy}	viable yellow obese mouse
BAT	brown adipose tissue
BA1	UCP1-expressing brown adipocyte
BA2	UCP2-expressing brown adipocyte
BA3	UCP3-expressing brown adipocyte
bp	base pairs
BNP	bacitracin zinc, neomycin sulfate, polymyxin B sulfate
borax	sodium tetraborate
BSA	bovine serum albumin
BW	body weight
B_0	total binding
cAMP	cyclic AMP
Cap	capsaicin
Cap-Des	capsaicin-desensitized
CC	central canal
cDNA	complementary DNA
C/EBP	CCAAT enhancer binding protein
CGRP	calcitonin gene-related peptide

CL	CL 316,243 (β_3-adrenergic receptor agonist)
CON	control mice
COX	cytochrome oxidase
cp/cp	corpulent rat
Cu	nucleus cuneatus
°C	degrees Celsius
DAB	3.3'-diaminobenzidine tetrahydrochloride
db/db	diabetic mouse
dbh KO	NA deficient transgenic mouse
dL	decilitre
DMP-30	tri (dimethylaminomethyl phenol)
DMV	dorsal motor nucleus of the vagus
DNA	deoxyribonucleic acid
DTA	diphtheria toxin A chain
ECL	enhanced chemiluminescence
EDTA	ethylenediamine tetraacetic acid
EWAT	epididymal white adipose tissue
fa/fa	fatty rat
fa^k/fa^k	hypertensive Koletsky rat
fat/fat	fat rat
FFA	free fatty acid
g	centrifugal force
GDP	guanosine 5'-diphosphate
GDPB	GDP binding
G protein	guanine nucleotide regulatory protein

Gr	nucleus gracilis
GTG	gold thioglucose
H & E	hematoxylin and eosin
HCl	hydrochloric acid
HSL	hormone sensitive lipase
H_2O_2	hydrogen peroxide
IBAT	interscapular brown adipose tissue
IgG	immunoglobulin
INWAT	inguinal white adipose tissue
JAK	*janus* kinase
kb	kilobases
KCl	potassium chloride
K_2HPO_4	dipotassium phosphate
KH_2PO_4	potassium phosphate
KOH	potassium hydroxide
LPL	lipoprotein lipase
M	mol/litre
mA	milliampere
ml	millilitre
mM	millimole/ litre
mm	millimetre
mRNA	messenger ribonucleic acid
MSG	monosodium glutamate
MWAT	mesenteric white adipose tissue
μCi	microcurie

μg	microgram
μl	microlitre
μm	micron
μM	micromolar
N	normal
NA	noradrenaline
NaCl	sodium chloride
Na_2EDTA	ethylenediamine tetraacetic acid (disodium salt)
NaOAc	sodium acetate
NaOH	sodium hydroxide
Na_2SO_4	sodium sulphate
NCM	nitrocellulose membrane
N.D.	not done
NH_4OH	ammonium hydroxide
$NiCl_2$	nickel chloride
nm	nanometre
NPY	neuropeptide Y
N.S.	not significant
NSB	nonspecific binding
NTS	nucleus of the solitary tract or nucleus tractus solitarius
ob/ob	genetically obese mouse
OB-R/ Ob-R	leptin receptor
PAGE	polyacrylamide gel electrophoresis
PBS	phosphate buffered saline
PPARγ	peroxisome proliferator-activated receptorγ

PPO	2.5-diphenyloxazole
PVN	paraventricular nucleus
PWAT	parametrial white adipose tissue
pg	picogram
pm	picomolar
1% solution	1 gram/100 millilitres
RIA	radioimmunoassay
rpm	revolutions per minute
RWAT	retroperitoneal white adipose tissue
s.c.	subcutaneous
SDS	sodium dodecyl sulfate
SEM	standard error of the mean
SLB	sample loading buffer
SM	standard medium
SNS	sympathetic nervous system
SP	substance P
SSC	sodium chloride, sodium citrate, sodium hydroxide
STAT	signal transducers and activators of transcription
STE	sodium-tris-EDTA
TBS	Tris buffered saline
TCA	trichloroacetic acid
TCT	Triton X-100, carrageenan, in Tris buffer
TE	Tris-EDTA
Tg	transgenic mouse
Tricine	Tris(hydroxymethyl) methyl glycine

Tris	Tris (hydroxymethyl) aminomethane
tub/tub	tubby mouse
Tween-20	polyoxyethylene sorbitan monolaurate
T_3	3,3,5'-triiodothyronine
T_4	thyroxine
$T_4$5'-D	thyroxine 5'-deiodinase
UCP	uncoupling protein
UCP1-KO	UCP1 knockout transgenic mice
UCP-DTA	transgenic mice with partial ablation of brown adipose tissue: diptheria toxin A chain driven by UCP1 promoter
V	volts
Veh	vehicle treated
VMH	ventromedial hypothalamus
vs.	versus
4V	4th ventricle
v/v	volume/volume
v/w	volume/weight
w/v	weight/volume
WAT	white adipose tissue
wk	week

Chapter 1: General introduction

Obesity is a disorder of energy balance occurring when energy intake chronically exceeds energy expenditure. In humans, obesity is a serious problem; it is a multifactorial disease with both genetic and environmental influences. In Western society, the prevalence of obesity is high. The many health risks associated with obesity include heart disease, non-insulin-dependent diabetes mellitus, hyperlipidemia and hypertension; each of which represents a major health problem.

The causes of obesity and consequently its treatments have remained elusive. In the past few years, researchers have made significant inroads into understanding the function of tissues that hold the key to excessive energy storage and intake, and to differences in energy expenditure; white adipose tissue (WAT) and brown adipose tissue (BAT).

WAT can be defined as a specialized connective tissue that functions to store a large amount of triglycerides; it serves as an energy storage depot. BAT is also a specialized connective tissue; its classification as an adipose tissue arose from its stores of triglycerides. The function of BAT is thermogenesis, or the production of heat, and the lipid that it stores is one of its fuels for thermogenesis. BAT possesses a protein called uncoupling protein (UCP) in its inner mitochondrial membrane whose function is to produce heat. The possession of this protein with its unique ability to uncouple oxidative phosphorylation has been the defining property of BAT.

BAT and obesity have both been studied for many years using biochemical and physiological experimental approaches. The arrival of molecular biology has allowed for the

determination of some of the control mechanisms of these tissues and has sparked a new interest in this rapidly expanding field.

Energy Balance and Obesity

Energy balance has two components: energy intake (food intake) and energy expenditure. Obesity results when energy intake chronically exceeds energy expenditure. Many rodent models of genetic and experimentally produced obesity exist, with deficits in one or both components of energy balance. These models are used to study the causes and consequences of obesity.

Experimental obesity is classified in four categories (Bray & York 1971). These categories include hypothalamic injury, endocrine-induced imbalance, dietary, and genetically transmitted. A fifth category of transgenically induced obesity must now be added.

Obesity can be produced by the selective destruction of regions in the hypothalamus (Bray & York 1971). These lesions are generated using heat, knife cuts, or by electrolytic means. Chemical agents can also be used to disrupt areas of the hypothalamus, causing obesity and hyperphagia (Bray & York 1971).

Parasagittal knife cuts between the ventromedial hypothalamus (VMH) and the lateral hypothalamus, ventromedial hypothalamic lesions (either electrolytic or radiofrequency), and paraventricular nucleus (PVN) lesions cause hyperphagia and obesity in rats (Himms-Hagen 1989a).

Obesity is due to both hyperphagia and an increase in metabolic efficiency in rats with parasagittal knife cuts (Coscina *et al.* 1985; Vander Tuig *et al.* 1985) and VMH rats (Vilberg & Keesey 1984; Walgren & Powley 1985), or is solely due to hyperphagia in PVN lesioned rats (Leibowitz 1988; Weingarten *et al.* 1985).

Injection of gold thioglucose (GTG) into mice produces hypothalamic lesions in the VMH and the arcuate nucleus that induce a transient hyperphagia and obesity (Djazayery *et al.* 1979). GTG mice have a lowering of body temperature (torpor) (Himms-Hagen 1989a), and defective control of BAT (Cooney *et al.* 1987; Eley & Himms-Hagen 1989; Hogan & Himms-Hagen 1983), both decreasing their energy expenditure and contributing to their high metabolic efficiency. Another model of chemically induced hypothalamic lesions causing obesity is the monosodium glutamate (MSG) treated mouse that becomes obese despite being normophagic (Djazayery *et al.* 1979; Moss *et al.* 1985a; Moss *et al.* 1985b; Tokuyama & Himms-Hagen 1986; Tokuyama & Himms-Hagen 1989), as a result of torpor (Tokuyama & Himms-Hagen 1986) and physical inactivity which cause a high metabolic efficiency. BAT of the MSG mouse is normal; it can respond to both cold (Tokuyama & Himms-Hagen 1986) and diet stimuli (Moss *et al.* 1985a; Moss *et al.* 1985b).

Insulin, hypercorticosteroidism induced by tumours or corticosteroids, and gonadectomy can all produce obesity in rodents (Bray & York 1971).

A high fat diet will cause some strains of rats and mice to become obese (Bray & York 1971; Himms-Hagen 1989a). Much variation is seen between strains in susceptibility

to this type of obesity (Himms-Hagen 1989a); not all strains are susceptible, suggesting that genetic factors play a role in diet-induced obesity.

Genetically obese rodents develop obesity because of a single gene mutation; these mutant alleles are carried on highly inbred lines (Johnson *et al.* 1991). Genetically transmitted obesity can be divided into two groups, the dominantly inherited A^{vy} (viable yellow), and the recessively inherited *ob* (obese), *db* (diabetic), *cp* (corpulent), *tub* (tubby), *fat* (fat), fa^k (hypertensive Koletsky) and *fa* (fatty) alleles.

The number of transgenic mice increases weekly; technology exists to knockout, overexpress, replace, and relocate genes, and to ablate cell types completely with lethal genes. Many transgenic mice are genetically engineered to alter the expression of key genes in WAT and BAT in an effort to discern their function.

The obese rodent models above have a deficit in one or both components of energy balance (intake or expenditure), resulting in obesity. Studies with a variety of obese laboratory rodents have shown that most of them have some kind of deficit in energy expenditure for thermogenesis (Himms-Hagen 1989b).

Thermogenesis

Thermogenesis is an inherent component of thermal balance; thermal balance can be defined as body temperature regulation at a given level by physiological control of facultative thermogenic mechanisms and of heat loss mechanisms.

Obligatory thermogenesis:

All metabolic reactions are inefficient and result in some energy loss as heat (Lehninger 1982). This is referred to as obligatory thermogenesis which is an element of all metabolic processes involved in maintenance of the body in the living state, and occurs in all organs (Himms-Hagen 1989b). Obligatory processes are controlled mainly by thyroid hormone (Himms-Hagen 1989b). Circulating thyroid hormone has a thermogenic effect on organisms, largely due to widespread metabolic stimulation in tissues other than BAT (Mory *et al.* 1981; Triandafillou *et al.* 1982).

Obligatory thermogenesis can be divided into two categories: essential and endothermic thermogenesis and the thermic effect of food (Himms-Hagen 1989b). Essential and endothermic thermogenesis is the heat produced in the cells of all organs due to inefficient cellular reactions. The thermic effect of food refers to the energy expended for ingesting, digesting, and processing food. This expenditure occurs in the intestine, liver, and WAT (Himms-Hagen 1989b).

Facultative thermogenesis:

Facultative thermogenesis differs from obligatory thermogenesis in that it is not always active: it can be rapidly switched on and off by the nervous system (Himms-Hagen 1989b). Skeletal muscle and BAT are the two tissues involved in this type of thermogenesis.

Energy expenditure in skeletal muscle falls into two different categories of facultative thermogenesis, exercise-induced and cold-induced shivering (Himms-Hagen 1989b). This expenditure is controlled by the central nervous system via motor nerves supplying the muscles. Mammals derive much of their body heat from metabolic activity in contracting muscles: exercise provides great quantities of heat (Lehninger 1982). Shivering is a physiological response that makes muscles contract and generate heat when a mammal is cold (Lehninger 1982).

The foremost function of BAT is heat production. Energy expenditure in BAT falls into two different categories of facultative thermogenesis, diet-induced and cold-induced nonshivering (Himms-Hagen 1989b). This expenditure is controlled by the sympathetic nervous system via sympathetic nerves supplying BAT. These nerves release noradrenaline (NA), which acts on adrenergic receptors (ARs) to stimulate heat production in BAT.

When a mammal's body temperature decreases, sympathetic nerves in BAT release NA, stimulating thermogenesis (cold-induced nonshivering thermogenesis). Diet-induced thermogenesis in BAT helps to balance energy intake (Himms-Hagen 1989b), effectively burning off excess calories.

Thermoregulatory thermogenesis (nonshivering in BAT, and shivering in muscle) is available for the organism to maintain body temperature (Himms-Hagen 1989b). Body temperature is kept within a very narrow range, due to a stringent control of thermal balance (Himms-Hagen 1989b). Energy balance is more loosely controlled than thermal balance and energy stores can vary over an extremely wide range. Neural control of BAT in relation to its thermoregulatory requirements takes precedence over the control in relation to its energy balance (Himms-Hagen 1989a). Physiological states causing increased heat production and body temperature such as growth, pregnancy and lactation, will lead to a suppression of BAT thermogenesis (Himms-Hagen 1989b).

Thermoregulation is a complex process: it will be affected by the physiological states mentioned above, as well as factors that are innate to a given animal such as set point of body temperature, torpor, body fat, thyroid status, and tumours. Behavioural thermogenesis to conserve body heat such as huddling, putting on clothing, or turning up a thermostat also play a role in overall thermoregulation.

Energy balance and BAT:

As an energy expending processes, thermogenesis is a possible means for the control of energy balance. Energy expenditure in BAT can serve in the regulation of energy balance, maintaining leanness in overeating lean animals and promoting obesity under conditions of decreased neural stimulation (Table 1.1).

Table 1.1: Examples of states of altered energy balance associated with altered BAT function, and some exceptions

Obesity associated with impaired control of BAT thermogenesis and often with defective thermoregulatory capacity	
Genetic obesity:	*ob/ob* and *db/db* mice
	fa/fa and *cp/cp* rats
	A^{vy} mice
Hypothalamic obesity:	Medial hypothalamic lesions in rats and mice (surgical or chemical)
Diet-induced obesity:	High-fat diet in rats and mice
Endocrinological obesity:	Ovariectomy in rats
	Excess glucocorticoids
Leanness associated with enhanced BAT function	
Hypothalamic leanness:	Lateral hypothalamic lesions in rats
Exceptions	
Capsaicin-desensitized rats have atrophied BAT but do not become obese.	
DIO rats may have hypertrophied BAT but still become obese.	

Adapted from: Himms-Hagen, J. (1990b)

BAT in genetically obese rodents:

The concept that a deficit in energy expenditure due to lack of BAT thermogenesis might contribute to the development of obesity has long been established (Himms-Hagen 1979), and has formed the basis of many studies of BAT in obese animals performed by many different researchers. Most obese rodents have a deficit in energy expenditure for thermogenesis either in BAT, or in all organs due to torpor (Himms-Hagen 1989a). A partial deficit may exist in these rodents; only diet-induced, only cold-induced, or both aspects of BAT thermogenesis may be affected (Himms-Hagen 1989a). Determining the contribution of this deficit towards obesity has been hard, the eventual hyperphagia that occurs in obesity outweighs the high metabolic efficiency seen.

Evidence for the link between BAT and obesity is provided in the UCP-DTA mouse. This mouse has diphtheria toxin A chain (DTA) gene linked to its UCP promoter. In cells where UCP is expressed, DTA is produced and the cell is killed. BAT is partially ablated in this transgenic model and the mouse becomes hyperphagic and obese (Lowell *et al.* 1993); these mice will be discussed later (Chapter 6).

Brown Adipose Tissue

Structure/Morphology:

BAT is found in small depots throughout the body. The primary superficial sites are in the interscapular, subscapular, and axillary regions; deeper sites are the perirenal and pericardiac regions (Néchad 1986). Patches of BAT are present along the major blood vessels in the thoracic and peritoneal cavities and along major arteries. The relative proportions of the depots vary from species to species, and with the physiological status of the animal: depots of BAT are especially pronounced in newborn mammals and in species that hibernate. In rats and mice, the major depot is the interscapular (IBAT), and this is the one most studied.

BAT makes up about 1-5% of an animal's body weight. The morphology of the tissue depends on the state of BAT, a tissue with a large capacity for atrophy, growth and regeneration. In older animals and humans, a quantity of BAT becomes dormant, but it can be activated by exposure to cold, or by thermogenic drugs.

BAT contains numerous cell types including brown adipocytes, interstitial cells, preadipocytes, mast cells, endothelial cells, and cells of the vasculature (Bukowiecki *et al.* 1982; Bukowiecki *et al.* 1986; Géloën *et al.* 1988; Néchad 1986). Mature brown adipocytes and endothelial cells are the predominant cell types in BAT, and they are equally abundant (each represent about 40% of the population) (Himms-Hagen & Ricquier 1997). Interstitial cells can be induced to proliferate and differentiate with chronic NA stimulation. Protoadipocytes and preadipocytes are stages in the differentiation of new mature cells, only

detectable with hyperplasia due to chronic stimulation (Géloën *et al.* 1988; Géloën *et al.* 1990; Goglia *et al.* 1992). A few white adipocytes are also present in BAT (Morroni *et al.* 1995; Sbarbati *et al.* 1991).

The mature brown adipocyte has many triglyceride droplets of different sizes, and is therefore described as multilocular. This cell is packed with large mitochondria containing closely packed cristae (Himms-Hagen & Ricquier 1997). These cristae are the site of UCP.

Brown adipocytes are not limited to discrete depots, but are more widely distributed throughout the mammalian body (Himms-Hagen & Ricquier 1997). Mature brown adipocytes that are multilocular and contain UCP can be found in WAT depots. Under chronic stimulation these are quite numerous (Himms-Hagen & Ricquier 1997). These potential brown adipocytes do not express very much UCP under non-stimulated conditions and have been referred to as convertible adipose tissue (Loncar 1991), masked brown adipocytes (Cousin *et al.* 1992), and dormant brown adipocytes (Himms-Hagen & Ricquier 1997).

The brown colour of BAT is due to the brownish cytochrome pigments found in the abundant mitochondria of the mature brown adipocyte, and to its high degree of vascularity. The brown adipocyte does not just have more mitochondria than the white adipocyte; the mitochondria are structurally different to promote thermogenesis at the expense of phosphorylation.

Vasculature: The extensive vasculature of BAT allows for very high rates of blood flow (up to 200 fold increase) when the tissue is stimulated (Closa *et al.* 1993; Foster 1986; Foster & Frydman 1978; Foster & Frydman 1979). IBAT is bilaterally symmetrical, and it has a symmetrical arterial and venous blood supply. A single and centrally placed vein, the Sulzer's vein, provides the major venous drainage of the depot. BAT can rapidly and extensively increase or decrease its blood flow via its arteriovenous anastomoses (Nnodim & Lever 1988). When closed, blood is shunted into the capillary bed that supplies the parenchymal cells of BAT. When open, blood is shunted directly into the venous drainage, which deprives the parenchymal cells of oxygen, and inhibits thermogenesis.

Innervation: Individual intercostal nerves supply the several lobes of IBAT, with no cross-innervation between the two sides (Foster *et al.* 1982; Watanabe *et al.* 1994). Paravascular nerves run along the symmetrical arteries and veins. These nerves are markedly heterogeneous with respect to the neurotransmitters they contain (Flaim *et al.* 1976; Lever *et al.* 1988; Lever *et al.* 1989; Mukherjee *et al.* 1989; Nnodim & Lever 1988; Norman *et al.* 1988). Within BAT, nerves supply the blood vessels and arteriovenous anastomoses, and course between and terminate on parenchymal cells. The cells in brown adipose tissue are linked by gap junctions for the propagation of neural input (Schneider-Picard *et al.* 1984; Schneider-Picard *et al.* 1980).

Nerves containing NA supply the blood vessels, arteriovenous anastomoses, and parenchymal cells. Neuropeptide Y (NPY) is colocalized with NA in nerves to blood vessels but not in nerves to parenchymal cells (Cannon *et al.* 1986; Nnodim & Lever 1988; Norman

et al. 1988). Both types of nerves are presumed to be sympathetic nerves. There are also nerves supplying the blood vessels and parenchymal cells that contain calcitonin gene-related peptide (CGRP), nerves supplying the blood vessels that contain substance P (SP), and CGRP containing nerves supplying the arteriovenous anastomoses (Himms-Hagen *et al.* 1990; Lever *et al.* 1988; Lever *et al.* 1989; Mukherjee *et al.* 1989). These are presumed to be different types of sensory nerves.

Adrenergic receptors: NA elicits its effects on BAT through adrenergic receptors. Cells in BAT have β_1 -, β_2 -, β_3 -, α_1 -, and α_2 -ARs. ARs possess a high degree of homology and share a number of characteristics: seven hydrophobic, α-helical, transmembrane-spanning domains, three intracellular and extracellular loops interspersed between the membrane-spanning regions, and all are coupled to their second messenger systems through guanine nucleotide regulatory proteins (G proteins) (Ruffolo 1991). G proteins are composed of α, β, and γ subunits. Once ligand is bound to the receptor, signal transduction occurs through one or more G proteins; GDP dissociates from the α-subunit of the G protein (Ruffolo 1991). GTP can now bind the α-subunit, causing the GTP-bound G protein to dissociate from the receptor-agonist complex. The dissociated GTP-α-subunit complex releases the β/γ dimer. The GTP-α-subunit activates the catalytic subunit of adenylate cyclase, causing an increase in cAMP (Ruffolo 1991).

Precursor cells contain β_1 -ARs and will proliferate and differentiate in response to NA stimulation; in mice DNA synthesis in interstitial cells is due to the exclusive stimulation of β_1 -ARs by NA (Bronnikov *et al.* 1992; Nedergaard *et al.* 1994). As the brown adipocyte

differentiates, it acquires β_3 -ARs (Klaus *et al.* 1995; Nedergaard *et al.* 1994). The β_3 -AR is a late marker of differentiation (Bronnikov *et al.* 1992; Himms-Hagen *et al.* 1994) that is present on mature brown adipocytes, on dormant brown adipocytes present in WAT, and in the brown and white adipocytes of most small mammals (Himms-Hagen & Ricquier 1997).

Chronic treatment with a β_3 -AR agonist does not induce hyperplasia of BAT in rats (Ghorbani *et al.* 1997; Ghorbani & Himms-Hagen 1997; Himms-Hagen *et al.* 1994). Selective β_3 -AR agonists are unable to recruit new cells in BAT since they lack the β_1 -AR mediated effect of NA in precursor cells (Himms-Hagen & Ricquier 1997).

The β_3 -AR is the predominant β -AR in BAT of the rat (Muzzin *et al.* 1992). β_3 -ARs mediate responses that are insensitive to most standard β -AR antagonists, have low affinity for NA, can be activated by certain antagonists of β_1 - and β_2 -ARs such as CGP 12177, and are activated by novel agonists (Himms-Hagen & Ricquier 1997), BRL37344 and CL 316,243 (CL) (Arch & Kaumann 1993; Giacobino 1995; Granneman 1995b; Himms-Hagen & Danforth 1996; Lafontan 1994; Lafontan & Berlan 1993; Largis *et al.* 1994; Lowell & Flier 1995; Strosberg & Pietri-Rouxel 1996).

Mature brown adipocytes of rodents possess both β_1 -ARs and β_3 -ARs; at low concentrations, NA stimulates respiration in brown adipocytes mainly through β_1 -ARs (D'Allaire *et al.* 1995; Zhao *et al.* 1994). β_1 -AR stimulation of adenylate cyclase of rat BAT occurs at low NA concentration whereas activation of β_3 -ARs only occurs at higher concentrations of NA (Galitzky *et al.* 1995; Lafontan 1994). β_3 -ARs may represent the physiological receptors for the NA secreted from sympathetic nerve endings where its

concentration is very high and for when the high-affinity β_1 -ARs are desensitized (D'Allaire *et al.* 1995; Zhao *et al.* 1994). β_3 -ARs are down-regulated under chronic stimulation (Granneman & Lahners 1992), but the capacity of the response to NA is preserved by an increase in the synthesis of adenylate cyclase type III (Granneman 1995a). β_3 -AR agonists increase UCP mRNA in rats (Muzzin *et al.* 1989; Ricquier *et al.* 1986), and UCP synthesis in differentiated brown adipocytes in primary culture (Champigny *et al.* 1992; Klaus *et al.* 1991; Kopecký *et al.* 1990; Rehnmark *et al.* 1990).

α_1 -AR stimulation constitutes a substantial part of the thermogenic response to NA (Horwitz & Hamilton 1984; Mohell *et al.* 1987; Schimmel *et al.* 1986). This stimulation does not involve adenylate cyclase (Schimmel *et al.* 1986), it involves instead an ATPase type of control mechanism rather than uncoupling of oxidative phosphorylation (Horwitz & Hamilton 1984; Mohell *et al.* 1987). It is likely involved in the propagation of the stimulatory signal, and the initiation of the trophic response (Himms-Hagen 1990a). Stimulation of α_1 -AR activates the phosphatidylinositol bisphosphate cycle, causing an increase in diacylglycerol and inositol trisphosphate, leading to the release of Ca^{2+} from intracellular stores and the translocation of protein kinase C to the plasma membrane. The thermogenesis associated with α_1 -AR mediated component of stimulation is related to the increased utilization of ATP for ion pumping, primarily by the Na^+K^+ -ATPase, which is necessary for re-establishing ion gradients that are dissipated through the opening of ion channels following phosphatidylinositol bisphosphate cycle activation (see Himms-Hagen, 1990).

Synergism between α_1 -, β_1 -, and β_3 -AR responses account for the many responses of BAT to NA stimulation (Himms-Hagen & Ricquier 1997). α_1 -ARs interact synergistically with β_3 -ARs to stimulate the activity of adenylate cyclase (Granneman 1995a; Ma & Foster 1984), to cause induction of adenylate cyclase type II (Granneman 1995a) and to induce c-*fos* expression (Thonberg *et al.* 1994). In rats, these receptors act synergistically to increase thyroxine 5'-deiodinase ($T_4$5'-D) activity. This enzyme converts thyroxine (T_4) to the thermogenically active 3,5,3' -triiodothyronine (T_3). A selective increase in UCP synthesis results from the synergistic action of T_3 on the cyclic AMP (cAMP)-mediated induction of UCP synthesis (Bianco *et al.* 1992; Raasmaja & Larsen 1989; Rabelo *et al.* 1995; Silva 1988). In mice, β_3 -ARs alone mediate this increase (Pavelka *et al.* 1993). Sympathetic control of blood flow is due to the synergistic actions of NA on α- and β -ARs (Foster 1985). In some species, α_2 -ARs play an important inhibitory role in brown adipocyte responsiveness to NA but in most they do not (Himms-Hagen & Ricquier 1997).

The ratio of α/β -ARs in different adipose tissue depots affects the lipolytic rate, with depots containing higher levels of α -ARs more prone to lipogenesis (Collins *et al.* 1994). The ratio of β_1: β_2: β_3 -AR mRNAs in mouse adipose tissue is approximately 3:1:150 (Collins *et al.* 1994).

Biochemical mechanisms/ BAT thermogenic pathway:

When a mammal's body temperature decreases, sympathetic nerves in BAT release NA. NA acts on β -ARs, resulting in an increase in cAMP. cAMP has two actions: it stimulates the protein kinase A dependant phosphorylation of hormone sensitive lipase (HSL), and it increases the synthesis of lipoprotein lipase (LPL) (Carneheim *et al.* 1988). The HSL breaks down stored triglyceride within the brown adipocyte, rapidly increasing the intracellular free fatty acid (FFA) concentration. LPL acts at the cell surface to hydrolyze triglyceride in blood borne chylomicrons and lipoproteins. A third source of FFAs, intracellular lipogenesis, may also be stimulated by NA. FFAs are both the fuel for thermogenesis, and they directly activate UCP (Himms-Hagen & Ricquier 1997).

In the mitochondria, protons in the matrix are pumped outside the inner membrane by the electron transport chain. Under normal conditions, the electron transport chain is limited by the proton gradient that it generates. The energy produced by the gradient is used to generate ATP through the proton-translocating ATP synthetase by a process called oxidative phosphorylation. ATP synthesis will only occur when ADP is available from cellular use of ATP. UCP uncouples oxidative phosphorylation and no ATP is produced. This uncoupling allows for the futile cycling of protons; protons can reenter the mitochondria through the UCP, rather than building up a gradient. The energy generated by the electron transport chain is instead released as heat. As the electron transport chain is no longer limited by a proton gradient, it will continue at a faster rate. Speeding up of electron transport leads to an increase in the activity of the mitochondrial dehydrogenases, which in turn leads to

acceleration of the reactions that supply the substrates for these enzymes. The result is an increase in overall substrate oxidation (Himms-Hagen 1991).

Uncoupling protein homologues:

During the last three months, homologues of UCP have been found that are expressed in other tissues, as well as in BAT (Boss *et al.* 1997b; Fleury *et al.* 1997; Gimeno *et al.* 1997; Larrouy *et al.* 1997; Vidal-Puig *et al.* 1997). UCP1, the first of the uncoupling proteins to be cloned (Bouillaud *et al.* 1985), is expressed only in BAT; throughout this thesis UCP refers to UCP1, unless otherwise stated.

UCP2 is 56% identical to UCP1 and it is also able to uncouple mitochondrial respiration (Fleury *et al.* 1997). UCP2 is ubiquitously expressed in mouse tissues; the tissues with the highest level of UCP2 expression are WAT and BAT (Fleury *et al.* 1997; Gimeno *et al.* 1997). It is also widely expressed in adult human tissues, including tissues rich in macrophages (Fleury *et al.* 1997). Studies on the regulation of UCP2 have yielded conflicting results, but it appears that this homologue is not subject to the same regulation as UCP1 (Fleury *et al.* 1997). In mice the levels of UCP2 mRNA in BAT and WAT have been reported to be unchanged by β_3 -AR agonist administration (Fleury *et al.* 1997), to be unaffected by cold exposure of mice (Fleury *et al.* 1997), or conversely to increase with cold exposure of rats in BAT, heart, and muscle (Boss *et al.* 1997a). UCP2 mRNA is increased in adipocytes containing large amounts of lipid; both white adipocytes of *ob/ob* and *db/db* mice (Gimeno *et al.* 1997), and brown adipocytes of transgenic mice deficient in UCP1 (UCP1-KO mice) (Enerbäck *et al.* 1997). UCP2 is upregulated in WAT in response to fat

feeding (Fleury *et al.* 1997): fasting did not affect the level of UCP2 mRNA in BAT and heart of rats, though it caused a marked increase in levels in muscle (Boss *et al.* 1997a). UCP2 may be responsible for the substantial mitochondrial proton leak that has been reported in other tissues of the body (Harper & Brand 1993; Nobes *et al.* 1990; Porter & Brand 1993). It is a thermogenic protein that is directly regulated by the diet (Fleury *et al.* 1997), and it could regulate body weight by influencing energy expenditure and thermogenesis. In support of this, UCP2 maps to regions of human chromosome 11 and mouse chromosome 7 linked to hyperinsulinemia and obesity.

Another UCP homologue, UCP3, has also been cloned (Boss *et al.* 1997b; Vidal-Puig *et al.* 1997). At the amino acid level, human UCP3 is 71% identical to human UCP2 and 57% identical to human UCP1 (Vidal-Puig *et al.* 1997). UCP3 is distinctive in its abundant and preferential expression in skeletal muscle in humans, and BAT and skeletal muscle in rodents (Boss *et al.* 1997b; Vidal-Puig *et al.* 1997). UCP3 mRNA is present in small amounts in mouse WAT, brain, kidney, liver and colon (Boss *et al.* 1997b). UCP3 expression is not increased in the cold in muscle (20 day exposure), but it is increased in BAT (Boss *et al.* 1997b; Vidal-Puig *et al.* 1997). UCP3 mRNA level is decreased in BAT of *fa/fa* rats (as is that of UCP1) whereas UCP2 is increased (Boss *et al.* 1997b; Vidal-Puig *et al.* 1997). Skeletal muscle and BAT are important in thermogenesis and therefore energy expenditure in both humans and rodents, so UCP3 is likely to play an important role in thermogenesis.

Considering the discovery of new UCP homologues, each under different control, with the data that will be presented in this thesis, I believe that there exists two or more

distinct types of brown adipocyte, each expressing a different UCP homologue, and each subject to different control.

Dark- and light-staining (and electron dense) multilocular adipocytes in BAT have been reported previously (Pellet & Lheritier 1975; Vallin 1970). The authors suggested that the pattern of staining was an indication of two different cell types, which was disputed and thought to be an artefact. Recently, immunocytochemical evidence has provided further evidence for the existence of more than one type of brown adipocyte (Cinti *et al.* 1997). When staining with a specific anti-UCP1 antibody, IBAT assumes a patchy staining (intensely stained cells close to less coloured and negative ones) defined as Harlequin-like (Cinti *et al.* 1997). IBAT with a Harlequin appearance has been reported in CL-treated rats (2 days treatment), and in cold-acclimated rats (2 weeks at 4°C) (Cinti *et al.* 1997). The authors suggest that the UCP gene does not react in the same way in all of the brown adipocytes in IBAT under thermogenic stimuli (Cinti *et al.* 1997). This will be discussed further in Chapter 8.

Triggers for thermogenesis in BAT:

Two types of external triggers for thermogenesis exist: the ingestion of food, and prolonged exposure to cold temperatures. Both stimulate the tissue via sympathetic innervation, which causes an increase in thermogenesis, mediated by the action of NA on brown adipocytes.

Hypertrophy:

BAT hypertrophies in response to chronic stimulation by NA; this includes hyperplastic growth, as well as an increased capacity for thermogenesis. Within BAT, nerves supply the blood vessels and arteriovenous anastomoses, and course between and terminate on parenchymal cells, allowing for a consolidated response from all components of the tissue. The extensive vasculature of BAT is highly innervated and will allow for very high rates of blood flow when the tissue is stimulated (Closa *et al.* 1993; Foster 1986; Foster & Frydman 1978; Foster & Frydman 1979).

Growth occurs by an increase in cell number, or hyperplasia. Hypertrophy includes an increase in all cellular constituents of BAT, with a selective increase in certain components. Mature brown adipocytes and dormant brown adipocytes are responsible for a rapid increase in thermogenesis, mediated by the β_3 -AR. The increase in thermogenic capacity of BAT when it is stimulated by NA is mediated by an increase in UCP, and the activities and levels of LPL and T_4 5'-D.

The morphology of the tissue depends on the state of BAT. Chronically stimulated BAT will have smaller lipid droplets, and much more abundant mitochondria, with an increased total content of UCP (Himms-Hagen & Ricquier 1997).

Atrophy:

BAT atrophies under conditions of decreased neural input (Himms-Hagen 1991). Atrophied BAT has a decreased capacity for thermogenesis resulting from a very low content of UCP (Himms-Hagen 1991; Himms-Hagen & Ricquier 1997; Hogan & Himms-Hagen 1980; Holt *et al.* 1983). The brown adipocytes not only have a low UCP content; they have less mitochondria with fewer cristae (Himms-Hagen 1991). The atrophied brown adipocyte may contain only one large triglyceride droplet and is then described as unilocular.

Differentiation:

Interstitial cells present in BAT proliferate and differentiate when stimulated by NA (Himms-Hagen & Ricquier 1997). These cells differentiate first into protoadipocytes, then preadipocytes and finally into mature cells (Géloën *et al.* 1992; Géloën *et al.* 1988; Géloën *et al.* 1990). Interstitial cells have no β_3 -ARs; proliferation and initial differentiation are mediated by β_1 -ARs (Bronnikov *et al.* 1992).

Differentiation of interstitial cells and protoadipocytes into preadipocytes and then mature adipocytes (whether brown or white) is complex, and it occurs via an sequential expression of adipocyte-specific genes, triggered by an assortment of interacting transcription factors. The most important transcription factors involved in the ordered expression of adipocyte-specific genes during differentiation are the nuclear receptor peroxisome proliferator-activated receptorγ2 (PPARγ2), and CCAAT enhancer binding proteins (C/EBP) (Auwerx *et al.* 1996). Several other transcription factors are involved, including ADD1 (Auwerx *et al.* 1996).

ADD1 mRNA is expressed predominantly and at high levels in BAT in vivo, and is regulated during both determination and differentiation of cultured adipocyte cell lines, suggesting that it plays a role in differentiation of brown adipocytes (Tontonoz *et al.* 1993).

The PPARs belong to the superfamily of nuclear hormone receptors (together with steroid, thyroid hormone, retinoid and vitamin D receptors) which act as transcription factors (Shalev & Meier 1996). PPARs recognize and bind to response elements in the promoter region of target genes as a heterodimer with RXR (Shalev & Meier 1996). PPARγ2 is crucial for early adipocyte differentiation (Hu *et al.* 1995; Tontonoz *et al.* 1994c). Expression of PPARγ in adipose tissue decreased with fasting and diabetes, increased with high fat diet, and in DTA transgenic mice (unchanged in *ob/ob* and GTG) (Vidal-Puig *et al.* 1996). PPARγ is a regulator of differentiation-dependent expression of UCP (Sears *et al.* 1996), adipocyte P2 (aP2) (Tontonoz *et al.* 1994a; Tontonoz *et al.* 1994b), and phosphoenolpyruvate carboxykinase (Tontonoz *et al.* 1995), and is able to inhibit leptin expression (De Vos *et al.* 1996; Kallen & Lazar 1996).

The natural ligand for PPARγ is 15-deoxy-$\Delta^{12,14}$-prostaglandin J_2 (a prostaglandin metabolite) (Forman *et al.* 1995; Kliewer *et al.* 1995). Anti-diabetic thiazolidinediones are synthetic, and possibly therapeutic, ligands of PPARγ (Lambe & Tugwood 1996; Lehmann *et al.* 1995).

Much remains unknown about differentiation of adipocytes; modulation of transcription factors (pharmacologically, or with diet) might influence differentiation and therefore obesity.

Measures for assessing BAT function:

Wet weight: BAT tissue weight reflects the state of energy balance and of lipid stores (Trayhurn & Milner 1989). BAT weight is not an indication of thermogenic activity or capacity; quiescent BAT in an obese animal will quite often contain more lipid and weigh more than that of lean controls.

Protein: The total protein content of BAT provides a crude index of the active tissue mass (Trayhurn & Milner 1989).

DNA: The DNA content of BAT is used as a measure of cellularity of the tissue. A given BAT depot consists of several different types of cells; over half the cells present may be non-brown adipocyte cells (Bukowiecki *et al.* 1982; Bukowiecki *et al.* 1986; Géloën *et al.* 1988; Néchad 1986). Measurement of cell number by measuring DNA will overestimate the number of brown adipocytes, but is useful in providing an indication of major changes in thermogenic capacity of BAT (Trayhurn & Milner 1989).

Cytochrome oxidase (COX): Mitochondria are the site of thermogenesis in BAT; measure of the total mitochondrial content of the tissue is useful for assessing its capacity for thermogenesis. The activity of a mitochondrial marker enzyme such as COX will give a determination of relative changes in mitochondrial mass. Some of the mitochondria measured will be from cell types other than brown adipocytes (Bukowiecki *et al.* 1982; Bukowiecki *et al.* 1986; Géloën *et al.* 1988; Néchad 1986); however, the mitochondrial contribution from other cells should be small compared with the large number from brown adipocytes (Trayhurn & Milner 1989).

UCP: The immunological detection of UCP has been regarded as providing the definitive criterion of whether an adipose tissue is functionally brown or white (Trayhurn & Milner 1989).

Antiserum to UCP is prepared using UCP purified from BAT mitochondria. As previously mentioned, UCP homologues have now been cloned (Boss *et al.* 1997b; Fleury *et al.* 1997; Gimeno *et al.* 1997; Larrouy *et al.* 1997; Vidal-Puig *et al.* 1997); all three isoforms of UCP are present in BAT. In view of the similarity in structure of the three isoforms it must be assumed, unless otherwise proven, that previous UCP antibodies measured all UCP types present in a tissue. Data published concerning amounts of UCP must now be carefully looked at, as BAT contains all three UCP homologues (Boss *et al.* 1997b; Fleury *et al.* 1997; Gimeno *et al.* 1997; Larrouy *et al.* 1997; Vidal-Puig *et al.* 1997). The level of UCP2 or UCP3 protein in BAT and other tissues is as yet unknown.

UCP mRNA: Detection of UCP message in an adipose tissue identifies the tissue as BAT, or the cell type as a brown adipocyte (Trayhurn & Milner 1989).

GDP binding (GDPB): GDP binds specifically to a site on UCP; its level depends on both the concentration and the thermogenic state of UCP. An acute increase in GDPB suggests the unmasking of binding sites that occurs when thermogenesis is stimulated by NA. GDPB is a measure of the activity of the proton conductance pathway (Trayhurn & Milner 1989). The level of GDPB is an index of the response of BAT to different stimuli, it reflects both the concentration of UCP in the mitochondria and the extent to which the binding sites on UCP are available (Trayhurn & Milner 1989).

BAT temperature: Heat is the main product of BAT; an increase in BAT temperature demonstrates an increased activity of the tissue. BAT will be activated by a decrease in core temperature, which can be measured simultaneously.

Blood flow through BAT: The amount of blood flowing through BAT is a good measure of the response of the tissue to altered neural control and can provide a direct measure of thermogenesis in BAT (Foster 1986; Foster & Frydman 1978; Foster & Frydman 1979).

Control of BAT

Central regulation:

Electrical or chemical stimulation and lesions to discrete areas of the brain have provided information on the central control of BAT thermogenesis and growth (see Himms-Hagen, 1991). No absolute delineation of the control has been determined, but many pieces of evidence have been accumulated.

The lateral hypothalamus generally exerts an inhibitory influence on BAT, while the VMH exerts an excitatory influence (Himms-Hagen 1991). Electrical stimulation of the VMH (Woods & Stock 1994; Woods & Stock 1996a) induces a biphasic response in the temperature of BAT; a decrease in BAT temperature was seen during the stimulation, and a large increase in BAT temperature was seen once the stimulation had stopped. The lateral hypothalamus is involved in this response, and the intact innervation of BAT is required. The authors suggest that the decrease in temperature seen during stimulation is mediated by the opening of the arteriovenous anastomoses caused by a release of neuropeptides. Once the

stimulation stopped, an increase in temperature would occur with the closing of the arteriovenous anastomoses. When the arteriovenous anastomoses are closed, blood is shunted into the capillary bed, and NA can act directly on the parenchymal cells. α_1 -ARs are thought to be responsible for the closing of the arteriovenous anastomoses; NA in the blood would be carried into the capillary bed and can then act on β_3 -ARs on brown adipocytes to increase thermogenesis. Foster (1986) has shown a synergism between α_1 - and β -ARs in the increase in blood flow in BAT, which is explained by this theory. Also explained by this is the failure of selective β_3-agonists to cause the same increase in blood flow through BAT (Thurlby & Ellis 1986), the selective agonist would not be able to stimulate α_1 -ARs to close the arteriovenous anastomoses.

Peripheral regulation:

Neural control (BAT innervation): Sympathetic noradrenergic innervation of BAT and its central control are responsible for the control of both BAT thermogenesis and the hyperplastic growth of BAT in response to chronic stimulation (Géloën *et al.* 1992; Himms-Hagen 1991; Takahashi *et al.* 1992).

Substantial evidence exists for the role of NA and sympathetic nerves in the control of BAT, including data from nerve stimulation, denervation, effects of NA, NA turnover rate and firing of noradrenergic nerves (Himms-Hagen 1991). Electrical stimulation of nerves that supply BAT results in metabolic changes in BAT, mimicking the tissue's response to cold or NA (Flaim *et al.* 1977; Girardier & Seydoux 1986; Minokoshi *et al.* 1988; Minokoshi *et al.* 1990).

BAT can be denervated both surgically and chemically. Surgical denervation can be done unilaterally, as each side of IBAT is separately innervated (Foster *et al.* 1982). This is beneficial for studying denervated and innervated pads in the same animal, and under the same conditions. Surgical denervation removes most NA from the tissue and prevents various responses to stimulation of BAT (Granneman & Campbell 1984; Minokoshi *et al.* 1986).

Surgical denervation abolishes the cold-induced increase in blood flow to BAT (Foster *et al.* 1982) and diminishes the longterm cold-induced increases in protein, UCP, GDPB, and T_4 5'-D activity (Himms-Hagen *et al.* 1990; Park & Himms-Hagen 1988; Rothwell & Stock 1984), as does chemical sympathectomy with 6-hydroxydopamine (Depocas *et al.* 1984; Desautels & Dulos 1988). Chronic infusion of NA prevents the effect of denervation on UCP and on GDPB in BAT of rats (Desautels & Dulos 1988).

Chemical denervation offers a more selective way of removing neural influences on BAT but has effects on other organs as well as on BAT (Himms-Hagen 1991). NA can be removed using 6-hydroxydopamine, and sensory neuropeptides can be removed using capsaicin (Cap), a process called Cap-desensitization.

Transgenically sympathectomized mice have been generated that cannot synthesize NA. These mice are cold intolerant as is expected since they are unable to activate thermogenesis in their BAT and to activate peripheral heat conservation mechanisms. These NA deficient mice have increased food intake but are not obese because of an increased basal metabolic rate caused by an increased heat loss (Thomas & Palmiter 1997).

Cold increases NA turnover in BAT (Young *et al.* 1982; Zaror-Behrens & Himms-Hagen 1983). In the rat, a palatable diet or addition of sucrose or fat to chow can increase NA turnover in BAT (Fisler *et al.* 1984; Rappaport *et al.* 1982; Vander Tuig & Romsos 1984; Walgren *et al.* 1987) and promote BAT growth and thermogenesis, while fasting does the opposite (Young *et al.* 1982).

Innervation of mature brown adipocytes by noradrenergic nerves and of the vasculature of BAT by noradrenergic nerves that also contain NPY is well established (Cannon *et al.* 1986; Nnodim & Lever 1988; Norman *et al.* 1988). However, the long-known heterogeneity of the five intercostal nerves that innervate IBAT (Flaim *et al.* 1976) is now realized to be attributable to the presence of a variety of neuropeptide-containing nerves that innervate mature brown adipocytes, the vasculature and the arterio-venous anastomoses (Lever *et al.* 1988; Lever *et al.* 1989; Mukherjee *et al.* 1989; Nnodim & Lever 1988; Norman *et al.* 1988). The presence of SP and CGRP within nerves in BAT, both neuropeptides characteristic of afferent autonomic 'sensory' nerves (Himms-Hagen *et al.* 1990; Lever *et al.* 1988; Lever *et al.* 1989; Mukherjee *et al.* 1989), implicates non-noradrenergic nerves in the control of BAT function.

Hormonal control: BAT activity is also modified by several hormones including insulin, glucagon, corticosteroids, and thyroid hormone.

Insulin plays an important role in the control of BAT in relation to energy balance. It has a direct influence on glucose transport into BAT (Greco-Perotto *et al.* 1987; Marette & Bukowiecki 1989; Slot *et al.* 1991), and on lipogenesis (Saggerson *et al.* 1988). Insulin indirectly stimulates BAT via modulation of the neural control of BAT (Géloën & Trayhurn 1990a; Géloën & Trayhurn 1990b). The sensitivity of BAT to insulin action is enhanced when the tissue is stimulated (Vallerand *et al.* 1990), and it develops a resistance to insulin in obese rodents (Himms-Hagen & Ricquier 1997). Insulin is required for maintenance of the thermogenic capacity of BAT, and is important for the synthesis of UCP and the glucose transporter GLUT 4 (Burcelin *et al.* 1993; Géloën & Trayhurn 1990b), indirectly mediated by its capacity to simulate $T_4$5'-D (Mills *et al.* 1987; Silva & Larsen 1986) to increase T_3 levels in BAT.

Animals that are diabetic due to treatment with streptozotocin have atrophied BAT with low levels of total protein, COX and UCP (Géloën & Trayhurn 1990b). BAT also has a low sympathetic activity (Yoshida *et al.* 1984; Yoshioka *et al.* 1989). Chronic treatment with insulin restores BAT thermogenic capacity, with a normal level of UCP (Géloën & Trayhurn 1990b). Treatment with a β -AR agonist has a similar effect (Arch *et al.* 1986), suggesting that the low level of sympathetic tone is the primary cause of the atrophy of BAT in the diabetic state. Surgical denervation markedly attenuates the effect of insulin in increasing UCP content (Géloën & Trayhurn 1990a). Therefore, insulin has a dual trophic

effect on BAT; partially mediated by nerves. The site of presumed central action of insulin is not known. Glucagon administration will induce a hyperplastic growth of BAT (Billington *et al.* 1987). Glucagon levels are increased in cold exposed and cold acclimated rats, and glucagon has been implicated in the control of BAT growth (Kuroshima *et al.* 1984). A physiological role of this hormone in the control of BAT is unlikely considering the high concentrations needed to exert its effects (Himms-Hagen 1989a).

Glucocorticoids suppress the neural activation of BAT, and large amounts can cause atrophy of the tissue (Galpin *et al.* 1983; Holt *et al.* 1983; Tokuyama & Himms-Hagen 1987; York *et al.* 1985a). Glucocorticoid induced atrophy of BAT is most marked in obese rodents. Adrenalectomy improves BAT thermogenic responsiveness in old, obesity-prone rats (Fukushima *et al.* 1985; Marchington *et al.* 1986), in rats with parasagittal knife cuts (Romsos *et al.* 1987), in *fa/fa* rats (Allars *et al.* 1987; Marchington *et al.* 1986; York *et al.* 1985a; York *et al.* 1985b), and in *ob/ob* and *db/db* mice (Saito & Bray 1984; Shimomura *et al.* 1987; Tokuyama & Himms-Hagen 1987; Tokuyama & Himms-Hagen 1989).

T_3 concentration is locally regulated in BAT. Rapid changes in BAT T_3 may occur without changes in plasma T_3 because BAT can produce T_3 from circulating T_4 via the action of a unique T_4 5'-D present in BAT (Leonard *et al.* 1983). In BAT, T_4 5'-D is stimulated by the sympathetic nervous system (Silva & Larsen 1985), mediated by both α_1 - and β -ARs (Bianco *et al.* 1992; Raasmaja & Larsen 1989; Rabelo *et al.* 1995; Silva 1988), and by insulin (Mills *et al.* 1987; Silva & Larsen 1986). When an animal is exposed to the cold, there is a rapid increase in T_4 5'-D. T_3 produced by this enzyme increases the thermogenic

capacity of BAT by increasing transcription of UCP (Bianco *et al.* 1988; Rabelo *et al.* 1996a; Rabelo *et al.* 1996b; Rabelo *et al.* 1995; Silva 1988; Silva & Rabelo 1997).

The UCP promoter contains thyroid response elements (Bianco *et al.* 1988). The burst of T_3 produced is enough to saturate the BAT nuclear receptors; these receptors bind thyroid response elements and increase the expression of UCP (Bianco *et al.* 1988; Bianco & Silva 1987; Silva 1988).

Control at the cellular level:

UCP: The uncoupling protein found in BAT mitochondria (UCP1), has always been thought to be unique to BAT. It is now known that it is simply this isoform that is unique to BAT (Boss *et al.* 1997a; Boss *et al.* 1997b; Fleury *et al.* 1997; Gimeno *et al.* 1997; Larrouy *et al.* 1997; Vidal-Puig *et al.* 1997).

The intracellular control of UCP depends mainly on the concentration of FFAs that interact with UCP to lower the membrane potential for proton translocation (Bukowiecki 1986; Nicholls *et al.* 1986; Nicholls & Rial 1984).

The exact mechanism of ion transport by UCP has not been explained; three models for H^+/OH^- transport exist (Ricquier & Cassard-Doulcier 1993): fatty acids are activators that stimulate the H^+-translocating pathway; fatty acid anions are translocated by UCP (Garlid *et al.* 1996); the carboxyl group of fatty acids acts as a H^+ acceptor and donor.

Intracellular purine nucleotides (mainly ADP and ATP) bind to a specific site on the UCP to inhibit proton translocation, and have to be removed for the UCP to function (Lanoue

et al. 1982). An unmasking of binding sites occurs when thermogenesis is stimulated by NA, permitting proton translocation to occur (Klingenberg 1984; Klingenberg 1988).

UCP synthesis is highly regulated at the transcriptional level (Silva & Rabelo 1997); mRNA stabilization plays a role in maintenance of a high level of UCP mRNA (Picó *et al.* 1994; Rehnmark *et al.* 1992), possibly mediated by T_3 (Guerra *et al.* 1996). NA is the main physiological activator of UCP synthesis, acting via its second messenger cAMP (Himms-Hagen 1991; Nedergaard & Cannon 1992). Stimulation of any of the three β -ARs in a brown adipocyte will lead to an increase in UCP mRNA (Klaus *et al.* 1994; Rohlfs *et al.* 1995). In the HIB 1B brown adipocyte cell line, β_3 -ARs accounted for 30-40% of the catecholamine stimulated increase in UCP mRNA, while β_1 - and β_2 -ARs were responsible for the remaining 60-70% (Klaus *et al.* 1994). In cells isolated from a mouse hibernoma, stimulation of any of the β -ARs led to an increase in UCP synthesis; the greatest response was seen when all three subtypes were stimulated (Rohlfs *et al.* 1995).

T_3 is required to achieve a maximal increase in UCP synthesis; it has been shown to act synergistically with NA, increasing the transcriptional response of the UCP gene to NA fourfold (Bianco *et al.* 1988; Guerra *et al.* 1994; Guerra *et al.* 1996; Klaus *et al.* 1991; Rehnmark *et al.* 1992; Silva 1993). Insulin is also necessary for a full response of UCP (Géloën & Trayhurn 1990a; Géloën & Trayhurn 1990b; Klaus *et al.* 1991).

UCP expression is also affected by other hormones: positively by IGF-1 (Guerra *et al.* 1994) and retinoids (Alvarez *et al.* 1995; Boyer & Kozak 1991; Cassard-Doulcier *et al.* 1993; Rabelo *et al.* 1996a), negatively by glucocorticoids (Moriscot *et al.* 1993).

The UCP gene promoter has been extensively analysed. The basic promoter runs from -157 to +144 base pairs (bp) and it contains a non cell-specific cAMP response element in rats and in mice (Kozak *et al.* 1994). In non-BAT cells of mouse and rat, UCP expression is reduced due to a repressor area at -400 to -160 bp (Cassard-Doulcier *et al.* 1993).

A powerful enhancer at -2.49 to -2.28 kilobases (kb) in the rat UCP gene was identified as an activator element (Cassard-Doulcier *et al.* 1993), seen also in the mouse gene (Kozak *et al.* 1994), and has now been extensively characterized. An area between -2.32 and -2.28 kb is responsible for the synergism between cAMP and T_3 in the rat (Silva & Rabelo 1997). Two T_3 response elements have been identified in the rat, at -2.33 kb and -2.39 kb (Cassard-Doulcier *et al.* 1994; Rabelo *et al.* 1996b; Rabelo *et al.* 1995). A complex 90 bp regulatory element is found between -2.49 and -2.40 kb, which contains numerous *cis*-acting elements (Rabelo *et al.* 1996a; Yubero *et al.* 1994b). These include a cAMP response element identified in mouse (Kozak *et al.* 1994), a retinoic acid responsive element with binding sites for retinoic acid receptor and retinoid X receptor in the rat (Alvarez *et al.* 1995; Larose *et al.* 1996; Rabelo *et al.* 1996a), a cell-specific enhancer in the mouse (Kozak *et al.* 1994), and a putative PPARγ element in the mouse (Sears *et al.* 1996).

Numerous *cis*-elements have been identified within the UCP gene; including cAMP-response elements in the enhancer and in the proximal region of the mouse promoter (Kozak *et al.* 1994), possible CCAAT enhancers have been identified in the rat UCP promoter (Yubero *et al.* 1994a). The CCAAT/enhancer binding protein family of transcription factors

may play an important role in adipose differentiation (Yubero *et al.* 1994b). Other putative trans factors include NF1, Ets1, and Sp1 (Cassard-Doulcier *et al.* 1994).

Glucose: Glucose is not a substrate for thermogenesis (Cawthorne *et al.* 1987; Isler *et al.* 1987; Lopez-Soriano & Alemany 1986; Saggerson *et al.* 1988; Smith *et al.* 1986; Wilson *et al.* 1987). Glucose entry is mediated by glucose transporters (predominantly the translocatable GLUT 4). NA stimulation causes an increase in glucose uptake that is not due to translocation but to activation of the transporter. When stimulated by NA, glucose use (Cooney *et al.* 1987; Cooney & Newsholme 1984; Shibata *et al.* 1989; Vallerand *et al.* 1987; Young *et al.* 1984b; Young *et al.* 1985) and lactate production (Ebner *et al.* 1987; Isler *et al.* 1987; Ma & Foster 1986) increase in the brown adipocyte.

Insulin also increases glucose uptake by the brown adipocyte via a translocation of GLUT4 to the plasma membrane. This occurs after a meal, when the glucose that enters is used for synthesis of triglycerides, both fatty acids and the glycerol backbone, to replenish fat stores in the brown adipocyte.

Glucose that enters the cell is metabolized via glycolysis. ATP for BAT is generated from substrate level phosphorylation at a time when ATP production in oxidative phosphorylation is curtailed (Himms-Hagen 1989a). Lactate is the end product of glycolysis (Himms-Hagen 1989a). The excess lactate produced in BAT is shunted to the liver, where it is reconverted to glucose by gluconeogenesis (Himms-Hagen 1989a). Some of the pyruvate produced in glycolysis is converted to fatty acids via lipogenesis.

BAT secretions

Heat can be regarded as a BAT secretion. BAT thermogenesis has been hypothesized to play a regulatory role in the control of meal size in animals living at temperatures below thermoneutrality, when it is required for thermoregulation (Himms-Hagen & Ricquier 1997). This hypothesis predicts a failure to terminate meals normally, and therefore overeating, when BAT function is impaired. Support for this hypothesis comes from the hyperphagia of the UCP-DTA mice (Lowell *et al.* 1996). UCP-DTA mice become massively obese and have insulin resistance, hyperglycemia, hyperinsulinemia, and hyperlipidemia characteristic of noninsulin-dependent diabetes mellitus (Hamann *et al.* 1995; Hamann *et al.* 1996; Lowell *et al.* 1993). The hyperphagia of these mice (Lowell *et al.* 1993) supports a role for BAT in the control of food intake.

Leptin is one satiety factor shown to be secreted from BAT in newborn rats (Dessolin *et al.* 1997), and from cultured brown adipocytes (Deng *et al.* 1997). Leptin is the product of the *ob* gene, which is defective in the *ob/ob* mouse, causing its obese phenotype (Zhang *et al.* 1994). Leptin expression in BAT has been investigated and was reported to be weak (Frederich *et al.* 1995b; MacDougald *et al.* 1995; Maffei *et al.* 1995a; Masuzaki *et al.* 1995b; Moinat *et al.* 1995; Murakami *et al.* 1995; Vydelingum *et al.* 1995) or not detectable (Murakami & Shima 1995; Trayhurn *et al.* 1995). The expression of leptin in BAT is inducible, as obese animals have an increased leptin expression in their BAT (Frederich *et al.* 1995b; Masuzaki *et al.* 1995b; Murakami & Shima 1995; Ogawa *et al.* 1995; Vydelingum

et al. 1995). Sympathetic stimulation in the form of acute cold exposure or β_3 -AR agonist, reduces leptin expression in BAT (Deng *et al.* 1997; Moinat *et al.* 1995).

Leptin is important in energy homeostasis in rodents; it remains to be seen whether the amount produced by BAT plays any role in this. Leptin is secreted from BAT at birth (Dessolin *et al.* 1997); the authors suggest that it is involved in the regulation of food intake at this point in development.

Many other factors are produced in BAT and secreted, the importance of most of them has yet to be determined. Adipose tissues are the most important source of angiotensinogen (Himms-Hagen & Ricquier 1997). Brown adipocytes from multiple anatomical sites in the rat express angiotensinogen mRNA and secrete angiotensinogen (Campbell & Habener 1987; Cassis *et al.* 1988; Crandall *et al.* 1994; Frederich *et al.* 1992). Angiotensinogen may be processed to the angiotensin peptides in rat BAT, and angiotensin II was able to modulate NA release when tested in BAT slices (Cassis & Dwoskin 1991; Cassis & Dwoskin 1994). Angiotensin II participates, through interaction with its receptors, in the enhanced sympathetic activity of cold-induced thermogenesis of rats (Cassis 1993).

An active role of BAT thermogenesis in acute fever development has been reported, and it was attributed to a central effect of interleukin-1β and TNFα (Dascombe *et al.* 1988; Rothwell *et al.* 1990). Brown adipocytes show an increased expression of interleukin-1α and interleukin-6, as well as an increased secretin of interleukin-6 when stimulated (Burýsek & Houstek 1997). These effects were mediated in primary culture by catecholamines acting on β_3 -ARs. Interleukin-1α is an early acting inducer of other inflammatory cytokines including

interleukin-1, TNFα, interleukin-6, interleukin-8, and interferons (Burýsek & Houstek 1997). The interleukin-6 produced may have a paracrine role, or it could contribute to the systemic level of interleukin-6 under certain physiological conditions (Burýsek & Houstek 1997).

Adipsin is expressed in BAT and WAT and is factor D of the alternative pathway of complement activation, and other factors of this pathway are present in BAT (Spiegelman *et al.* 1993). WAT, and most likely BAT, secrete prostaglandins and monobutyrin (Himms-Hagen & Ricquier 1997). Prostaglandins are involved in the regulation of lipolysis and adipose differentiation (Ailhaud *et al.* 1992); the metabolite 15-deoxy-$\Delta^{12,14}$-prostaglandin J_2 is a ligand for PPARγ (Forman *et al.* 1995; Kliewer *et al.* 1995). Monobutyrin is formed from the acylation of diacylglycerol by butyryl-CoA, and it stimulates both angiogenesis and vasodilatation of microvascular beds (Ailhaud *et al.* 1992; Wilkison & Spiegelman 1993).

BAT in humans

BAT is well developed and important in the thermal and energy balance of the human infant (McIntyre *et al.* 1993). BAT is stimulated in human infants exposed to mild cold (22°C-27°C) (Brück 1978; Lean 1992a). Six main depots in the human infant constitute 90% of the BAT: cervical, axillary, perirenal, periadrenal, and pericardiac regions; and the remaining 10% of the BAT is found in the posterior part of the abdominal cavity: along thoracic aorta, intercostal arteries, abdominal aorta, saphenous veins, and in omentum well (Lean *et al.* 1986; Nedergaard & Cannon 1992). BAT has been implicated in thermoregulatory feeding in human infants (Himms-Hagen 1995).

BAT accumulates lipid and takes on the histological appearance of WAT with age (Himms-Hagen & Ricquier 1997). Adult fat occurring at sites present as BAT in human infants can be considered as inactive BAT (Himms-Hagen & Ricquier 1997). Clusters of BAT-type multilocular cells have been found at these sites (Himms-Hagen & Ricquier 1997). Brown adipocytes are more readily identified in younger humans and in those exposed to cold temperatures, but they have been found in humans of all ages (Huttunen *et al.* 1981; Kortelainen *et al.* 1993; Lean 1992b; Lean & James 1986; Lean *et al.* 1986). Under certain conditions, BAT in humans can be stimulated, as seen by a decreased lipid content, multilocular appearance, and an increased number of mitochondria. A NA secreting tumour (pheochromocytoma) can activate perirenal fat (Garruti & Ricquier 1992; Melicow 1957), and tumours of BAT (hibernomata) are thermogenically active (Bouillaud *et al.* 1988). Garruti & Ricquier (1992) investigated the possible association of UCP and its message with pathological conditions other than pheochromocytoma. The authors suggest that BAT is likely to be present in more adults than expected. NA and β_3 -AR agonists increased UCP mRNA level in primary culture of human perirenal adipocytes (Champigny & Ricquier 1996), which were presumed to be dormant brown adipocytes.

BAT as a target for antiobesity drugs acting on β_3 -ARs

BAT is probably not important in temperature control or metabolic regulation in adult humans (Lean 1992b; Lean *et al.* 1986); it follows that it would not play a role in the etiology of human obesity. However, BAT in adult humans is a possible target for antiobesity drugs.

More than one type of β -AR is present in BAT (Himms-Hagen & Ricquier 1997). Administering drugs to activate BAT using β -AR agonists can produce unwanted effects in other tissues. β_1 -ARs are present in the heart and its agonists will cause tachycardia, while agonists of β_2 -ARs will cause tremors. The β_3 -AR was cloned in 1989 (Emorine *et al.* 1989) and is expressed mainly in brown and white adipocytes of small mammals, except the guinea pig (Carpéné *et al.* 1994; Himms-Hagen *et al.* 1995).

The selective β_3 -AR agonist CL can both prevent and reverse diet-induced obesity in rats (Ghorbani *et al.* 1997; Ghorbani & Himms-Hagen 1997; Himms-Hagen *et al.* 1994), hypothalamic obesity in MSG-treated mice (Yoshida *et al.* 1994b), and genetic obesity in *fa/fa* rats (Ghorbani & Himms-Hagen 1997; Himms-Hagen & Ghorbani 1995) and yellow KK mice (Yoshida *et al.* 1994a). CL appears to work by liberating FFAs from WAT, while activating BAT to consume the FFAs (Himms-Hagen & Danforth 1996). This drug is in phase II clinical trials, but it is not very effective for the human β_3 -AR (Himms-Hagen & Danforth 1996). An effective drug for treatment of human obesity must be effective on the human β_3 -AR (Himms-Hagen & Danforth 1996).

White adipose tissue

Structure/ Morphology:

WAT functions to store surplus energy as triglycerides in lipid droplets. When this stored energy is needed, the triglycerides are hydrolyzed and released as FFAs and glycerol. Both the storage and release of energy from fat cells are regulated by hormonal, neural, and local factors (Lönnroth & Smith 1992). WAT can expand and contract markedly under different conditions of age, endocrine status, and energy balance (Benjamin *et al.* 1961; Di Girolamo & Rudman 1968; Rudman & Di Girolamo 1967).

Adipose tissue consists of adipocytes and stromal-vascular cells (Gurr & Kirtland 1978; O'Brien *et al.* 1996). The stromal-vascular fraction is composed primarily of adipose stromal cells but also contains some vascular endothelia, macrophages, and mast cells (Bloom & Fawcett 1993; O'Brien *et al.* 1996). Adipose stromal cells are precursors of adipocytes but also play an important role in the paracrine regulation of adipocyte function and thus fat distribution (O'Brien *et al.* 1996). During differentiation, the preadipocytes fill with lipid and may take on a multilocular appearance (Gurr & Kirtland 1978).

Mature fat cells have accumulated lipid and have a single lipid droplet. Preadipocytes have no, or very little triacylglycerol but may develop into mature fat cells by hypertrophy (Gurr & Kirtland 1978). The fat cell is the largest cell in the body and lipid is the major proportion of the adipocyte. The proportion of cellular lipid to protein changes as the tissue matures and the fat cells enlarge (Gurr & Kirtland 1978). Mature WAT contains 90% triglyceride by weight (Newby *et al.* 1990).

WAT is found in depots throughout the body. Each fat depot has different characteristics, including patterns of development and differentiation (Cousin *et al.* 1993), and response to various stimuli. The pattern of distribution of fat cell size will vary between different WAT depots in the body and between species (Gurr & Kirtland 1978). A bimodal distribution of fat cell diameters is seen; a large portion of the cells have diameters with a classic distribution of 35-150 microns, and a small proportion of very small cells exists with diameters of 8-35 microns (DeMartinis & Francendese 1982).

Fibroblast-like, replicating, undifferentiated preadipocytes can be recovered from the stromal-vascular fraction of fat tissue digests. In the presence of media enriched with substrates and hormones, preadipocytes can be induced to differentiate into lipid-filled fat cells in vitro (Björntorp *et al.* 1978; Kirkland *et al.* 1993). As they differentiate, preadipocytes lose their capacity to divide while acquiring biochemical characteristics of fat cells (Kirkland *et al.* 1993): altered contents of various cytoskeletal proteins, and increases in activities of lipogenic enzymes. Many studies have been done on cells in culture in an effort to determine the biochemical mechanisms of differentiation and metabolism of white adipocytes.

Activation of white adipocyte adenylate cyclase by β -AR agonists produces cAMP as in BAT. cAMP activates the cAMP-dependent protein kinase (protein kinase A). This kinase phosphorylates and activates HSL, which hydrolyzes stored triglycerides to glycerol and FFAs (Strålfors *et al.* 1984). FFAs are released from the cell through an energy-requiring

transporting process also triggered by increased intracellular cAMP levels (Abumrad & Perry 1985).

The acute effects of catecholamines on the regulation of glucose and lipid metabolism in WAT have been well documented (Shimazu 1981). In WAT, β -AR agonist treatment stimulates basal glucose uptake (Kashiwagi *et al.* 1983; Ludvigsen *et al.* 1980; Lupien *et al.* 1990), and lipolysis (Scheidegger *et al.* 1984; Yang & McElligott 1989). In white adipose cell lines or in the primary culture of adipose precursors, β -AR agonists are triggers of the adipose conversion of adipocyte precursors and play a dominant antilipogenic role in mature fat cells (Antras *et al.* 1991).

Insulin has numerous effects within the adipocyte: glucose and amino acid transport, intracellular glycolytic and antilipolytic effects, and regulation of protein synthesis and cell growth (Lönnroth & Smith 1992). LPL activity, rates of LPL synthesis and LPL mRNA levels in adipocytes are all increased by insulin (Ailhaud 1991; Chan *et al.* 1988; Ong *et al.* 1988; Pradines-Figueres *et al.* 1988; Raynolds *et al.* 1991; Speake *et al.* 1985; Spooner *et al.* 1979).

WAT as an endocrine organ:

The adipocyte is metabolically very active; it functions as a secretory cell releasing numerous bioactive mediators that may have both autocrine and paracrine affects (Flier 1995). Secreted from both BAT and WAT, and already discussed with reference to BAT secretions were angiotensinogen, adipsin, prostaglandins, and monobutyrin. Adipocytes

synthesize and secrete LPL and cholesterol ester transfer protein, both regulators of triglyceride and lipoprotein metabolism.

Leptin, the product of the *ob* gene, is secreted from adipose tissue (Zhang *et al.* 1994; Zhang *et al.* 1995). Leptin is produced and secreted by adipocytes; its regulation and many actions will be discussed in the following sections.

TNFα was originally isolated as the mediator of hypertriglyceridemia and wasting (cachexia) (Beutler *et al.* 1985) in parasitically infected animals. TNFα is a cytokine that has been shown to have numerous direct effects on adipocyte metabolism (see Hotamisligil, 1994). In vitro, TNFα suppresses the expression of adipocyte-specific genes, including the enzymes involved in lipogenesis (Hotamisligil & Spiegelman 1994), and causes a suppression of LPL (Roberts & Greenberg 1996). In humans, body fat has been linked to a marker near TNFα (Roberts & Greenberg 1996). Adipose tissue expression of TNFα has been proposed to play a direct role in obesity linked insulin resistance (Hotamisligil *et al.* 1993; Hotamisligil & Spiegelman 1994).

Leptin and its Receptors

Leptin:

Leptin is a term coined by Halaas *et al.* (1995). It is derived from the Greek root leptos meaning thin and refers to the product of the *ob* gene, which is defective in the *ob/ob* mouse (Halaas *et al.* 1995). In December 1994, Zhang *et al.* cloned the *obese* gene encoding leptin. The absence of leptin leads to hyperphagia and the multiple neural and endocrine abnormalities in the *ob/ob* mouse (Ahima *et al.* 1996). Leptin is currently referred to as a satiety factor. The role of leptin in the control of food intake will be discussed below.

The gene product is an 18 kilodalton protein (Zhang *et al.* 1994). When secreted from adipose tissue it is 16 kilodaltons (after cleavage of its signal sequence) (Zhang *et al.* 1994). Leptin is highly conserved among vertebrates (Zhang *et al.* 1994), and it was confirmed to be present in rodent serum as detected by Western blotting (Frederich *et al.* 1995b). The promoter must contain elements conferring tissue specificity as leptin is only expressed in adipose cells (He *et al.* 1995).

Leptin is important in energy homeostasis in rodents. Its expression and protein levels are regulated as a function of energy stores (Frederich *et al.* 1995b; Maffei *et al.* 1995a), and of nutritional status (Ahima *et al.* 1996; Frederich *et al.* 1995a; Mantzoros *et al.* 1996). Leptin expression and protein levels are increased in various forms of rodent obesity (Frederich *et al.* 1995b; Maffei *et al.* 1995a). Leptin increases with increasing fat mass, and with a high fat diet (Frederich *et al.* 1995a), and it decreases with decreased fat mass and fasting (Ahima *et al.* 1996; Frederich *et al.* 1995b). Circulating leptin levels were decreased

by fasting and cold exposure in lean but not *fa/fa* rats (Hardie *et al.* 1996). Leptin is also secreted from brown adipose tissue (Deng *et al.* 1997; Dessolin *et al.* 1997), see section on BAT secretions.

Leptin is present in abundance in human adipose tissue but not in other tissues (Masuzaki *et al.* 1995a). One case of an '*ob*-like' mutation has been reported in humans (Montague *et al.* 1997), but generally leptin is not mutated in human obesity (Considine *et al.* 1995; Hamilton *et al.* 1995). As in rodents, leptin concentration is a function of energy stores and its expression is increased with obesity in humans (Considine *et al.* 1995; Hamilton *et al.* 1995).

The crucial signal that induces *ob* gene expression and leptin production in fat cells is still unknown. Insulin, catecholamines, and corticosteroids (Wabitsch *et al.* 1996), are all candidates for the regulation of leptin expression and secretion.

In the *ob/ob* mouse the message for leptin is present, but it contains a mutation and the mouse fails to produce the protein, leading to the obese phenotype. Leptin mRNA is overexpressed in the *ob/ob* mouse because no protein is present to signal the tissue to decrease transcription of the gene. Administration of purified recombinant leptin to mice validated the physiological effects of leptin; obesity was reversed in the *ob/ob* mouse with leptin administration (Campfield *et al.* 1995; Halaas *et al.* 1995; Pelleymounter *et al.* 1995).

Leptin receptors:

In December of 1995, Tartaglia *et al.* (1995) reported on the identification and expression cloning of a leptin receptor (OB-R), which is a single membrane-spanning receptor (Tartaglia *et al.* 1995).

The OB-R has at least five alternatively spliced transcripts (Chen *et al.* 1996; Lee *et al.* 1996), (Table 1.2). Several of these cDNA clones diverge from OB-R at the carboxyl terminus, two at the extreme amino terminus. Four clones (Ob-Ra, Ob-Rb, Ob-Rc, and Ob-Rd) have identical C-terminal sequences until Lys 889, which includes the extracellular domain and the transmembrane domain (Lee *et al.* 1996), and are consequently membrane bound receptors. Each of the four clones has a different cytoplasmic tail (intracellular domain), all of which are short except that of Ob-Rb. Ob-Re may encode a soluble receptor, as it has no region encoding a transmembrane domain (Lee *et al.* 1996). Ob-Rb is the normal product of the mutated *db* (Chen *et al.* 1996; Chua *et al.* 1996a; Lee *et al.* 1996), *fa* (Chua *et al.* 1996a; Chua *et al.* 1996b), and fa^k genes (Takaya *et al.* 1996), and is therefore the physiologically important receptor gene which when defective accounts for the obese phenotype of these rodents. Ob-Ra may function as a transporter across the blood brain barrier, based on its location in the choroid plexus.

	OB-Ra	OB-Rb	OB-Rc	OB-Rd	OB-Re
Extracellular domain	✔	✔	✔	✔	✘
Transmembrane domain	✔	✔	✔	✔	✘
Intracellular domain					
Length	S	L	S	S	✘
BOX 1	✔	✔	✔	✔	✘
BOX 2	✘	✔	✘	✘	✘
Tissue Distribution	**Hy**, T, F, B	**Hy**, T, F	**F**, S, H, T, L, B	**T**, **F**,Hy, L, H, S	**H**, **F**, T, Hy, B
Putative Function	transport	energy balance	?	?	transport
***Mutations in:**	*fa*, *fa*^{k}	***db***, *fa*,*fa*^{k}	*fa*, *fa*^{k}	*fa*, *fa*^{k}	*fa*, *fa*^{k}

Table 1.2: Ob-R Summary Table. Four of the clones have identical extracellular domains, and transmembrane domains. Ob-Re lacks a transmembrane domain, and may be a soluble receptor. The membrane bound receptors differ in the sequence and length of their cytoplasmic tail, or intracellular domain. Ob-Ra, -Rc, and -Rd all have short tails (S), while Ob-Rb has a long tail (L). All of the transmembrane receptors have BOX 1 sequence present in their intracellular domain, while only Ob-Rb has BOX 2. BOX 1 and 2 are motifs for JAK and STAT binding. Tissues in bold are those where the message was most abundant. Tissues are listed in order of abundance. B-brain, Hy-hypothalamus, L-liver, H-heart, T-testis, F-fat, S-spleen. Some faint bands not recorded in table.
* Mutations of the OB-R are discussed below.

Mutations in the leptin receptor: Study of the physiological consequences of the mutation present in each of these obese rodent models should provide insight into the functions of leptin.

The *db/db* mouse produces a transcript for the long form of OB-R (OB-Rb) but with a 106 nucleotide insertion that prematurely ends the intracellular domain (Lee *et al.* 1996). The portion of the cytoplasmic domain that is missing must be required for signal transduction and in eliciting the effects of leptin on body weight and feeding regulation.

A mutation causing an amino acid substitution in the C domain (Phillips *et al.* 1996), a region conserved in all isoforms of OB-R, causes the *fa* phenotype. The affinity of the receptor for leptin is unchanged (Chua *et al.* 1996b; Rosenblum *et al.* 1996). A decrease in total cell surface binding to the mutated receptor occurs (Chua *et al.* 1996b; Rosenblum *et al.* 1996), possibly due to a decreased dimerization of the receptor, causing leptin resistance (Rosenblum *et al.* 1996).

The Koletsky rat spontaneously develops obesity, hyperlipidaemia, hyperinsulinemia, and proteinuria with kidney disease. A single recessive gene (fa^k) is responsible for this phenotype. A nonsense mutation in the fa^k allele in the portion coding for the extracellular domain results in a stop codon (Takaya *et al.* 1996) within part of the receptor common to all known OB-R. This may provide the first 'null' OB-R model.

No mutation in the OB-R has been reported in obese humans. In obese humans, as in obese rodent models, high levels of leptin are seen; indicating a resistance to the action of leptin. Obese humans do not have any change in the expression of hypothalamic OB-R

(Considine *et al.* 1996). The cerebrospinal fluid/ serum ratio of leptin was fourfold higher in lean humans as compared with obese humans (Caro *et al.* 1996). This suggests that leptin enters the brain by a saturable transport system, as reported in mice (Banks *et al.* 1996). A lower capacity for transport in obese individuals may provide a mechanism for decreased leptin action.

OB-R is predicted to be a member of the cytokine receptor superfamily (Madej *et al.* 1995). Members of this family of receptors have sites on their cytoplasmic tails for the binding of *janus* kinase (JAK), and STATS (signal transducers and activators of transcription) (Heim 1996). The STAT family has six members: STAT 1, 2, 3, 4, 5, 6 (Taniguchi 1995).

In the mutant Ob-Rb receptor of the *db/db* mouse, both the JAK and STAT sites are missing (Table 1.2). Wild type Ob-Rb can activate STAT 1 (Rosenblum *et al.* 1996), STAT 3 (Baumann *et al.* 1996; Ghilardi *et al.* 1996; Rosenblum *et al.* 1996; Vaisse *et al.* 1996), STAT 5 (Baumann *et al.* 1996; Ghilardi *et al.* 1996), and STAT 6 (Ghilardi *et al.* 1996). Ob-Ra and the mutated *db* short form of Ob-Rb cannot activate the STAT pathway (Ghilardi *et al.* 1996; Vaisse *et al.* 1996), while *fa* OB-R can (Rosenblum *et al.* 1996).

Actions of leptin:

In rodents and in man, leptin expression and levels generally increase in parallel to adipose stores (Frederich *et al.* 1995a; Maffei *et al.* 1995b). This fits in with the proposed role of leptin as a signal of adipocyte triglyceride stores. The mechanisms for this coupling of triglyceride stores and leptin expression and secretion have yet to be determined.

Leptin is believed to help to prevent obesity by reducing food intake and raising energy expenditure via an action in the hypothalamus. OB-Rs are present on cells in key hypothalamic nuclei including the arcuate nucleus (Mercer *et al.* 1996a; Mercer *et al.* 1996b; Schwartz *et al.* 1996), the VMH (Mercer *et al.* 1996b; Schwartz *et al.* 1996), the PVN (Mercer *et al.* 1996b; Schwartz *et al.* 1996; Woods & Stock 1996b), and the ventral premamillary nucleus (Mercer *et al.* 1996b).

Leptin can regulate the expression of key hypothalamic neuropeptide genes NPY and corticotrophin releasing hormone (Schwartz *et al.* 1996). The normal response to fasting is overridden by leptin and the brain is tricked into believing that an abundance of food is present (Schwartz *et al.* 1996). Leptin acts directly on cells that express NPY mRNA; OB-R and preproneuropeptide Y mRNA are coexpressed in the arcuate nucleus of mice (Mercer *et al.* 1996a).

While leptin has been proposed to act via suppression of NPY expression in the hypothalamus, the persistence of obesity in *ob/ob* mice unable to express NPY and the normal response of these mice to leptin injection (Erickson *et al.* 1996) suggests that other hypothalamic neuropeptides must also be involved.

Treatment with the β_3 -AR agonist CL decreases leptin mRNA and circulating leptin to 20% of baseline levels. Despite this decrease in leptin, CL still caused a decrease in food intake (Mantzoros *et al.* 1996). The insulin stimulated release of leptin seen in rat white adipocytes was completely blocked by a β_3 -AR agonist, suggesting that the β_3 -AR may play a role in regulating the release of leptin from the adipocyte (Gettys *et al.* 1996).

Leptin may play a role in the physiology of starvation (Ahima *et al.* 1996). Leptin levels decrease during starvation (Ahima *et al.* 1996), and the *ob/ob* mice have neuroendocrine abnormalities similar to those seen with starvation (Bray 1990).

Leptin administration decreases serum insulin levels in mice (Campfield *et al.* 1995; Halaas *et al.* 1995; Pelleymounter *et al.* 1995), this may be directly mediated by an OB-R that is present on β cells in the pancreas (Kieffer *et al.* 1996). In human hepatic cells containing an OB-R, leptin antagonizes insulin signaling (Cohen *et al.* 1996).

There are conflicting reports on the effects of insulin on leptin expression. Insulin has been reported to have no effect on leptin expression in lean and obese humans (Muscelli *et al.* 1996), or in rhesus monkeys (Hotta *et al.* 1996). Contrary to this, insulin administration has been shown to affect leptin levels both positively (Hardie *et al.* 1996; Utriainen *et al.* 1996; Wabitsch *et al.* 1996; Gettys *et al.* 1996), and negatively (Nolan *et al.* 1996).

In rats, thiazolidinediones caused a decrease in food intake, WAT weight, and a dose dependant decrease in leptin mRNA levels (De Vos *et al.* 1996) via activation of PPARγ. This decreased expression was shown to occur via a decreased activation of the leptin promoter in primary human adipocytes (De Vos *et al.* 1996).

Leptin's roles in systems other than energy balance need to be investigated. OB-Rs are present in the lung, kidney, liver, ovary, testis, prostate, intestines, spleen, primitive haematopoietic stem cells, pancreas and many brain areas. The functions of all of the isoforms of OB-R need to be determined.

Infertility is a characteristic shared by the *ob/ob*, and *db/db* mice, and by the *fa/fa* rat, possibly because of a defective hypothalamic-pituitary-gonadal axis (Bray & York 1971). Leptin could serve as metabolic signal informing the reproductive axis about the body's nutritional state; permitting reproduction if sufficient metabolic reserves are available (Ahima *et al.* 1996). In support of this, continuous administration of leptin in the *ob/ob* female corrects their sterility (Chehab *et al.* 1996), and leptin could stimulate the reproductive endocrine system in both male and female mice (Barash *et al.* 1996).

The bone marrow adipocyte is the most abundant stromal cell phenotype in adult human marrow (Gimble *et al.* 1996) where it may play a nurturing role (Bennett *et al.* 1996), and be involved in haematopoiesis (the production of multiple blood cell lineages throughout the lifespan of an organism) (Gimble *et al.* 1996). OB-Rs are expressed in primitive haematopoietic cell populations (Bennett *et al.* 1996; Cioffi *et al.* 1996), and in both human and murine stem cell populations (Bennett *et al.* 1996). Haematopoietic stroma express leptin and leptin has a proliferative effect at the level of a multi lineage progenitor (Bennett *et al.* 1996).

The understanding of obesity and the control of food intake has been significantly affected by the discovery of leptin along with the validation of its role as a satiety factor and modulator of energy balance in reversing obesity in the *ob/ob* mouse. The regulation of leptin's expression and its mode of action are yet to be explained; the search should be constructive in supplying information on the control of energy balance.

The question remains as to what role if any leptin secreted from BAT (see section on BAT secretions) plays in energy balance, and how BAT thermogenesis affects its regulation in this tissue. A glandular function for BAT has occasionally been commented on; its original name was 'hibernating gland'. Could BAT secrete a different, as yet unknown, cytokine that has a satiety effect like that of leptin? Studies of the atrophy of BAT have lead to some hypotheses on these topics and will be covered in this thesis.

Chapter 2: General objectives

Many rodent models of genetic and experimentally produced obesity exist, with deficits in either energy intake, energy expenditure, or both of these components of energy balance. In most obese rodents, energy expenditure for thermogenesis is at a deficit, usually caused by a suppression of BAT thermogenesis (Himms-Hagen 1989b).

The objective of this research was to examine the effects of atrophied BAT on energy balance and body composition in different rodent models. Three different rodent models were used in my studies, each with a deficit in BAT thermogenesis.

The Cap-Des rat has atrophied BAT, with impaired thermogenesis (Cui & Himms-Hagen 1992a; Cui *et al.* 1990). Despite this deficit, previous studies had shown leanness in Cap-Des rats up to 8 months after treatment (Cui & Himms-Hagen 1992b). The objective of the first study was to extend the period of study of the Cap-Des rat to one year after treatment, when aging-associated obesity usually develops, and to characterize the altered size of the WAT depots according to the number and size of their adipocytes and to their total number of cells. At this time the rats would be 13.5 months old and expected to display an aging-associated, hyperplastic obesity, characteristic of old rats (Newby *et al.* 1990). IBAT was also studied in these rats, to assess whether the partial atrophy persisted in the older animals. The results are presented in Chapter 4.

Rats with a lesion in the nucleus of the solitary tract (NTS) were reported to have an impaired capacity to increase their oxygen uptake and the temperature of their IBAT after administration of catecholamines (Fyda *et al.* 1991). A similar impairment was seen in the

Cap-Des rat (Cui *et al.* 1990), known also to sustain a lesion in the NTS, and associated with marked atrophy of the IBAT. The objective of the second study was to learn the role of NTS disruption on BAT atrophy and function. The results of these experiments are presented in Chapter 5.

The UCP-DTA transgenic mouse has a partial genetic ablation of its BAT due to expression of DTA linked to the UCP promotor. These mice were developed as an effective model for the near complete atrophy of the many diffuse BAT depots, to determine their role in energy balance and body composition. UCP-DTA mice become massively obese, and have insulin resistance, hyperglycemia, hyperinsulinemia, and hyperlipidemia characteristic of noninsulin-dependent diabetes mellitus (Hamann *et al.* 1995; Hamann *et al.* 1996; Lowell *et al.* 1993). These mice also became hyperphagic (Lowell *et al.* 1993), supporting a role for BAT in control of food intake.

The objective of the first study with these mice was to detect what role the deficit in BAT thermogenesis of the UCP-DTA mice plays in the phenotype of obesity and hyperphagia by raising transgenic and control mice at thermoneutrality. The results of this experiment are presented in Chapter 6.

UCP-DTA mice can regulate their body temperature in the cold (Lowell *et al.* 1993), and it had been shown that UCP is still expressed in the BAT of these mice. It was thought that a population of brown adipocytes had escaped ablation by the toxigene and were responsible for the expression of UCP in the tissue. Mice were adapted to mild cold to learn whether these UCP-expressing brown adipocytes could proliferate and compensate for the

ablated cells. The objective of the second study was to find out why UCP-DTA mice were not as cold-intolerant (as are mice with transgenic disruption of the UCP1 gene (Enerbäck *et al.* 1997)) and to determine the nature of the compensation in their BAT when exposed to cold. The results of this experiment are presented in Chapter 7.

Chapter 3: General methods

Animals

Rats:

Male Sprague-Dawley rats were obtained from Charles River Laboratories, ST. Constant, Québec. The rats were 5 weeks of age (long-term experiment, Chapter 4) or 8 weeks of age (NTS experiment, Chapter 5). They were housed individually in plastic cages at a temperature of 24°C with a 12:12 hour light-dark cycle (lights on at 0700 hours). The rats had free access to food (Agway R-M-H 3000 chow, 14.4% of energy from fat) and water.

Mice:

A colony of UCP-DTA mice was established with six female UCP-DTA mice (provided by Dr. Bradford B. Lowell, Beth Israel Hospital and Harvard Medical School, Boston, MA) and six male FVB/N mice (from Taconic, Germantown, NY). Female transgenic mice were heterozygous for the UCP-DTA transgene. Breeding pairs were housed at 24°C with free access to food (Agway R-M-H 4020 chow, 14.5 % of energy from fat) and water and lights on for 12 hours per day.

Pups were weaned at 19-21 days of age, and were housed with littermates of the same sex until used (for description of transgene and genotyping see Chapter 6).

Measurement of body weights and food intake

Body weight and food intake measurements were done at approximately the same time of day throughout each experiment. Unless otherwise stated, body weights and food were measured twice a week. Differences between initial and final body weights, or between weights on successive days, are referred to as body weight gain.

Food intake measurement varied according to how the animals were housed. Food was measured before it was given to the animals, and the food remaining was collected and measured. Spillage was always checked, and this amount was added to the bulk of food remaining. The food no longer remaining was the food eaten.

Preparation of serum

Animals were killed by decapitation and blood was collected immediately. The blood samples were left to clot on ice for 0.5-2 hours, after which they were centrifuged at 3,000 rpm, 1,500*g* at 4°C for 15-30 minutes (Sorvall RC-5B or RC2-B). Serum was then transferred to Eppendorf microcentrifuge tubes and flash frozen in liquid nitrogen. Frozen serum samples were stored at -80°C until use.

Brown adipose tissue

In all experiments, IBAT was removed immediately after blood collection. BAT was placed in ice-cold isolation medium (0.25 M sucrose, 1 mM *N*-2-hydroxyethylpiperazine-*N'*-2-ethanesulfonic acid, 0.2 mM potassium EDTA, adjusted to pH 7.2 with 1.0 M KOH) or in plastic weigh boats on ice (for experiments with mice). IBAT was subsequently dissected clean of muscle and WAT, blotted dry and weighed. For rats, the BAT was homogenized in

10 ml of isolation medium (Brinkmann Polytron PT 10, setting 4 for 30 seconds) and samples of the homogenate were frozen for later analysis. For mice, samples were taken for histology, the tissue was reweighed and then frozen for later homogenizing. Mouse BAT was thawed on ice, and homogenized in a volume of ice-cold isolation medium approximately four times its weight (OMNI 1000 Hand held Rechargeable Homogenizer, Diamed Lab Supplies).

Protein:

The protein content of tissue homogenates was measured using a Lowry assay (Lowry *et al.* 1951) as modified by (Schacterle & Pollack 1973). Bovine serum albumin (BSA) was used as a standard. BSA amounts for the standard curve were 0, 15, 30, 60, 90, and 120 μg of protein. Standards and samples were always assayed simultaneously and were treated identically. The homogenate to be assayed or the protein standards were aliquoted in triplicate into conical plastic tubes. Five ml of 12.5% TCA were added; the samples were mixed, covered with parafilm, and left to allow the protein to precipitate overnight in the cold (4° C). Following the overnight incubation, the tubes were centrifuged at 4,000 rpm for 30 minutes, using a Beckman J-6B refrigerated centrifuge. Suction was used to remove the infranatant and along with it any fat that could interfere with the assay. 0.5 N NaOH was added to the tubes (1.150 ml), and the tubes were mixed. All of the precipitated protein was redissolved by placing the tubes in a water bath at 55° C (heated with a Brinkmann Circulator model IC-2) for 10 minutes and then mixing. After the samples had cooled to room temperature, copper reagent (10% sodium carbonate, 0.1% potassium tartrate, 0.05%

cupric sulphate) was added to the samples, which were mixed and left to incubate for 10 minutes at room temperature. A purchased 2N phenol reagent (Folin & Ciocalteau) was diluted 1:16 with water just before use. Folin reagent was added; tubes were vortexed immediately and incubated at 55° C for 5 minutes. The tubes were placed on ice for 5-10 minutes to stop the reaction. The absorbance of the samples at 650 nm was read within 30 minutes on a Beckman DU-50 or DU-65 spectrophotometer equipped with linear software data pack. Values of triplicates that were within 10% were retained and analysed using a Lotus 1-2-3, or Microsoft Excel spreadsheet and then Prism software.

Cytochrome oxidase:

COX is the final enzyme in the electron transport chain. It is a metalloenzyme requiring both iron and copper as prosthetic groups. The COX content of BAT serves as a measure of mitochondrial mass. A spectrophotometric assay was used to measure the rate at which COX could oxidize its substrate cytochrome c based on the method of Yonetani & Ray (1965). This was done by measuring the disappearance of the reduced cytochrome c, which absorbs light at 550 nm.

BAT homogenates were solubilized with a 3% lubrol WX solution on ice for 1.5 hours. One μl of lubrol was added for every 10 μg of protein. The samples were all diluted to a final protein concentration of 0.65 mg/ml with phosphate buffer (0.1 M, pH 7.0).

A solution of reduced cytochrome c (horse heart, type III) was prepared fresh on the day of the experiment. To keep the cytochrome c in its reduced form, it was added to a

solution of ascorbic acid (1%). Immediately before the assay, the solution was diluted so that ascorbic acid was 0.025% and cytochrome c was 202 μM, pH 7.0.

The assay was carried out in phosphate buffer; a given volume of lubrol solubilized homogenate was added first and mixed well (7.8 μg protein/ assay for rat and 10.4 μg/ assay for mouse). Cytochrome c was added to the cuvettes and they were gently mixed by inversion. Immediately, the cuvettes were placed in a Beckman DU-65 spectrophotometer and the absorbance was read continuously for 1 minute.

Six different concentrations of cytochrome c were used for each assay (6.7, 13.4, 20.1, 26.8, 33.5, and 40.2 μM) to construct a Lineweaver-Burke plot and obtain the V_{max} for each sample. The Beckmann Kinetic Soft-Pac module (program 6: kindata) was used to process the data and to obtain reaction rates from the spectrophotometer.

At various times on the day of the experiment, the concentration of cytochrome c was measured spectrophotometrically. A correction was made for any oxidation of the substrate that had occurred. For calculations of concentration, an extinction coefficient of 0.0295 was used (Yonetani & Ray 1965).

Data was analysed using the program Inplot (and later Prism) and manipulated to obtain both the Michaelis-Menten and Lineweaver-Burke plots of the reaction. The intercept of the reciprocal Lineweaver-Burke plot yields $1/V_{max}$.

DNA:

The DNA content of tissue homogenates was measured using fluorescence spectroscopy. This method was adapted from (Downs & Wilfinger 1983). Homogenate volumes containing 5 or 10 mg of tissue were incubated with shaking at 37°C (Yamato constant temperature shaking bath Model BT-25) for 10 minutes in an ammonium hydroxide-Triton X-100 extraction solution (0.2% Triton X-100 in 1N NH_4OH). This lyses both cells and nuclei, allowing for the interaction of DNA and a fluorophore later in the assay. After lysis, homogenates were diluted with an equal volume of assay buffer (100 mM NaCl, 10 mM EDTA, 10 mM Tris Base, pH 7.0). The samples were then passed through a syringe with a 0.33 μ filter (Millipore) prior to the assay to remove any particulate matter.

DNA fluorescence was measured using a TKO 100 dedicated mini fluorometer (Hoefer Scientific Instruments). This fluorometer is designed specifically to detect relative fluorescence at 460 nm using a mercury lamp paired with a filtered detector. The lamp's emission spectrum peaks at 365 nm with a band width of 100 nm and the photo detector is filtered to read light emitted at 460 nm with a 10 nm peak width. Bis benzimidizole (Hoechst 33258) is a fluorophore that was added and will bind to the DNA in the samples. Fluorescence is directly related to the DNA concentration of the samples due to this interaction. A working dye solution of 0.01% Hoescht 33258 in TNE (10 mM Tris, 1 mM EDTA, 0.1 M NaCl, pH 7.4) was prepared fresh each day. The fluorometer was standardized using calf thymus DNA and the DNA concentrations of the diluted homogenates were read

directly. The total number of cells in the tissue was calculated from the DNA content using a value of 7 picograms of DNA per nucleus (Sober 1968).

Measurement of uncoupling protein content

All of the purified uncoupling protein used in my experiments was prepared in our lab by myself with the assistance of Dr. Anna-Lisa Kates. Dr. Gloria Zaror-Behrens prepared the rabbit anti-hamster UCP antiserum used in my experiments.

Preparation of purified UCP:

The method can be used for many species, including mice, rats, guinea pigs, and hamsters. Variables such as the age of the animals, and the length of time that the animals are acclimated to the cold are not critical.

Mitochondria were first prepared by the method of Slinde *et al.* (1975), in which mitochondria are isolated by differential centrifugation in isolation medium. Purification of UCP continued according to the method of (Lin & Klingenberg 1982) except that the sucrose density gradient centrifugation was omitted. Affinity chromatography with a hydroxyapatite column was used for the final purification step.

For the purifications performed by me, 24 control FVB/N mice, or 12 Sprague Dawley rats were kept at 4°C for 3-4 weeks. After the period of cold acclimation, the animals were killed by decapitation. IBAT was removed immediately and placed in ice-cold isolation medium. IBAT from each animal was cleaned and weighed individually. BAT was homogenized in approximately five times the tissue weight of isolation medium using a KONTES #21 glass/Teflon homogenizer (4,000 rpm on ice). The homogenates were pooled

at this point, the total volume was recorded, and a 1 ml aliquot was saved for later analysis. The pooled homogenate was divided between ten 50 ml centrifuge tubes.

Preparation of mitochondria:

The method followed for the preparation of mitochondria was that of Slinde *et al.* (1975), in which mitochondria were isolated by differential centrifugation in isolation medium. For all centrifugations, a Sorvall refrigerated centrifuge (RC-5B or RC2-B) was used with an HB-4 Rotor.

All of the tubes were centrifuged at 3, 000 rpm for 10 minutes. The supernatant was filtered through gauze and centrifuged at 10,000 rpm for 14 minutes. Isolation medium was added to resuspend the pellet, which was then centrifuged again at 3,000 rpm for 10 minutes. The supernatant from this centrifugation was first filtered through gauze and then centrifuged at 10,000 rpm for 14 minutes.

When both of the high speed centrifugations were complete, the supernatant was discarded and the pellets of the two centrifugations were resuspended and combined into one 50 ml tube. This was centrifuged at 10,000 rpm for 14 minutes. The supernatant was discarded and the pellet was resuspended in 42 ml isolation medium. At this step all of the tubes were combined into two final tubes during resuspending of the pellets. An aliquot of 500 μl was taken from each tube for later analysis.

The two tubes were centrifuged at 10,000 rpm for 14 minutes. At this step, the supernatant was discarded. Parafilm with small holes was used to cover the tube. Liquid nitrogen was used to flash freeze the mitochondria, and the tubes were stored at -80°C.

Purification of UCP continued according to the method of Lin & Klingenberg (1982). Mitochondrial protein was determined before proceeding. The following day, the frozen pellet was transferred into a glass/Teflon homogenizer. After thawing on ice for 5 minutes maximum, the pellet was chipped into four pieces. These pieces were quickly moved up to the lip of the tube and transferred into the homogenizer. For every 100 mg of mitochondrial protein, 3.6 ml of standard medium (20 mM 3-[N-Morpholino] propanesulfonic acid, 50 mM Na_2SO_4, 0.16 mM Na_2EDTA, pH 6.7) + 3.2% lubrol was added. The sample was homogenized and transferred to an ultracentrifuge tube. After mixing, the tubes were left on ice for 30 minutes to allow for the lubrol to remove both soluble and peripheral membrane proteins. Standard medium was added to the samples to fill the tubes, which were then balanced by weighing. The samples were centrifuged at 100,000 *g* (40,000 rpm for 30 minutes in a 60 Ti Rotor) in a Beckmann L8-55M ultracentrifuge. Following the centrifugation, the supernatant was poured off and cotton tipped applicators were used to dry and remove excess lubrol from the sides of the tube. Resuspension of the resulting membrane pellet was effected with Sucrose-Tris-EDTA (0.3 mM sucrose, 10 mM Tris Base, 2 mM EDTA, pH 7.2) using the homogenizer. An aliquot of 250 μl was saved for later analysis. The samples were centrifuged at 100,000 *g* (40,000 rpm for 30 minutes in 60 Ti Rotor). Parafilm was used to cover the pellets, which were frozen in liquid nitrogen, and kept at -80°C overnight.

On the following day, the pellets were resuspended in standard medium + 5% Triton X-100. For 500 mg of mitochondrial protein, 16 ml of solution was needed. A 30 minute

incubation on ice was followed by centrifugation at 100,000 *g* (40,000 rpm for 30 minutes in 60 Ti Rotor). The supernatant was kept and an aliquot of 250 μl was kept for later analysis. This final supernatant contained UCP-Triton micelles.

A hydroxyapatite column was prepared by suspending 15 g of hydroxyapatite in 100 ml of standard medium for every 500 mg mitochondrial protein. Fines were removed by washing the suspension a few times. The suspension was poured into a LKB 2137 chromatography column. Once settled, the column length was measured and the void volume was calculated ($v=l\pi r^2$) where l is the length, v is the void volume, and r is the radius of the column. A flow rate of approximately 1 ml/min was used.

The chromatography on hydroxyapatite is the final purification step. At this point in the procedure, only inner mitochondrial membrane proteins are present in Triton micelles. UCP will pass through the column at room temperature, while most other proteins are adsorbed onto the hydroxyapatite. The major contaminant is the ADP/ATP carrier and this protein is not stable at room temperature. At room temperature, the carrier protein is degraded and is retained by the column.

After reaching room temperature, the sample was applied to the column. The void volume was collected, after which 1 ml fractions were collected and kept. Protein concentration of the fractions was measured using a modified Lowry assay containing 1% SDS, while the Triton X-100 levels were measured spectrophotometrically at 276 nm. These values were plotted on a graph (See Figure 3.1) and the fractions containing protein were pooled. The UCP was aliquoted out in 500 or 1000 μl portions and stored at -80°C.

Elution profile of purified rat UCP from a hydroxyapatite column

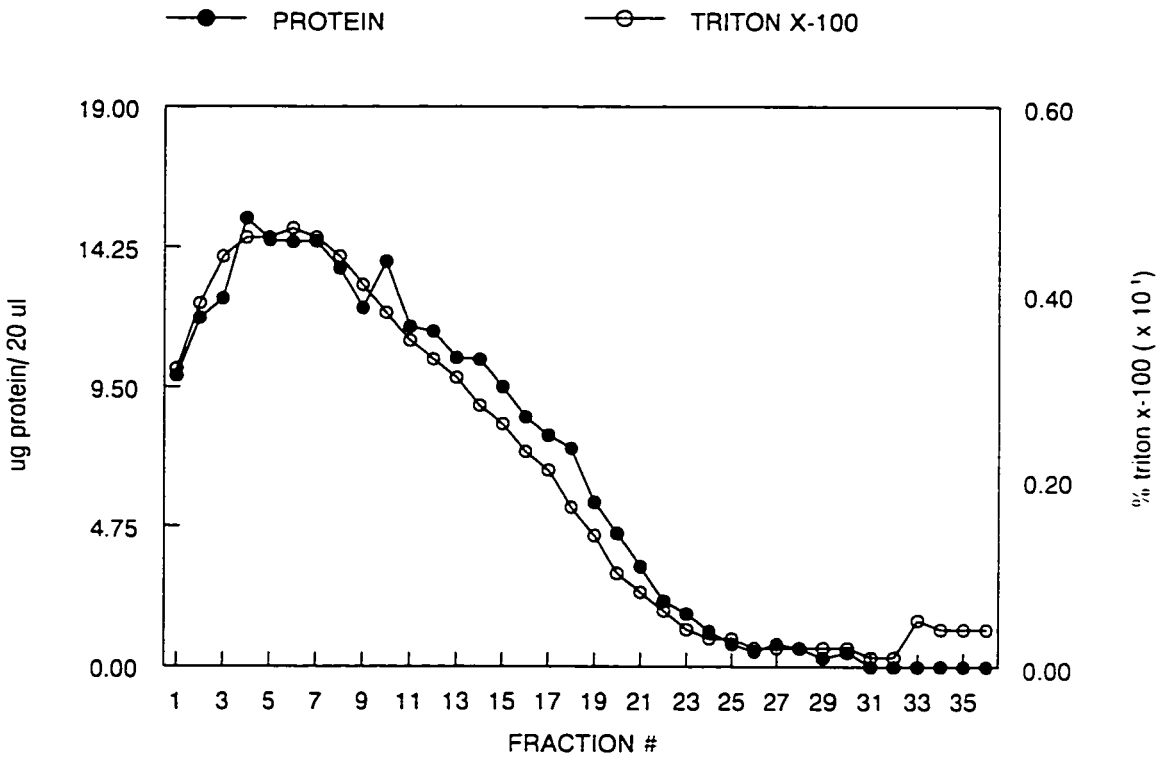

Figure 3.1: Protein and Triton X-100 content of each fraction eluted from a hydroxyapatite column. Protein measured is almost entirely rat UCP.

Preparation of UCP antibody:

The immunization schedule used for the development of antibody in rabbits was that of Fernandez *et al.* (1987). Three month old rabbits were allowed to acclimatize to the facility for one week. Pre-immune serum was prepared with blood collected from the ear vein of the rabbits. The next day, the rabbits were immunized with 100 μg of purified hamster UCP (isolated as above using cold-acclimated hamsters) mixed with Freund's complete adjuvant injected into each of five sites: intramuscularly into the hind legs and subcutaneously on the back. These injections were repeated the following week, using 100 μg UCP in Freund's incomplete adjuvant. After one week, a booster injection was given by injecting 100 μg UCP in a total volume of 500 μl of saline intravenously into the ear vein.

When the injections were complete, the rabbits were bled by cardiac puncture (the following week). After the blood was collected into polycarbonate tubes, it was left to clot at 4°C overnight. The tubes were then centrifuged at 2,500 x *g* for 30 minutes (Sorvall RC-5B or RC2-B). The serum was either frozen immediately at -80°C for later aliquoting, or diluted 1:1 (v/w) with glycerol and stored at -80°C.

Dr. Anna-Lisa Kates and Christine Villemeure conducted the UCP purification and the antibody preparation for the hamster UCP and the rabbit anti-hamster UCP antibodies that I used in my experiments.

UCP homologues:

Antibodies specific for UCP1 can react with at least one other UCP isoform. Larrouy et al. (1997) detected significant UCP1 reactivity in the rat liver using UCP1 antibodies. This staining is due to UCP2 reactivity, as UCP1 is not expressed in any cell type of rat liver and UCP2 mRNA is highly expressed in Küppfer cells (Larrouy *et al.* 1997). The cross immunoreactivity of UCP antibody to both UCP homologues was confirmed by the detection of UCP2 with anti-UCP1 antibody in yeast expressing UCP2 (Larrouy *et al.* 1997).

Due to the similarity of the isoforms of UCP, the possibility exists that the UCP standards used in my experiments could all contain UCP1, UCP2, and UCP3. Additionally, the antibody used to detect UCP in my experiments was raised with unpurified (with respect to UCP1, UCP2, and UCP3) protein. The antiserum could contain antibodies against UCP1, UCP2, and UCP3; or alternatively a single antibody type to UCP1 that reacts with all three homologues. Regardless, we have shown that the antibody used in my experiments is not specific for UCP1 as we had thought. The antibody used in all of the research for this thesis reacts with UCP2 (Figure 3.2). Immunohistochemistry was performed by Linda Jui, for detailed method please refer to the immunohistochemistry section in this chapter.

Immunohistochemistry of rat liver: Detection of UCP2

Figure 3.2: Immunohistochemical detection of UCP2 in 10 μm sections of rat liver. Magnification x 200. Red stained areas are Küppfer cells of rat liver, which do not express UCP1 (Larrouy *et al.* 1997), showing that these cells are positive for UCP2. Detection performed with the rabbit anti-hamster UCP antibody used for assays of UCP in my experiments.

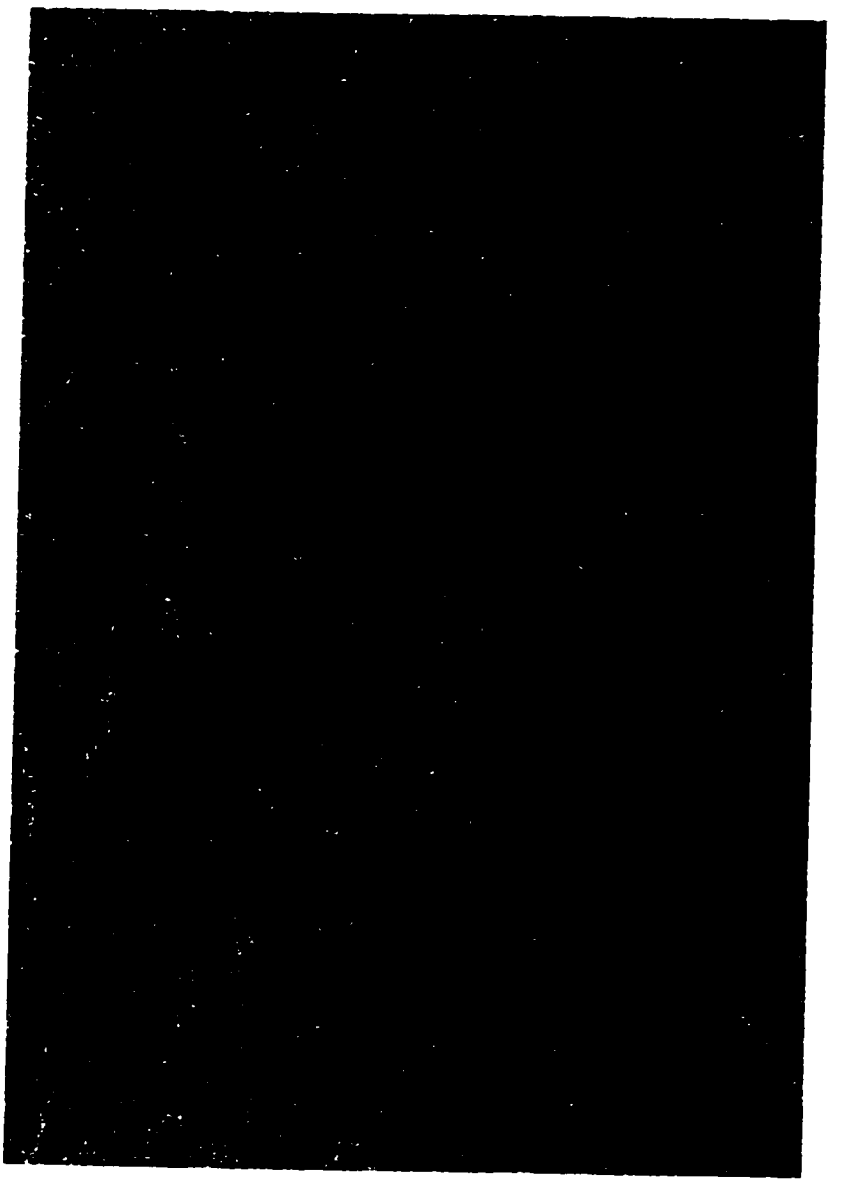

UCP detection by Western blotting:

UCP was detected in BAT homogenates using polyacrylamide gel electrophoresis (PAGE) and Western blotting. An equal volume of sample loading buffer {2% SDS, 0.1 M Tris-Cl, 4 mM PMSF in isopropanol, 2 mM EDTA with bromophenol, 25% glycerol (w/v), and 10% β-mercaptoethanol (v/v)} was added to homogenates containing either 10, 15, or 20 μg of protein. The samples were combined with sample loading buffer on the day of the assay, and they were boiled for 3 minutes before being loaded on the gel. Rainbow™ coloured protein molecular weight markers (Amersham) were prepared by combining them 1:3 with sample loading buffer and boiling them for 1 minute before loading. Purified mouse or rat uncoupling protein (0.10 μg) was loaded as a standard on each gel.

For casting and running the gels, the PROTEAN® II Mini Electrophoresis Cell (Bio-Rad) was used. The separation gel used was 10% acrylamide, 0.13% bisacrylamide, 9% Tris, 0.1% SDS, and 0.1% ammonium persulfate. This gel was poured the day before the experiment, overlaid with distilled water, covered with SaranWrap™, and left to polymerize in the cold room (4°C) overnight.

Following polymerization, the water was removed by inversion of the assembly apparatus, and the stacking gel was poured. The composition of the stacking gel was 3.4% acrylamide, 0.05% bisacrylamide, 0.8% tris base, 0.1% SDS, and 0.1% ammonium persulfate. Combs were inserted and the gel was left to polymerize for 0.5 hours. When the stacking gel had polymerized, the combs were removed, and the gels were placed in the electrophoresis cell. Running buffer (0.3% Tris base, 1.42% glycine, 0.1% SDS, and 0.01%

PMSF) was added to the chamber. The samples were loaded using a Hamilton syringe, and the gels were run for 1 hour at 180 V.

At the end of the run, the gels were removed from between the glass plates and placed in transfer buffer to equilibrate (30 minutes at room temperature, with shaking). The transfer buffer was 0.72% glycine, 0.15% tris-base, 20% methanol (v/v), and 0.01% PMSF. For transferring the proteins, a Mini Trans-Blot® Cell (Bio-Rad) was used. The gels were set up in the transfer cassettes as follows: filter pad, 2 pieces of filter paper, equilibrated gel, nitrocellulose membrane (NCM), 2 pieces of filter paper, filter pad. Each component for the transfer was soaked in transfer buffer for one hour before assembling. The cassette was placed into the trans-blot cell and the transfer proceeded at 4°C and 120 V for exactly one hour.

After the transfer was complete, the NCM was removed, wrapped in SaranWrap™ and stored at -20°C until further processing.

All of the following blotting steps were done at room temperature and with shaking on a Belly Dancer® Shaker (Stovall Life Science Inc.) unless otherwise stated. The NCM was removed from the SaranWrap™ and placed in phosphate buffered saline (PBS, 5.3 mM K_2HPO_4, 1.5 mM KH_2PO_4, 140 mM NaCl, 3 mM KCl, pH 7.4) with 0.05% Tween-20 and blocked for 30 minutes. The blot was incubated with the primary antibody (rabbit anti-hamster UCP) diluted 1:32,000 in PBS + 0.05% Tween-20 for one hour.

PBS + 0.2% SDS, 0.375% Triton X-100, and 0.375% BSA was used for washing the blot after the primary antibody incubation. Three 15 minute washes were done, each with 250 ml of buffer and vigorous shaking.

The blot was then incubated with the secondary antibody (goat anti-rabbit IgG horseradish peroxidase conjugate, Cedarlane Labs Ltd.), diluted 1:10,000 in PBS + 0.05% Tween-20 for one hour.

PBS containing decreasing amounts of Tween-20 was used to wash the blots as follows: four 5 minute incubations in PBS + 0.3% Tween-20, four 5 minute incubations in PBS + 0.1% Tween-20, and finally two 5 minute incubations in PBS alone.

Detection of the secondary antibody conjugate was done using a commercially available kit (Amersham RPN 2109). Enhanced chemiluminescence (ECL™) Western blotting is a light emitting non-radioactive method for detection of immobilized specific antigens, conjugated with horseradish peroxidase-labeled antibodies.

The homogenate proteins are immobilized on the NCM after which the primary rabbit anti-hamster UCP antibody is bound specifically to UCP. The secondary antibody was goat anti-rabbit IgG horseradish peroxidase conjugate which is bound to the primary antibody and therefore indirectly to the UCP.

Enhanced chemiluminescence is achieved by performing the oxidation of the added luminol substrate by the horseradish peroxidase in the presence of chemical enhancers such as phenols. Light is produced by the reaction and is detected by exposure of the NCM to Kodak X-OMAT™ film (Figure 3.3). Exposure was carried out in a Kodak X-Omatic cassette; the films were then developed either manually using Kodak GBX fixer and replenisher, and GBX developer and replenisher or with an automated system.

UCP assay by radioimmunoassay:

Uncoupling protein was also measured in BAT homogenates using a solid phase radioimmunoassay (RIA) based on the method developed by Lean *et al.* (1983). The method was adapted in our lab by Dr. Gloria Zaror-Behrens.

Before the assay, the samples were prepared by solubilization. The values listed are for rats, with those for mice in brackets. Samples of homogenate were initially diluted to a protein concentration of 2.0 mg/ml (0.5 mg/ml) with PBS. Triton X-100 (5%) was used to solubilize the diluted samples: diluted sample 12.5 μl (180 μl), PBS 32.5 μl (0), 5% Triton X-100 5.0 μl (20 μl). The samples were mixed and left to incubate at room temperature for 30 minutes. After solubilizing, the samples were diluted five times with PBS, mixed and centrifuged in an Eppendorf 3200 centrifuge for 2 minutes. To eliminate fat from the sample, the infranatant was carefully poured off into clean microfuge tubes. At this point, the samples were stored at - 20°C for no more than one month.

Enhanced chemiluminescence

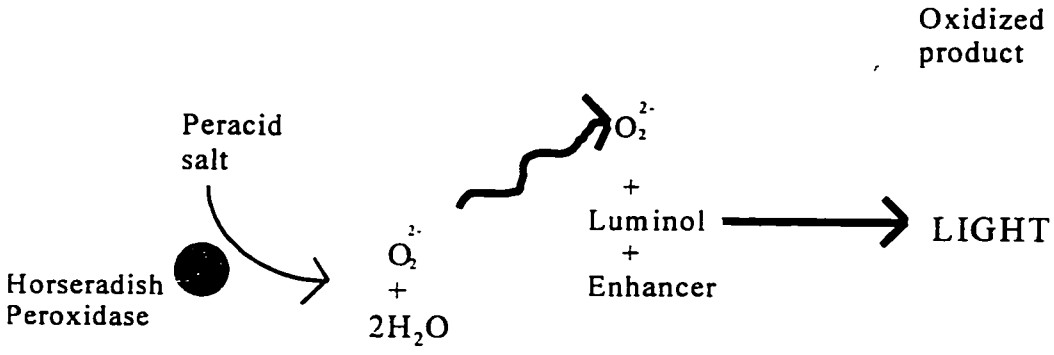

Figure 3.3: The principles of enhanced chemiluminescent detection. ECL is achieved by performing the oxidation of the added luminol substrate by the horseradish peroxidase in the presence of chemical enhancers such as phenols. Light is produced by the reaction and is detected by a film.

On the day of the assay, the rat samples were diluted again; 200 μl of PBS and 750 μl of PBS + 0.02 % Triton X-100 were added to 50 μl of sample. Each well contained 0.2 μg protein, with a Triton X-100 concentration of 0.02% (rat), or 3.6 μg protein with 0.1% Triton X-100 for mice.

When measuring the rat samples, the standards were prepared on the day of the experiment. For mice, the standards were prepared ahead of time in large quantities, aliquoted out, and frozen at -20°C to ensure consistency between assays. Rat or mouse UCP was purified in the lab as outlined above. Dilution of the purified UCP with PBS gave a working stock with a concentration of 4.7 μg/ml for rats, or 5.3 μg/ml for mice. The standards for the rat assays were diluted with PBS + 0.02% Triton X-100 and contained 63.67, 31.83, 15.92, 7.96, 3.98, and 1.99 ng UCP/well. The standards for the mouse assays were diluted with PBS + 0.01% Triton X-100 and contained 212.5, 141.70, 70.83, 35.42, 17.71, 8.85, and 4.43 ng UCP/well.

Falcon® 3912 MicroTest III™ flexible assay plates were used in the assays. These plates have 96 flat-bottom wells, with a well capacity of ~0.3 ml (Becton Dickinson). Before use, the plates were washed to remove residual chemicals from the manufacturing process. The plates were soaked in RBS pF detergent concentrate (PIERCE chemical company) (20 ml / 1 L H_2O) for at least 30 minutes. After soaking, the plates were rinsed three times in hot tap water, then three times in cold tap water, and finally three times in distilled water. Paper towels were used to absorb the water from the plates left to air dry upside down and were then stored until needed.

For coating the plates, the UCP concentration was adjusted to 10 μg/ml with PBS, allowing 50 μl/well. Purified rat UCP was prepared the day of the experiment for coating the plates when rat homogenates were being analyzed. Mouse UCP for coating was prepared in large amounts ahead of time, aliquoted out and stored at -20°C until used, to reduce variability between assays. The UCP for coating was prepared in siliconized glass or plastic tubes.

Total binding (B_0) and total nonspecific binding (NSB) were measured for the entire plate, and for samples and standards. Fifty μl of PBS + Triton X-100 were added to each NSB well (uncoated wells). The coated wells (B_0) had 50 μL of UCP in PBS.

The plates were covered with parafilm (rats) or with MicroTest III™ flexible assay plate lids (mice). Incubation for coating of the plates was 37°C for 2 hours (Isotemp® Incubator, Fisher Scientific). All liquid in the wells was dumped into a waste container, and then the plates were inverted onto a stack of Kleenex. Removal of any remaining liquid was achieved by forcibly slapping the plate on the stack of Kleenex. The plates were washed with PBS + 1% BSA and 0.1% sodium azide (PBS-BSA). A multipipetter was used for the first two washes (200μL). Removal of liquid from the wells was repeated between each wash step. After the addition of PBS-BSA for the third wash, the plate was loosely covered and put back into the oven at 37°C for 10 minutes. This step will block all uncoated portions of the well. Three more washes were performed with PBS-BSA delivered using a siphon. The plates were left inverted on the Kleenex after the last wash to drain for 5 minutes.

For the competition step, sample, standard, or PBS + Triton X-100 were added along with anti-UCP antibody. Competition occurs between the coated UCP and the UCP in solution to bind the antibody that is also in solution.

Lanes 1 and 2 in Figure 3.4 had 40 μL of PBS + Triton X-100 added to each well; these lanes are for total binding and total NSB. Lanes 3, 4, 5, 6, and 7 all had 40 μl of standard added to each well. Lanes 8, 9, 10, 11, and 12 all had 40 μl of sample added to each well. In all lanes but one and two, each row represents a different standard or sample, each with duplicate NSB, and triplicate B_0. The antibody was diluted in PBS. Ten μl of this diluted antibody were added to every well; the final antibody dilution in each well was 1:1600.

The plates were covered with a lid or parafilm and incubated overnight at 4°C. The next day, the plates were washed as outlined above.

^{125}I-Protein A (30 μCi/ml ICN Biomedical) was used to detect the antibody that remained bound to the plate. To obtain 60000-70000 cpm/well (50 μl/ well), the protein A was diluted with PBS. Protein A was added to each well, and the plates were left to incubate loosely covered with a zip-lock bag, or covered with a lid for 1.5 hours at room temperature. Total counts added per 50 μl were also measured after every 2 lanes.

UCP radioimmunoassay: Layout of assay plate

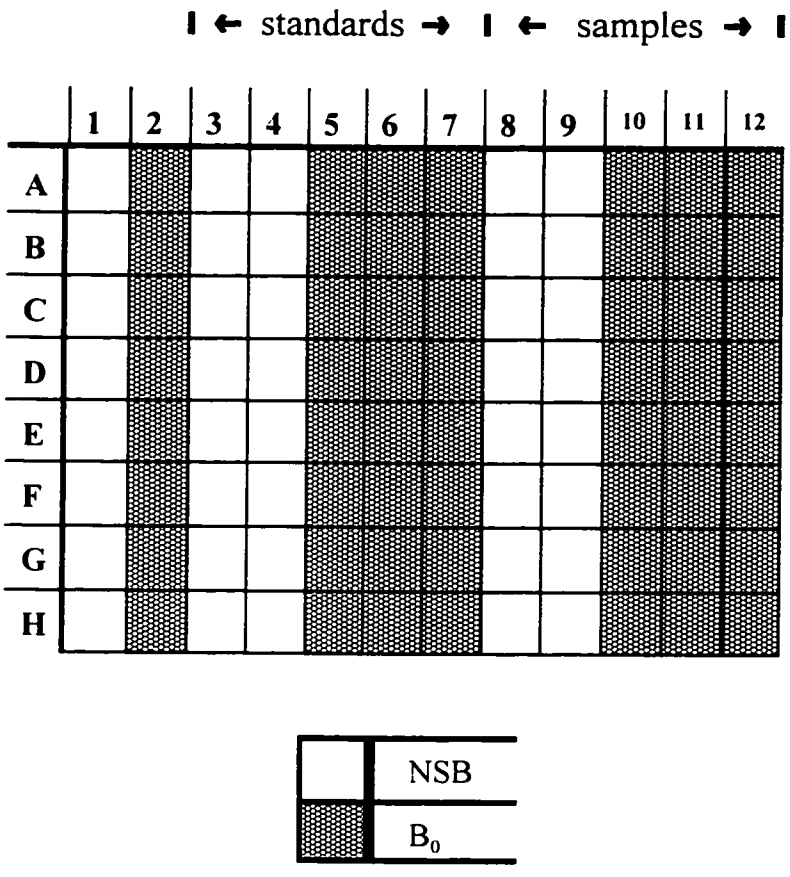

Figure 3.4: Layout of the assay plate for the UCP radioimmunoassay. Lanes 1&2: NSB and B_0 respectively. Lanes 3-7: NSB and B_0 of standards. Lanes 8-12: NSB and B_0 of samples.

Washing was repeated as above. The wells were cut out into plastic tubes (Sarstedt 5 ml polypropylene tubes) and counted in a Beckman 5500 gamma counter. The results were corrected for nonspecific binding and then the UCP per sample was calculated using the linear regression line of logit-ln UCP. A Lotus 1-2-3 spreadsheet was used for calculations initially (rats), and later Microsoft Excel and Prism were used. The results were expressed as μg UCP/mg protein in BAT homogenates.

White adipose tissue

WAT was removed from the animal and placed on ice. For the experiments with rats, it was weighed and frozen immediately. For mice, samples were taken for osmium fixation and histology after which the tissue was reweighed and then frozen.

Homogenates were made of the frozen tissue as described for BAT with one exception. The homogenates were centrifuged in a refrigerated J6B centrifuge at 1500 rpm for 5-10 minutes. The fat cake was carefully removed from the top using a spatula. Infranatants were vortexed, the volume was measured, and after mixing again, they were aliquoted out into Eppendorf microcentrifuge tubes and frozen at -80°C.

Protein and DNA assays were performed as for BAT.

Osmium fixation of adipocytes:

Samples of WAT depots were shredded and placed onto discs of 540 μm NITEX (B&SH Thompson), which were previously washed in chloroform-methanol (2:1) mixture, allowed to air dry, and tared. The tissue shreds of < 200 mg total wet weight were placed on

the discs and then washed many times with small quantities of warm isotonic saline (0.9% NaCl) to free them from oil droplets. Filter paper was used to blot the undersurface of the disc and the wet weight of the tissue was obtained.

After obtaining the weight, the filter disc and tissue were immediately put into a plastic scintillation vial containing 5 ml of a 2% osmium tetroxide solution in 0.05 M cacodylate, pH 7.4.

The vials were incubated at 37°C for 72 hours with shaking (Gyratory Water Bath Shaker, New Brunswick Scientific Co. Inc.) to fix the tissue, and then the vials were stored at room temperature until later isolation and counting of adipocytes (Hirsch & Gallian 1968).

For isolation of the fixed adipocytes, all of the glassware and instruments to be used were siliconized and then rinsed with diluted Kodak Photo-Flo 200 solution (1:5 with distilled water). These steps were carried out to prevent the fixed adipocytes from sticking to each other and to the materials used in the isolation of the adipocytes.

Approximately 1 ml of diluted Photo-Flo was added to a 500 ml Erlenmeyer sidearm flask, and a large stirring magnet was placed in the flask. The contents of the scintillation vial were washed into the flask through a 253 μm NITEX filter with distilled water while stirring. During the washing step, the tissue shreds were gently rubbed by hand on the filter. This step was done under suction.

A 10 μm NITEX filter was used to catch cells as the filtrate was washed into another 500 ml Erlenmeyer. Copious amounts of distilled water were used to wash the trapped cells.

The flask with the original filtrate was rinsed well, and if necessary, was left to stir with diluted Photo-Flo to remove the remaining cells from the flask.

The adipocytes were rinsed into siliconized and tared plastic 50 ml Corning tubes with saline. A few drops of Photo-Flo were added to prevent sticking of the adipocytes. As much liquid as possible was removed using a 10 ml syringe (without needle) after allowing the adipocytes to settle overnight. The cell suspension was weighed, and the adipocytes were counted.

A 0.2 mm deep Fuchs Rosenthal counting chamber was used to count the adipocytes under a light microscope (Carl Zeiss, Germany). Adipocyte size was calculated from the number of adipocytes counted and the weight of the tissue using an assumed lipid content of 90% of the wet weight (Newby *et al.* 1990).

Histology

For studies in which BAT and WAT samples were taken for histological analysis, the tissue was initially weighed and then cut with a razor blade. Representative samples were taken from the depot, and the remaining tissue was reweighed and frozen at -80°C until homogenized.

Paraffin Embedding of Sections:

Pieces of freshly cut tissue were placed in 10 times the volume of 10% buffered formalin. The tissue pieces were left to fix in formalin for at least three days. All of the following preparation of slides and staining was done by Linda Jui.

The tissue pieces were placed in plastic cassettes (HISTOSETTE® I, Simport Plastics). The tissue was then processed in an automatic machine in the following manner. First the tissue was dehydrated using increasing amounts of ethanol (60%, 70%, 80%, 90%, 100%). The tissue was then cleared with xylene twice, and finally with paraffin. The tissue was embedded in paraffin by hand.

These blocks were then sectioned on a microtome (Tissue-Tek® "820" microtome, Spencer). The blocks were cut into different thicknesses; 4 μm for hematoxylin and eosin (H & E) staining, and 10 μm for immunohistochemical detection. The sections were placed onto Superfrost Plus slides.

Staining of thick sections:

The tissue was rehydrated, stained, dehydrated with increasing amounts of ethanol, cleared with xylene, and then mounted with Permount.

For H&E staining, the slides were first incubated in filtered Delafield's Haematoxylin for 6 minutes, and then rinsed in water differentiated in alcohol (30% alcohol + 1% HCl). The slides were then washed with lithium carbonate (1g/100 ml distilled water) until the

section was blue. After a wash in running water for 10 minutes, the slides were placed in eosin for 2 minutes and then processed as described above.

Immunohistochemistry:

Immunohistochemistry for UCP was performed in WAT and BAT. The sections were first deparaffinized with two 5-10 minute washes in xylene, and then rehydrated with decreasing amounts of ethanol. Each wash was 3-5 minutes, starting with two washes of 100% ethanol, one of 95% ethanol, 70% ethanol, water, and finally Tris- buffered saline (TBS, 0.1 M Tris, 0.14 M NaCl, pH 7.7).

Rabbit anti-hamster UCP antibody was diluted 1:100 in TCT (0.3% Triton X-100, 0.6% carrageenan, in Tris buffer). The sections were left to incubate in this primary antibody solution overnight at 4°C in a humidified chamber. Following the incubation, the sections were washed in TBS twice for 7 minutes each.

The secondary antibody (donkey anti-rabbit Ig, biotinylated species-specific whole antibody, Amersham) was diluted 1:50 in TCT. The sections were left to incubate for 60 minutes at room temperature in a humidified chamber. Following the incubation, the sections were washed in TBS twice for 7 minutes each.

After washing the sections, the slides were neutralized with 3% freshly made hydrogen peroxide (H_2O_2) for 10 minutes. Again the slides were washed twice in TBS.

Streptavidin-horseradish peroxidase conjugate (Amersham) was diluted with TCT (1:50) and added to the sections that were then incubated for 60 minutes at room temperature in a humidified chamber. Again the sections were washed in TBS twice.

The sections were incubated in the dark with freshly made DAB (3,3'-diaminobenzidine tetrahydrochloride) for 15 minutes at room temperature. Working stock was 1% DAB (10 mg/ml stock in water), 0.07% $NiCl_2$, and 0.006% H_2O_2 in TBS. The washing step was repeated with TBS, for 7 minutes twice.

Increasing amounts of ethanol (70%, 80%, 95%, 100%, 100%) were used to dehydrate the sections, which were then cleared with two 5 minute xylene washes. The slides were mounted with Permount.

Two sections were immunostained for each tissue; the second set was counterstained with hematoxylin before being dehydrated.

Immunohistochemistry of liver sections:

Method used for the detection of UCP2 in Figure 3.2 is that of Larrouy *et al.* (1997). The rat livers were fixed in 10% buffered formalin, dehydrated in ethanol and paraffin embedded. 10 μm sections were deparaffinized, rehydrated and incubated with rabbit anti-hamster UCP antibody (dilution 1:100 in TCT as above). The secondary antibody used was donkey anti-rabbit Ig coupled to alkaline phosphatase (1:2000 dilution in TCT). Alkaline phosphatase activity was revealed using Sigma Fast Red TR/Naphtol AS-MX tablets as substrate and sections were counterstained with hematoxylin.

Semi-thin sections:

Small pieces of freshly cut tissue (size 1-2 mm^3) were placed in cold 0.1 M cacodylate buffer (pH 7.4) + 2% paraformaldehyde and 2.5% glutaraldehyde. These samples were shaken well and left in the cold until processed.

The tissues were washed with cacodylate buffer with 3-4 changes. The tissues were then post-fixed with 1-2% osmium tetroxide in cacodylate buffer for 1-2 hours at room temperature on a rotator. Two changes of distilled water were used to wash the tissues. Following these washes, the tissues were dehydrated with graded ethanol (60%, 80%, 90%, and 100% ethanol) for 10-15 minutes each. The tissue was then incubated twice in propylene oxide for 10-15 minutes at room temperature.

Epon mixture was used to embed the tissue samples. Epon mixture is 49% Jembed resin, 29.6% dodecenyl succinic anhydride, 19.7% nadic methyl anhydride, and 1.5% DMP-30 (tri(dimethylaminomethyl phenol)). Before embedding, the samples were incubated in a 1:1 mixture of Epon mixture and propylene oxide for one hour on a rotator. The incubation was repeated with undiluted Epon mixture.

To embed the tissue, pieces were placed in the tips of the wells of the embedding molds. Each well was filled with freshly made Epon mixture. The molds were placed in the oven for 72 hours to dry and harden. The temperature of the oven was increased as follows: 24 hours at 40°C, 24 hours at 60°C, and 24 hours at 70°C.

Sections were cut 0.5 to 1 μm thick using a glass knife. The sections were then lifted off the surface of the water using an eyelash stick, and placed on a drop of water on a glass microscope slide. Several sections were placed in each drop of water. The slide was put on a 65°C hot plate, and once the water had evaporated, the sections were covered with stain.

For staining a mixture of 0.5% methylene blue, 0.5% borax (sodium tetraborate) and 0.5% azure II was used. The sections were stained for 4-5 minutes at room temperature and then rinsed well with water. The sections were dried completely on the hot plate, and then allowed to cool to room temperature. A cover slip was mounted on each slide using Permount.

Photography:

Sections were viewed using a light microscope under 200x magnification and were photographed using an attached camera. Film used was Ilford XP2 35 mm 400 ASA (black and white) or Fuji 100 ASA (colour). Film was taken to a photographic shop for processing.

Carcass analysis

Thawed carcasses were cut into pieces with a guillotine (rats) or scissors (mouse). The tails and paws were removed, and then the carcass pieces were homogenized (refer to experiments for homogenizer used) in distilled water. Samples of the homogenate were dried in duplicate in extraction thimbles in the oven overnight at 55°C. The thimbles were placed in a Soxhlet extraction assembly, and the lipid was extracted with petroleum ether (35-60°C fraction).

Lipid content of the sample aliquot was determined using the weight of lipid collected and the weight of the sample remaining after extraction. The lipid content of the WAT depots removed (90% of their wet weight; Newby *et al.* 1990) was added to the carcass fat extracted to obtain the total carcass fat.

Data presentation and statistical analysis

All data are expressed as means ± SEM (standard error of the mean) unless otherwise stated. Statistical analysis was performed using the mainframe program SAS, or using Instat software.

Chapter 4: Resistance to aging-associated obesity in capsaicin-desensitized rats one year after treatment

Introduction

Sensory nervous system:

The sensory nervous system enables an organism to react to changes in its external and internal environment to maintain homeostasis (Holzer 1988). As its name suggests, this system has traditionally been thought of as a receptive and afferent system. Afferent neurons not only play a sensory role, but they take part in local effector systems such as inflammatory response.

The cell bodies of primary afferent neurons are found in the spinal cord (dorsal root ganglia) or cranial sensory ganglia (Holzer 1988). Fibres from the cell bodies run both centrally and peripherally (Holzer 1988). The endings of the peripheral fibres may be receptors themselves or may connect to special sensory structures (Holzer 1988).

Sensory nerve endings may have local effector roles such as regulating blood flow, vascular permeability, immunological processes, activity of autonomic ganglia and visceral smooth muscle. Local functions of sensory nerve endings have been determined pharmacologically, using capsaicin (Holzer 1988).

Sources and chemical properties of capsaicin (Cap):

Cap is the pungent ingredient in a variety of red peppers of the genus capsicum. Cap is a chemical derivative of vanillyl amide, and is widely used as a probe for sensory neuron mechanisms. At doses very much higher than those used to spice food, this compound is a very selective neurotoxin for afferent neurons having small cell bodies (C-type afferent neurons) (Holzer 1988).

Relationship of Capsaicin and sensory nerves:

Cap sensitive sensory nerves cannot be identified by any other characteristic than the fact that they are Cap-sensitive (Maggi & Meli 1988). These nerves send chemical and physical signals to the central nervous system. They arise from the viscera and the skin and activate a variety of visceromotor and neuroendocrine reflexes. These reflexes occur at different levels: peripheral organs, prevertebral ganglia, spinal and supraspinal level (Maggi & Meli 1988).

The action of Cap on sensory nerves has been documented (Maggi & Meli 1988). First the sensory terminal is excited; this is accompanied by the activation of both the sensory and efferent functions of the nerve. Following the excitatory phase produced by a maximally effective dose of Cap, the sensory terminal becomes unexcitable to both natural and artificial stimuli (Maggi & Meli 1988). Initially the nerves' terminals still contain neurotransmitter, though they can neither transmit sensory information, nor release neurotransmitter. Subsequently, the neurotransmitter is depleted from both the central and peripheral terminals.

The effect of administered Cap on rodents varies with the dose and schedule of delivery. At low doses (μg/kg range), Cap exerts a powerful excitatory effect on peripheral sensory nerve endings. Excitation is followed by desensitization and nerve conduction is blocked.

The systemic administration of high doses (mg/kg range) has a neurotoxic effect on a population of sensory neurons; the extent of damage depends on the dosage, the route of administration, animal species, and age of the animals. Systemic treatment of newborn rats produces the most extensive and consistent lesions. A single dose of 50 mg/kg Cap results in a permanent loss by degeneration of 50-90% of all unmyelinated fibres with no change in the myelinated afferent fibres (Holzer 1988).

Cap-desensitization of rodents results from the systemic administration of large doses of subcutaneous (*s.c.*) Cap to newborn rats (Maggi & Meli 1988). The consequence of this treatment is the lifelong degeneration and death of Cap sensitive sensory nerves. Cap-desensitization in newborn animals causes an irreversible destruction of ~50% of the cells in the sensory ganglia (Maggi & Meli 1988).

Cap-desensitization was executed on adult rats (six weeks of age) in our lab (Cui & Himms-Hagen 1992a; Cui & Himms-Hagen 1992b; Cui *et al.* 1990; Himms-Hagen & Cui 1991; Himms-Hagen *et al.* 1990) as described by others (Castonguay & Bellinger 1987). The rats were anesthetized with halothane and injected with Cap (12.5 mg/kg *s.c.*). The injections

were repeated in conscious rats twice the next day (25 mg/kg each time) and again the day after (62.5 mg/kg).

Background on the Capsaicin-Desensitized (Cap-Des) rat:

Cap-Des rats exhibit a potentiation of endotoxin-induced fever (Szekely & Szelenyi 1979; Szekely & Szolcsanyi 1979). This potentiation includes an enhancement of the increase in BAT temperature that accompanies the development of fever. Normally, the hypothalamus will sense warmth and suppress thermogenesis in BAT; it was postulated that the hypothalamic sensing of warmth was impaired.

The basis for studying the Cap-Des rat was the impairment of central and peripheral warmth reception. This defect was predicted to diminish the hypothalamic suppression of BAT thermogenesis in response to the increase in body temperature induced by ingestion of food (the combined effect of diet induced thermogenesis and the thermic effect of food). It was initially expected that diet-induced thermogenesis in BAT would be amplified in the Cap-Des rat. However, BAT was atrophied in Cap-Des rats (Cui *et al.* 1990), suggesting that sensory neuropeptides may have a trophic influence on BAT, among other possibilities.

Model of the Cap-Des rat:

IBAT is atrophied both short (1 day) (Cui & Himms-Hagen 1992a), and medium term (8 months) (Cui & Himms-Hagen 1992b) in Cap-Des rats. Atrophy includes a reduced total protein content, a loss of cells, loss of mitochondria, as little as 10% of the normal content of UCP, and the tissue is depleted of CGRP (Cui *et al.* 1990). A reduction of almost 40% of

the overall thermogenic response to infused NA was seen in anesthetized Cap-Des rats, attributable to the atrophied BAT. Feeding a palatable diet had a delayed thermogenic effect and no trophic effect on BAT. Food intake and selection were normal in the Cap-Des rats; diet-induced weight gain was the same as control.

Exposure of the Cap-Des rat to the cold for one or seven days exerted a normal thermogenic effect on BAT but a delayed trophic effect. The cold-induced increase in $T_4$5'-D in BAT occurred normally. At one day of cold exposure, the Cap-Des rats were hypothermic; by seven days of cold exposure, they were normothermic.

The body fat content of the Cap-Des rat is lower than in control rats (Cui & Himms-Hagen 1992a; Cui & Himms-Hagen 1992b) and they become less obese than control rats even on high-fat diet for the first 3 months after treatment (Himms-Hagen & Cui 1991). This resistance to obesity was surprising due to the smaller amount of thermogenically active BAT in Cap-Des rats (Cui & Himms-Hagen 1992a; Cui & Himms-Hagen 1992b; Cui *et al.* 1990; Himms-Hagen *et al.* 1990), a state usually associated with obesity in rodents (Himms-Hagen 1989a; Himms-Hagen 1991). This connection has been supported by the massive obesity seen in the UCP-DTA transgenic mouse (Lowell *et al.* 1993). The reduction in obesity of the Cap-Des was not characterized (Cui & Himms-Hagen 1992b).

The reason for the atrophied state of BAT in the Cap-Des rat has not been explained. Central brain lesions are present as a consequence of the treatment, a role for these lesions

in both the atrophy of BAT and in the altered energy balance seen in the Cap-Des rat is possible.

The atrophied BAT of Cap-Des rats is depleted of the sensory neuropeptide CGRP (Himms-Hagen *et al.* 1990), which is normally present in afferent autonomic (sensory) nerves in BAT (Lever *et al.* 1988; Nnodim & Lever 1988; Norman *et al.* 1988).

Afferent autonomic nerves are also present in WAT (Fishman & Dark 1987), and sensory information from WAT may play an important role in the regulation of regional and total body fat mass. These nerves may be destroyed by Cap-Des, causing the lower fat level seen in these rats.

Aging-associated obesity:

Newby *et al.* (1990) described a model of spontaneous obesity in chow-fed male Wistar rats. This aging-associated obesity probably resulted from a combination of aging, unrestricted access to chow, and limited spontaneous locomotor activity due to cage restriction. Similar to human obesity, this is a model of moderate obesity, characterized by a slow, progressive increase in fat cell size and number (Newby *et al.* 1990).

The weight of the epididymal WAT (EWAT) depot was linearly related to body weight, but not body lipid. An exponential relationship was shown between the weight of the retroperitoneal WAT (RWAT) and body weight, while a linear relationship was shown with body lipid (Newby *et al.* 1990). Significant regional differences exist in adipose depot composition and cellularity; the RWAT becomes hyperplastic, while the EWAT does not.

Objectives

The objective of this study was to extend the period of study of the Cap-Des rat to 1 year after treatment and to characterize the altered size of the WAT depots according to the number and size of their adipocytes and their total cell number. At this time the rats would be 13.5 months old and expected to display an aging-associated, hyperplastic obesity, characteristic of old rats (Newby *et al.* 1990). IBAT was also studied in these rats, to assess whether the partial atrophy persisted in the older animals.

Materials and methods

Animals:

Male Sprague-Dawley rats were obtained from Charles River Laboratories at 5 weeks of age. They were housed individually in plastic cages at 24°C with a 12:12 hour light-dark cycle (lights on at 0700 hours).

Cap-desensitization:

At six weeks of age, rats were anesthetized with halothane and injected with Cap (12.5 mg/kg *s.c.*) or an equal volume of the vehicle (vehicle-treated rats, Veh) in which the Cap was dissolved (80% saline, 10% Tween 80, 10% ethanol). Injections were repeated in conscious rats twice the next day (25 mg/kg each time) and again the day after (62.5 mg/kg). Doses and times were as used by others (Castonguay & Bellinger 1987) and by our lab previously (Cui & Himms-Hagen 1992a; Cui & Himms-Hagen 1992b; Cui *et al.* 1990; Himms-Hagen & Cui 1991; Himms-Hagen *et al.* 1990). Cap was obtained from Fluka,

through Terochem Laboratories, Canada, and contained 65% capsaicin and 35% dehydrocapsaicin (Fluka Chemical, Ronkonkoma, NY).

Body weight determination:

Rats were weighed weekly for one year after treatment. All body weight and food intake measurements were done by Gisèle Larose.

Food intake determination:

Rats had free access to food (Agway chow R-M-H 3000, 14.4 % energy from fat) and water. Food intake was measured weekly for one year after treatment.

Termination:

Rats were brought to the laboratory, where they were weighed and then killed by decapitation. Rectal temperatures were measured immediately using a BAT-8 digital thermometer equipped with a flexible Teflon-sheathed probe inserted to a depth of 6 cm. IBAT was quickly removed and placed in ice-cold isolation medium (see Chapter 3). EWAT and RWAT were removed and placed in plastic weigh boats on ice until weighed and frozen. Twelve rats were killed per day. Carcasses (minus tail, paws, and the adipose depots removed) were frozen for later analysis.

Tissue processing:

Brown adipose tissue: IBAT was dissected away from adhering WAT and muscle and then weighed. IBAT was then homogenized in ice-cold isolation medium (Chapter 3) and samples of homogenate were frozen in liquid nitrogen and stored at -80°C for later assays.

Analyses of BAT and its activity: Protein, DNA, UCP by radioimmunoassay, and COX were measured as outlined in Chapter 3.

White adipose tissue: WAT depots were cleaned, weighed, and then cut into pieces. Some pieces were used for osmium fixation as outlined in Chapter 3. The remaining tissue was reweighed and frozen. The WAT was homogenized and protein and DNA were measured as outlined in Chapter 3.

Carcass analysis:

Carcasses were homogenized in water. At the beginning of the experiment carcasses were homogenized without autoclaving and with a Polytron (Brinkmann) PT45 with a PT45/2K generator. At the end of the experiment, the carcasses were first autoclaved and then homogenized with a Waring Commercial Heavy Duty blender. Lipid content of samples of homogenate was determined as outlined in Chapter 3. Carcass analysis was done by Stefanie Foster.

Immunohistochemistry:

SP and CGRP were detected in sections of spinal cord as described previously (Himms-Hagen *et al.* 1990) except that deeply anesthetized rats were perfused with buffered glutaraldehyde solution to fix the tissue. Immunohistochemistry of the spinal cord of Cap-Des and Veh rats was done by the lab of Dr. W. A. Staines of the Department of Anatomy and Neurobiology of the University of Ottawa.

Data presentation and analysis:

Data are presented as the mean of each group ± SEM unless otherwise stated. Statistics were performed using Instat software and a two-tailed unpaired t-test, with $P<0.05$ regarded as a significant difference. Where data showed a non-Gaussian distribution of data (Table 4.1), a Mann-Whitney test was also used.

The computer program SlideWrite Plus (Advanced Graphics Software, Inc.; Carlsbad, California) was used to generate the graphs, and the regression lines in Figures 4.3, and 4.4.

Results

Body composition/ food intake:

Initial body weights of Cap-Des rats before desensitization were not significantly different from those of Veh rats (Table 4.1, Figure 4.1). After 1 year, the mean body weights of the Cap-Des rats were significantly lower than those of Veh rats (Table 4.1, Figure 4.1). The body weight distribution differed between the two groups in that most of the Cap-Des rats (80%) were in a 550 to 700 g range (Figure 4.2). The median weights differed by more than 100 grams (Table 4.1, legend).

Carcass analysis showed a lower total carcass fat in Cap-Des rats (Table 4.1). This was not simply due to their lower body weight since percent body fat was also significantly lower (Table 4.1).

Average food intakes per day over the 52 weeks of the study were significantly lower in the Cap-Des rats than in the Veh rats (Table 4.1). When it is expressed per 100 grams of body weight, the food intake was higher in the Cap-Des rats. A plot of food intake per 100 grams body weight as a function of body weight for all of the rats during the study showed that smaller rats ate more per 100 grams body weight than did larger rats (4 g per 100 g for 400 g rats, 3.3 g per 100 g for 900 g rats) (Figure 4.3). Consequently, the smaller Cap-Des rats would be expected to eat more per 100 grams body weight. An identical relationship between average food intake and body weight was seen for the two groups (Figure 4.4). The Cap-Des rats ate an amount that was normal for their smaller body size.

NOTE TO USERS

Page(s) not included in the original manuscript are unavailable from the author or university. The manuscript was microfilmed as received.

101 THRU 104

UMI

Food intake: Average over 52 weeks

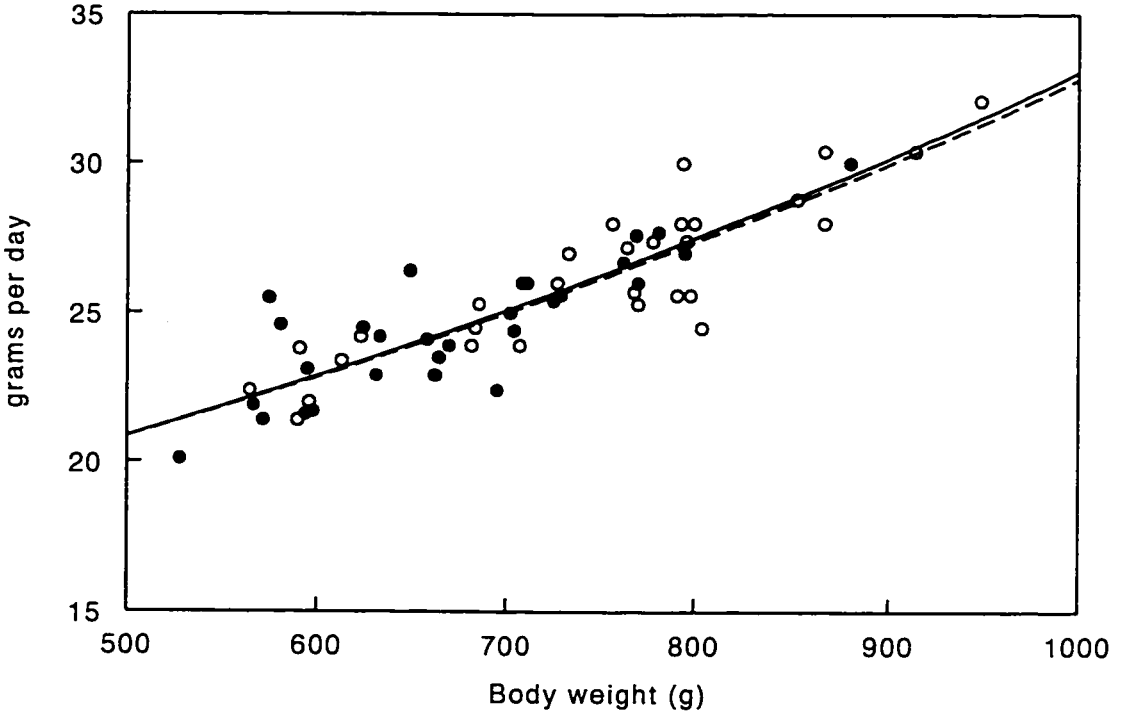

Figure 4.4: Average food intake (grams of chow per rat per day) of individual rats plotted against their body weights. Open circles and broken line, Veh rats (n=29). Closed circles and solid line, Cap-Des rats (n=30). The relationship between food intake and body weight is identical in the two groups.

The Cap-Des rats were not stunted in their growth, as the nasoanal lengths of Cap-Des and Veh rats were not different (Figure 4.5a). No significant difference was seen in the relationship between nasoanal length and body weight for the two groups (Figure 4.5b).

The Lee index of obesity was calculated using the nasoanal length of the rats and their body weight at the time. Figure 4.6 shows that the Veh rats are significantly more obese than the Cap-Des rats (332.7 ± 2.1 vs. 325.4 ± 2.3, p=0.023).

Another index of obesity is the weight of the retroperitoneal depot alone (Figure 4.7). An exponential relationship exists between RWAT weight and body weight (Newby *et al.* 1990), which is seen as the obesity develops in the older and heavier Veh rats. Cap-Des rats fail to progress to an obese state as they age (Figure 4.7).

White adipose tissue:

Weights of two major abdominal WAT depots, the epididymal and retroperitoneal depots, were lower in Cap-Des rats (for EWAT P=0.0310 and for RWAT P=0.0048). (Figure 4.8).

The Cap-Des rats had a lower protein content in their WAT (Figure 4.9). However, this difference did not reach significance between the two groups for either depot (P=0.0565 for EWAT, and P=0.1653 for RWAT).

Nasoanal lengths

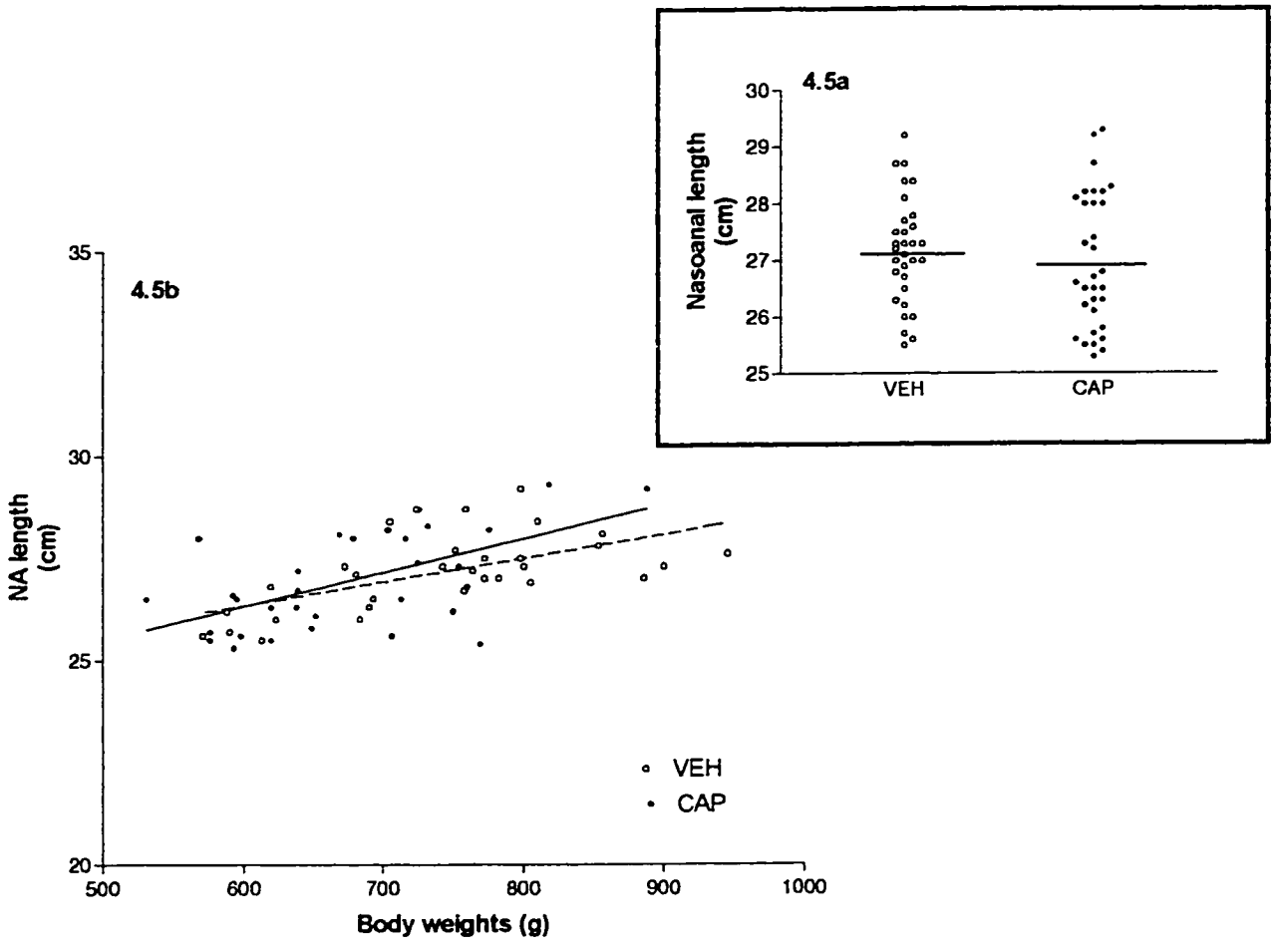

Figure 4.5: Nasoanal lengths of Cap and Veh rats. Rats were briefly anesthetized with halothane 1 week before they were to be killed. Open circles and broken line, Veh rats (n=29). Closed circles and solid line, Cap-Des rats (n=30). Nasoanal lengths were not different between the two groups; Veh 27.17 cm ± 0.17, Cap-Des 26.97 cm ± 0.21 (Figure 4.5a). The relationship between nasoanal length and body weight was not different between the two groups (Figure 4.5b).

Lee index of obesity

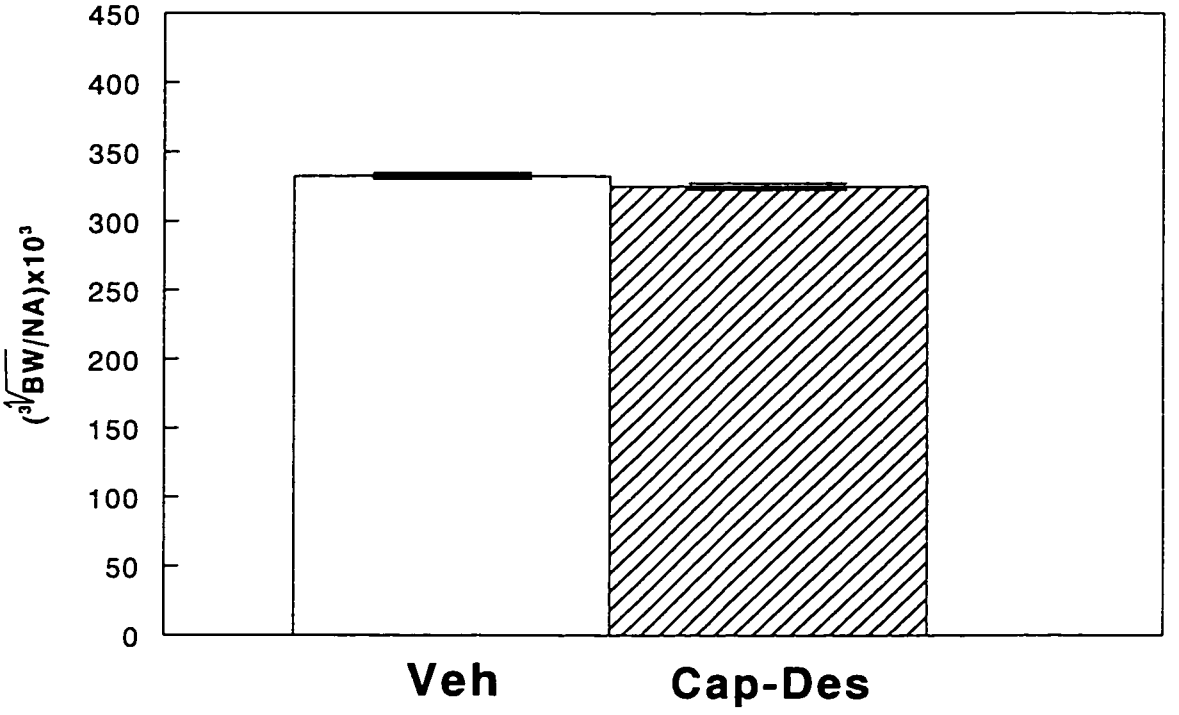

Figure 4.6: Relative obesity of Cap-Des and Veh rats, as determined by the Lee index of obesity, was significantly different between the two groups. The Veh rats (n=29) were more obese than the Cap-Des rats (n=30), (332.7 ± 2.1 vs. 325.4 ± 2.3, p=0.023). The Lee index of obesity was calculated for each rat using the nasoanal lengths from Figure 4.5 and the body weight of the rat at the same time $\{(\sqrt[3]{\text{body weight in g}} \div \text{nasoanal length in cm}) \times 10^3\}$.

Weight of RWAT as an index of obesity

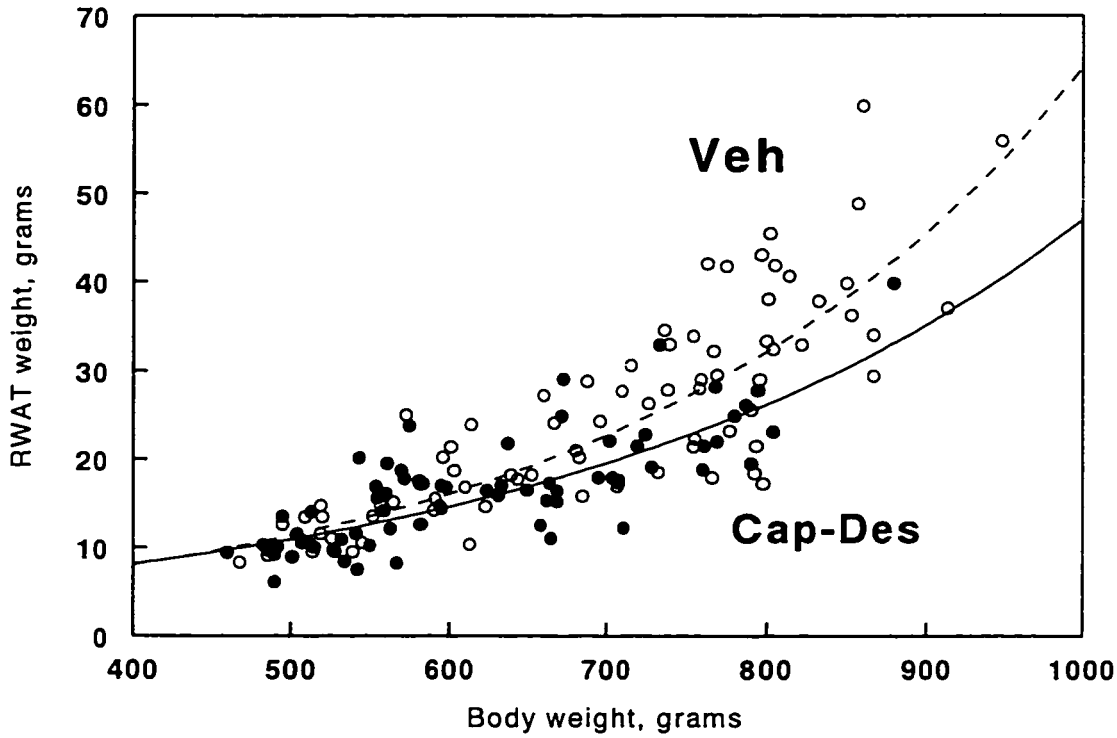

Figure 4.7: Weight of RWAT, an index of obesity (Newby *et al.* 1990), as a function of the body weight of Veh and Cap-Des rats between 10 weeks and 52 weeks after treatment. Data from present study and from previous studies of Veh and Cap-Des rats eating chow (Cui & Himms-Hagen 1992a; Cui & Himms-Hagen 1992b; Himms-Hagen & Cui 1991); age range 4 to 13.5 months. Closed circles and solid line, Cap-Des rats (n=70). Open circles and broken line, Veh rats (n=78), some points hidden under those of Cap-Des rats. Lines show the known exponential relationship (Newby *et al.* 1990) as obesity develops in the older and heavier Veh rats; not seen in Cap-Des rats. Mean values for RWAT weight for all rats shown are 24.8 ± 1.31 g for Veh rats and 16.7 ± 0.77 g for Cap-Des rats ($P<0.0001$), a reduction of 33%.

Weight of two WAT depots

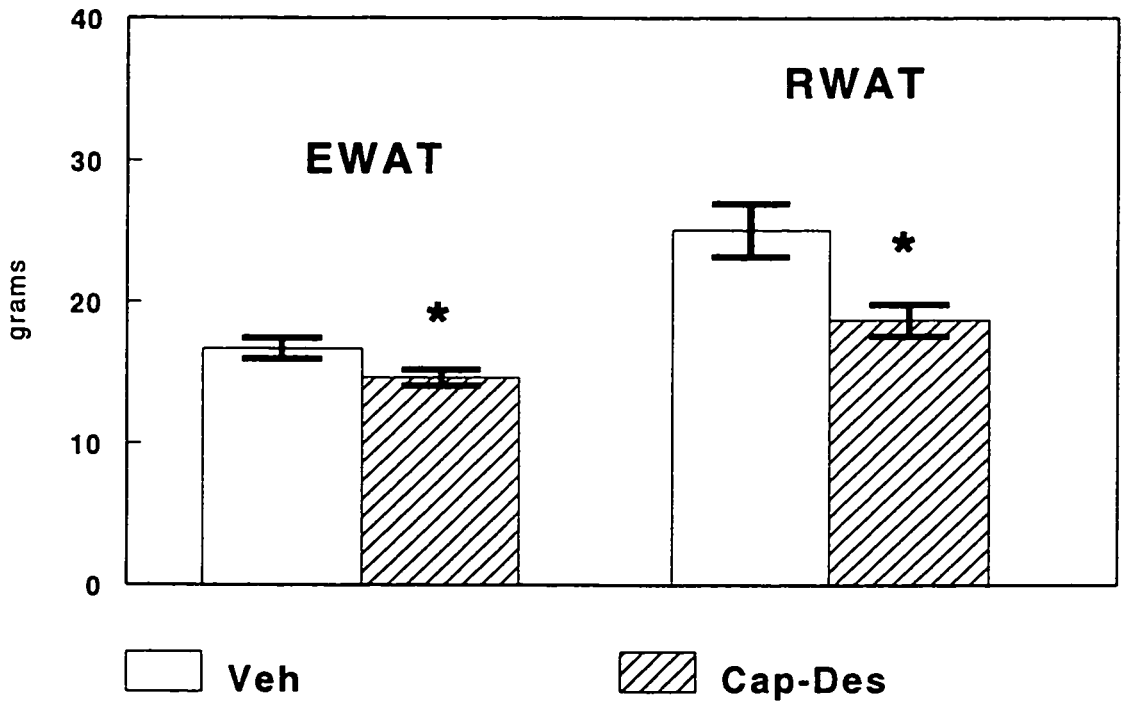

Figure 4.8: Wet weight of two major abdominal WAT depots, EWAT and RWAT, in Veh (n=29) and Cap-Des (n=30) rats 1 year after treatment. Weight is significantly less in Cap-Des rats, both for EWAT (P=0.0310) and for RWAT (P=0.0048).

Total protein content of two WAT depots

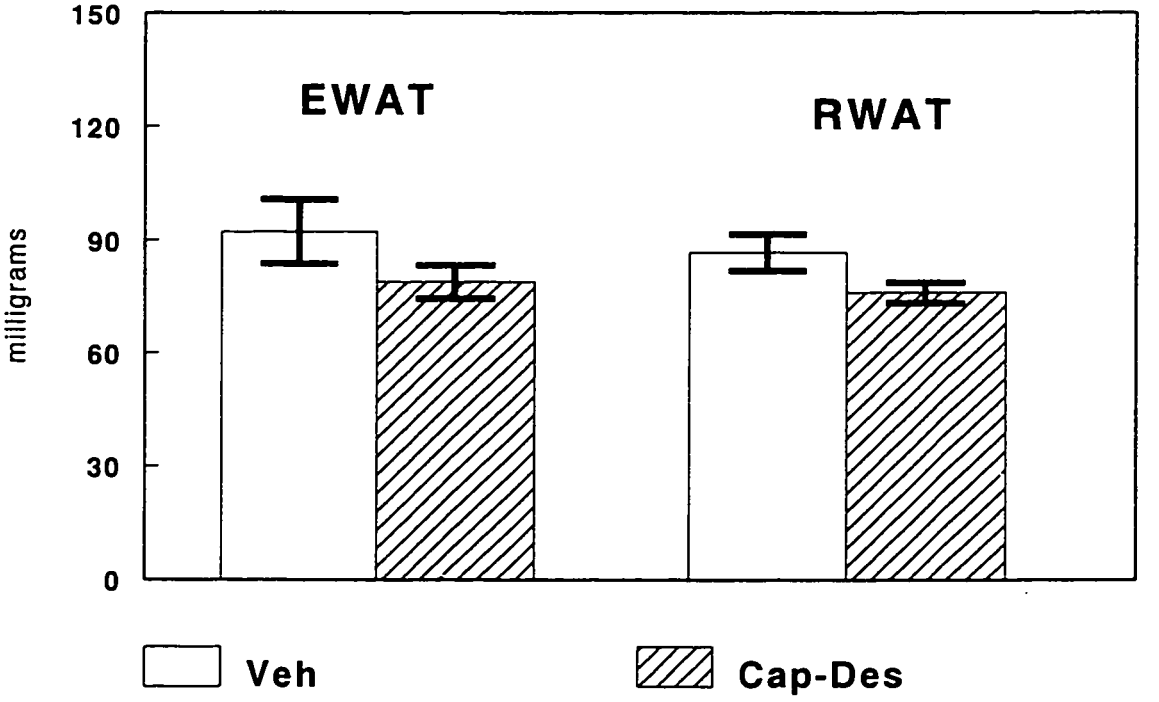

Figure 4.9: Total protein of EWAT and RWAT depots of Veh (n=29), and Cap-Des (n=30) rats. No significant difference exists between the two groups with respect to the total protein content of their WAT depots. (P=0.0565 for EWAT, and P=0.1653 for RWAT).

White adipocyte number, as assessed by the osmium fixation technique of Hirsch & Gallian (1968), was considerably less in the retroperitoneal depot of the Cap-Des rats but not in the epididymal depot (Figure 4.10). Mature white adipocyte size was not altered by the Cap-Des treatment (Figure 4.11).

Total cell number, as assessed by DNA content, was less in the Cap-Des rats. This decrease reached statistical significance for EWAT. Due to a large variation, the difference did not reach statistical significance in RWAT (Figure 4.12). More mature adipocytes and other cell types were seen in RWAT than in EWAT (Figures 4.10 and 4.12). Adipocyte size was the same in the two depots (Figure 4.11). Cell types other than mature white adipocytes are presumably endothelial cells associated with the vasculature and also interstitial cells and preadipocytes.

Interscapular brown adipose tissue:

IBAT of the Cap-Des rats weighed less and had less protein (Figure 4.13) and COX (Figure 4.14) than that of Veh rats. DNA and UCP contents were not different (Figure 4.15).

Immunohistochemistry:

Immunohistochemical staining of the spinal cord for CGRP and SP showed a persistent depletion of these neuropeptides, particularly in SP. The depletion was seen in the substantia gelatinosa and Lissauer's tract (Figure 4.16).

Adipocyte number in two WAT depots

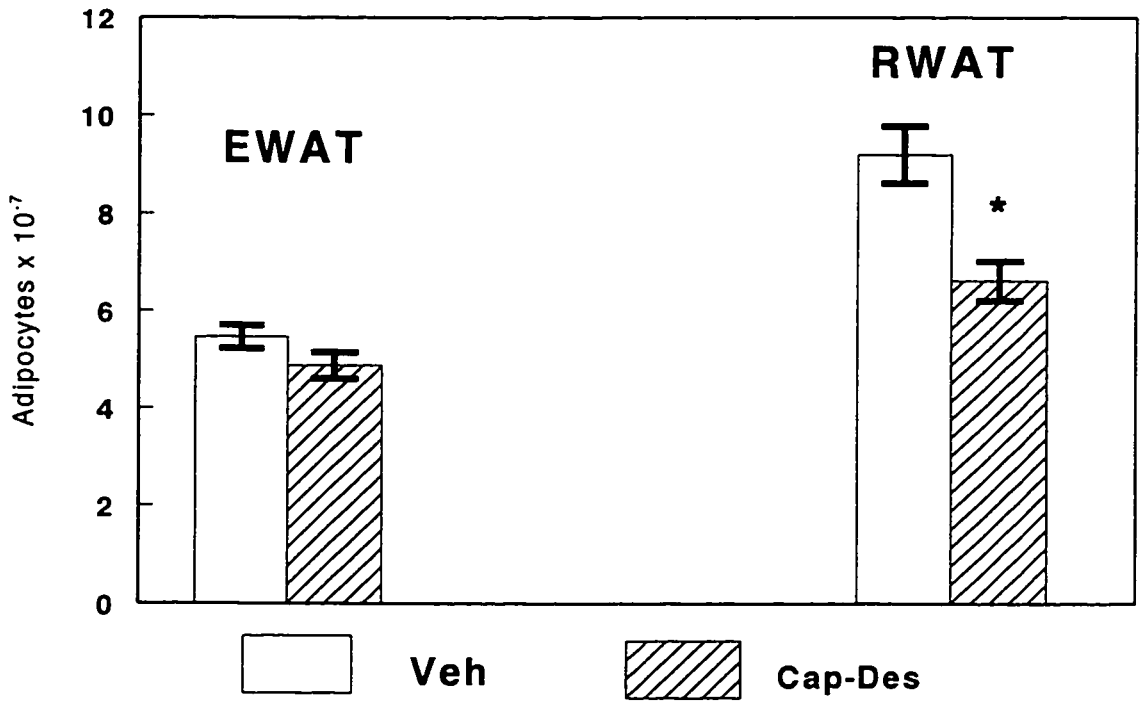

Figure 4.10: Mature white adipocyte number in two abdominal WAT depots. Abbreviations and numbers as in Figure 4.8. Mature adipocytes were assessed by osmium fixation and counting (Hirsch & Gallian 1968). The number is significantly less for RWAT of Cap-Des rats (P=0.0006) but not for EWAT.

Adipocyte size in two WAT depots

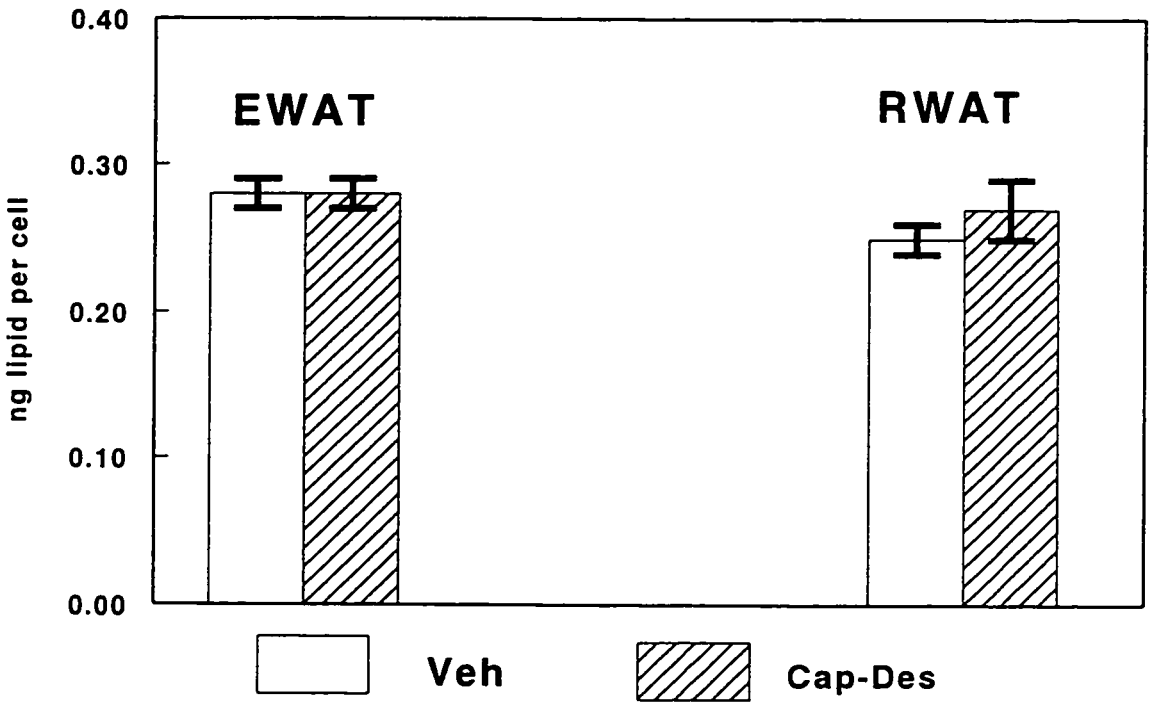

Figure 4.11: Adipocyte size in two abdominal WAT depots. Numbers and abbreviations as in Figure 4.8. See legend to Figure 4.10 for more information. Size calculation based on assumption of 90% lipid content of WAT by weight (Newby *et al.* 1990). No significant effects of Cap-Des are seen.

Total cells (from DNA) in two WAT depots

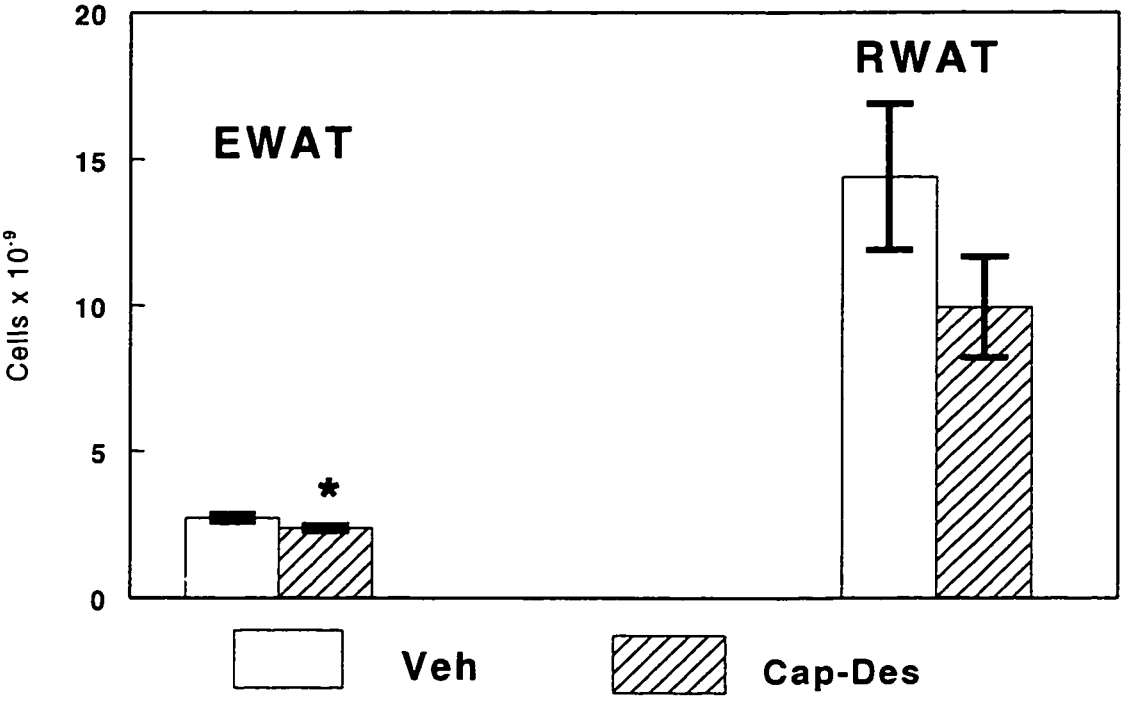

Figure 4.12: Cellularity of two WAT depots as assessed by DNA content (factor used, 7 pg DNA per nucleus). Abbreviations and numbers as in Figure 4.8. Cellularity is significantly less in EWAT (P=0.0315) but not in RWAT (P=0.141). Note that DNA content is a measure of all cell types, not only mature white adipocytes but also endothelial cells, interstitial cells, and preadipocytes.

Interscapular BAT weight and protein content

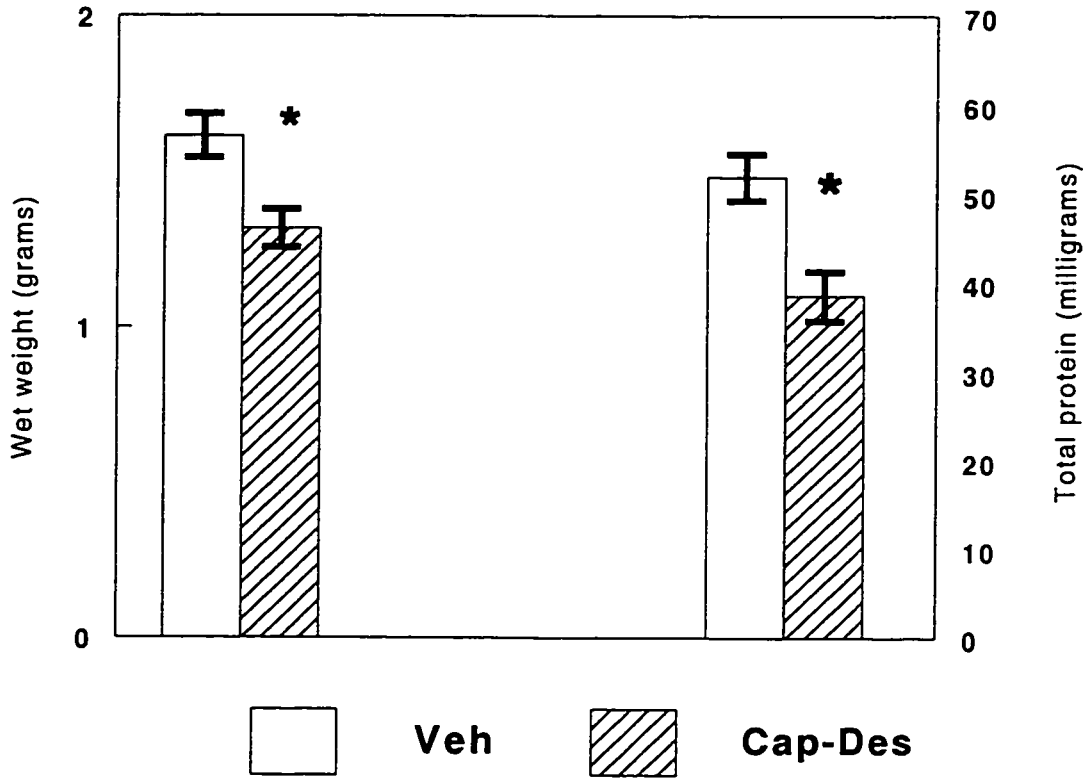

Figure 4.13: Wet weight and total protein of interscapular brown adipose tissue. Wet weight of IBAT is significantly lower (P=0.0021) in Cap-Des rats, as is the protein content of the tissue (P=0.0009). Veh, n=29; Cap-Des, n=30.

Interscapular BAT cytochrome oxidase activity

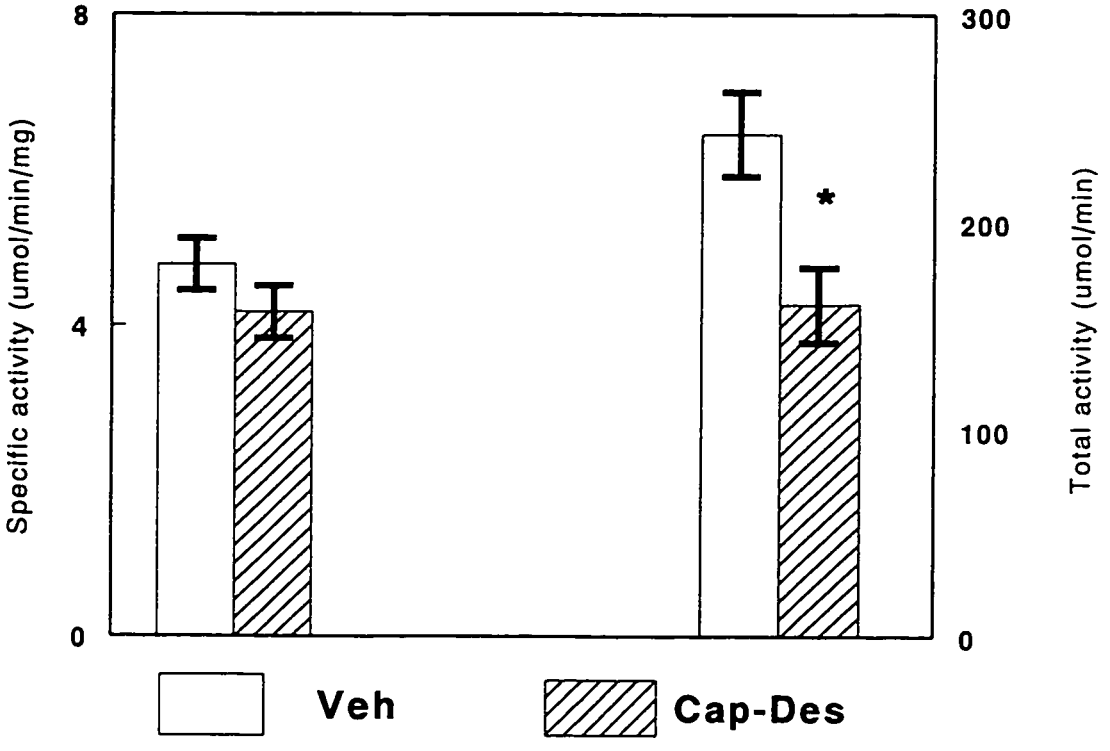

Figure 4.14: Interscapular brown adipose tissue COX activity. Specific activity (activity per mg protein) was not different. Total COX was significantly lower in Cap-Des rats (P=0.0037). Numbers of animals as in Figure 4.13.

Interscapular BAT DNA and UCP content

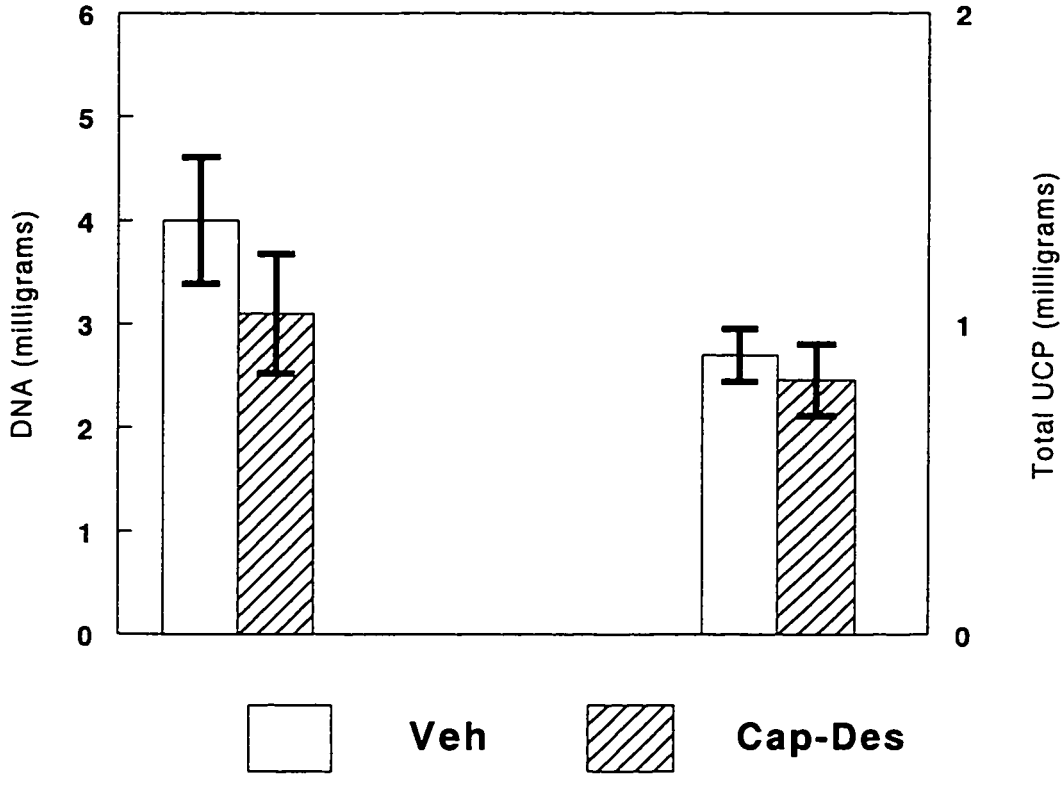

Figure 4.15: Interscapular brown adipose tissue DNA and UCP content. No significant difference exists between groups for either of these measures. Numbers of animals as in Figure 4.13.

Immunohistochemistry of spinal cord sections

Figure 4.16: Immunohistochemical detection of CGRP and substance P (SP) in spinal cord sections of control and Cap-Des (lesion) rats. Studies showed a persistent depletion, particularly in substance P, in the substantia gelatinosa and Lissauer's tract.

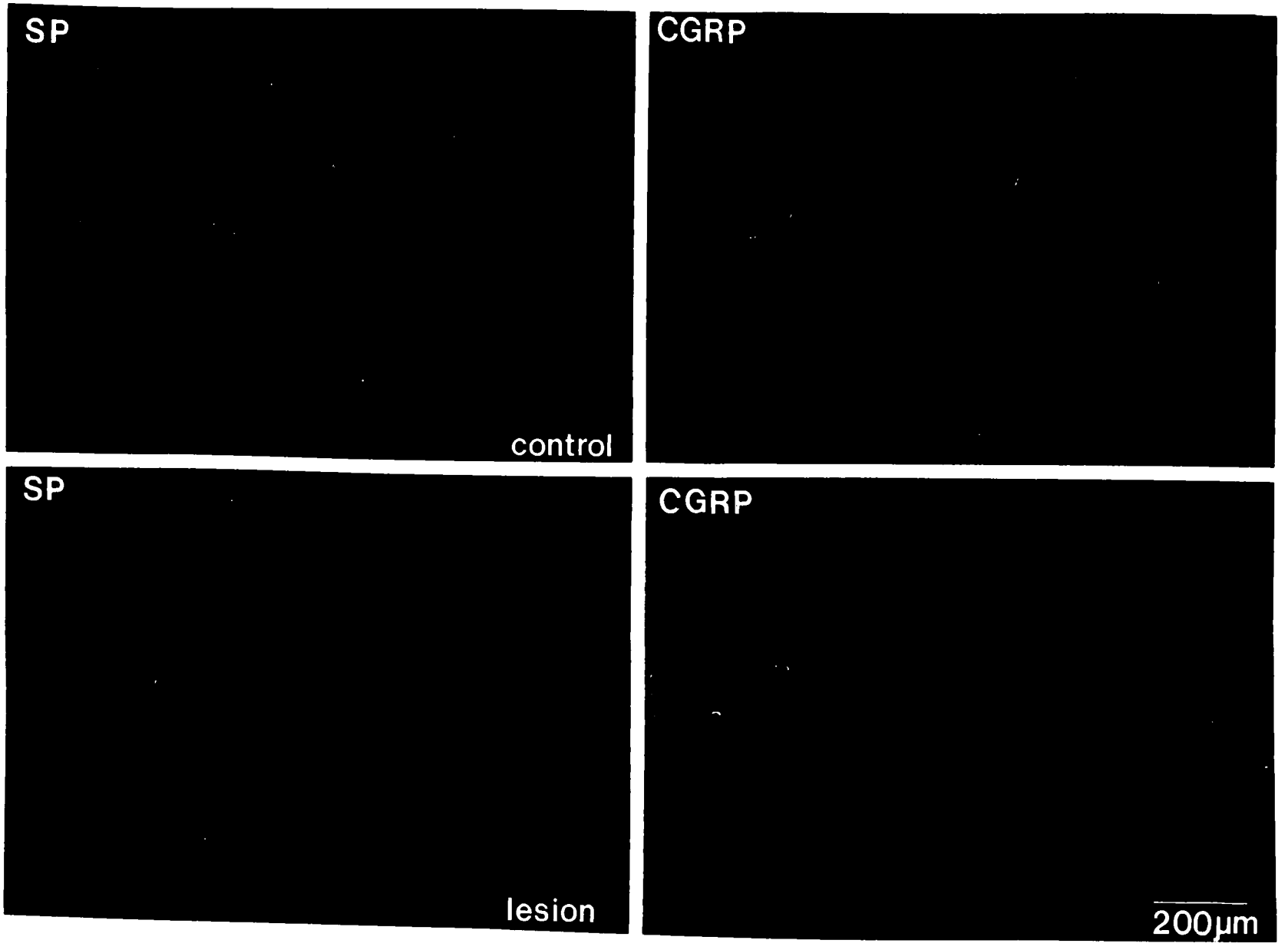
SP
CGRP
control
SP
CGRP
lesion
200µm

Discussion

The principal finding in this study was that Cap-Des rats remained leaner and smaller than Veh rats up to one year after treatment. Their food intake was normal for their smaller body size. The Cap-Des rats were not stunted in their linear growth.

Using the Lee index, the sum of the WAT depots and the RWAT weight as indices of obesity, the Cap-Des rats were less obese than the Veh rats. (Figures 4.6, 4.7, and 4.8). At this age Veh rats exhibit a high prevalence of aging-associated obesity. Using the wet weight of the RWAT depot as an index of obesity (Newby *et al.* 1990), the exponential increase in adiposity of older and larger rats can be seen (Figure 4.7). All except one Cap-Des rat failed to become obese (Figure 4.7). The number of mature white adipocytes in this depot is known to increase with the development of obesity in the aging rat (Newby *et al.* 1990). In the Cap-Des rat this increase in number was retarded.

In contrast, the number of mature white adipocytes in EWAT does not increase with aging in rats (Newby *et al.* 1990), and was not altered in the Cap-Des rats. The adipocyte number in EWAT in our study is similar to that reported for this depot in old Wistar rats (Newby *et al.* 1990). Our value for adipocyte number in RWAT is almost twice as high as in old Wistar rats, as is the wet weight of this depot, possibly a characteristic of old Sprague-Dawley rats.

We conclude that the aging-associated, hyperplastic obesity that develops in 13.5-month-old Sprague-Dawley rats was prevented by Cap-desensitization at the age of 1.5 months.

Another finding of this study is the low proportion of mature white adipocytes in the total cell population (as measured by DNA content) of EWAT and particularly of RWAT depots. Similar findings have been reported previously for EWAT (Cleary *et al.* 1979) and for RWAT (Ghorbani & Himms-Hagen 1997) of *fa/fa* Zucker rats and their lean littermates. The low contribution of mature white adipocytes to the total cell number in RWAT of *fa/fa* Zucker rats was visualized in sections stained with propidium iodide and viewed by fluorescence microscopy (Ghorbani & Himms-Hagen 1997). This treatment allowed for the observation of all of the nuclei present in the section and it clearly showed the abundance of non-adipocyte nuclei. The non-adipocyte nuclei measured could be from the endothelial and smooth muscle cells of the vasculature; they could also be from interstitial precursor cells, preadipocytes, mast cells, and possibly dormant brown adipocytes (Cousin *et al.* 1993). These are all very small cells compared with the large size of the adipocytes and are not readily assessed by routine histology.

In our lab, it was previously shown that the BAT of the Cap-Des rat is atrophied (Cui & Himms-Hagen 1992a; Cui & Himms-Hagen 1992b; Cui *et al.* 1990; Himms-Hagen & Cui 1991; Himms-Hagen *et al.* 1990). This atrophy of BAT is accompanied by a depletion of its

CGRP (Himms-Hagen *et al.* 1990), which has raised the possibility of a local effector function of sensory neuropeptides in the maintenance of BAT.

Atrophy of BAT is generally associated with obesity rather than leanness (Himms-Hagen 1989a; Himms-Hagen 1991) and the genetic ablation of BAT in mice induces massive obesity (Lowell *et al.* 1993). The resistance of the Cap-Des rat to the development of obesity, both aging-associated (this study) and diet-induced (Himms-Hagen & Cui 1991) cannot be attributed to the lack of any known function of BAT.

No clear relationship exists between the leanness in the Cap-Des rat and any known function of Cap sensitive sensory nerves, neither to their local effector functions in all peripheral tissues nor to the function of their central projections.

Perspectives:

Some speculative suggestions for another mechanism conferring the resistance to obesity seen in old Cap-Des rats can be offered. Provided in this section is a review of the literature supporting our proposal that the attenuated age-associated increase in circulating CGRP (derived mainly from Cap-sensitive nerves) in the Cap-Des rat (Wimalawansa 1993) results in a lower degree of aging-associated insulin-resistance, hence in a lesser degree of obesity.

CGRP is in circulation and may lead to insulin resistance:

CGRP is present in the circulation of rats (Diez Guerra *et al.* 1988; Emson & Zaidi 1989; Zaidi *et al.* 1986); its sources are the thyroid gland and perivascular nerves (Diez Guerra *et al.* 1988; Emson & Zaidi 1989; Zaidi *et al.* 1986). At least 50% of circulating CGRP may arise from sensory neurons (Diez Guerra *et al.* 1988); the acute administration of Cap causes a substantial release of CGRP into the circulation (Diez Guerra *et al.* 1988; Emson & Zaidi 1989) from these nerves.

The function of circulating CGRP may be to act with amylin in regulation of fuel metabolism; the two peptides are structurally similar and have similar biological effects in many tissues (Cooper 1994). CGRP and amylin act as noncompetitive antagonists of insulin in skeletal muscle (the main site of insulin resistance) (Cooper 1994; Kreutter *et al.* 1993; Rossetti *et al.* 1993; Yamaguchi *et al.* 1990) and have been shown to induce states of insulin resistance in whole animals (Cooper 1994; Leighton & Cooper 1990).

A disorder in the homeostasis of amylin and/or CGRP is an early event in the insulin resistance of non-insulin dependant diabetes mellitus and obesity in humans (Cooper 1994). Circulating amylin is increased in human obesity (Cooper 1994), and in all animal models of obesity and insulin resistance (Cooper 1994). An increase in CGRP concentration in the blood has been linked with obesity and insulin resistance in *fa/fa* rats (Seitz & Cooper 1987) and in obese humans (Zelissen *et al.* 1991).

In rats, the concentration of CGRP in the circulation increases with age. This is due to an increased output of CGRP into the circulation from the thyroid gland (Wimalawansa 1991); the major source of CGRP in the old rat (Emson & Zaidi 1989; Zaidi *et al.* 1986). This can be linked to the rise in insulin resistance reported in old rats, starting between 2 and 4 months of age and reaching a maximum at 12 months (Cincotta *et al.* 1993; Gulve *et al.* 1993; Narimiya *et al.* 1984; Nishimura *et al.* 1988). This insulin resistance is characterized by a decrease in insulin action on muscle (Gulve *et al.* 1993; Narimiya *et al.* 1984) and was associated with an increased body weight.

Furthermore, the concentration of CGRP in the blood of old rats (about 70 pM) (Wimalawansa 1991; Wimalawansa 1993), could antagonize the action of insulin, since a maximum inhibition of insulin-stimulated glucose uptake by soleus muscle in vitro is achieved at a peptide concentration of 10 pM (Kreutter *et al.* 1993).

Cap-desensitization decreases circulating CGRP and improves insulin resistance:

Cap-desensitization destroys sensory nerves that normally release CGRP. In vitro Cap decreased the CGRP levels in stripped soleus muscle preparations by nearly 40% (Leighton & Foot 1995), while rats treated neonatally with Cap exhibited a depletion of >50% of CGRP in various tissues (Wimalawansa 1993). Plasma levels of CGRP are also significantly decreased throughout the lifespan of Cap-Des rats; a one-year-old Cap-Des rat has a concentration of CGRP in its blood equal to that characteristic of a five-week-old rat (Wimalawansa 1993).

Insulin sensitivity is enhanced in stripped soleus muscle preparations from adult Cap-Des rats (Leighton & Foot 1995), and in the Cap-Des mouse (Karlsson *et al.* 1994; Zhou *et al.* 1990).

Consequently, the leanness of the Cap-Des rat reported here, associated with a reduced concentration of CGRP in the blood (Wimalawansa 1993), would be expected to be associated with a lesser degree of aging-associated insulin resistance, therefore with a lesser propensity to obesity. The nature of the connection between the CGRP-amylin system and energy balance remains for further investigation.

The system composed of the neurotransmitter, CGRP, and the closely related circulating hormone derived from pancreatic islets, amylin, has been likened to the sympathetic nervous system, with its neurotransmitter, NA and its circulating hormone derived from the adrenal medulla, adrenaline (Leighton & Cooper 1990). A role for the sympathoadrenal system in energy balance is well known, with low sympathetic nervous system activity (but not low adrenal medullary activity) being associated with obesity (Bray 1990). A related role for the CGRP-amylin system is conceivable, with high activity associated with obesity and insulin resistance, and low activity of the CGRP system, as in the Cap-Des rats of the present study, with leanness.

Chapter 5: Brown adipose tissue in rats with lesions in the nucleus of the solitary tract

Introduction

The control of BAT growth and thermogenesis by sympathetic noradrenergic nerves is well known. These nerves are under central control and stimulate the tissue under dietary influences and the influence of a cold environment (Géloën *et al.* 1992; Himms-Hagen 1991; Himms-Hagen & Ricquier 1997; Takahashi *et al.* 1992). The verification of NA as the principal stimulus of BAT thermogenesis and growth was covered in Chapter 1.

The heterogeneity of the nerves innervating BAT (Flaim *et al.* 1976), and the presence of nerves containing SP and CGRP (Himms-Hagen *et al.* 1990; Lever *et al.* 1988; Lever *et al.* 1989; Mukherjee *et al.* 1989), has also implicated non-noradrenergic nerves in the control of BAT function.

SP and CGRP are both neuropeptides characteristic of afferent autonomic 'sensory' nerves (Himms-Hagen *et al.* 1990; Lever *et al.* 1988; Lever *et al.* 1989; Mukherjee *et al.* 1989). As discussed in Chapter 4, Cap-desensitization of rats, a treatment known to destroy a subpopulation of afferent autonomic sensory nerves (Holzer 1988; Holzer 1991a; Holzer 1991b; Maggi 1991; Maggi & Meli 1988), depletes BAT of its CGRP content, leaving intact the noradrenergic innervation (Himms-Hagen *et al.* 1990).

This treatment induces an atrophy of BAT, characterized by loss of cells (reduced DNA content) and of mitochondria (reduced UCP and COX contents) (Cui & Himms-Hagen

1992a; Cui & Himms-Hagen 1992b; Cui *et al.* 1990). In Cap-Des rats, the atrophy of BAT is not associated with obesity as is normally seen in other animal models (Himms-Hagen 1989a). It is associated with a lack of diet-induced activation of BAT thermogenesis (Cui *et al.* 1990; Himms-Hagen & Cui 1991), and conversely, with leanness. A lesser degree of diet induced obesity was observed in Cap-Des rats when they were fed a palatable high fat diet (Cui & Himms-Hagen 1992b; Himms-Hagen & Cui 1991), and these animals also showed a lesser degree of aging-associated hyperplastic obesity, as discussed in Chapter 4.

Sensory nerves are also present in WAT (Fishman & Dark 1987), suggesting a role for Cap-sensitive sensory nerves in both BAT and WAT involved in the regulation of adipose tissue metabolism and of energy balance.

Cap-Des rats are known to have central brain lesions in addition to the peripheral lesions that they sustain from the treatment. These central lesions include a lesion of the nucleus of the solitary tract (or nucleus tractus solitarius: NTS) (Castonguay & Bellinger 1987; Ritter & Dinh 1988; Ritter & Dinh 1990; Ritter & Dinh 1992).

Lesions in specific brain areas are known understandably to alter energy balance, and to change control of BAT thermogenic activity and capacity (Himms-Hagen 1991). The areas of the brain controlling these functions are mainly in the hypothalamus but also in the brain stem.

Rats with lesions of the nucleus of the solitary tract resemble Cap-Des rats in that both exhibit a normal rate of weight gain but a lack of catch-up growth after a period of rapid weight loss (Cui & Himms-Hagen 1992a; Cui & Himms-Hagen 1992b; Himms-Hagen & Cui

1991; Hyde & Miselis 1983; Kott *et al.* 1984). During desensitization, the Cap-Des rat falls behind in weight compared with the control rat; the NTS-lesioned rat falls behind controls due to weight loss after lesioning. In contrast, rats deprived of food will lose weight but when given free access to chow; they will eventually grow and catch-up to control fed rats.

Differences are seen between the two types of rats in their regulation of feeding. The NTS-lesioned rat overeats during short-term exposure to palatable food (Edwards & Ritter 1986; Ritter & Edwards 1984), the Cap-Des rat does not (Himms-Hagen, J. unpublished results). However, during long-term exposure to palatable foods, both types of animals react the same as controls with respect to total consumption. Lesions to the NTS cause an increased responsiveness to highly palatable foods in rats (Ritter & Edwards 1984), without disabling the animal's ability to control total caloric intake (Hyde & Miselis 1983; Ritter & Edwards 1984). When exposed to a palatable diet, the Cap-Des rat (Cui *et al.* 1990) consumes the same amount of calories as control rats, and diet-induced weight gain is the same.

Glucose and fatty acids can function as metabolic controls of food intake. The positive feeding responses induced by lack of these stimuli are respectively called glucoprivic and lipoprivic. NTS-lesioned rats lack both glucoprivic and lipoprivic feeding responses (Ritter & Taylor 1989) whereas Cap-Des rats lack lipoprivic feeding responses but not glucoprivic feeding responses (Ritter & Taylor 1989; Ritter & Taylor 1990).

The sympathetic control of BAT-mediated thermogenesis may be regulated in part through mechanisms or pathways similar to those involved in the afferent arm of the

baroreceptor reflex (Fyda *et al.* 1991; Nagasaka *et al.* 1984; Saito *et al.* 1985). Afferent baroreceptor fibres first synapse in the NTS and lesioning of this region effectively denervates baroreceptors (Fyda *et al.* 1991), impairing the reflex in these animals. Cap-Des rats do not have impaired baroreceptor-mediated reflex responses (Takano *et al.* 1988).

Fyda *et al.* (1991) observed that the metabolic and temperature responses to NA and isoproterenol (increase in whole body oxygen uptake and an increase in temperature of IBAT) were decreased in NTS-lesioned rats. NTS lesions caused the attenuation of the metabolic, core and BAT temperature responses typically seen during cold exposures to graded cold ambient temperatures (Fyda & Wilson 1991). This group suggests that the ability of BAT to respond to adrenergic stimulation with an increase in metabolism is impaired due to lesioning of the NTS.

An important similarity between NTS-lesioned rats and Cap-Des rats in the context of the present study is that both have a reduced capacity to respond to administered NA by an increase in whole body oxygen uptake and an increase in temperature of IBAT (Cui *et al.* 1990; Fyda *et al.* 1991). In the Cap-Des rat, this deficiency is attributable to the atrophied state of its BAT (Cui *et al.* 1990). This led to our hypothesis that NTS-lesioned rats would have atrophied BAT like Cap-Des rats, associated in both with a lesion in the NTS.

Objectives

The objective of the present study was to assess by biochemical means the thermogenic capacity of IBAT in NTS-lesioned rats.

Materials and methods

Animals:

Male Sprague-Dawley rats aged 8 weeks were obtained from Charles River, St. Constant, Québec. Their initial weight on arrival was in the range 268 to 293 grams. They were housed singly in plastic cages with free access to food (Agway R-M-H 3000 chow, 14.4% energy from fat) and water. The temperature of the animal care facility was 24 °C, and it had a 12 hour lighting schedule (lights on at 0730 h).

Experimental groupings:

Because of the possibility that the reduced food intake known to occur after an NTS-lesion might influence the thermogenic capacity of the lesioned rats, we studied not only sham-lesioned control rats but also a group of sham-lesioned rats pair-fed to the NTS-lesioned rats.

Body weights were measured daily for one week and the largest and smallest gainers were discarded to obtain the three equivalent groups of rats studied. On day 0, 16 rats received sham NTS lesions. The following day (day 1), 9 rats received NTS lesions.

Lesions:

All of the lesions done in this experiment were performed by Thu Dinh. For the lesions and sham-lesions, rats were anesthetized with methoxyflurane (Metafane, Pitman-Moore Ltd.) and placed in a stereotaxic instrument with the head in a ventroflexed position. A midline incision was made between the occipital crest and the midcervical level. The foramen magnum was exposed by blunt dissection of the overlying musculature. The atlanto-

occipital ligature and meninges were excised and the foramen magnum was enlarged slightly with rongeurs. The cerebellum was then gently lifted to allow visualization of the obex. Obex was defined as the most caudal extent of the area postrema, viewed from its dorsal surface. Stainless steel electrodes (A-M systems, Inc., Everett WA) were lowered bilaterally into the NTS 0.3 mm rostral, ±0.5 mm lateral and 0.4 mm ventral to the obex. A DC constant current lesion maker (Model DC-LM5, Grass Instruments, Quincy, MA) was used to pass 0.5 mA of anodal current through the electrode for 5 seconds with a rectal cathode. For sham-operated controls, the same surgical approach was made but the electrode did not penetrate the NTS and no current was passed. The skin was closed with surgical silk. At the end of the operation rats were injected intraperitoneally with 0.1 ml per 100 g body weight ampicillin sodium, 125 mg per ml (Pentritin-250, Ayerst) and BNP ointment was placed in their eyes (bacitracin zinc, neomycin sulfate, polymyxin B sulfate in white petrolatum and mineral oil, Vetcom Inc.). They were kept in incubators at 37°C until fully recovered form the anesthesia, then returned to their cages.

Body weight determination:

Rats were weighed daily from day zero (sham-lesioning) for 20 or 22 days.

Food intake determination:

Ad libitum fed rats (NTS-lesioned and one sham-lesioned group) had free access to chow (Agway chow R-M-H 3000, 3.5 kcal/g, 14.4 % energy from fat) and water. Food was placed on the floors of the cages and intake was measured daily. An amount of food equal to the mean amount eaten by all the lesioned rats on one day was given to a group of sham-lesioned rats the following day. These restricted-fed rats ate all the food provided.

Termination:

At 20 to 22 days after surgery, the rats were killed by decapitation. The rats were transferred to the laboratory, where they were weighed before killing. Heads of lesioned rats were placed in 10 % buffered formalin for later shipment to Thu Dinh at Washington State University. Blood was collected into a 42 ml centrifuge tube with the aid of a plastic funnel and kept on ice. Rectal temperatures were measured after blood collection, using a BAT-8 digital thermometer equipped with a flexible Teflon-sheathed probe inserted to a depth of 6 cm. IBAT was quickly removed and placed in ice-cold isolation medium (see Chapter 3). EWAT and RWAT were removed and placed in plastic weigh boats on ice until weighed and frozen. Carcasses (minus tail, paws, and the adipose depots removed) were frozen for later analysis.

Tissue processing:

Brown adipose tissue: IBAT was dissected away from adhering white adipose tissue and muscle and then weighed. IBAT was then homogenized in ice-cold isolation medium (Chapter 3) and samples of homogenate were frozen in liquid nitrogen and stored at -80°C for later assays.

Analyses of BAT and its activity: Protein, DNA, UCP by radioimmunoassay, and COX were measured as outlined in Chapter 3.

White adipose tissue: WAT depots were cleaned, weighed and frozen at -80°C for later analysis. Frozen WAT depots were thawed at 4°C and the entire depot was then homogenized. Homogenates were processed, and protein and DNA were measured as outlined in Chapter 3.

Carcass analysis:

Carcasses were homogenized in water with a Polytron (Brinkmann) PT45 with a PT45/2K generator. Lipid content of samples of homogenate was determined as outlined in Chapter 3. Carcass analysis was done by Gisèle Larose.

Brain histology:

All of the brain histology was done by Thu Dinh, and the interpretations of the extent of the lesions was done by Sue Ritter at Washington State University. The brains were removed from the skulls, post-fixed in formalin solution and cryoprotected in 30 % sucrose solution. Frozen sections (30 μm in thickness) were mounted on slides and stained with cresyl violet. Sections were examined microscopically to determine the extent of the lesion. Areas cauterized or obliterated by the lesion and the surrounding zone of heavy glial infiltration were drawn on anatomically corresponding plates from stereotaxic atlas of the rat brain (Paxinos & Watson 1982).

Data presentation and analysis:

Data are presented as the mean of each group ± SEM unless otherwise stated. Statistical analysis used analysis of variance followed by Student-Newman-Keuls post-hoc test where appropriate.

Results

Lesions:

Lesions were identified by the obliteration of brain tissue, by the presence of cauterized tissue and by dense glial infiltration obscuring the presence of normal cells. In all rats the lesion was confined to an area largely medial to the solitary tract and extending approximately 1.0 mm rostral and 0.3 mm caudal to the obex. Examples of a small and a large lesion are illustrated in Figure 5.1; most lesions resembled that shown in Figure 5.1 B.

Lesions were centered in the medial and dorsomedial subnuclei of the NTS and were most severe in areas of the NTS coextensive with the area postrema. The commissural subnucleus was also damaged extensively by the lesion, but never was this subnucleus totally destroyed in regions caudal to the obex. The area postrema sustained heavy glial infiltration in all animals. The dorsal motor nucleus of the vagus was spared in most cases, with visible unilateral damage in only three rats. The medial aspect of the nucleus gracilis immediately adjacent to the area postrema was slightly damaged in all rats.

NTS lesions

Figure 5.1: Diagram of coronal sections through the nucleus of the solitary tract showing areas of electrocoagulation and glial infiltration resulting from electrolytic lesions (cross-hatched areas). Panel A shows the smallest lesion and panel B shows the largest lesion. Abbreviations: 4V, 4th ventricle; AP, area postrema; CC, central canal; Cu, nucleus cuneatus; DMV, dorsal motor nucleus of the vagus; Gr, nucleus gracilis; NTS, nucleus of the solitary tract.

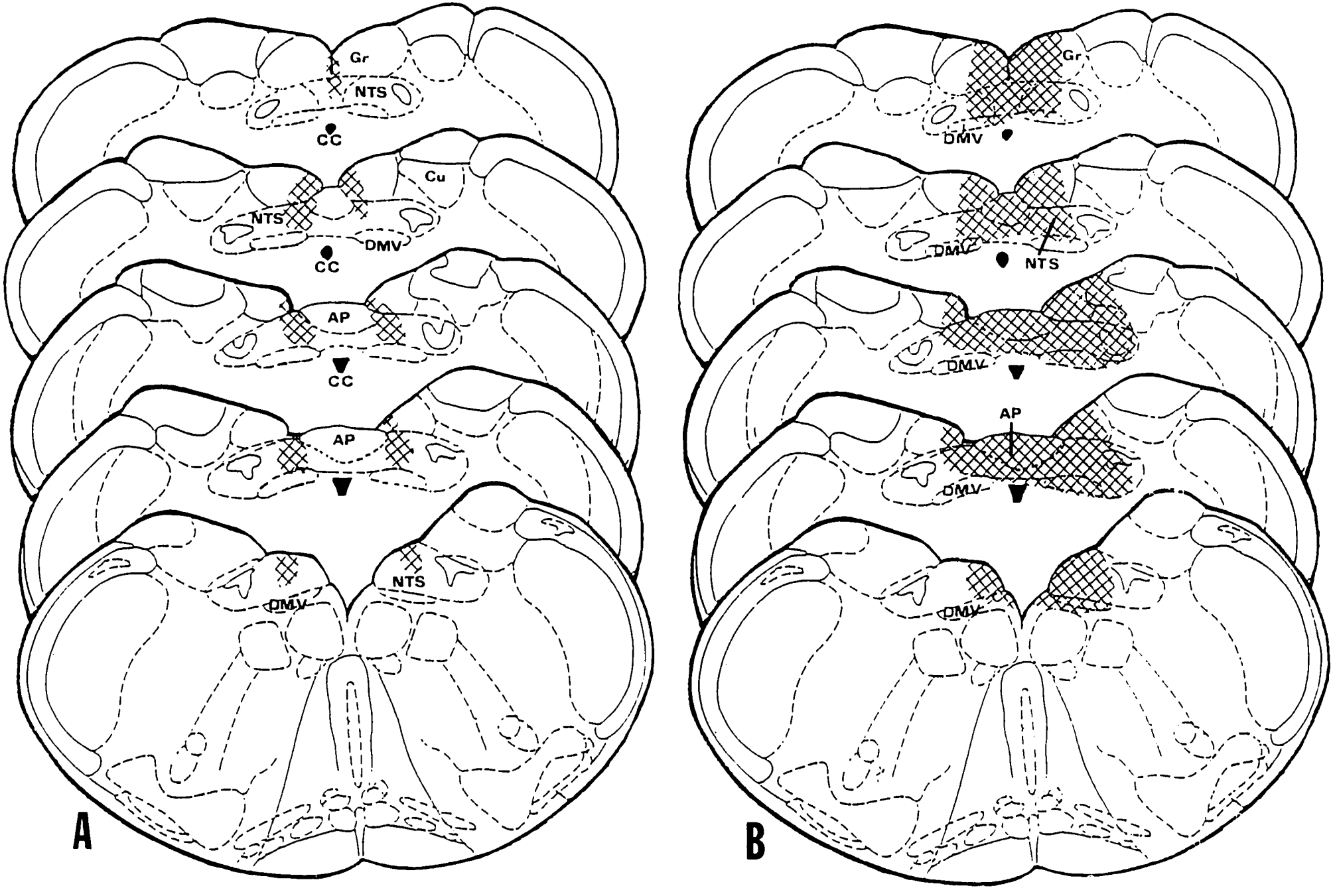
Gr
NTS
CC
Cu
NTS
DMV
CC
AP
CC
AP
DMV
NTS
A
Gr
DMV
DMV
NTS
DMV
AP
DMV
DMV
B

Initial calculations for all rats (9 lesioned, 8 sham-lesioned and restricted-fed, 8 sham-lesioned and ad libitum fed) showed no effect of lesion on any parameter measured except weight gain (Table 5.1) and food intake.

The lesioned rats clearly separated into two distinct groups based on their weight gain as shown in Figure 5.2. The low group (n=4) gained 50.0 ± 2.27 g and had a final body weight of 382.5 ± 4.75 g, while the high group (n=5) gained 81.4 ± 3.59 g and had a final body weight of 424.4 ± 3.67 g (P=0.0002 for both).

Further calculations were done for those rats showing the greatest functional impairment as suggested by their low weight gain. The rats with the greatest impairment could not be distinguished from the rats showing the greater weight gain based on the histological appearance of their lesions. A matched group of restricted-fed sham-lesioned rats (n=4) was used for comparison (see Figure 5.2). Data are presented only for these subgroups.

Food intake:

Food intake decreased transiently the night after surgery in the sham-lesioned rats. A more profound and prolonged decrease occurred in the NTS-lesioned rats (Figure 5.3). Food intake returned to a steady level by 8 days post-lesion.

Table 5.1: Weights, weight gain, carcass fat, and WAT measures

	Sham-lesioned	Sham-lesioned Restricted-fed	NTS-lesioned
Number of animals	**(8)**	**(8)**	**(9)**
Body weight, grams			
Initial	323 ± 2.90	328 ± 3.79	338 ±3.05*
Final	423 ± 6.45	399 ± 3.76*	406 ± 7.91
Gain	100 ± 5.69	71 ± 5.12*	67.5 ±5.90*
Carcass fat, grams	20.2 ± 1.87	18.2 ± 1.50	18.0 ± 1.20
Carcass fat, %	4.75 ± 0.39	4.54 ± 0.33	4.41 ± 0.24
EWAT, g	3.86 ± 0.22	3.61 ± 0.20	3.75 ± 0.17
RWAT			
Wet weight, g	3.24 ± 0.29	3.07 ± 0.36	2.96 ± 0.24
Protein, mg	31.6 ± 2.63	33.8 ± 3.28	31.0 ± 1.90
Cells x 10^{-5}	8.87 ± 0.61	9.56 ± 1.21	9.89 ± 0.83
Cells x 10^{-5}/g	2.84 ± 0.13	3.14 ± 0.12	3.50 ± 0.32
IBAT			
Wet weight, mg	589 ± 25	566 ± 30	561 ± 38
Protein, mg	25.9 ± 2.0	24.9 ± 1.4	26.0 ± 2.3
Cells x 10^{-5}	6.06 ±0.27	5.85 ± 0.26	5.70 ± 0.33
Cells x 10^{-5}/g	10.3 ± 0.3	10.4 ± 0.2	10.2 ± 0.2
UCP, mg	3.22 ± 0.552	3.11 ± 0.58	3.78 ± 0.39
UCP, mg/mg	123 ± 16.3	119 ± 18.1	145.3 ± 7.72
COX μmol/min	141.5 ± 19.4	140.6 ± 12.1	116.8 ± 9.4
COX μmol/min/mg	5.68 ± 0.86	5.70 ± 0.46	4.70 ± 0.49
UCP/COX ratio	24.8 ± 4.90	22.5 ± 4.6	33.8 ± 4.0

*$P < 0.05$ compared with sham-lesioned controls
There are no significant differences between restricted fed rats and NTS-lesioned rats.

Initial and final body weights

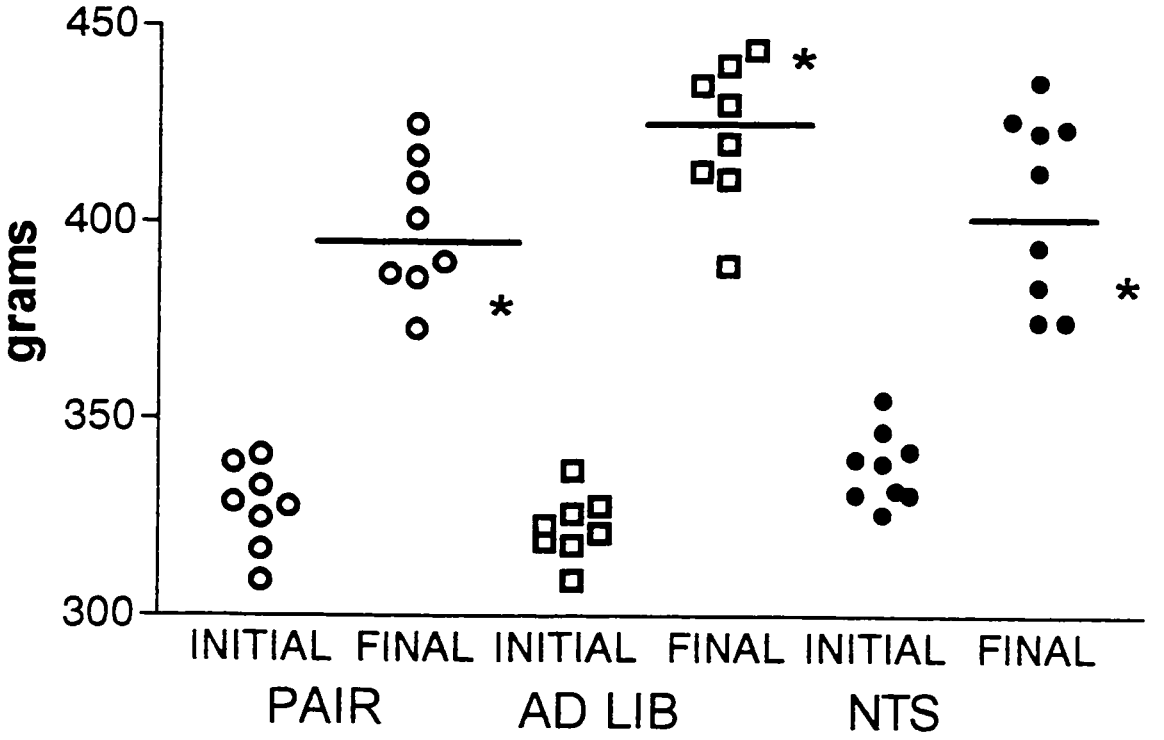

Figure 5.2: Initial and final body weights of original experimental rats. The lesioned rats clearly separated into two distinct groups based on their weight gain. The low group (n=4) gained 50.0 ± 2.27 g and had a final body weight of 382.5 ± 4.75 g, while the high group (n=5) gained 81.4 ± 3.59 g and had a final body weight of 424.4 ± 3.67 g (P =0.0002 for both). * denotes new experimental groupings.

Daily food intake

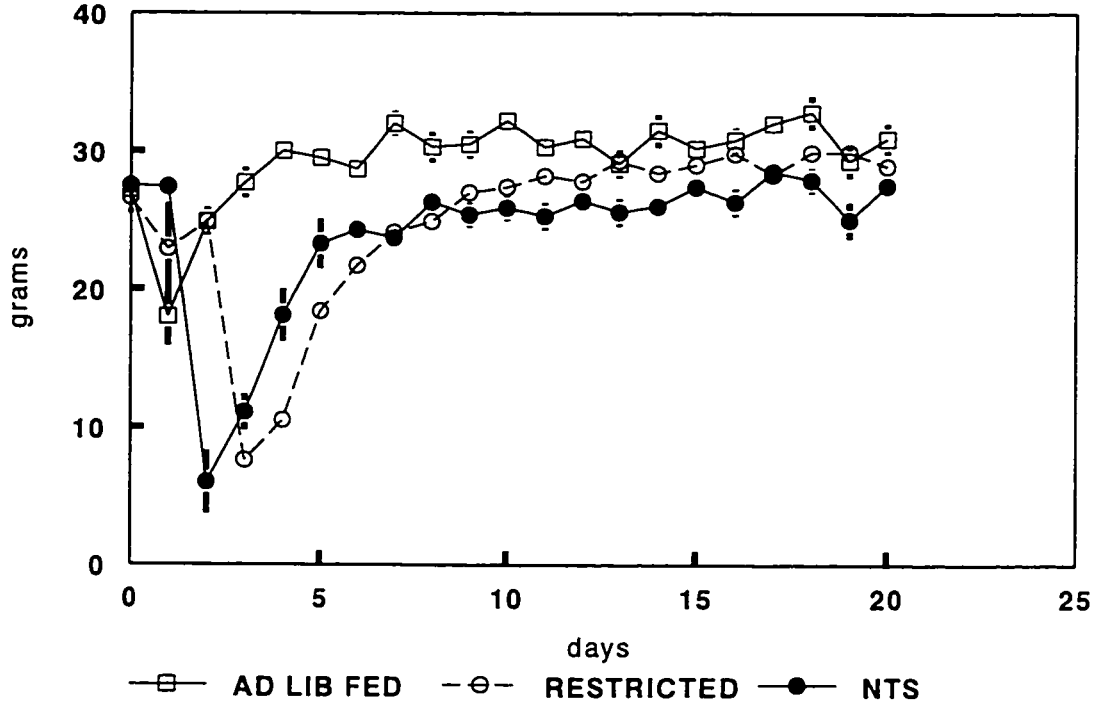

Figure 5.3: Daily food intake (grams of chow) of sham-lesioned (open squares), restricted-fed sham-lesioned (open circles) and NTS-lesioned (closed circles) rats. The sham-lesioned rats received lesions on day 0. The NTS-lesioned rats received lesions on day 1. Restricted-fed sham-lesioned rats received the mean amount eaten by all the ad libitum-fed NTS-lesioned rats the day before from day 3 to day 20.

Body weights/ body composition:

Body weights of the lesioned rats decreased substantially post-lesion and body weight gain of these rats and the restricted-fed sham-lesioned rats subsequently paralleled that of the ad libitum-fed sham-lesioned rats (Figure 5.4). Final body weights and overall body weight gain were less in the NTS-lesioned rats and the restricted-fed sham-lesioned rats than in the ad libitum-fed sham-lesioned rats (Table 5.2). Weight gain of NTS-lesioned rats was not significantly different from that of the restricted-fed sham-lesioned rats (Table 5.2). Final carcass fat content did not differ significantly between groups (Table 5.2).

White adipose tissue:

There was no significant difference in the weights of epididymal and retroperitoneal WAT depots between groups (Table 5.2). Protein content and cellularity (calculated from DNA content) of RWAT were also not altered by the lesion.

Interscapular brown adipose tissue:

IBAT was not significantly different in NTS-lesioned rats. Wet weight, protein content, cellularity, and UCP and COX contents were not altered by the lesion (Table 5.3). The ratio of UCP to COX content was also not significantly different between groups.

Body weight gain

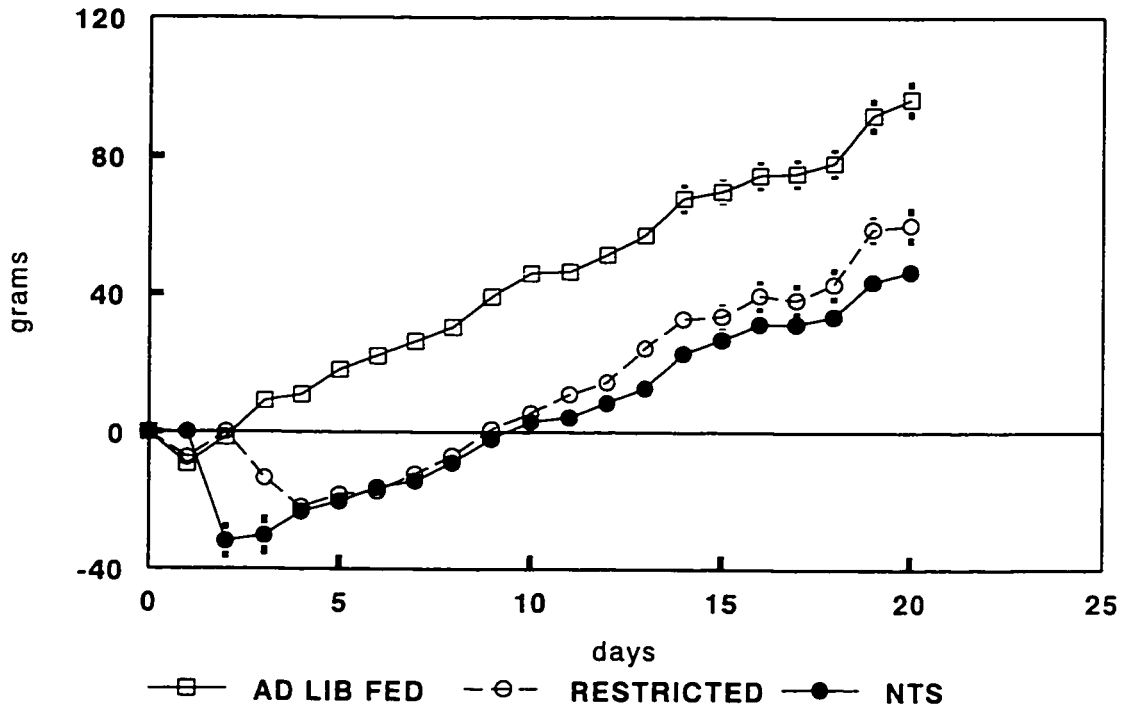

Figure 5.4: Body weight gain of sham-lesioned, restricted-fed sham-lesioned, and NTS-lesioned rats. Symbols are the same as in Figure 5.2. For sham-lesioned rats the gain is calculated from day 0. For NTS-lesioned rats the gain is calculated from the weight on day 1 when these rats were lesioned.

Table 5.2: Weights, weight gain, carcass fat, and WAT measures

	Sham-lesioned	Sham-lesioned Restricted-fed	NTS-lesioned
Number of animals	**(8)**	**(4)**	**(4)**
Body weight, grams			
Initial	323 ± 2.90	324 ± 3.76	332 ± 2.92
Final	423 ± 6.45	384 ± 3.76*	382 ± 4.53*
Gain	100 ± 5.69	60 ± 5.70*	50 ± 2.27*
Carcass fat, grams	20.2 ± 1.87	15.7 ± 0.97	15.1 ± 1.52
Carcass fat, %	4.75 ± 0.39	4.08 ± 0.25	3.94 ± 0.41
EWAT, g	3.86 ± 0.22	3.31 ± 0.18	3.30 ± 0.17
RWAT			
Wet weight, g	3.24 ± 0.29	2.57 ± 0.29	2.64 ± 0.33
Protein, mg	31.6 ± 2.63	27.8 ± 2.15	29.3 ± 3.28
Cells x 10^{-5}	8.87 ± 0.61	7.91 ± 1.08	10.12 ± 1.71

*P<0.05 compared with sham-lesioned controls
There are no significant differences between restricted fed rats and NTS-lesioned rats.

Table 5.3: Interscapular brown adipose tissue*

	Sham-lesioned	Sham-lesioned Restricted-fed	NTS-lesioned
Number of rats	**(8)**	**(4)**	**(4)**
Wet weight, mg	589 ± 25	590 ± 45.3	492 ± 41.7
Protein, mg	25.9 ± 2.0	25.4 ± 1.11	22.8 ± 1.10
Cells x 10^{-5}	6.06 ± 0.27	5.95 ± 0.34	5.14 ± 0.34
COX μmol/min	141.5 ± 19.4	125.1 ± 5.64	113.8 ± 20.05
UCP, mg	3.22 ± 0.552	3.47 ± 0.584	3.15 ± 0.281
UCP/COX ratio	24.8 ± 4.90	28.3 ± 5.68	30.8 ± 7.04

* There are no significant differences between groups.

Discussion

The main finding of this study was that the thermogenic capacity of BAT in NTS-lesioned rats was unchanged. There was no change in the weight, protein content, cellularity, content of mitochondria or content of UCP in BAT of the NTS-lesioned rats.

The reported reduced capacity of NTS-lesioned rats to respond to administered NA or isoproterenol by an increase in whole body oxygen uptake and by an increase in BAT temperature (Fyda *et al.* 1991) is not explained by our findings. In those experiments, NTS-lesioned rats displayed the expected impairment of the baroreflex arc, as shown by the lack of bradycardia in response to administration of phenylephrine (Fyda *et al.* 1991). However, since the baroreceptor-mediated suppression of BAT thermogenesis that would have been expected (Nagasaka *et al.* 1984; Shibata 1982) was not seen in the non-lesioned rats (Fyda *et al.* 1991), it is not clear whether this particular baroreflex arc was disrupted in the NTS-lesioned rats. The impaired thermogenic response of BAT to both isoproterenol and to NA in the NTS-lesioned rat (Fyda *et al.* 1991) cannot, however, in the light of our results, be attributed to atrophy of the BAT.

The suggestion of a loss of β_3-ARs (Fyda *et al.* 1991) would not be compatible with the down-regulation of these receptors by the sympathetic nervous system activity in BAT (Granneman & Lahners 1992) and the apparently normal trophic influence of the sympathetic nervous system on BAT in our NTS-lesioned rats, as judged from its normal thermogenic capacity. The reason for the lack of thermogenic response of BAT of the NTS-lesioned rat to β-AR stimulation (Fyda *et al.* 1991) remains unclear.

It is known that the hypothalamus can exert an apparently inhibitory influence on BAT thermogenesis (Woods & Stock 1994), mediated most probably by control of the vasculature of BAT and involving maintenance of arteriovenous anastomoses in the open state (Woods & Stock 1996a). This inhibitory influence prevents perfusion of the capillary bed supplying the BAT parenchymal cells (Woods & Stock 1996a), probably impairing the stimulatory influence of the hypothalamus on these cells. It is conceivable that this inhibitory influence prevails in the NTS-lesioned rat.

Perhaps of note in this context is that the pressor response to phenylephrine or NA is much greater in the NTS-lesioned rat (Fyda *et al.* 1991), reflecting perhaps lack of closure of the arteriovenous anastomoses and therefore a failure of opening of the capillary bed supplying the thermogenic parenchymal cells. Normally this capillary bed of IBAT experiences a 200-fold increase in blood flow when stimulated by NA (Foster *et al.* 1980), or by a spontaneous oscillation in sympathetic activity (Closa *et al.* 1993), and a 100-fold increase in the proportion of cardiac output directed through the BAT. The lack of the thermogenic response would thus be due not to lack of thermogenic capacity of the BAT but to prevention of any increase in oxygen supply to the stimulated parenchymal cells.

It is also possible, however, that the lesions produced by Fyda *et al.* (1991) differed from ours in causing more extensive damage to sensory afferents, sufficient to induce atrophy of BAT. The coordinates used in the two studies were the same but their lesions, induced with a current of 0.8 mA for 5 seconds, appear larger than ours, produced with a current of 0.5 mA for 5 seconds. Our lesions were quite well-limited to the NTS but in no

case destroyed the NTS totally. In view of the need of their rats, but not ours, for artificial respiration with oxygen and a concomitant extended period of anesthesia, a difference in the placement and size of the lesions is likely. Our lesions did, however, produce the anticipated loss of body weight, followed by resumption of normal growth rate but no catch-up growth (Hyde & Miselis 1983; Kott *et al.* 1984).

The NTS rats in this study differ from Cap-Des rats, which also sustain a lesion in the NTS but have atrophied BAT (Cui & Himms-Hagen 1992a; Cui & Himms-Hagen 1992b; Cui *et al.* 1990). The atrophy of BAT in the Cap-Des rat is thus unlikely to be due to a lesion in the NTS.

Another difference between the NTS-lesioned rat and the Cap-Des rat revealed by the present study is that NTS-lesioned rats, while weighing less than sham-lesioned rats, have a normal proportion of body fat whereas Cap-Des rats have a low proportion of body fat (Cui & Himms-Hagen 1992b; Himms-Hagen & Cui 1991; Melnyk & Himms-Hagen 1995), Chapter 4. The reduced body weight of the NTS-lesioned rats can be attributed to their failure to compensate for a period of markedly reduced food intake by catch-up growth; their body fat content is not altered.

It is important to note that Cap-Des induces a selective punctate chemical lesion in the NTS-lesioned rat (Castonguay & Bellinger 1987), whereas lesions induced surgically are much less selective regarding neuronal type damaged and produce more extensive abnormalities, even when induced in very well-defined brain areas.

In summary, the NTS lesions in our rats had no effect on the thermogenic capacity of BAT. Atrophy of BAT cannot explain the lack of thermogenic response of BAT to catecholamines seen by others in NTS-lesioned rats (Fyda *et al.* 1991) and an NTS lesion cannot explain the atrophy of BAT seen in the Cap-Des rat (Cui & Himms-Hagen 1992a; Cui & Himms-Hagen 1992b; Cui *et al.* 1990; Himms-Hagen & Cui 1991; Himms-Hagen *et al.* 1990), Chapter 4.

Chapter 6: Raising at thermoneutrality prevents obesity and hyperphagia in transgenic mice with partial ablation of BAT

Introduction

In obese rodent models, obesity is associated with atrophy of BAT (Himms-Hagen 1989a; Himms-Hagen 1990b). BAT thermogenesis is a component of energy balance (Himms-Hagen 1989b). All genetic and acquired forms of rodent obesity are characterized by a decrease in sympathetic nervous system activity in BAT (Himms-Hagen 1991). It has not been possible to ascertain a direct role of BAT in the development of obesity by its surgical removal or denervation as this tissue is present in many discrete depots throughout the body and it has a great capacity to regenerate and hypertrophy. To address this problem (Lowell *et al.* 1993), created mice with genetically ablated BAT by using a "suicide DNA vector" in which the UCP promoter drives the BAT specific expression of DTA. The vector was constructed from a UCP-1 minigene (Boyer & Kozak 1991), shown to be expressed exclusively in BAT. The DTA was inserted into the first exon at position +120 bp, and precedes the UCP start codon at +232 bp (Lowell *et al.* 1993).

UCP-DTA transgenic mice have a partial ablation of brown adipocytes (Lowell *et al.* 1993), become obese at a very early age, and later hyperphagic (Lowell *et al.* 1993). It has been shown that BAT produces leptin at birth (Dessolin *et al.* 1997). The authors suggest that it is involved in the regulation of food intake at this point in development; this could possibly contribute to the early onset of obesity in the UCP-DTA mice. Eventually the UCP-DTA

mice become massively obese, and have insulin resistance, hyperglycemia, hyperinsulinemia, and hyperlipidemia characteristic of noninsulin-dependent diabetes mellitus (Hamann *et al.* 1995; Hamann *et al.* 1996).

When fed a high fat diet (41% of calories from fat) from the time of weaning, UCP-DTA mice remain hyperphagic and exhibit the usual increased efficiency of deposition of body fat characteristic of animals eating such a diet (Hamann *et al.* 1996). UCP-DTA mice also overexpress TNFα (Hamann *et al.* 1995) and leptin (Frederich *et al.* 1995b) in their WAT. Their obesity and hyperphagia are not prevented by leptin treatment (Hamann *et al.* 1997). In contrast to *ob/ob* and *db/db* mice, they do not exhibit hypercorticosteronemia, are not stunted, and are fertile (Frederich *et al.* 1995b; Lowell *et al.* 1993; Lowell *et al.* 1996).

The development of obesity following BAT ablation was predicted by the hypothesis that mice would suffer from a deficit in energy expenditure (Lowell *et al.* 1993). The hyperphagia seen in these mice was unexpected, and suggests a role for BAT in the control of food intake. BAT thermogenesis has been hypothesized to play a regulatory role in the control of meal size in animals living at temperatures at which BAT thermogenesis is required for thermoregulation (below thermoneutrality). This hypothesis predicts a failure to terminate meals normally, and therefore overeating, when BAT function is impaired. It has been developed based on the hyperphagia of the UCP-DTA mice and on the literature (Himms-Hagen 1995).

When normal mice live at the environmental temperatures usually used for rodents in animal care facilities (21-24°C) they are partially cold-acclimated. The sympathetic

nervous system activity in their BAT is much higher than in mice living at 35°C (Romsos *et al.* 1985; Zaror-Behrens & Himms-Hagen 1983), and their BAT has a much greater content of UCP than that of mice living at a thermoneutral environmental temperature (between 32-35°C; (Ashwell *et al.* 1983)).

To determine whether the development of both obesity and hyperphagia in the UCP-DTA transgenic mouse was due to lack of BAT thermogenesis and not to another impairment, we raised mice at thermoneutrality (35°C). At this temperature, the external stimulus of cold on BAT thermogenesis is removed. This would annul the deficit in BAT thermogenesis that occurs when the mice are raised at 21-24°C and would prevent both the development of the obesity and the hyperphagia.

Objectives

The objective of this study was to obviate any deficit in BAT thermogenesis by raising transgenic and control mice at thermoneutrality, where both would have equally inactive BAT, to see whether this would prevent the obesity and hyperphagia.

Materials and methods

Animals:

A colony of UCP-DTA mice was established with six female UCP-DTA mice (provided by Dr. Bradford B. Lowell, Beth Israel Hospital and Harvard Medical School, Boston, MA) and six male FVB/N mice (from Taconic, Germantown, NY). Female transgenic mice were heterozygous for the UCP-DTA transgene. Breeding pairs were housed

at 24°C with free access to food (Agway R-M-H 4020 chow, 14.5 % of energy from fat) and water and lights on for 12 hours per day.

Pups were weaned at 19-21 days of age, and were housed with littermates of the same sex until used.

Experimental setup:

Some male mice were killed at 3 weeks (wks) of age. At weaning (at exactly 3 wks) other male mice were separated into groups of the same genotype and housed at 24°C or in a transparent incubator maintained at 35°C in the same room for the next 5 wks (usually 3 mice per cage, although occasionally a mouse was alone in a cage for a short time until other mice in the colony were weaned). These mice were killed at 8 wks of age.

Body weight determination:

Body weights were measured twice weekly.

Food intake determination:

Food intake was measured twice weekly. Food eaten was divided by the number of age and genotype-matched mice in cage. Mice had free access to food (Agway R-M-H 4020 chow, 3.5 kcal/g, 14.5 % energy from fat) and water.

Termination:

At 3 or 8 wks of age, mice were killed by cervical dislocation and exsanguination. IBAT and four WAT depots (EWAT, RWAT, inguinal {INWAT} and mesenteric {MWAT}) were removed and weighed. The tissues were processed as listed below, the remaining tissue was reweighed and frozen at -80°C for later analysis.

Tissue processing:

White adipose tissue: Osmium fixation and analysis of adipocyte number and size were performed on samples of INWAT as outlined in Chapter 3 (Hirsch & Gallian 1968). The remaining tissue was frozen for later analysis.

White adipose tissue assays: INWAT was thawed on ice and homogenized. DNA and protein were measured on homogenates.

Brown adipose tissue: IBAT was dissected away from adhering white adipose tissue and muscle, and then weighed. Samples were fixed in glutaraldehyde for semi-thin sectioning. The remaining BAT was weighed and frozen at -80°C.

Analyses of BAT and its activity: IBAT was thawed on ice and homogenized in ice-cold isolation medium as outlined in Chapter 3. Samples of homogenate were frozen in liquid nitrogen and stored at -80°C for later assays.

UCP was measured by a solid-phase radioimmunoassay as before (Himms-Hagen *et al.* 1994) with the use of mouse UCP as a standard. The UCP/cytochrome oxidase ratio ($\mu g.\mu mol^{-1}.min^{-1}$) was calculated as a measure of the concentration of UCP in BAT mitochondria.

Histology:

Separate groups of control or DTA mice were maintained at 35°C or at 24°C from weaning to 8 wks of age, or alternatively sacrificed at weaning as above. Samples of IBAT and INWAT were fixed in a volume of 10% buffered formalin roughly 10 times the tissue size. These samples were then embedded in paraffin, and sectioned for light microscopy as described in Chapter 3.

Serum assays:

Cholesterol and triacylglycerol were measured by enzymatic assays using Sigma diagnostic kits as before (Lowell *et al.* 1993). Serum leptin was measured using a mouse leptin RIA kit from LINCO Research, Inc. (CEDARLANE Laboratories Ltd.).

Carcass analysis:

Carcasses were autoclaved, then homogenized in water in a Waring heavy-duty commercial blender. Lipid content of samples was measured after Soxhlet extraction with petroleum ether. Lipid content of the WAT depots removed was assumed to be 90 % of the wet weight, and this amount was added to the estimate of carcass fat.

Data presentation and analysis:

All data are expressed as means ± SEM. Instat software was used for analysis of variance followed by Tukey-Kramer post hoc tests.

Genotyping of transgenic mice

Isolation of genomic DNA from mouse tails:

The method used for genotyping control and transgenic mice was modified from that outlined in (Bothwell *et al.* 1990).

One centimetre of tail was put into a microfuge tube with 500 μl of Sodium-Tris-EDTA (STE: 100 mM NaCl, 20 mM Tris; pH 7.5, 10 mM EDTA, 1% SDS) and 25 μl Proteinase K (10 mg/ml in water). For digestion an incubation of 5 hours to overnight at 55°C with shaking was used.

After the incubation, 500 μl of phenol (tris-equilibrated)[1] was added. The tubes were mixed gently, incubated for one hour, centrifuged in a microcentrifuge, and the aqueous phase was removed. To the aqueous phase (in a fresh tube), 500 μl of phenol:chloroform[2] was added, mixed gently, incubated for one hour, and centrifuged in a microcentrifuge. The aqueous phase was removed and the above step was repeated with 500 μl of chloroform.

Two volumes (1 ml) of isopropanol were used to precipitate the DNA, after which it was washed with 70% ethanol. The precipitates were dried using a Speed Vac Concentrator

---

[1] The phenol was equilibrated as in Maniatis *et al.* (1982) with 0.1 M Tris (2-3 times or until the pH of the aqueous phase was near 8.0). This was done after adding 0.1% hydroxyquinoline to the melted phenol.

[2] The chloroform used was chloroform:isoamyl alcohol in the ratio of 24:1 according to standard protocols.

(Savant, Farmingdale NY), and then dissolved in 200-300 μl Tris-EDTA (TE: 10 mM Tris, 1 mM EDTA) with 1/10 volume of sodium acetate (NaOAc, pH 5.2).

To clean the DNA further, it was reprecipitated with 2 volumes of ethanol, washed with 70% ethanol and dried again in a Speed Vac. Two hundred μl of TE were used to dissolve the DNA. The concentration of DNA in each tube was approximately 1 μg/μl as determined spectrophotometrically using the A_{260}/A_{280} ratio. Absorbances were measured by taking 3-4 μl of the redissolved DNA samples in 500 μl TE (with TE as a blank) in a Beckman DU-65 spectrophotometer.

Digestion/electrophoresis of DNA:

5-7 μl of each sample ($\leq$ 10 μg DNA) were used for digestion with Pst I (~ 23 units), the samples were left to digest for 3 hours at 37°C. Loading buffer (6X :0.25% bromophenol blue, 0.25% xylene cyanol, 30% glycerol in water, 4°C) was added to the samples, they were warmed to 50°C, and left on ice until loading.

The digested samples and their undigested controls were run on a 1% agarose gel, in (1.14 M Tris-acetate, 0.001 M EDTA) with fluorescein-11-labeled λ-Hind III markers.

The gels were run for 90 minutes at 70 V, or until the bands of the loading buffer separated the gel into thirds. Following electrophoresis, the gel was stained with ethidium bromide, photographed to confirm digestion of the DNA, destained in water, and then denatured in 0.4 N NaOH.

Southern analysis of DNA:

DNA was transferred onto nylon membranes (Hybond-N) by capillary transfer as in (Maniatis *et al.* 1982), with 0.4 N NaOH overnight. The gel was stained again with ethidium bromide, to ensure that all DNA had transferred.

Neutralization of the membrane was achieved by washing in 2 x SSC (NaCl, sodium citrate, NaOH, pH 7.0), after which it was cross linked in a Strata linker (automode).

Probe:

The probe was supplied by Dr. B. B. Lowell in the pUC plasmid (selection was ampicillin). Expansion of the plasmid was effected in DH5α cells (were transfected and grown up on agar). After the selection of cells that had taken up plasmid, DNA was isolated. The plasmid was digested with Kpn 1 and Hind III to free the insert. This generated 3 bands: the 3.2 kb plasmid backbone, a 1.8 kb UCP genomic sequence 5' to Kpn I site and a 0.9 kb UCP genomic sequence 3' to Kpn I site (Figure 6.1).

The digest was run on an agarose gel, ethidium bromide stained, and the separated insert was cut out of the gel. The 0.9 kb fragment was gel purified using a Qiagen gel extraction kit (QIAquick).

The probe was labeled using the Fluorescein Gene Images™ random prime labeling module (RPN 3540 Amersham). In this system, the probe is labeled with a hapten (fluorescein), and alkaline phosphatase is introduced later as an anti-fluorescein alkaline phosphatase conjugate. Fluorescein is incorporated into the probe as fluorescein-11-dUTP.

pUC Plasmid with UCP insert

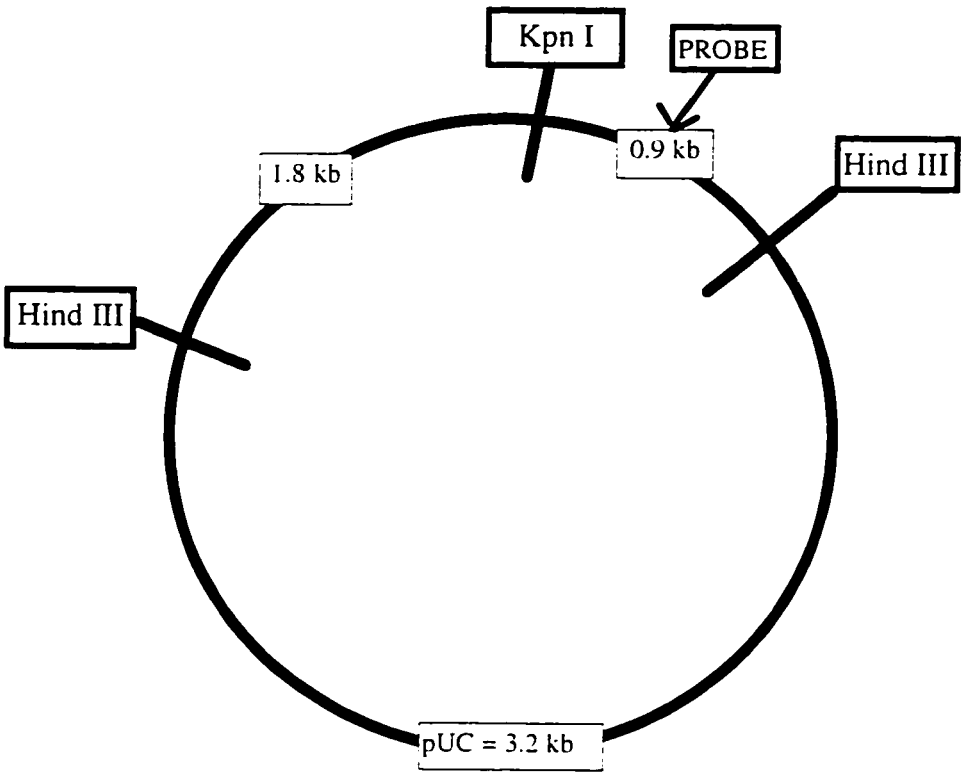

Figure 6.1: Diagram of pUC plasmid with UCP insert. Plasmid with insert supplied by Dr. BB Lowell. Digestion with Kpn I and Hind III generated 3 bands: the 3.2 kb plasmid backbone, a 1.8 kb UCP genomic sequence 5' to Kpn I site and a 0.9 kb UCP genomic sequence 3' to Kpn I site.

Hybridization:

The hybridization steps followed the protocol in the Fluorescein Gene Images™ dioxetane detection module (RPN 3510 Amersham) with slight modifications. All hybridizations were carried out in a hybridization chamber.

Hybridization buffer (5X SSC, 0.1% SDS, 5% dextran sulfate {10% solution in water}, and 5% (v/v) liquid block supplied in kit) was used for pre-hybridization of the membrane. This step was carried out for one hour at 60°C.

The membrane was hybridized overnight at 60°C. Approximately 200 ng of labeled probe (10 μl) was boiled and chilled before adding to 20 ml of hybridization buffer.

The next day, the membrane was washed twice in 1X SSC, 0.1% SDS for 15 minutes. These were followed by two washes in 0.5X SSC, 0.1% SDS, for 15 minutes each. All of the washes were carried out with shaking at 60°C. The total volume of all washes was 500 ml.

Detection:

For detection, the membrane was washed first in diluent buffer (100 mM Tris HCl, 300 mM NaCl, pH 7.5). The diluent buffer was prepared fresh and autoclaved to eliminate any exogenous alkaline phosphatases that would interfere with the signal generation.

Next the membrane was blocked with liquid block (which was supplied in the kit) 1:10 in diluent buffer, for 60 minutes at room temperature with shaking. Following blocking, the membrane was rinsed in diluent buffer.

The alkaline phosphatase conjugated anti-fluorescein antibody was diluted 1:5000 in diluent buffer + 0.5%BSA and incubated with the membrane for 60 minutes at room temperature with shaking. After this, the membrane was washed three times in diluent buffer + 0.3% Tween for 10 minutes each wash, at room temperature with shaking.

At this stage, the digested genomic DNA is immobilized on the membrane. The fluorescein labeled probe is specifically bound to the UCP sequence. Anti-fluorescein alkaline phosphatase conjugate is bound specifically to the fluorescein and therefore indirectly to the UCP sequence.

Diluent buffer was used to rinse the membrane, and all excess liquid was drained off. A plastic folder was provided in which to place the membrane, after which it was sprayed with liquid dioxetane. The plastic was folded over to cover the membrane, and the dioxetane was spread evenly over the surface.

Chemiluminescence is based on the production of light by a chemical reaction (see Figure 3.3). Alkaline phosphatase catalyzes a chemiluminescent reaction with dioxetane and the resulting signal is captured on light sensitive film. The membrane was transferred to SaranWrap™ and exposed to Hyperfilm-MP in a Kodak X-Omatic cassette. Exposure times varied; either 1-2 hours immediately, or for 4-16 hours after a delay of a few hours. The films were developed using an automated system.

Genotype was determined by the bands present after detection. The wild-type UCP gene showed one band of 3.3 kb, while the transgene showed up as a 3.2 kb band (Figure 6.2). Accordingly, control mice exhibited one band of 3.3 kb; the heterozygous transgenic mice used in this experiment exhibited 2 bands, one of 3.3 kb and one of 3.2 kb.

Wild-type and transgenic UCP genes

WILD TYPE:

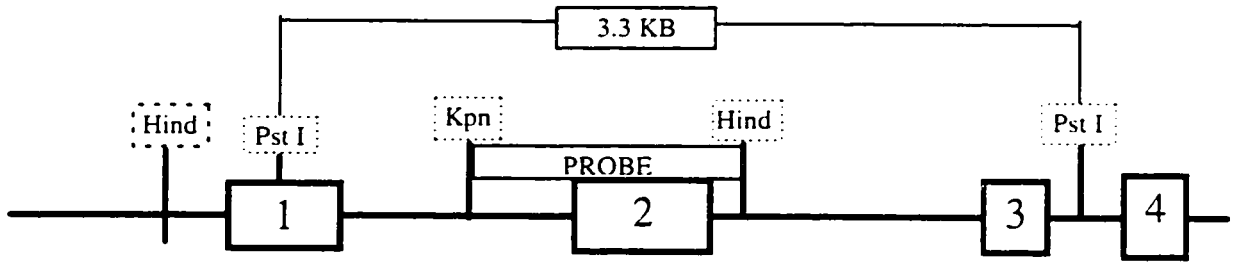

TRANSGENE:

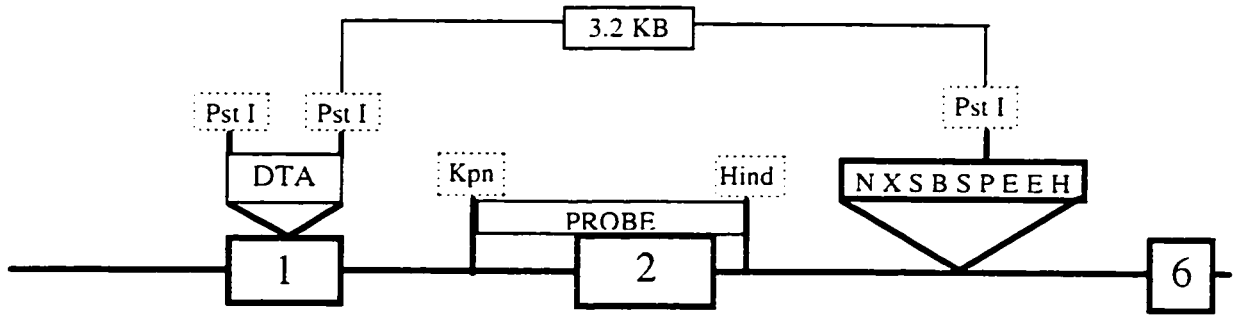

Figure 6.2: Diagram of probe interaction with the wild-type and transgenic UCP genes. Transgenic animals are heterozygous and show two bands on the Southern blot (3.2. and 3.3 kb). Control animals show one band of 3.3 kb.

Results

Body weights and food intake:

Weight gain was similar in control and transgenic mice up to 5 wks of age when they were raised at the usual animal facility temperature of 24°C. After this age the body weights of transgenic mice exceeded those of control mice (Figure 6.3). The weight gain of the transgenic mice raised at 35°C paralleled that of the control mice at this temperature during the entire period of study (Figure 6.3). Weights of all mice raised at 35°C were not different from those of control mice raised at 24°C (Figure 6.3).

Food intake was similar in control and transgenic mice up to 4 wks of age when they were raised at 24°C, but the food intake of transgenic mice exceeded that of control mice after this age (Figure 6.4). Housing control mice at 35°C reduced their food intake to 50% of that of control mice at 24°C (Figure 6.4). Transgenic and control mice housed at 35°C ate the same low amount, only 40% of that eaten by the hyperphagic transgenic mice at 24°C.

Growth of mice from 3 to 8 weeks of age

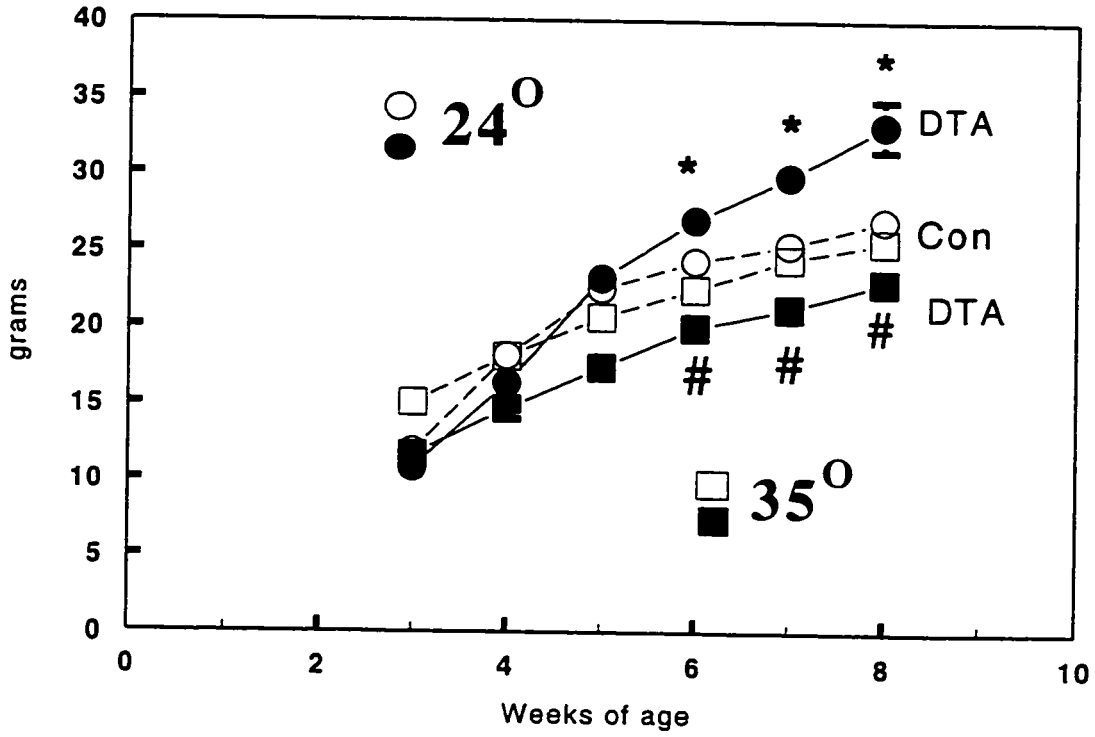

Figure 6.3: Growth of mice from 3 to 8 wks of age. Control (CON) mice, open symbols; transgenic (DTA) mice, solid symbols. Mice at 24°C, circles; mice at 35°C, squares. Numbers of mice: CON at 24°C, 18; DTA at 24°C, 16; CON at 35°C, 14; DTA at 35°C, 11. Means ± SEM for weekly body weights. Body weights of mice killed at 3 wks of age were CON 11.9 ± 0.55 g (n=10) and DTA 9.0 ± 0.41 g (n=10). Body weights of transgenic mice at 24°C are significantly greater than those of control mice at 24°C at 6 wks and older. There are no significant differences in body weights of control and transgenic mice at 35°C.
* denotes a significant effect of transgene, # denotes a significant effect of temperature

Food intake of mice from 3 to 8 weeks of age

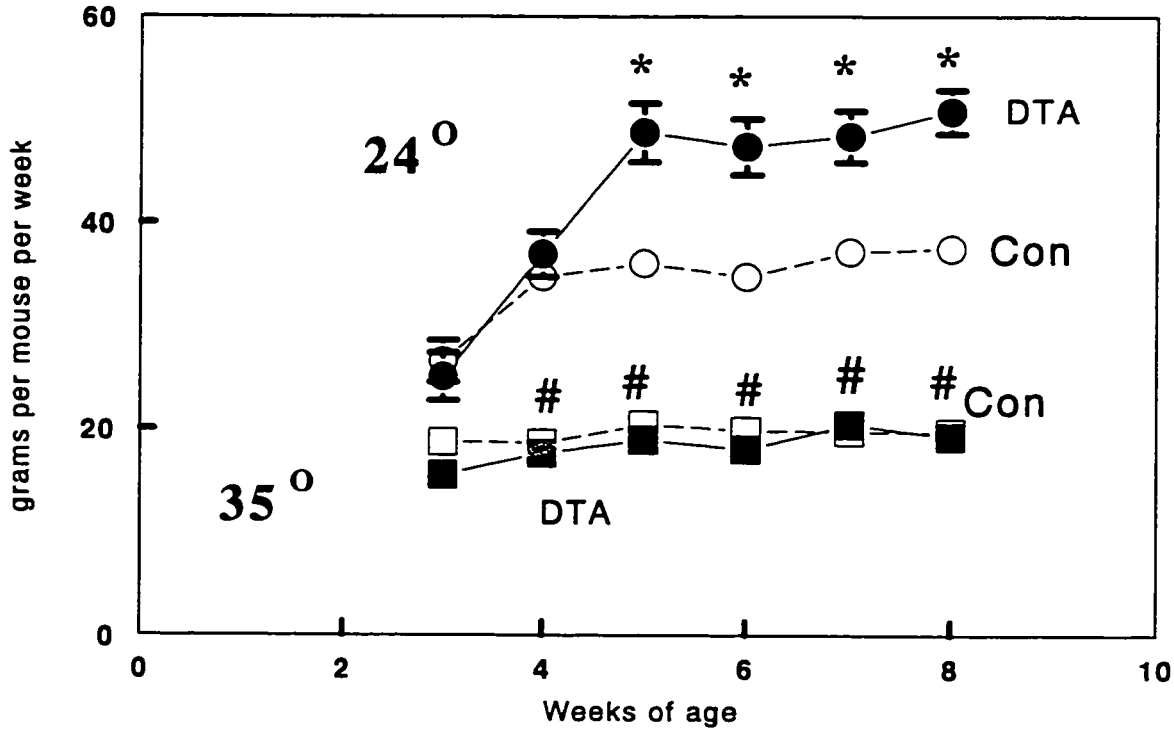

Figure 6.4: Food intake of mice from 3 to 8 wks of age. Control (CON) mice, open symbols; transgenic (DTA) mice, solid symbols. Mice at 24°C, circles; mice at 35°C, squares. Same mice as represented in Figure 6.3. Numbers of mice as in Figure 6.3. Means ± SEM for weekly food intake. Food intake of transgenic mice at 24°C is significantly greater than that of control mice at 24°C from 5 wks of age. There are no significant differences between control and transgenic mice at 35°C.
* denotes a significant effect of transgene, # denotes a significant effect of temperature

Serum measurements:

Serum leptin was four times higher in 8 wk old transgenic mice at 24°C compared with controls (8.57 ng/ml ± 2.25 vs. 2.28 ± 0.25 ng/ml, $P<0.001$; Figure 6.5). At 3 wks of age, transgenic mice already have leptin levels double those of the controls. Leptin did not change significantly with age over the five wks studied. When transgenic mice are raised at thermoneutrality, no differences in the serum leptin are seen when compared to control mice at any age or temperature. No change in serum leptin was seen with age, nor with temperature in the control mice.

There were no differences in either serum cholesterol concentration or in serum triacylglycerol concentration between transgenic and control mice at any age or temperature (Table 6.1).

Effect of thermoneutrality on serum leptin in mice

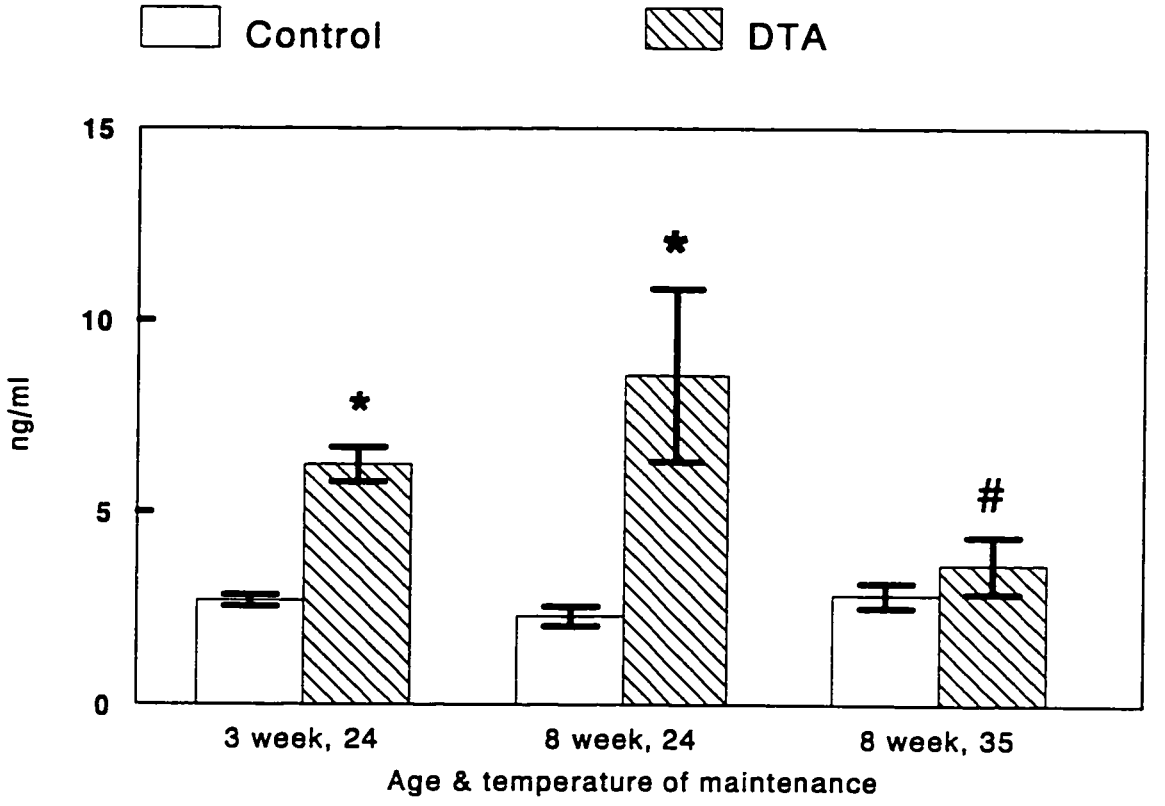

Figure 6.5: Serum leptin concentration of mice. Control mice, open bars; transgenic mice, hatched bars. Leptin of 8 wk old transgenic mice was higher than controls at 24°C. The serum leptin of UCP-DTA mice at 35°C is not different from that of control mice at any age or temperature. No change in serum leptin was seen with age, nor with temperature in the control mice. Difference between 3 wk old transgenic mice and 3 wk old control mice (6.24 ± 0.45 ng/ml vs. 2.68 ± 0.14 ng/ml) did not reach statistical significance; however, an unpaired t-test revealed a statistically significant difference ($P<0.0001$) between these two values.

* denotes a significant effect of transgene, # denotes a significant effect of temperature

Table 6.1: Serum cholesterol and trigylcerides

		Serum Cholesterol (mg/dL)†	Serum Triglycerides (mg/dL)†
3 week, 24°C	CON	113.61 ± 2.24	131.1 ± 9.37
	DTA	125.06 ± 8.91	104.17 ± 12.11
8 week, 24°C	CON	178.22 ± 4.31	222.23 ± 19.23
	DTA	164.59 ± 5.9	253.89 ± 17.46
8 week, 35°C	CON	146.53 ± 3.76	241.06 ± 11.86
	DTA	139.05 ± 6.23	203.47 ± 15.28

† There were no differences in serum cholesterol concentrations or serum triacylglycerol concentrations between the groups of mice.

Development of obesity:

Carcass analysis showed the expected development of obesity in the 8 wk old transgenic mice raised at 24°C, with twice as much carcass fat as control mice at the same age and temperature (Figure 6.6). Transgenic mice were not obese at 3 wks of age (Figure 6.6). Raising transgenic mice at 35°C completely prevented the development of obesity at 8 wks of age (Figure 6.6). A normal age-associated increase in body fat occurred in both control and transgenic mice raised at 24°C (Figure 6.6).

Weights of all four WAT depots studied were much greater in the 8 wk old transgenic mice raised at 24°C than in 8 wk old control mice at this temperature (Figure 6.7). Raising transgenic mice at 35°C completely prevented the exaggerated increase in the weight of all four WAT depots between 3 and 8 wks of age (Figure 6.7).

Transgenic mice housed at 24°C had hypertrophic obesity. The adipocyte number in the INWAT was normal but adipocyte size was increased (Figure 6.8, 6.9). This increase in the size of the adipocytes was prevented in transgenic mice raised at 35°C (Figure 6.9). (Adipocyte size and number could not be assessed in the 3 wk old mice because not enough tissue was available). The enlarged INWAT depot of transgenic mice raised at 24°C (Figure 6.7) also had more total cells (from DNA assay) (Figure 6.10) and more total protein (Figure 6.11) than that of control mice. These changes were not seen in the transgenic mice raised at 35°C (Figures 6.7, 6.9, 6.10, 6.11).

Carcass fat of control and transgenic mice

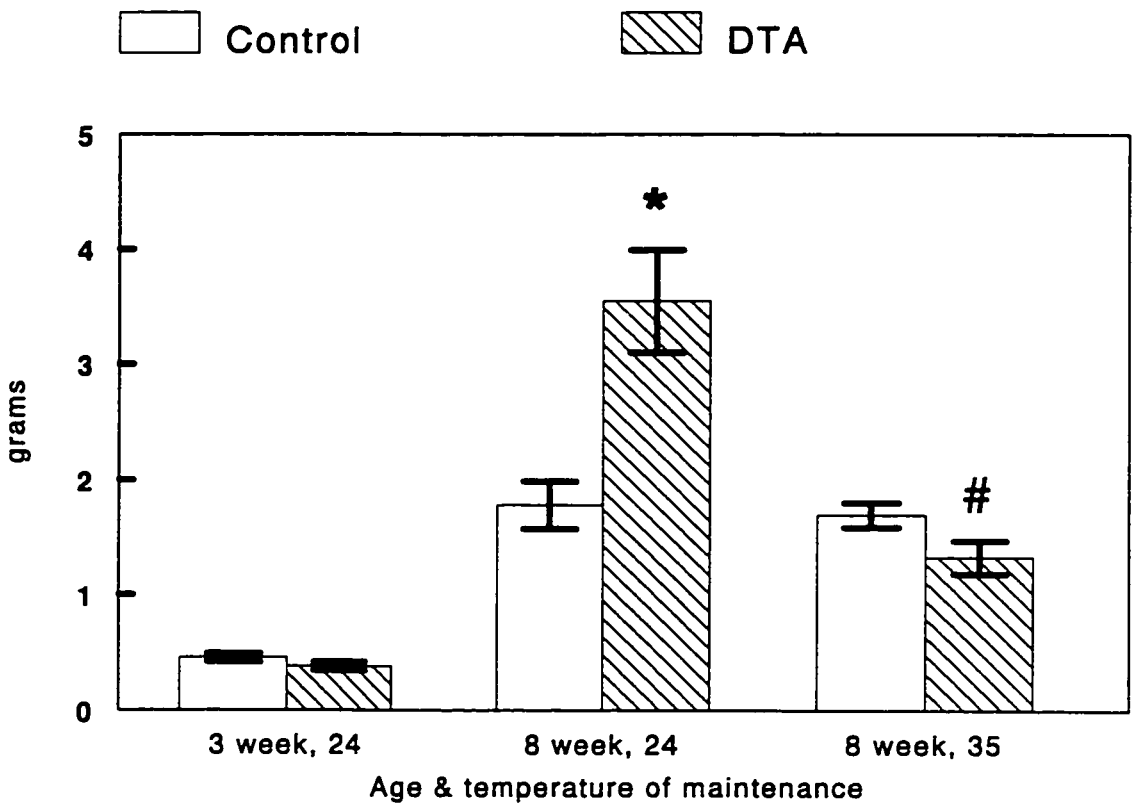

Figure 6.6: Carcass fat weight as determined by Soxhlet extraction. Control mice, open bars; transgenic mice, hatched bars. Total carcass fat is significantly greater in 8 wk old transgenic mice at 24°C than in 8 wk old control mice at 24°C ($P>0.001$). There are no other significant differences between control and transgenic mice at the same age and temperature. Body fat increased with age (8 vs 3 wks) and was not influenced by temperature in control mice. Body fat also increased with age in transgenic mice, but was significantly lower in transgenic mice at 35°C than in transgenic mice at 24°C.

* denotes a significant effect of transgene, # denotes a significant effect of temperature

Weight of four white adipose tissue depots

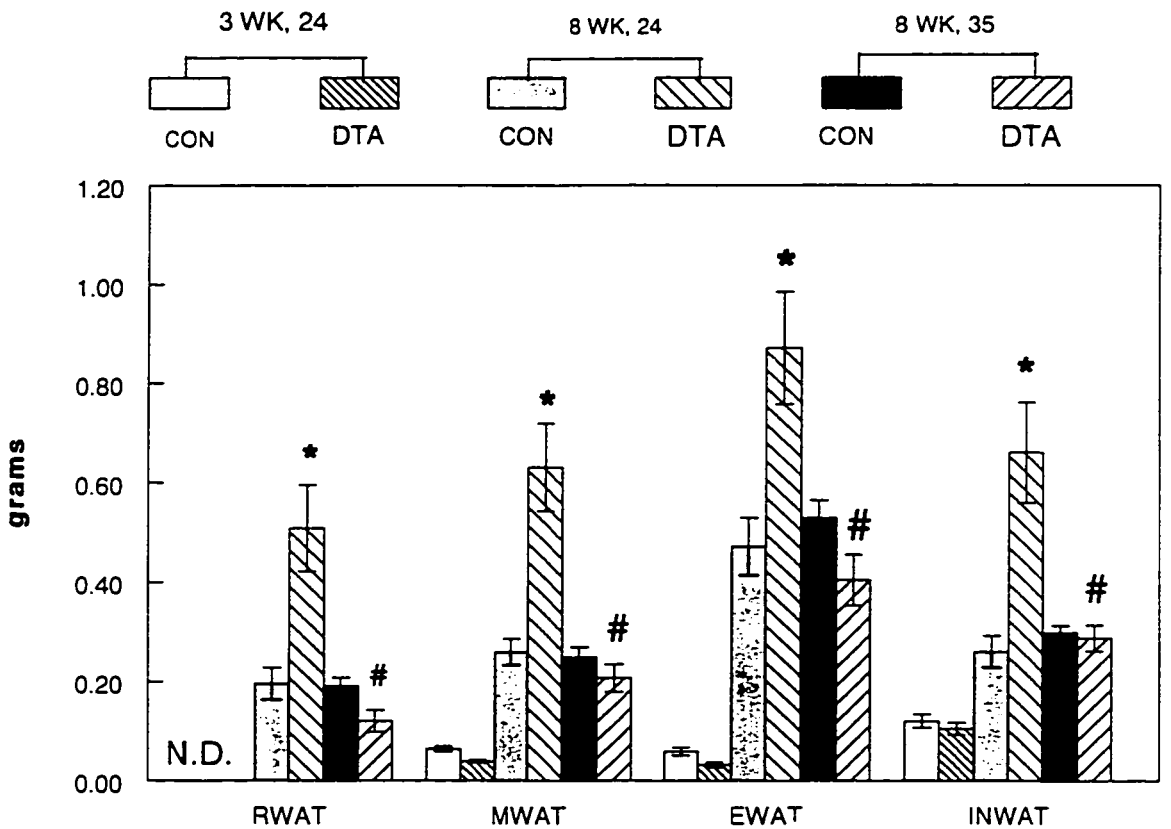

Figure 6.7: Weight of four white adipose tissue depots. RWAT, MWAT, EWAT, and INWAT. Weights of all four WAT depots were significantly greater in 8 wk old transgenic mice raised at 24°C compared with control mice at this age and temperature. Raising transgenic mice at 35°C completely prevented the increase seen in WAT weight between 3 and 8 wks of age. No difference was seen in WAT weights at 3 wks of age.
N.D. not done.
* denotes a significant effect of transgene, # denotes a significant effect of temperature

Number of white adipocytes in inguinal white adipose tissue

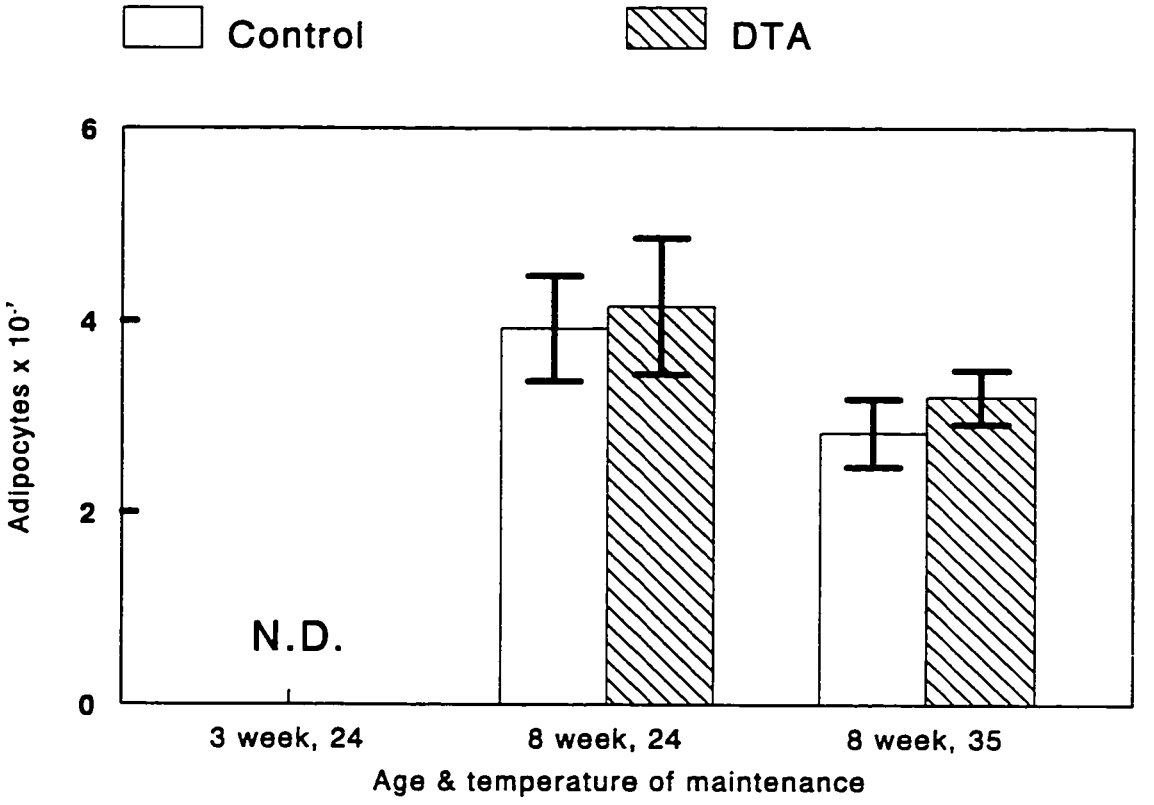

Figure 6.8: Number of white adipocytes in inguinal white adipose depot. Control mice, open bars; transgenic mice, hatched bars. N.D., not done because too little tissue was available. There are no significant differences in white adipocyte number.

Size of adipocytes in inguinal white adipose tissue

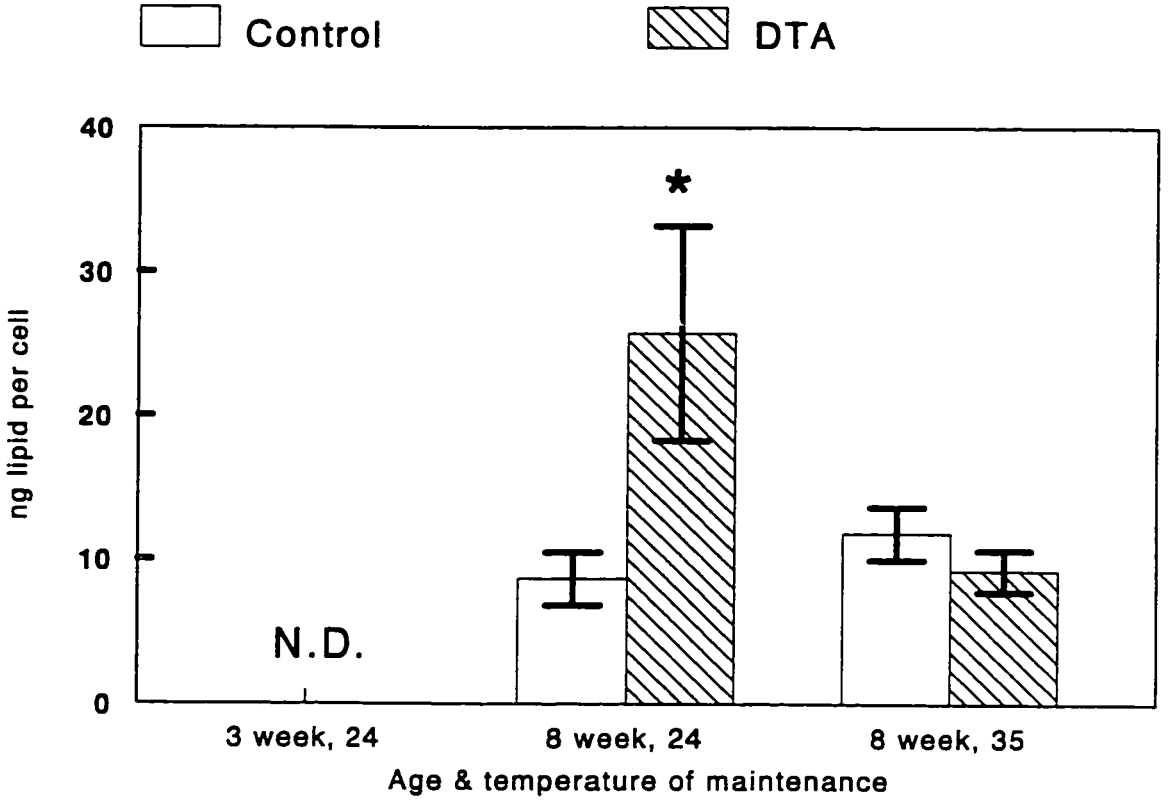

Figure 6.9: Size of white adipocytes in inguinal white adipose depot. Control mice, open bars; transgenic mice, hatched bars. N.D., not done because too little tissue was available. Adipocyte size is significantly greater in 8 wk old transgenic mice at 24°C than in 8 wk old control mice at 24°C ($P<0.05$). There is no difference in adipocyte size between 8 wk old transgenic mice at 35°C and 8 wk old control mice at 35°C.
* denotes a significant effect of transgene.

Total number of cells in inguinal white adipose tissue

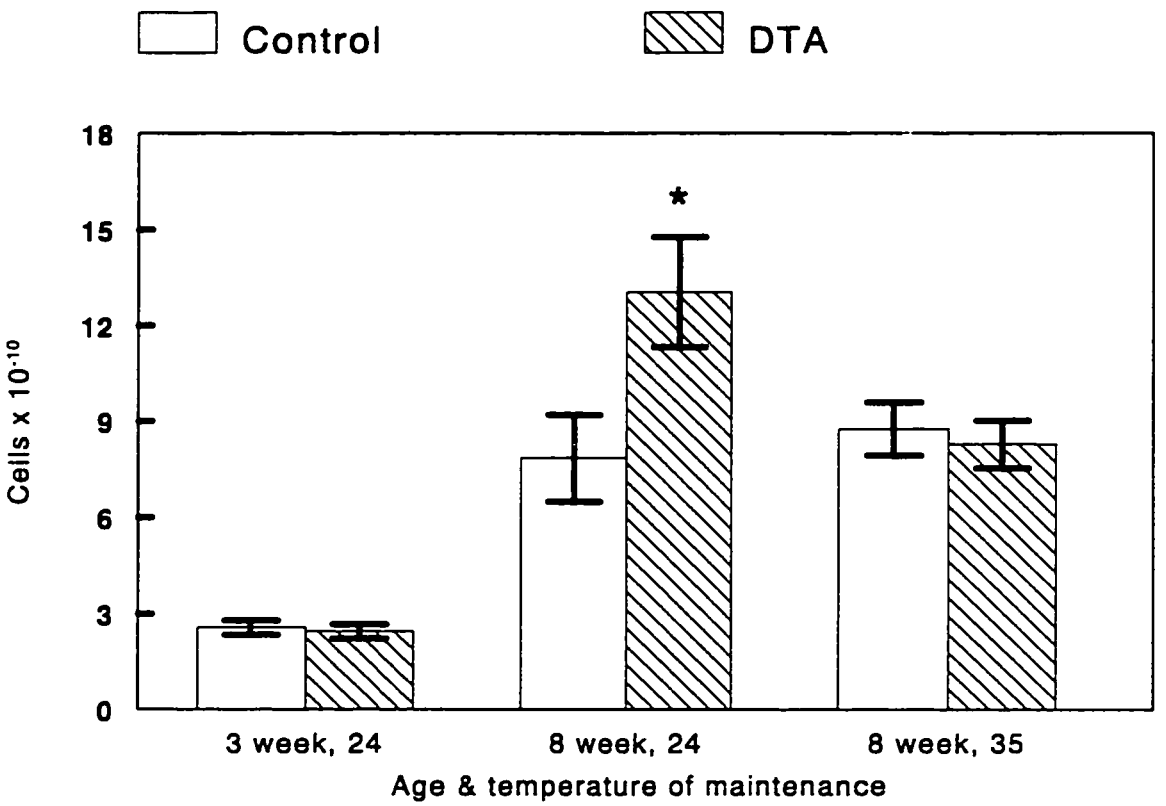

Figure 6.10: Total number of cells (from DNA content) in INWAT. Control mice, open bars; transgenic mice, hatched bars. Total number of cells (this means all cell types, not only adipocytes) is significantly greater in transgenic mice at 24°C than in control mice at 24°C ($P<0.05$) and in all 8 wk old mice compared with 3 wk old mice. There are no differences between 8 wk old control mice at 24°C, 8 wk old control mice at 35°C, and 8 wk old transgenic mice at 35°C.
* denotes a significant effect of transgene.

Total protein content of inguinal white adipose tissue

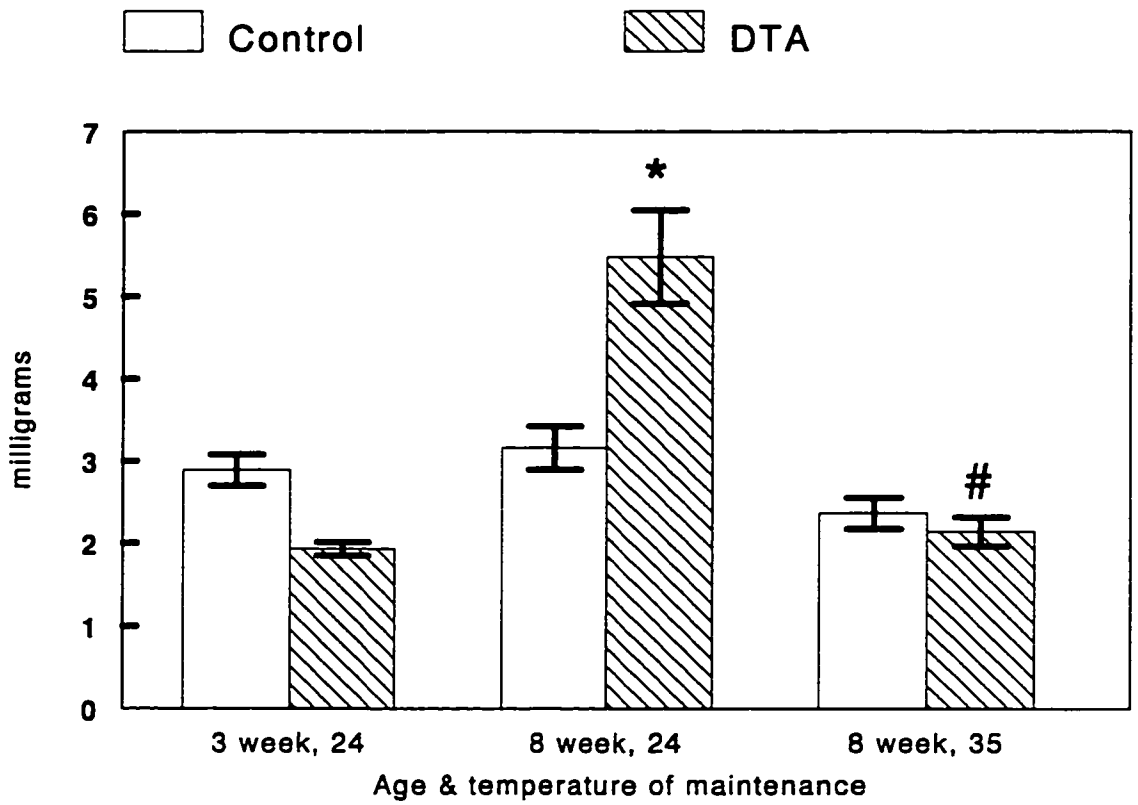

Figure 6.11: Total protein content of inguinal white adipose tissue depot. Control mice, open bars; transgenic mice, hatched bars. Protein content is significantly greater in 8 wk old transgenic mice at 24°C than in 8 wk old control mice at 24°C ($P<0.001$), than in 3 wk old transgenic mice, or in 8 wk old transgenic mice at 35°C ($P<0.001$ for each). There are no other significant differences.
* denotes a significant effect of transgene, # denotes a significant effect of temperature

Histology of inguinal white adipose tissue:

There was no difference in appearance of INWAT between control and transgenic mice at 3 wks of age (Figures 6.12 and 6.13; A, B). Multilocular adipocytes are visible among the unilocular white adipocytes (Figures 6.12, 6.13; A, B), and these are positive for UCP (Figure 6.13 A, B).

When the mice were raised at 24°C, by 8 wks of age the appearance of INWAT in control and transgenic mice is significantly different (Figures 6.12, 6.13; C, D). Multilocular adipocytes that are positive for UCP are present in both control and transgenic mice; these are more abundant in control mice (Figures 6.12, 6.13; C, D). Unilocular adipocytes are larger in the transgenic mice at 24°C than in control mice (Figures 6.12, 6.13; C, D). Multilocular brown adipocytes are not as abundant at 8 wks of age as they are at 3 wks of age (Figures 6.12, 6.13; A, B, C, D).

When mice are raised 35°C, adipocytes in their INWAT appear round and unilocular (Figures 6.12, 6.13; E, F). The lipid droplets present within these adipocytes are smaller than at 24°C (Figures 6.12, 6.13; E, F). A few sparse multilocular cells stain positive for UCP (Figure 6.13 E, F).

Histology of inguinal white adipose tissue

Figure 6.12: Hematoxylin and eosin stained 4μm sections of INWAT of 3 wk old control (A), 3 wk old UCP-DTA (B), 8 wk old control raised at 24°C (C), 8 wk old UCP-DTA raised at 24°C (D), 8 wk old control raised at 35°C (E), and 8 wk old UCP-DTA raised at 35°C (F). Magnification x 200. No difference in appearance of INWAT at 3 wks of age (A, B). Larger lipid droplets in 8 wk old UCP-DTA at 24°C compared with controls (D vs. C). Note the similar appearance of INWAT when mice are raised at 35°C (E, F).

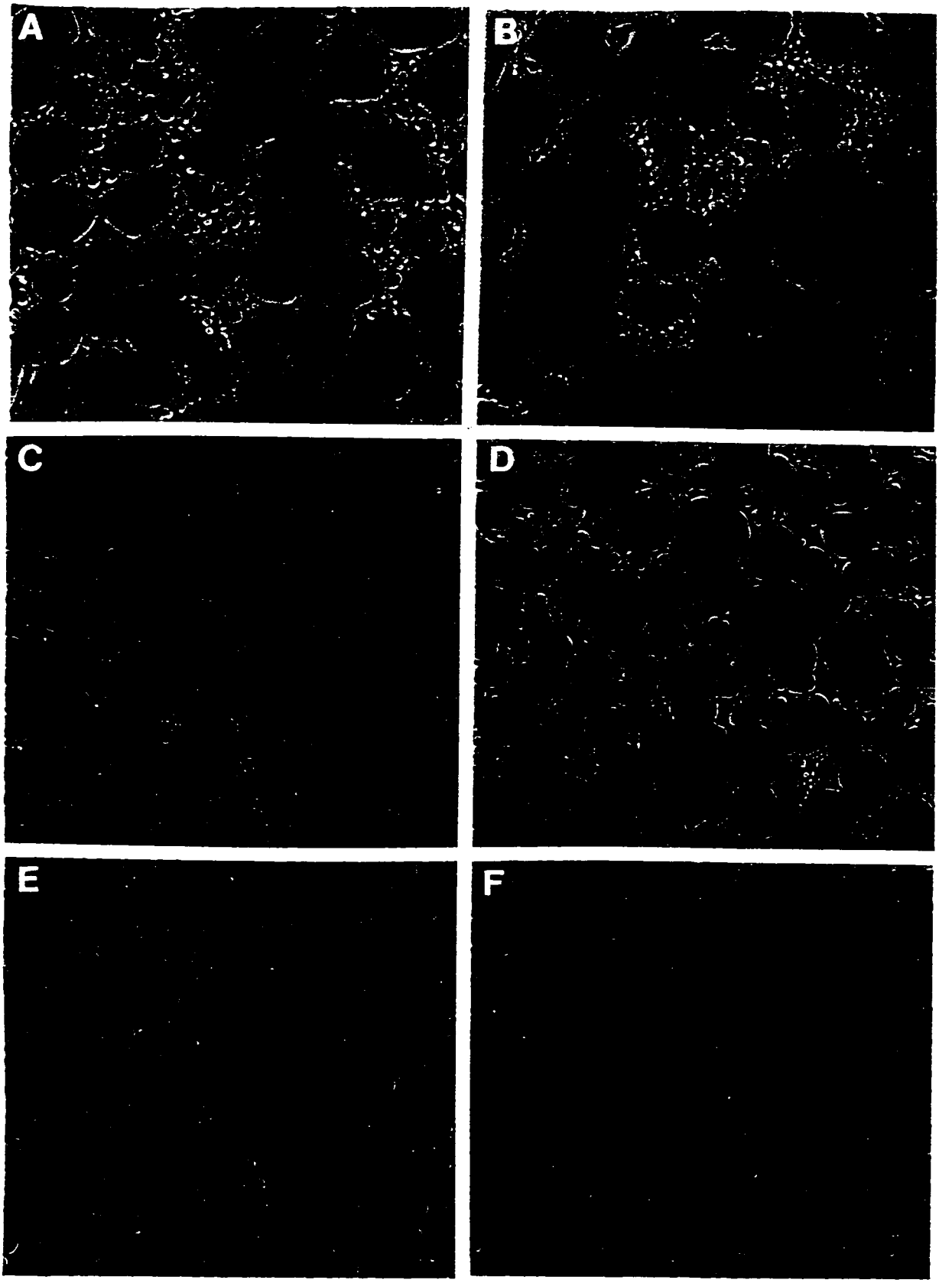
A
B
C
D
E
F

Immunohistochemical detection of UCP in INWAT

Figure 6.13: Immunohistochemical detection of UCP in INWAT of control and UCP-DTA mice, counter stained with hematoxylin. UCP in 10 μm sections of INWAT of 3 wk old control (A), 3 wk old UCP-DTA (B), 8 wk old control raised at 24°C (C), 8 wk old UCP-DTA raised at 24°C (D), 8 wk old control raised at 35°C (E), and 8 wk old UCP-DTA raised at 35°C (F). Magnification x 200. No difference in appearance of INWAT of control and UCP-DTA at 3 wks of age (A, B), nor at 35°C (E, F). Note the positively stained multilocular adipocytes present in INWAT at each age and temperature. Brown adipocytes are most abundant and appear most active at 3 wks of age (A, B). Lowest number of multilocular cells at 35°C (E, F). 8 wk old controls raised at 24°C have more abundant and more active appearing brown adipocytes than UCP-DTA mice at this age and temperature (C, D).

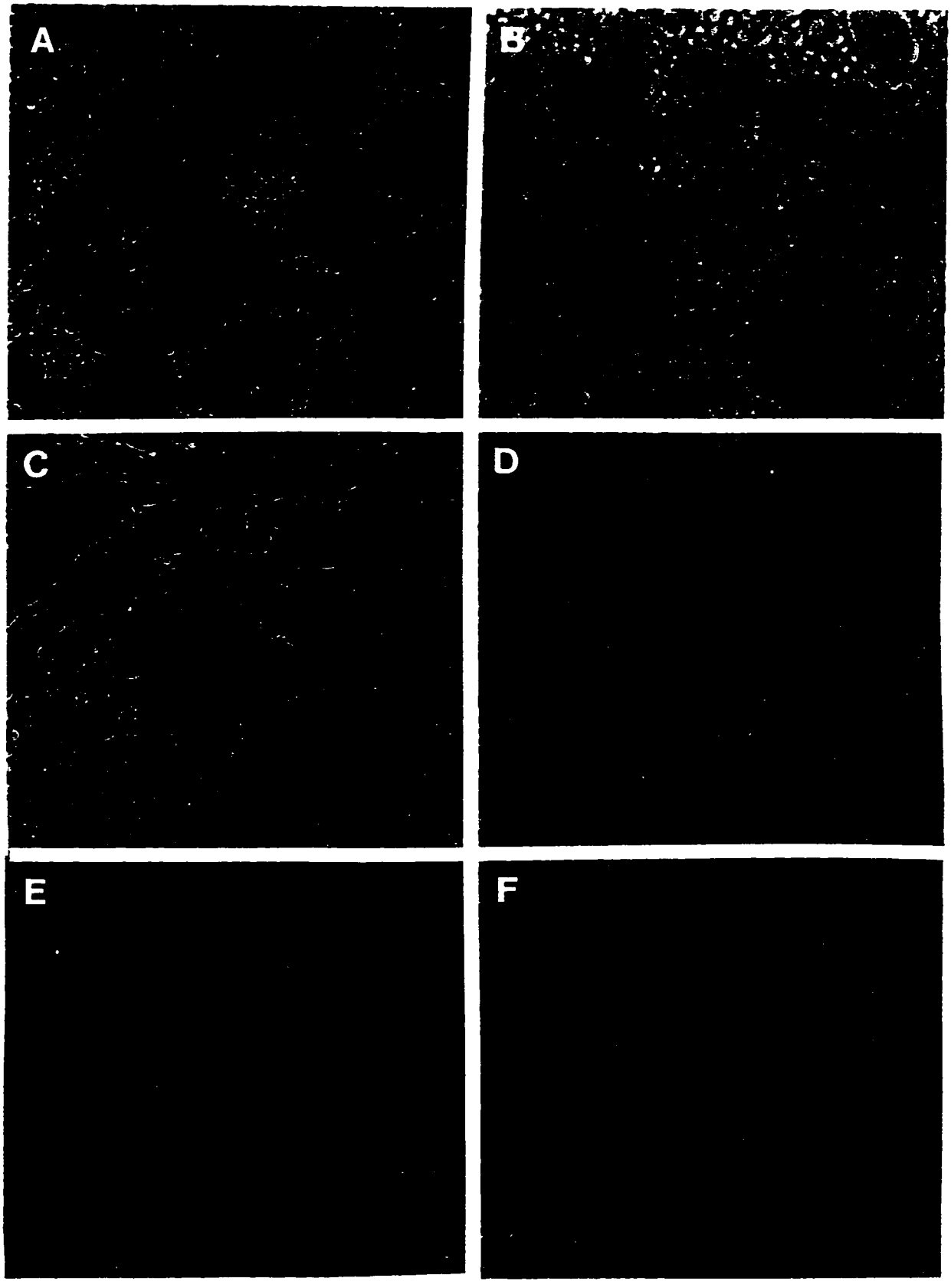
A
B
C
D
E
F

Interscapular brown adipose tissue:

The weight of IBAT of 8 wk old UCP-DTA mice was significantly higher than that of controls ($p<0.05$) when they were raised at 24°C (Figure 6.14). No differences in IBAT weight between transgenic and controls were seen at any other age or temperature. The weight of IBAT increased significantly with age in the UCP-DTA ($p<0.001$) but not in the control mice. Raising at thermoneutrality prevented this increase in IBAT weight in the UCP-DTA mice (Figure 6.14). Temperature of housing did not affect the IBAT weight of control mice.

IBAT of UCP-DTA mice raised at 24°C had more cells than control mice, as assessed by DNA content of the tissue ($p< 0.05$, Figure 6.15). There was no difference in cell number between transgenic and control mice either at 3 wks of age, or at 8 wks of age when raised at 35°C. There was no effect of age, or temperature on the total number of cells in the IBAT of control mice (Figure 6.15). A significant increase in cell number of IBAT with age was detected in UCP-DTA mice ($p<0.001$), which was prevented by raising the mice at thermoneutrality (Figure 6.15). IBAT of transgenic obese mice generally had less total protein and mitochondrial mass (as assessed by cytochrome oxidase content) than control mice (Figures 6.16 and 6.17) and a lower UCP content (Figure 6.18). In control mice, the expected age- and temperature-dependent decline in UCP content of BAT was seen (Figure 6.18); control mice raised at 35°C had very little UCP in their BAT, and transgenic mice raised at this temperature had even less (Figure 6.18).

Wet weight of interscapular brown adipose tissue

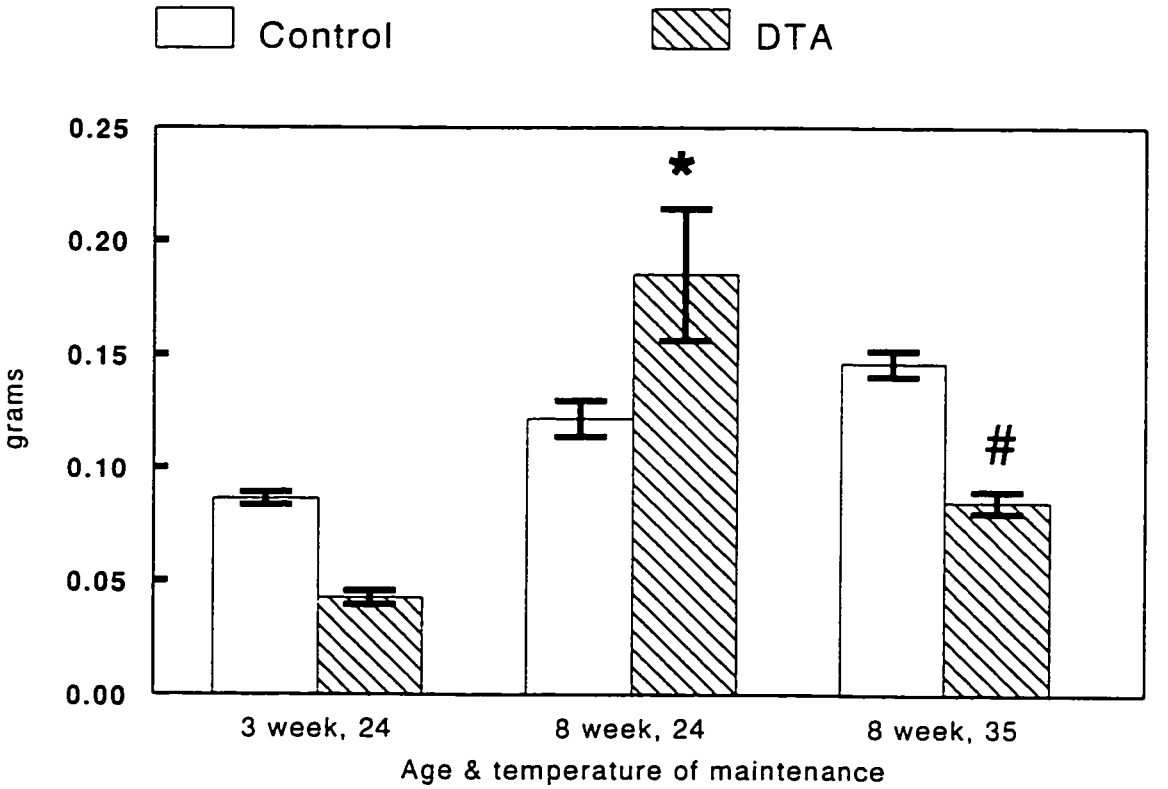

Figure 6.14: IBAT wet weight. Control mice, open bars; transgenic mice, hatched bars. The weight of IBAT was not significantly different in 3 wk old mice. The IBAT weight of 8 wk old DTA mice was significantly higher than that of controls ($p<0.05$) when raised at 24°C, though not at 35°C. The weight of IBAT increased with age in the DTA ($p<0.001$) but not in the control mice. Raising at thermoneutrality prevented this increase in IBAT weight in the DTA mice. Temperature of housing did not affect the IBAT weight of control mice.
* denotes a significant effect of transgene, # denotes a significant effect of temperature

Total cells in interscapular brown adipose tissue

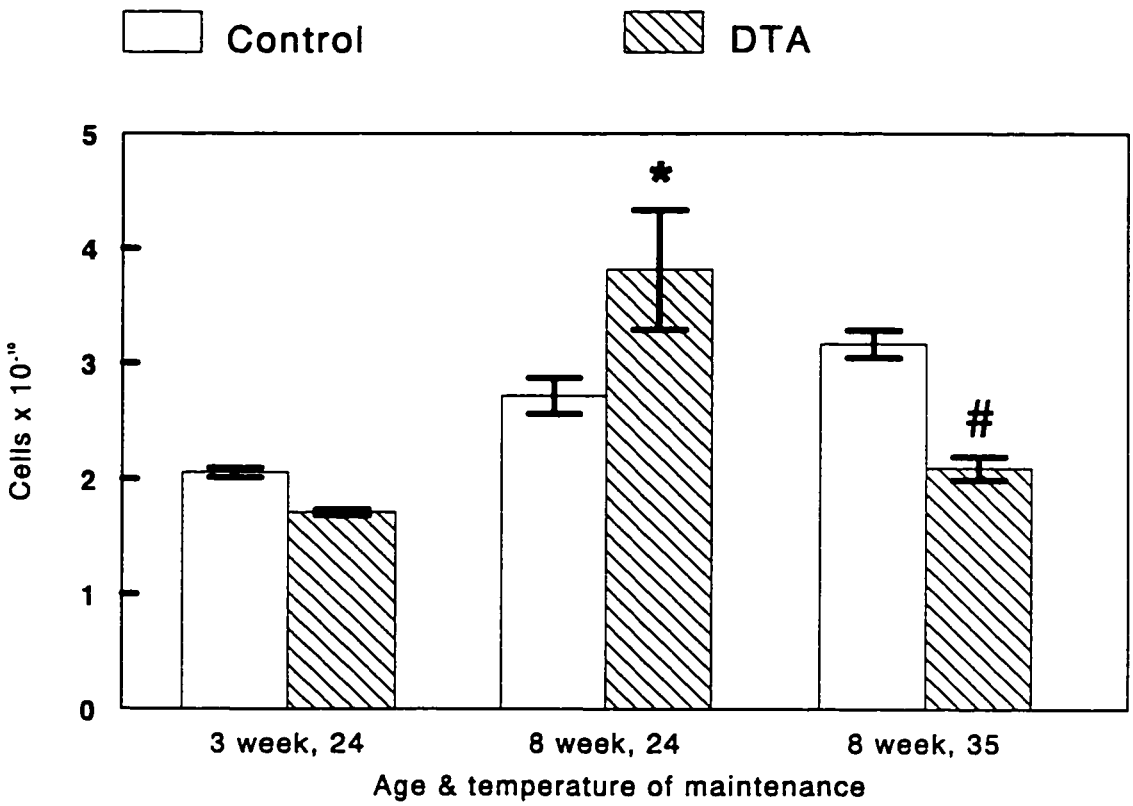

Figure 6.15: Total cells in IBAT as assessed by DNA. Transgenic mice raised at 24°C had significantly more cells than controls ($p<0.05$). No effect of age, nor temperature was seen in the control mice. Significant effect of age is seen in the UCP-DTA mice raised at 24°C that is abolished by raising the mice at 35°C.
* denotes a significant effect of transgene, # denotes a significant effect of temperature

Total protein of interscapular brown adipose tissue

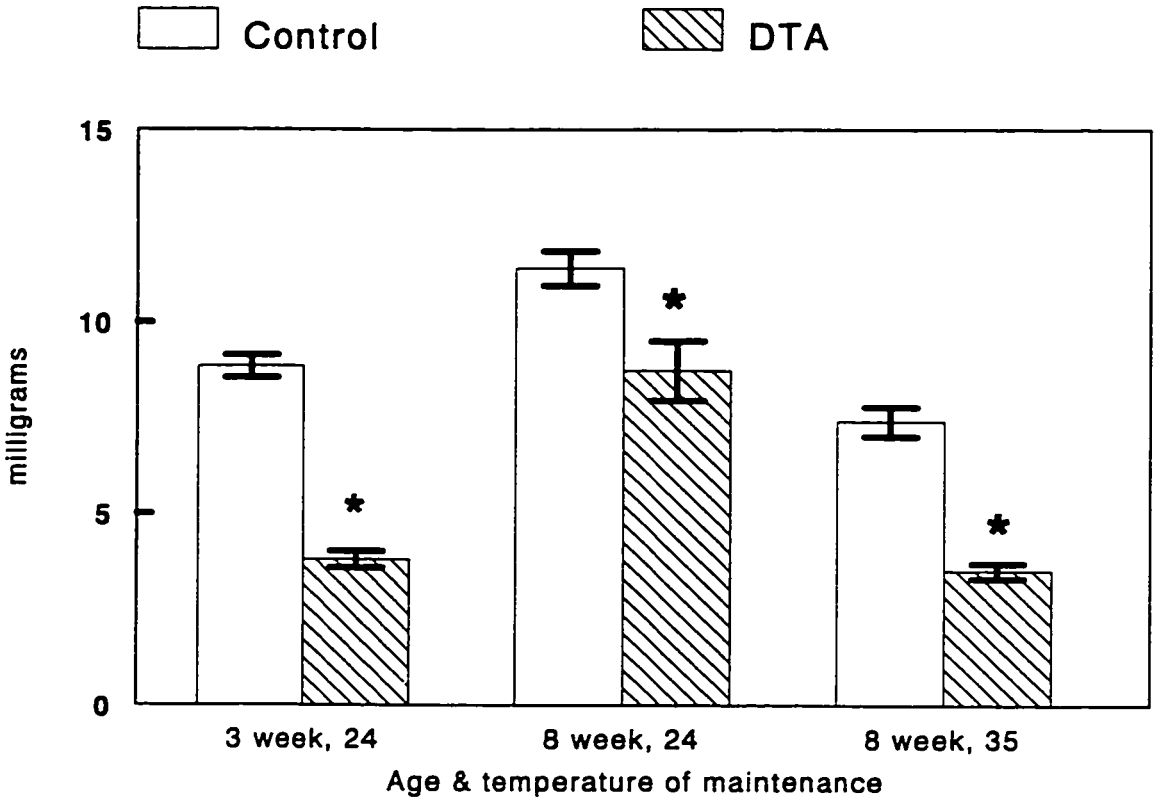

Figure 6.16: Total protein in IBAT. Control mice, open bars; transgenic mice, hatched bars. Protein content is significantly lower in transgenic mice compared with control mice at same age and temperature for 3 wk old mice ($P<0.001$), for 8 wk old mice at 24°C ($P<0.001$), and for 8 wk old mice at 35°C ($P<0.001$).
* denotes a significant effect of transgene.

Total cytochrome oxidase activity of interscapular brown adipose tissue

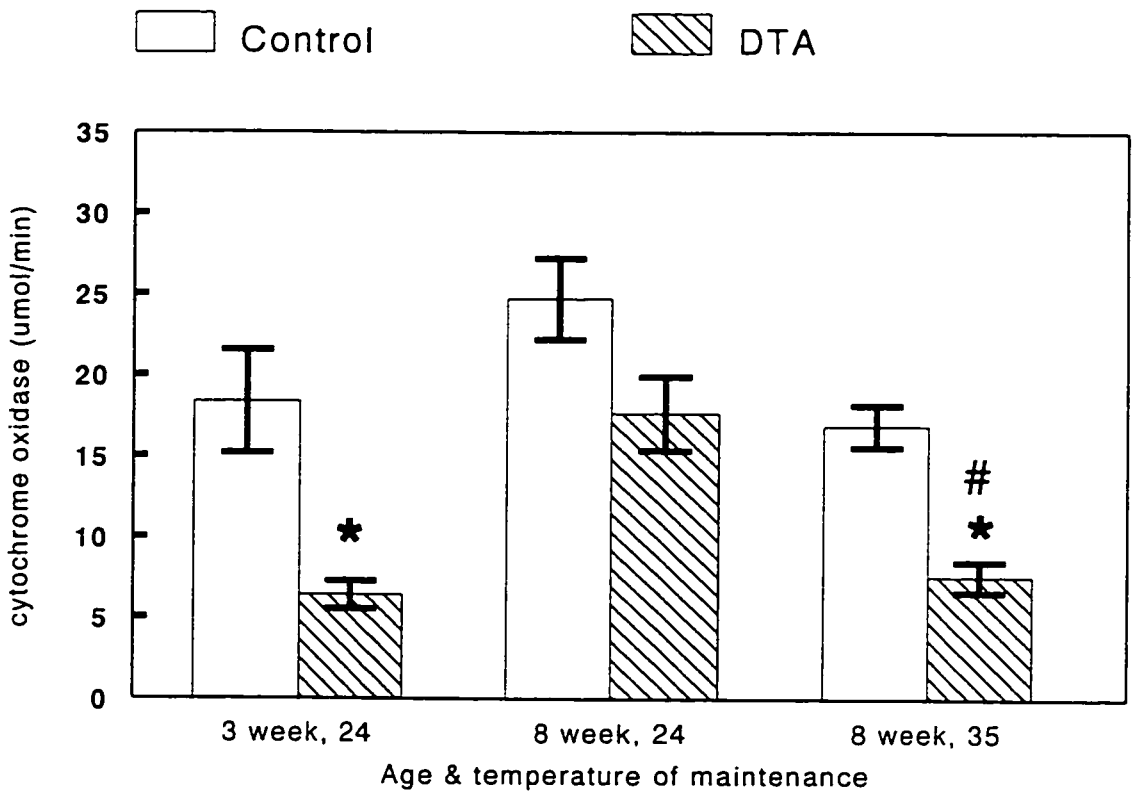

Figure 6.17: Total cytochrome oxidase activity (μmol/minute) in IBAT. Control mice, open bars; transgenic mice, hatched bars. Total cytochrome oxidase activity is significantly lower in 3 wk old transgenic mice than in 3 wk old control mice ($P<0.05$) and in 8 wk old transgenic mice at 35°C than in 8 wk old control mice at 35°C. It is significantly higher in 8 wk old transgenic mice at 24°C than in 3 wk old transgenic mice ($P<0.01$) or in 8 wk old transgenic mice at 35°C ($P<0.01$). The difference between control and transgenic mice at 24°C did not reach statistical significance.
* denotes a significant effect of transgene, # denotes a significant effect of temperature

Uncoupling protein content of interscapular brown adipose tissue

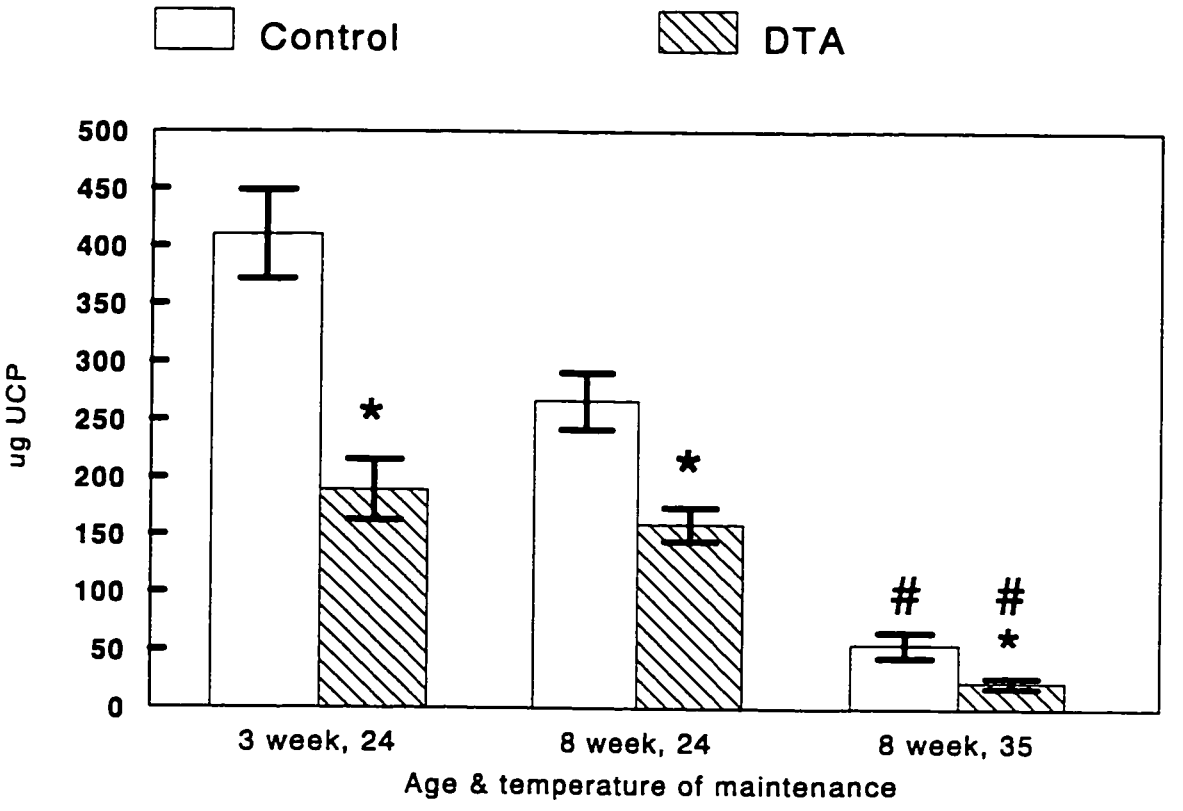

Figure 6.18: UCP content of IBAT. Control mice, open bars; transgenic mice, hatched bars. UCP content is significantly lower in 3 wk old transgenic mice than in 3 wk old control mice ($P<0.001$) and in 8 wk old transgenic mice at 24°C than in 8 wk old control mice at 24°C ($P<0.01$). Difference between 8 wk old transgenic mice at 35°C and 8 wk old control mice at 35°C did not reach statistical significance; an unpaired t-test revealed a statistically significant difference ($P<0.016$) between these two very low values, much lower than those for all other groups of mice ($P<0.001$).
* denotes a significant effect of transgene, # denotes a significant effect of temperature

The UCP/cytochrome oxidase ratio, a measure of UCP concentration relative to that of other mitochondrial proteins, was highest in the 3 wk old mice and lowest in the mice raised at 35°C (Figure 6.19). Thus UCP concentration in mitochondria decreased with age ($p<0.001$ for CON and UCP-DTA); much more so in the mice raised at 35°C than in the mice raised at 24°C. The UCP/ cytochrome oxidase ratio in BAT mitochondria of transgenic mice was, however, the same as in control mice in all groups (Figure 6.19); the transgenic mice suffer from depletion of mitochondria in their BAT, not from a lower concentration of UCP in the mitochondria that are present.

Histology of BAT:

Semi-thin sections (0.5 μm) of IBAT of 8 wk old mice show the fatty, inactive appearance of IBAT in UCP-DTA mice raised at 24°C, and in controls and transgenics raised at 35°C (Figure 6.20 B, C, D). When raised at 24°C, the IBAT of control mice has an active appearance, with multilocular adipocytes and abundant mitochondria (Figure 6.20 A). In UCP-DTA mice at 24°C, there are still some multilocular cells present, but these contain larger lipid droplets (Figure 6.20 B). At 35°C, IBAT of both control and transgenic mice has larger lipid droplets and fewer mitochondria (Figure 6.20 C, D).

UCP/cytochrome oxidase ratio of interscapular brown adipose tissue

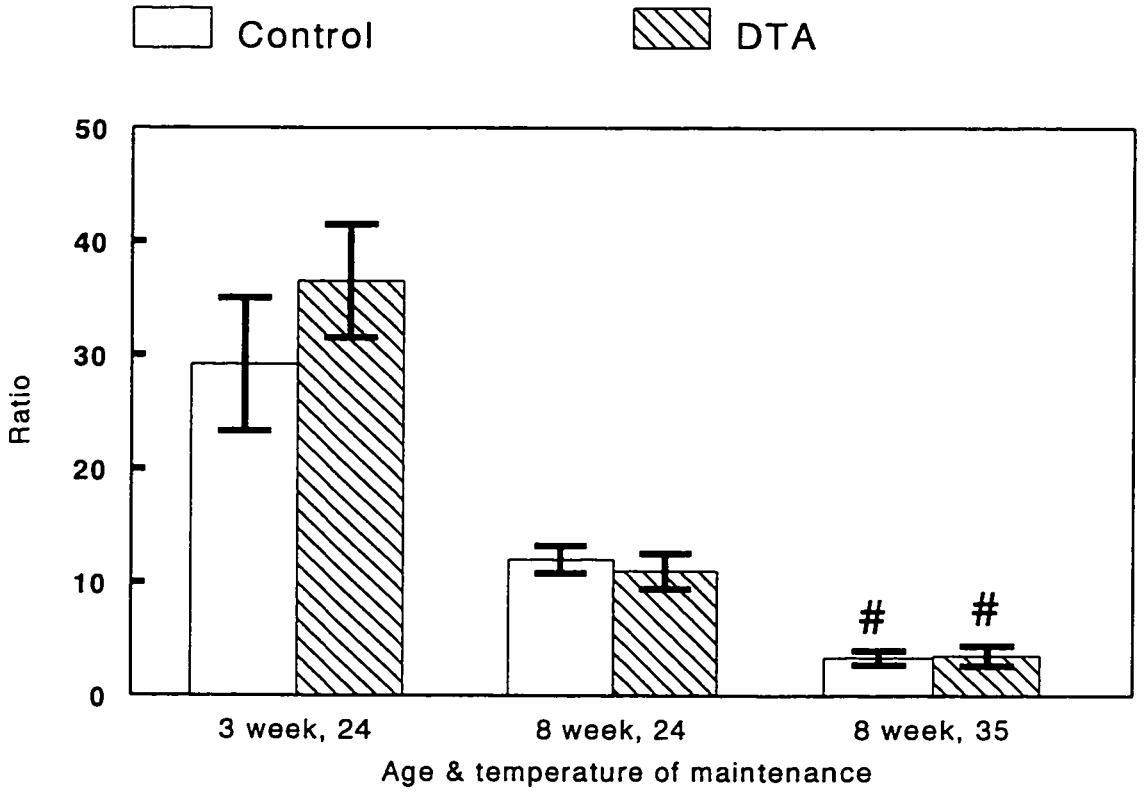

Figure 6.19: UCP/cytochrome oxidase ratio of IBAT. Control mice, open bars; transgenic mice, hatched bars. There are no significant differences in UCP/cytochrome oxidase ratio between groups of transgenic and control mice at same age and temperature. There is a decrease in the ratio with age ($P<0.001$) and with the higher temperature ($P<0.01$).
# denotes a significant effect of temperature

Semithin sections of interscapular brown adipose tissue

Figure 6.20: Semi-thin sections (0.5 μm) of IBAT magnification x 1000. Sections stained with methylene blue and azure blue II. **A:** 8 wk old control at 24°C, **B:** 8 wk old UCP-DTA at 24°C, **C:** 8 wk old control at 35°C, **D:** 8 wk old UCP-DTA at 35°C. At 24°C, IBAT of control mice has an active appearance, with multilocular adipocytes and abundant mitochondria (A). In UCP-DTA mice at 24°C, there are still some multilocular cells present, but these contain larger lipid droplets (B). At 35°C, IBAT of both control and transgenic mice has larger lipid droplets and fewer mitochondria (C, D).

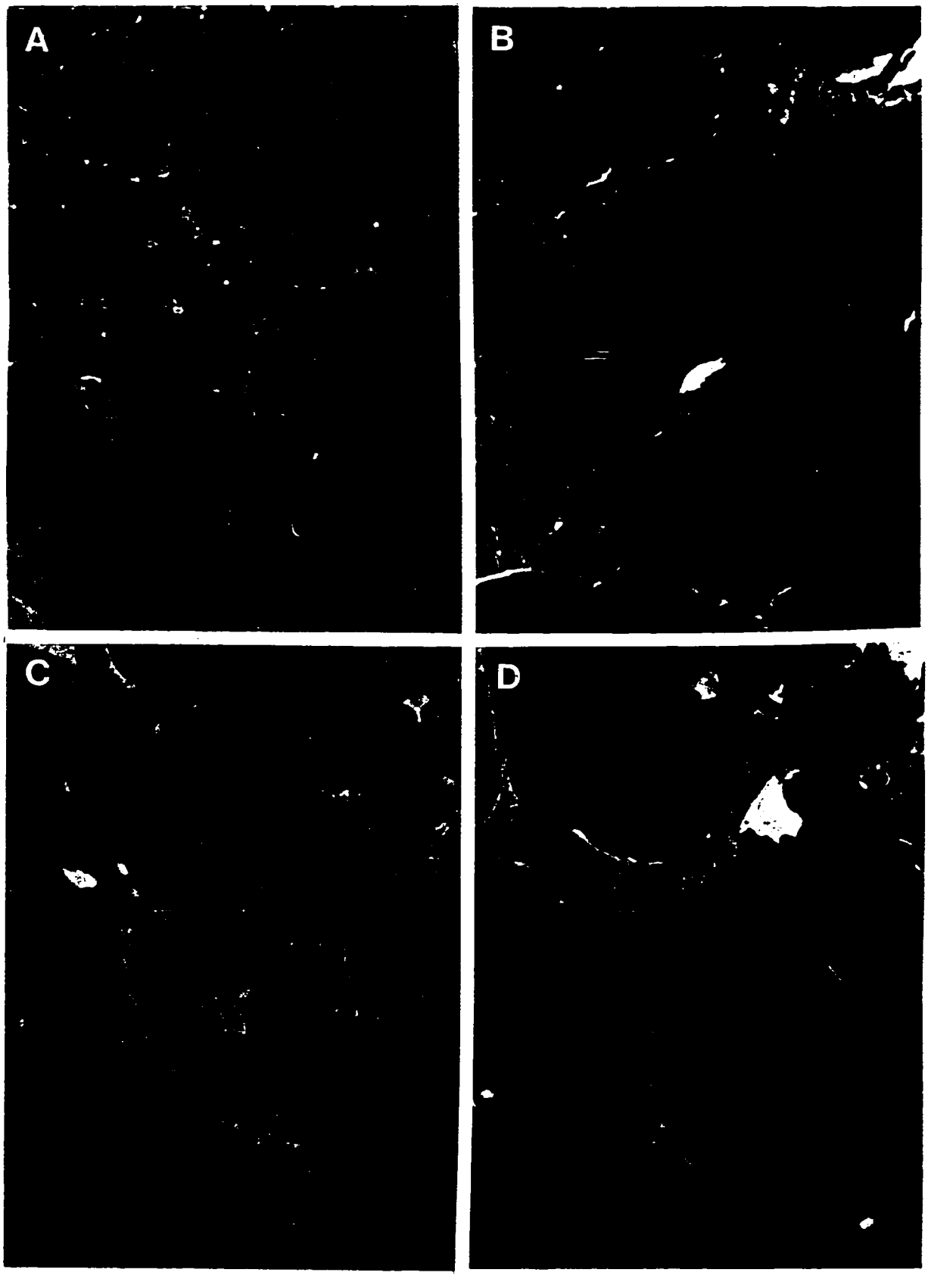
A
B
C
D

Stained 4 μm sections of IBAT of 8 wk old control mice at 24°C and 3 wk old control and transgenic mice had a thermogenically active appearance (Figures 6.21 and 6.22; A, B, C). Cells were multilocular, with small lipid droplets and were positively stained for UCP (Figure 6.22 A, B, C). Histology of BAT showed fatty inactive appearance in all mice at 35°C and in DTA mice at 24°C.

At 3 wks of age, the IBAT of control and UCP-DTA mice looks very similar (Figures 6.21 and 6.22; A, B).

The IBAT of control mice at 8 wks of age raised at 24°C contained all multilocular cells, and the Harlequin effect (Chapter 1: Brown adipose tissue, Uncoupling protein homologues, (Cinti *et al.* 1997)) was apparent (Figure 6.21, 6.22; C). In UCP-DTA mice at 8 wks of age raised at 24°C, IBAT contained unilocular cells, and had a very fatty appearance Figures 6.21, 6.22; D. Many multilocular adipocytes were also present, but these contain larger lipid droplets than control mice at this temperature (Figures 6.21, 6.22; C, D). These multilocular cells were positive for UCP (Figure 6.22 C, D).

The appearance of IBAT of control and UCP-DTA raised at 35°C was the same; the cells were mainly unilocular and very inactive looking with large round lipid droplets. The cells were very heterogeneous in size.

Histology of interscapular brown adipose tissue

Figure 6.21: Hematoxylin and eosin-stained 4μm sections of IBAT of 3 wk old control (A), 3 wk old UCP-DTA (B), 8 wk old control raised at 24°C (C), 8 wk old UCP-DTA raised at 24°C (D), 8 wk old control raised at 35°C (E), and 8 wk old UCP-DTA raised at 35°C (F). Magnification x 200. BAT of 8 wk old control mice at 24°C and 3 wk old control and transgenic mice had a thermogenically active appearance (C, A, B), cells are multilocular, with small lipid droplets. Note fatty, inactive appearance in all mice at 35°C and in DTA mice at 24°C (E, F, D).

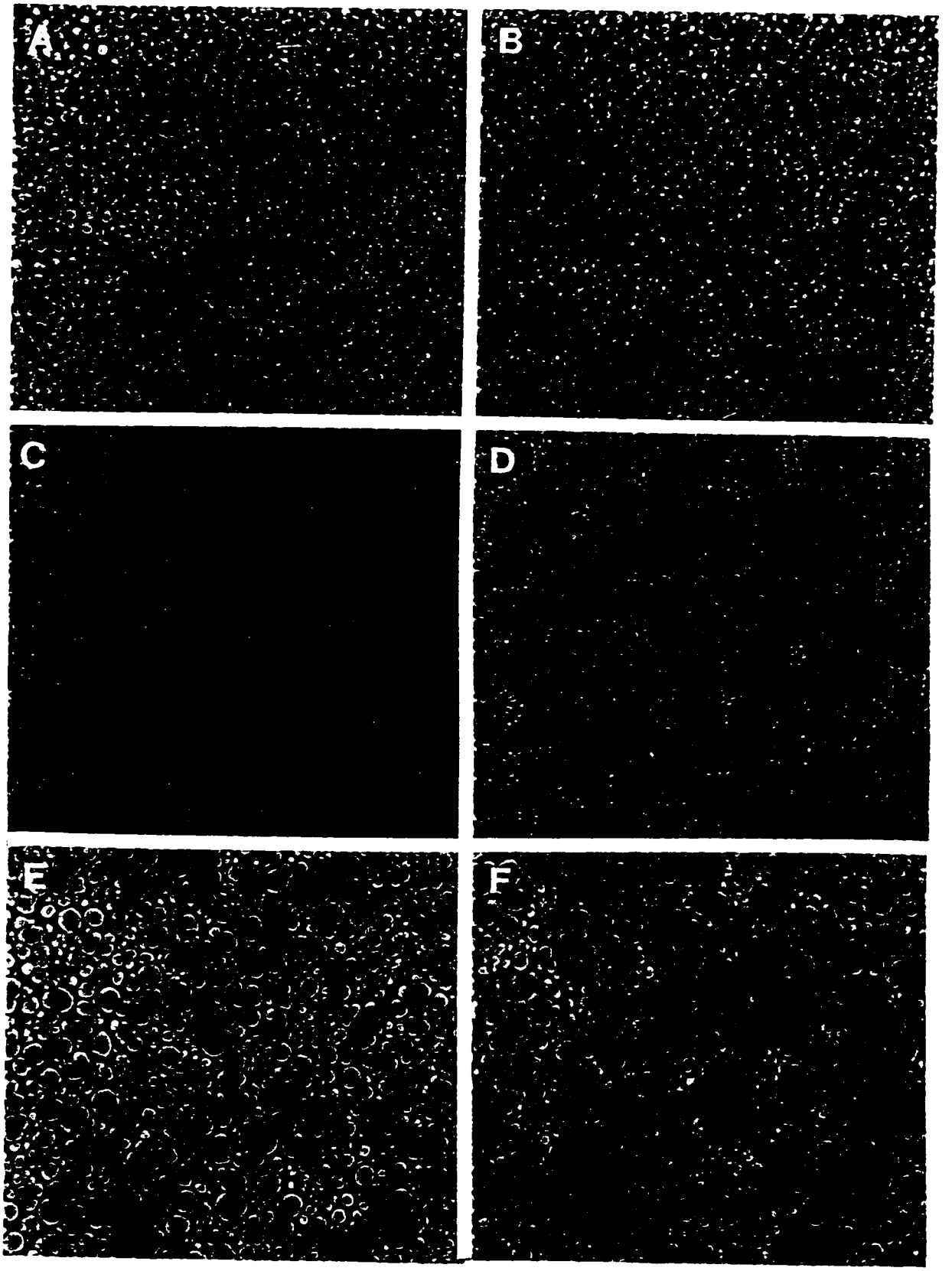
A
B
C
D
E
F

Immunohistochemical detection of UCP in IBAT

Figure 6.22: Immunohistochemical detection of UCP in IBAT of control and UCP-DTA mice, counter stained with hematoxylin. UCP in 10 μm sections of IBAT of 3 wk old control (A), 3 wk old UCP-DTA (B), 8 wk old control raised at 24°C (C), 8 wk old UCP-DTA raised at 24°C (D), 8 wk old control raised at 35°C (E), and 8 wk old UCP-DTA raised at 35°C (F). Magnification x 200. The IBAT of control mice at 8 wks of age raised at 24°C contained all multilocular cells, and the Harlequin effect was apparent (C).

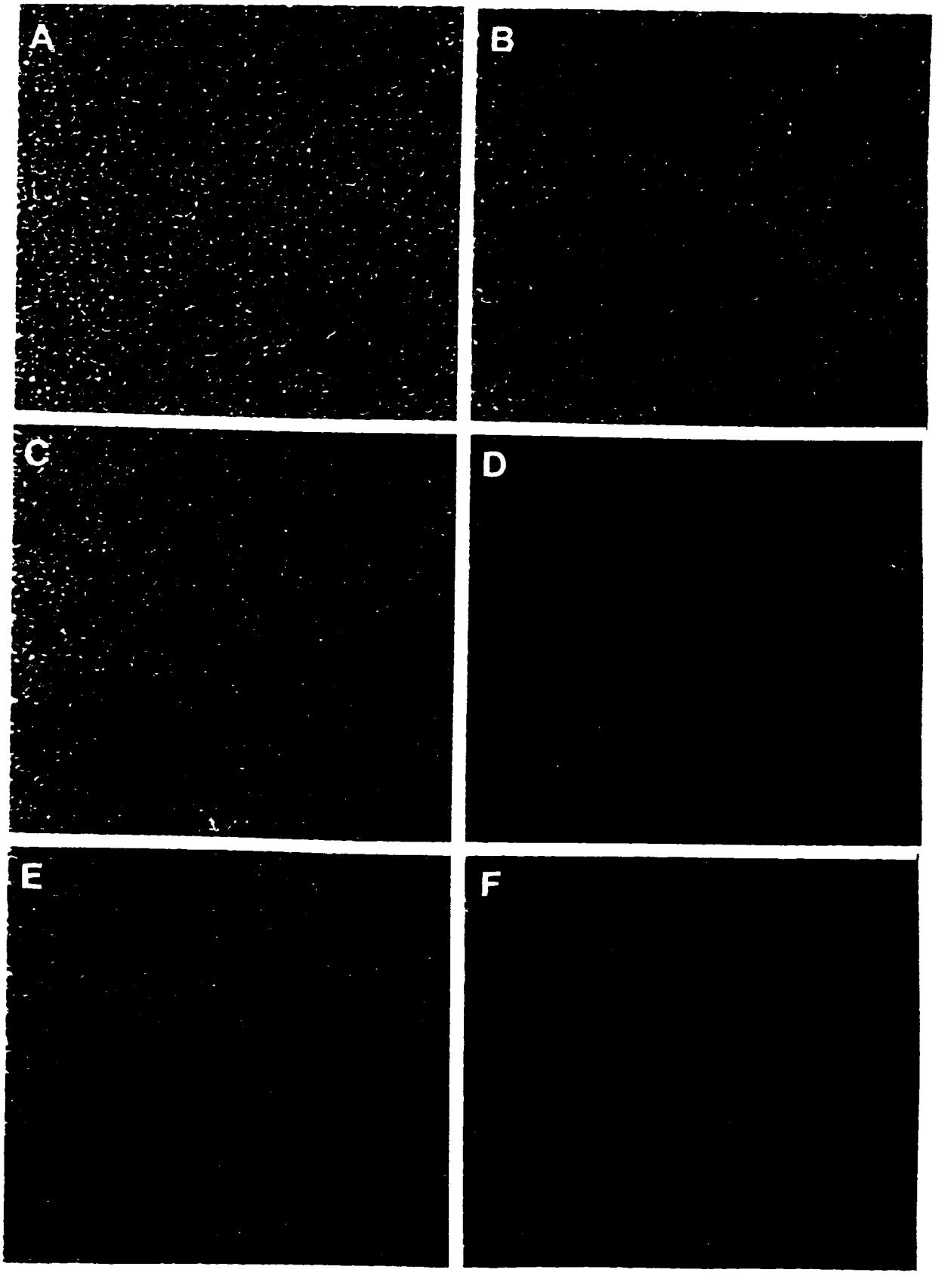
A
B
C
D
E
F

Discussion

The principal finding of this study is that both the development of obesity and the hyperphagia in UCP-DTA mice are temperature sensitive. Both were prevented when these mice were raised from weaning to the age of 8 wks in a thermoneutral environment. Under these conditions, BAT thermogenesis and BAT UCP content are expected to be at an equally low level in the transgenic and control mice.

Transgenic mice ate to adjust their energy intake precisely to their needs for growth and maintenance at this relatively high temperature, eating the same amount as control mice and acquiring the same amount of body fat as control mice. Control mice can precisely adjust their energy intake to meet their needs for growth and maintenance at the low temperature usually used for raising mice (24°C); at this temperature they eat twice as much as at 35°C but acquire the same amount of body fat as mice raised at the higher temperature.

UCP-DTA mice, in contrast, are unable to adjust their energy intake precisely to meet their needs for growth and maintenance at a lower temperature and eat 2.6 times as much as they do when raised at 35°C. This level of intake is in excess of their needs, which should be lower than in control mice because of the deficit in BAT thermogenesis at this temperature. The consequence is that UCP-DTA mice develop obesity.

An obligatory link may exist between a mouse's ability to use thermogenesis in BAT and its ability to adjust its food intake in accordance with environmental temperatures below thermoneutrality, uncorrelated with leptin concentration.

Serum leptin concentration was the same in control mice at 35°C and at 24°C, but their food intake at 35°C was only 50% of that at 24°C. Transgenic mice at 35°C had the same low serum leptin levels and food intake as control mice at this temperature. At 24°C UCP-DTA mice were hyperphagic, obese and had a threefold increase in leptin level. Weanling UCP-DTA mice had elevated serum leptin levels but normal food intake and body fat. Adjustment of food intake in accordance with temperature of adaptation is not mediated by changes in leptin concentration. This will be discussed further in Chapters 7 and 8.

Female UCP-DTA mice have recently been reported to have a normal plasma leptin concentration at 6 wks of age (Hamann *et al.* 1997), contrasting our results for 3 wk old mice. Leptin levels are increased when the mice are obese; it is apparent from our study that this increase precedes the development of obesity (as seen in 3 wk old mice). The male mice used in this study become obese at an earlier age (as seen previously (Lowell *et al.* 1993)), possibly explaining the difference in leptin levels.

In contrast to a previous study (Lowell *et al.* 1993), the weanling mice were not obese, although their BAT was definitely atrophied, as indicated by the reduction in mitochondrial content. In this study an accelerated weight gain appeared to coincide with the hyperphagia detected at 5 wks of age, as in the previous study (Lowell *et al.* 1993). Without detailed carcass analysis between 3 and 6 wks of age, we cannot pinpoint more precisely the age at which obesity started to develop. Obesity and hyperphagia apparently developed at the same time, suggesting an important role for hyperphagia in the development of obesity in UCP-DTA mice beyond the presumed deficit in energy expenditure in their BAT.

The biochemical assessment of BAT of the UCP-DTA mice suggests that the principal consequence of the expression of the toxigene is a loss of UCP1 expressing brown adipocytes and the abundant mitochondria contained within them. The control of UCP concentration in the mitochondria in relation to age (it decreases with age from 3 to 8 wks of age) and environmental temperature (it decreases even further at thermoneutrality) is normal in the cells that are present. The defect in the UCP-DTA mouse lies in its reduced capacity for thermogenesis, due to the lack of UCP1 expressing brown adipocytes, not in the central mechanisms that exert control over its BAT.

The obesity of the UCP-DTA mouse at 8 wks of age is hypertrophic, the doubling of body fat achieved by increased adipocyte size with no increase in adipocyte number. In WAT, the total number of cells increased, with a concomitant increase in protein content, interpreted as an increase in vascularity to support the expanded mass of tissue. Transgenic mice raised at 24°C to 8 wks of age had not yet developed the hypertriglyceridemia or hypercholesterolemia seen in older obese mice (Hamann *et al.* 1995; Hamann *et al.* 1996; Lowell *et al.* 1993).

Based on the assumption that only UCP1 containing brown adipocytes are destroyed in the BAT of UCP-DTA mice and on the presence of multilocular brown adipocytes expressing UCP, we propose that more than one brown adipocyte type may exist, expressing a UCP homologue other than UCP1.

This hypothesis is supported by the histology of BAT performed in this study, and by histological data of BAT from others (Cinti *et al.* 1997; Pellet & Lheritier 1975; Vallin

1970); see the discussion of the Harlequin effect (Cinti *et al.* 1997), Chapter 1: Uncoupling protein homologues.

IBAT of UCP-DTA mice at 24 °C has two different populations of adipocytes (Figure 6.22); large unilocular adipocytes and multilocular adipocytes. These adipocytes are presumed not to contain UCP1, possibly they contain other UCP homologues and are compensating for the loss of UCP1 brown adipocytes. At 3 wks of age, the IBAT of control and UCP-DTA mice looks very similar, but the protein and UCP content of UCP-DTA mice are only 50% of that in control mice suggesting that the tissue composition is not identical.

Multilocular brown adipocytes appear in INWAT of UCP-DTA mice, but are less abundant than in control mice (Figures 6.12, 6.13). These are presumed to be UCP1 expressing brown adipocytes in control mice; it is postulated that they express another UCP isoform in UCP-DTA mice.

A useful transgenic model to compare the UCP-DTA mouse with is the UCP1 knockout mouse (UCP1-KO) (Enerbäck *et al.* 1997). Neither of these mice expresses UCP1; the difference between the two models lies in the fact that UCP1 expressing brown adipocytes are destroyed in the UCP-DTA mice, while they are still present in the UCP-KO mice (though not expressing UCP1). In contrast to the UCP-DTA mouse, the UCP1-KO mouse is neither obese, nor hyperphagic (Enerbäck *et al.* 1997). We postulate that UCP1 expressing brown adipocytes normally secrete a satiety factor. Secretion of this factor would be higher when the UCP1 brown adipocytes are not stimulated by noradrenaline, as at thermoneutrality, less when they are stimulated at lower temperatures. We suggest in

addition that these adipocytes survive in UCP-DTA mice at thermoneutrality and secrete the postulated factor; consequently, food intake of the UCP-DTA mice is low. These adipocytes are lost at 24°C, and UCP-DTA mice lack the postulated factor and become hyperphagic. Further evidence for this theory is presented in Chapter 7.

In summary, the obesity and hyperphagia of the UCP-DTA mouse are temperature dependent, apparent only when the mouse lives at a temperature below thermoneutrality; temperatures at which BAT thermogenesis is switched on and UCP1 expressing brown adipocytes are destroyed. Both the obesity and the hyperphagia fail to develop at thermoneutrality. Under these conditions BAT thermogenesis is switched off and UCP1 expressing brown adipocytes are not killed off; suggesting a link between these cells and the development of hyperphagia and obesity.

Chapter 7: Acclimation to mild cold in transgenic mice with partial ablation of BAT

Introduction

Energy expenditure for thermogenesis in BAT maintains body temperature in the cold. Non-shivering thermogenesis in BAT is an important part of thermal balance (Himms-Hagen 1990b).

When an animal undergoes cold acclimation there is a chronic increase in the activity of sympathetic nerves innervating BAT, causing the tissue to hypertrophy (Himms-Hagen 1991). This hypertrophy includes hyperplastic growth, and an increased capacity for thermogenesis. The increase in cell number is mediated by β_1-ARs present on interstitial precursor cells, which when stimulated will proliferate and differentiate (Bronnikov *et al.* 1992).

The increase in capacity for thermogenesis results from an increase in all cellular constituents of BAT, with a selective increase in certain components. Mature brown adipocytes and dormant brown adipocytes are responsible for a rapid increase in thermogenesis, mediated by the β_3-AR (Himms-Hagen & Ricquier 1997). Specific components increased include UCP, and the activities and levels of LPL and T_4 5'-D.

The morphology of the tissue depends on the state of BAT. Chronically stimulated BAT will have smaller lipid droplets, and much more abundant mitochondria, with an increased total content of UCP (Himms-Hagen & Ricquier 1997).

Initially the prevention of obesity and hyperphagia in the UCP-DTA mouse when raised at thermoneutrality (Chapter 6) was interpreted as the result of the abolition of any deficit in BAT thermogenesis at this temperature. Brown adipocytes were thought to be equally thermogenically inactive in both control and in UCP-DTA mice with any potential deficit felt only at lower environmental temperatures. This interpretation has been revised in the light of a recent report of a transgenic mouse with targeted disruption of the UCP 1 gene in its brown adipocytes (Enerbäck *et al.* 1997). As discussed in Chapter 6, the difference between these mice and the UCP-DTA mice is that the UCP1 gene alone is knocked out, and not the brown adipocytes that express UCP1. The animals are not hyperphagic nor obese, suggesting that the presence of the UCP1 expressing brown adipocytes provides a satiety factor for the mouse. Another difference between the UCP1-KO mouse and the UCP-DTA transgenic mouse is extreme cold intolerance in the UCP1-KO mouse (Enerbäck *et al.* 1997). The UCP-DTA mice can survive for at least two days at a temperature that is very cold for mice (4°C) (Lowell *et al.* 1993).

The initial objective of the present experiments was to characterize further the ability of the UCP-DTA mouse to survive in a cold environment, in particular to assess whether its BAT could grow during cold acclimation to mild cold (14°C). Because of previous studies of cold-acclimated mice (Loncar 1991; Young *et al.* 1984a) and rats (Cousin *et al.* 1996; Cousin *et al.* 1992) and of mice (Collins *et al.* 1997) or rats (Ghorbani *et al.* 1997; Ghorbani & Himms-Hagen 1997; Nagase *et al.* 1996; Umekawa *et al.* 1997) treated chronically with a β_3 -AR agonist showing a cold- or drug-induced appearance of abundant multilocular

brown adipocytes and of UCP in WAT depots, we also studied the response of a WAT depot to the increased sympathetic nervous system activity that accompanies acclimation to cold in control and in UCP-DTA mice.

Objectives

The objective of this study was to characterize further the ability of the UCP-DTA mouse to survive in a cold environment, and to assess whether its BAT could grow during acclimation to mild cold (14°C) and whether its WAT could acquire brown adipocytes. An additional objective was to assess whether altered food intake in a cold environment correlated with altered leptin levels in the blood.

Materials and methods

Animals:

A colony of UCP-DTA mice was established with six female UCP-DTA mice (provided by Dr. Bradford B. Lowell, Beth Israel Hospital and Harvard Medical School, Boston, MA) and six male FVB/N mice (from Taconic, Germantown, NY). Breeding pairs were housed at 24°C with free access to food (Agway R-M-H 4020 chow, 14.5 % of energy from fat) and water. Lights were on for 12 hours a day.

Experimental setup:

Female mice from the colony were separated into single cages at 17 weeks of age (control, n=31; UCP-DTA, n=32). These mice were allowed free access to chow and water for one week before the experiment. At 18 weeks of age, mice were either killed (zero time), or they were put into a cold room kept at 14°C for up to 14 days. Groups of mice were killed at 1, 2, 7, and 14 days. Each group (including zero time) included 6-8 control mice and 6-8 UCP-DTA mice (Table 7.1).

Body weight and rectal temperature:

Rectal temperatures and body weights were measured at each time point shown and all mice available at each time point were included in mean values (Table 7.2). Body weights and rectal temperatures were all measured between 11:30 a.m. and 3:00 p.m.

Food intake:

Food intake was evaluated over the course of the experiment. Food left in the cage was weighed at same time that body weight and rectal temperature were measured. Mice had free access to food (Agway R-M-H 4020 chow, 3.5 kcal/g, 14.5 % energy from fat) and water. All mice available at each time point were included in mean values (Table 7.2).

Table 7.1: Numbers of mice in each group

Days in cold	0		1		2		7		14	
Type	Con	Tg	Con	Tg	Con	Tg	Con	Tg	Con	Tg
n	6	6	6	6	6	8	6	6	7	6

Table 7.2: Numbers of mice for measures of temperature, body weight, and food intake*

Days in cold	Type	Temperature	Body weight	Food intake
0	Con	31	31	5**
	Tg	31	32	3**
1	Con	25	25	25
	Tg	26	26	26
2	Con	19	19	19
	Tg	20	20	20
4	Con	13	13	13
	Tg	12	12	12
7	Con	13	13	13
	Tg	12	12	12
11	Con	/	7	7
	Tg	/	6	6
14	Con	7	7	7
	Tg	6	6	6

* For the above measurements, all available mice were included when determining mean at each time point.

** Values of food intake for zero time were taken from a previous study on the long term food intake of female control and UCP-DTA mice.

Termination:

Mice were killed between these 11:30 and 15:00 by cervical dislocation and exsanguination. IBAT, INWAT, and parametrial (PWAT) depots were removed, cleaned and weighed. Tissues were processed as listed below, remaining tissue was reweighed and frozen at -80°C for later analysis.

Tissue processing:

White adipose tissue: Samples of INWAT and PWAT were fixed in 10% buffered formalin for histological work. Remaining tissues were frozen for later analysis.

White adipose tissue assays: INWAT was processed by Masoud Ghorbani. INWAT was thawed on ice and homogenized in ice-cold isolation medium and protein content was measured in homogenates as outlined in Chapter 3. Remaining homogenate was frozen at -80°C.

Brown adipose tissue: IBAT was dissected away from adhering WAT and muscle, and then weighed. Samples were fixed in 10% buffered formalin for histology. The remaining BAT was weighed and frozen at -80°C.

Analyses of BAT and its activity: IBAT was thawed on ice and homogenized in ice-cold isolation medium as in Chapter 3. Samples of homogenate were frozen in liquid nitrogen and stored at -80°C for later assays (protein).

Serum assays:

Serum leptin was measured using a mouse leptin RIA kit from LINCO Research. Inc. (CEDARLANE Laboratories Ltd.).

Data presentation and analysis:

All data are expressed as means ± SEM. Instat software was used for analysis of variance followed by Tukey-Kramer post hoc tests.

Results

Body temperatures:

When housed at normal animal care facility temperatures (24°C), the body temperatures of transgenic mice are significantly lower than those of control mice (37.6 ± 0.1 °C (n=31) vs. 37.9 ± 0.1 °C (n=31), P=0.039, Figure 7.1). When they are exposed to mild cold (14°C), the body temperatures of both groups decline slightly. The temperature of both groups dipped on the first day of exposure to the cold; a significant increase from day 1 was seen at day 4 in both groups. UCP-DTA mice at 14°C have a significantly lower body temperature than control mice for the first week of acclimation (Figure 7.1). They could not, however, be described as hypothermic, maintaining a temperature consistently between 37.5°C and 38°C. After 14 days of acclimation to cold, both groups of mice can thermoregulate and maintain their body temperature at the temperature at which they started (Figure 7.1).

Body weights:

Female transgenic mice weigh almost 10 grams more than female control mice at 18-20 weeks of age (33.1 ± 0.9 g vs. 25.3 ± 0.4 g, P<0.001, Figure 7.2). The body weight of control mice is significantly higher after the two weeks of cold acclimation (Figure 7.2). The UCP-DTA mice did not weigh significantly more than the control mice after one week of cold exposure (Figure 7.2).

Cold-induced change in body temperature

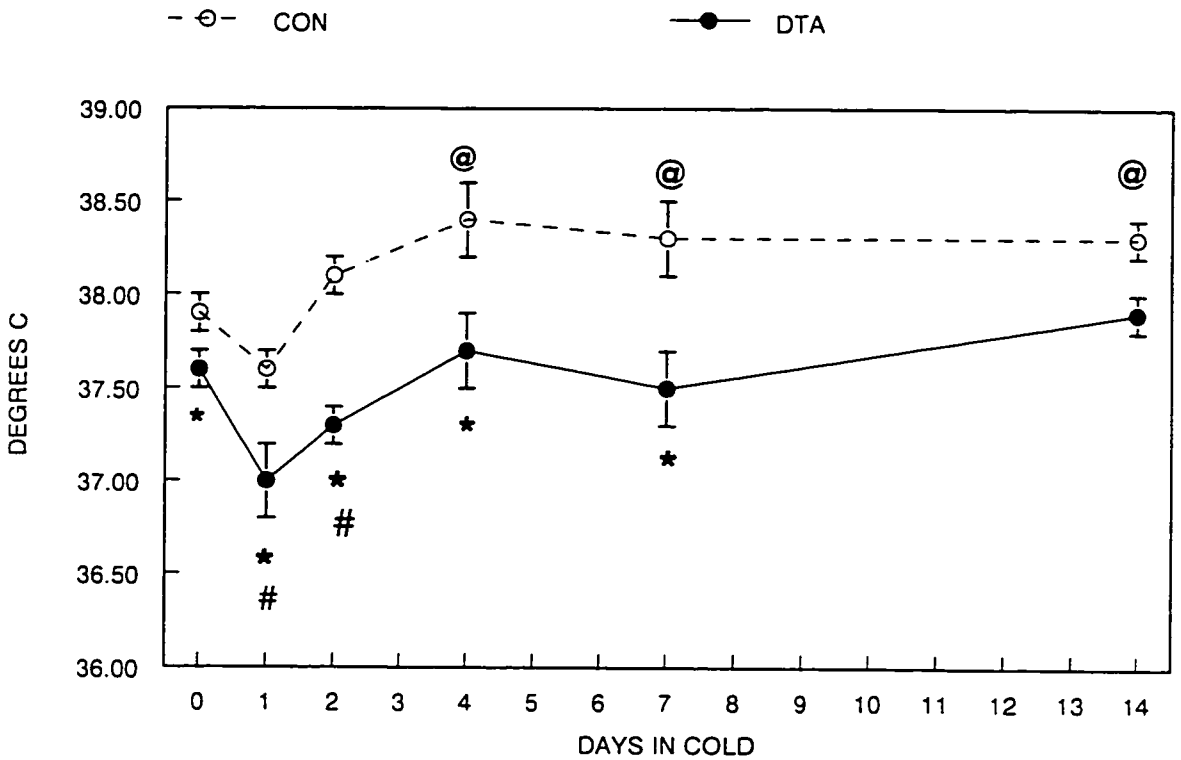

Figure 7.1: Body temperature (as measured with a rectal probe) in control and transgenic mice exposed to mild cold for 2 weeks. Both control and DTA mice were able to thermoregulate at 14°C. At Day 0, the body temperature of UCP-DTA mice is significantly lower than that of control mice (P=0.039). For numbers of mice see Table 7.2.
*denotes significant difference between UCP-DTA and control; @ denotes significant difference from control at day zero; # denotes significant difference from UCP-DTA at day zero.

Cold-induced change in body weight

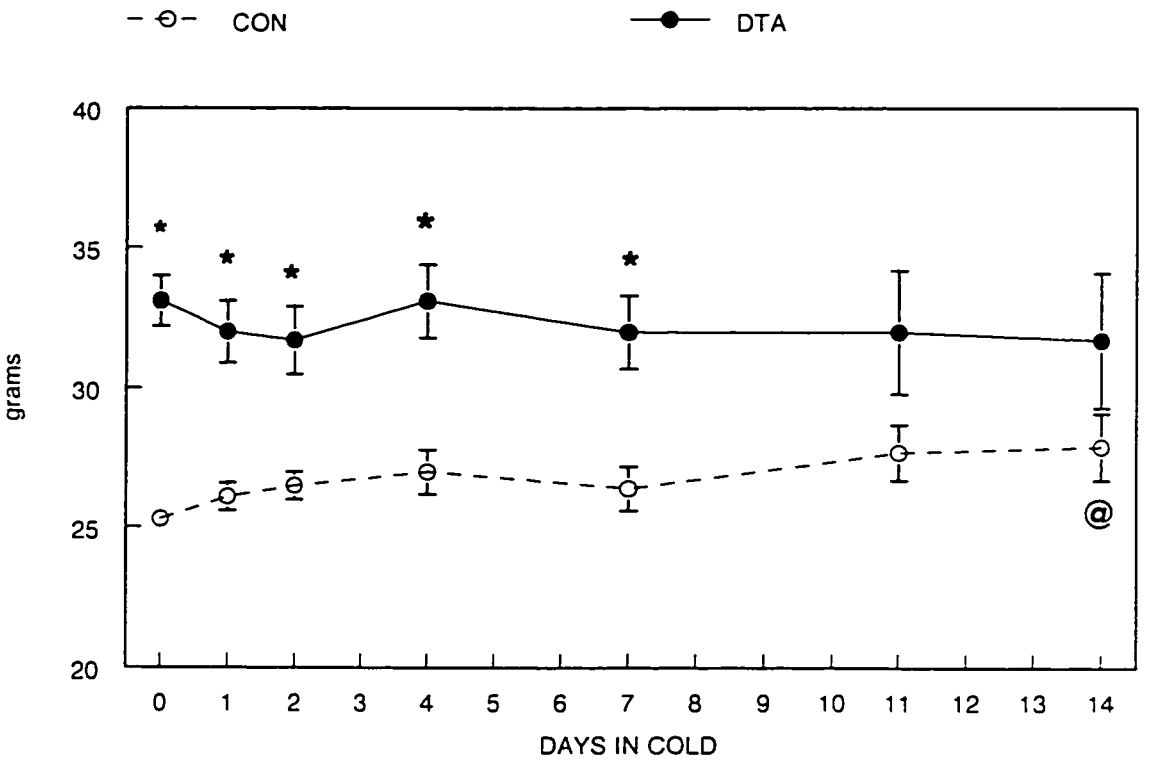

Figure 7.2: Body weights of control and transgenic mice exposed to mild cold for two weeks. For numbers of mice see Table 7.2.
*denotes significant difference between UCP-DTA and control; @ denotes significant difference from control at day zero.

Food intake:

Food intake of control mice at 14°C increased rapidly with exposure to cold. It increased 3 fold by the second day, and then remained at this elevated level for the remainder of the period of acclimation to 14°C (Figure 7.3). Food intake of UCP-DTA mice was almost double that of control mice before the exposure to cold on day zero but did not change during the first 4-7 days of exposure to cold (Figure 7.3); they were thus hypophagic compared with control mice. By 14 days, food intake of the UCP-DTA mice had increased slightly to reach the same high level as in the control mice.

Serum leptin:

The concentration of leptin in serum of control mice was low and did not change throughout the 14 days of acclimation to cold (Figure 7.4). At day zero, serum leptin levels were fivefold higher in the obese, 18 week old UCP-DTA mice as compared to controls (Figure 7.4). Serum leptin levels in transgenic mice dropped by 50% with one day of exposure to cold to a level not significantly different from that of control mice. The decrease in leptin level in UCP-DTA mice paralleled almost exactly the decrease in wet weight of their INWAT and PWAT, which likewise weighed only slightly greater than and not significantly different from that of control mice by day 14 (Figures 7.5, 7.6).

Cold-induced increase in food intake

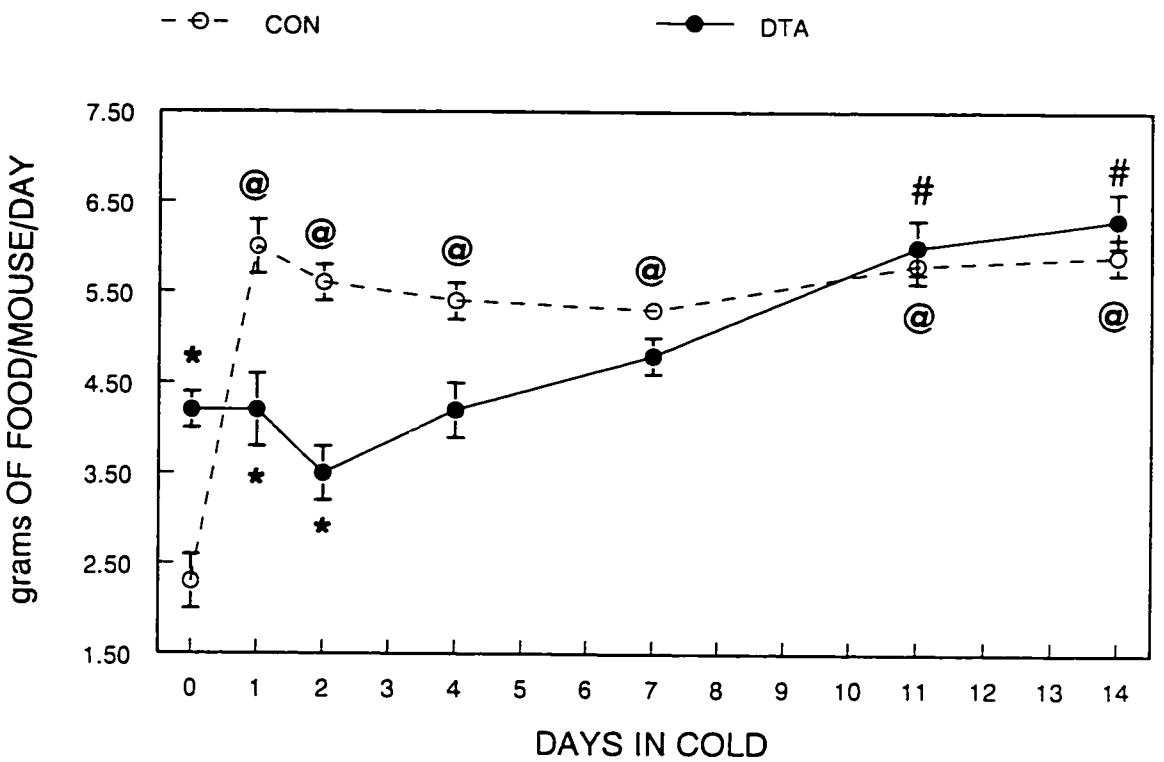

Figure 7.3: Food intake (grams of food/mouse/day) of control and transgenic mice acclimated to the cold for two weeks. For numbers of mice see Table 7.2. Values of food intake at zero time were taken from a previous study on long term food intake of female control and UCP-DTA mice.
*denotes significant difference between UCP-DTA and control; @ denotes significant difference from control at day zero; # denotes significant difference from UCP-DTA at day zero.

Cold-induced change in serum leptin

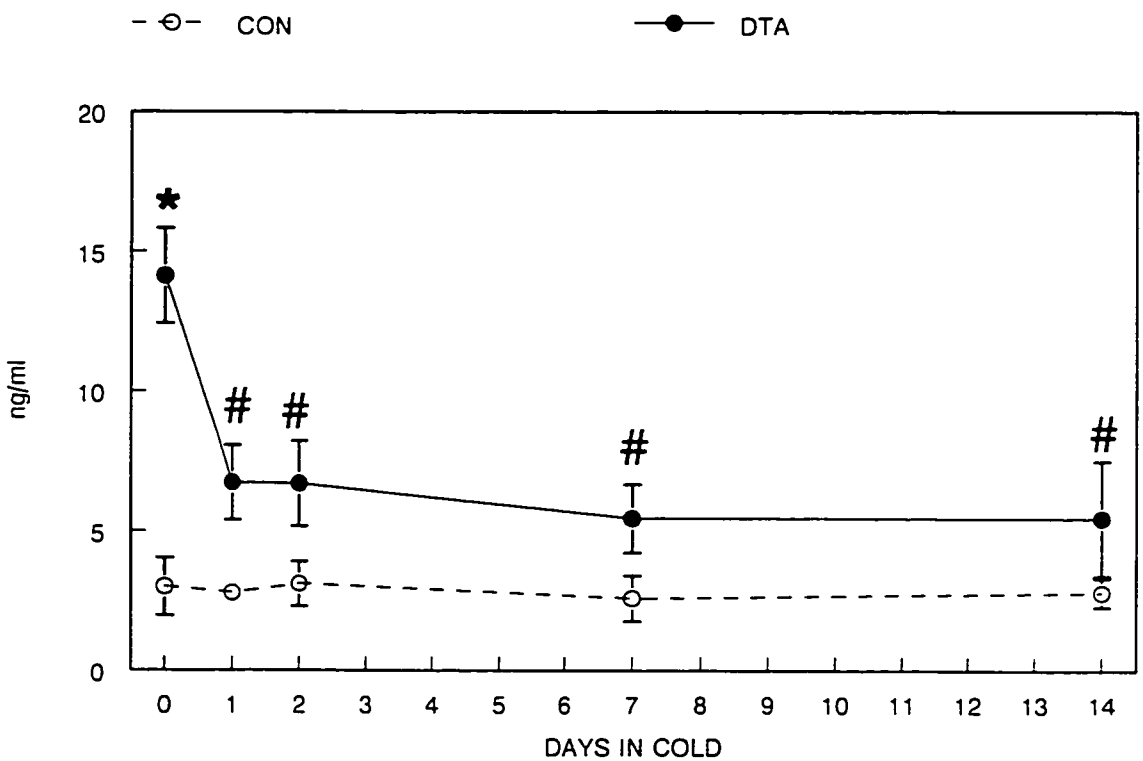

Figure 7.4: Serum leptin levels in transgenic and control mice. There is a significant difference in the leptin levels of DTA and control mice at day zero (14.13 ± 1.70, and 3.02 ± 1.03 respectively, $P<0.001$). A significant decrease is seen in the leptin levels of the DTA mice when exposed to cold ($P<0.001$). For numbers of mice see Table 7.1.
*denotes significant difference between UCP-DTA and control; # denotes significant difference from UCP-DTA at day zero.

Cold-induced change in inguinal WAT weight

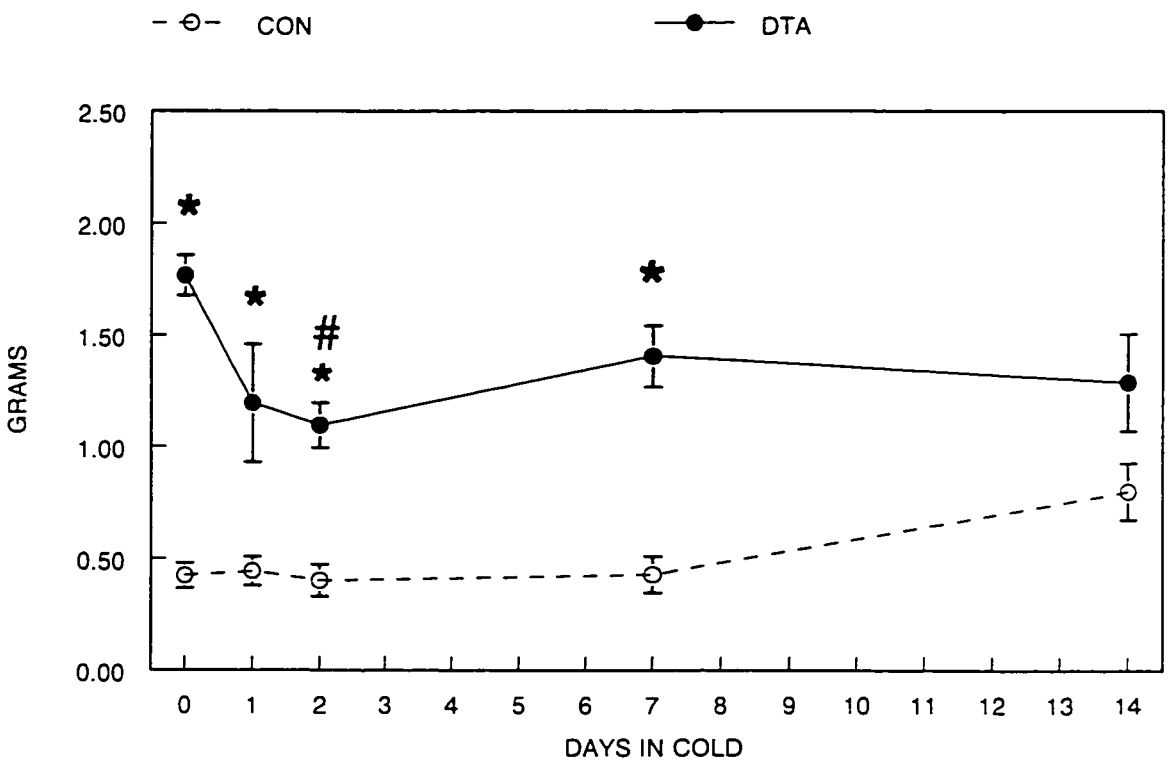

Figure 7.5: Wet weight of INWAT of control and transgenic mice. For numbers of mice see Table 7.1.
*denotes significant difference between UCP-DTA and control; # denotes significant difference from UCP-DTA at day zero.

Cold-induced change in parametrial WAT weight

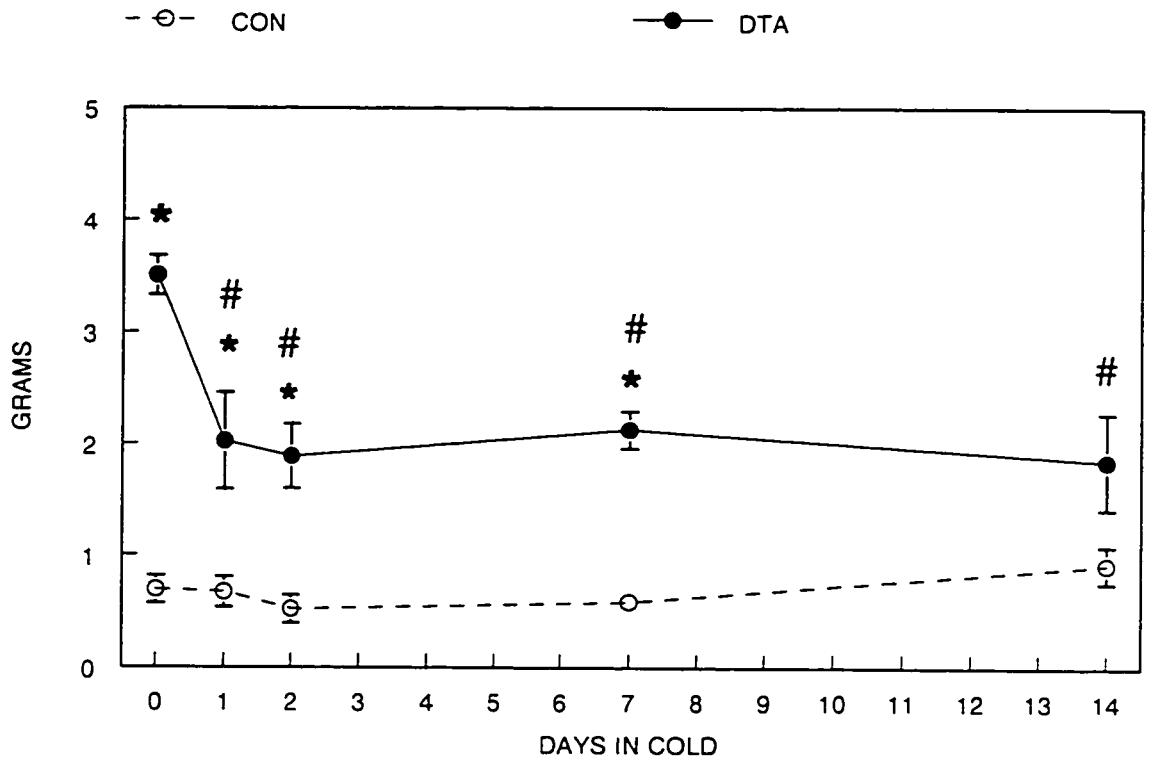

Figure 7.6: Wet weight of PWAT of control and transgenic mice. For numbers of mice see Table 7.1.
*denotes significant difference between UCP-DTA and control; # denotes significant difference from UCP-DTA at day zero.

White adipose tissue:

Using the weight of INWAT and PWAT as indices of obesity, female transgenic mice are obese at 18-20 weeks of age as compared with controls (Figures 7.5, 7.6). The weights of these fat pads are significantly greater in the transgenic mice for the first week of cold exposure (Figures 7.5, 7.6). The weights of fat depots in the transgenic mice decrease with acclimation to the cold temperature, weighing significantly less than those in non-exposed mice by 1 day (PWAT) or by 2 days in the cold (INWAT) (Figures 7.5, 7.6). By the end of the two weeks of cold exposure, the weights of the two WAT depots are not different between groups (Figures 7.5, 7.6).

Protein content in INWAT was initially lower in UCP-DTA mice than in control mice but increased significantly during acclimation (Figure 7.7). The higher initial level in control mice was not further increased by acclimation to cold.

Cold-induced increase in inguinal WAT protein

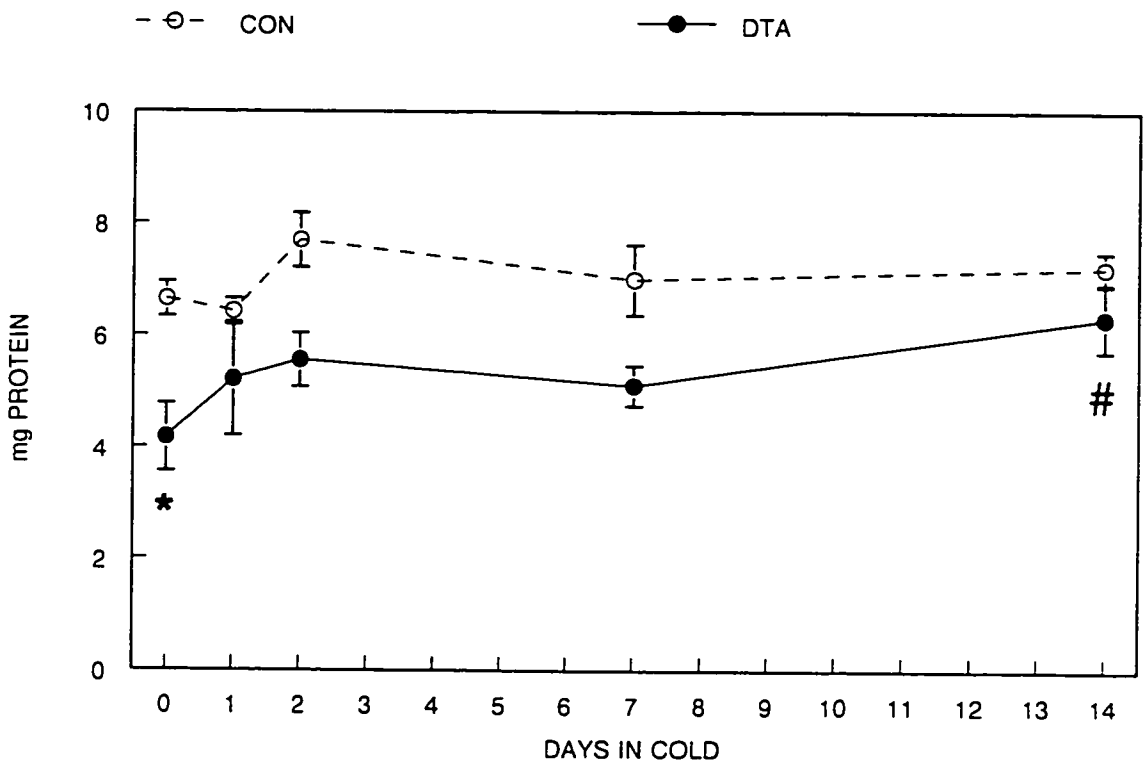

Figure 7.7: Total protein of INWAT. Protein content was initially lower in UCP-DTA mice than in control mice but increased significantly during acclimation. The higher initial level in control mice was not further increased by acclimation to cold. For numbers of mice see Table 7.1.

*denotes significant difference between UCP-DTA and control; # denotes significant difference from UCP-DTA at day zero.

Histology of inguinal white adipose tissue:

Appearance of INWAT of control mice differs from that of transgenic mice at 18 weeks of age (Figures 7.8 and 7.9; A, B). Multilocular adipocytes that are positive for UCP are present in control mice (Figures 7.8, 7.9; A), however none are apparent in the UCP-DTA mice at this age (Figures 7.8, 7.9; B). Unilocular adipocytes are larger in the transgenic mice than in control mice (Figures 7.8. and 7.9; A. B).

When mice are acclimated to 14 °C for two weeks, multilocular brown adipocytes are much more abundant in control mice, but are also apparent in UCP-DTA mice (Figures 7.8 and 7.9; C, D). Note the different appearance of multilocular brown adipocytes between the two groups of mice; they have a more dense appearance in the control mice (Figure 7.8 C). An increase in UCP is evident in both groups after two weeks of cold acclimation, as indicated by the dark staining in multilocular brown adipocytes (Figure 7.9; C, D).

Figures 7.10 and 7.11 show the effects of acclimation to 14 °C on INWAT appearance over time. Multilocular brown adipocytes increase in control mice and appear in UCP-DTA mice at day 1 (Figures 7.10 and 7.11; A, B). Brown adipocytes seem to proliferate at days 1 and 2 and then to take up lipid by day 7 (Figure 7.10). Note the increase in UCP immunostaining in the brown adipocytes in control and transgenic mice after two days of cold acclimation (Figure 7.11; C, D), and after 7 days in the cold (Figure 7.11; E, F).

Histology of inguinal white adipose tissue

Figure 7.8: Hematoxylin and eosin stained 4μm sections of INWAT of: control mice at day zero (A), UCP-DTA mice at day zero (B), control mice acclimated to 14°C for 14 days (C), and UCP-DTA mice acclimated to 14°C for 14 days (D). Magnification x 200. Multilocular brown adipocytes are present at day zero in control mice (A), only large unilocular cells are seen in UCP-DTA mice (B). Multilocular brown adipocytes appeared in UCP-DTA mice by day 14 of acclimation (D), and increased in control mice after this time (C). Note the difference in appearance of brown adipocytes in the two groups after 14 days of acclimation: they have a more dense appearance in control mice (C and D).

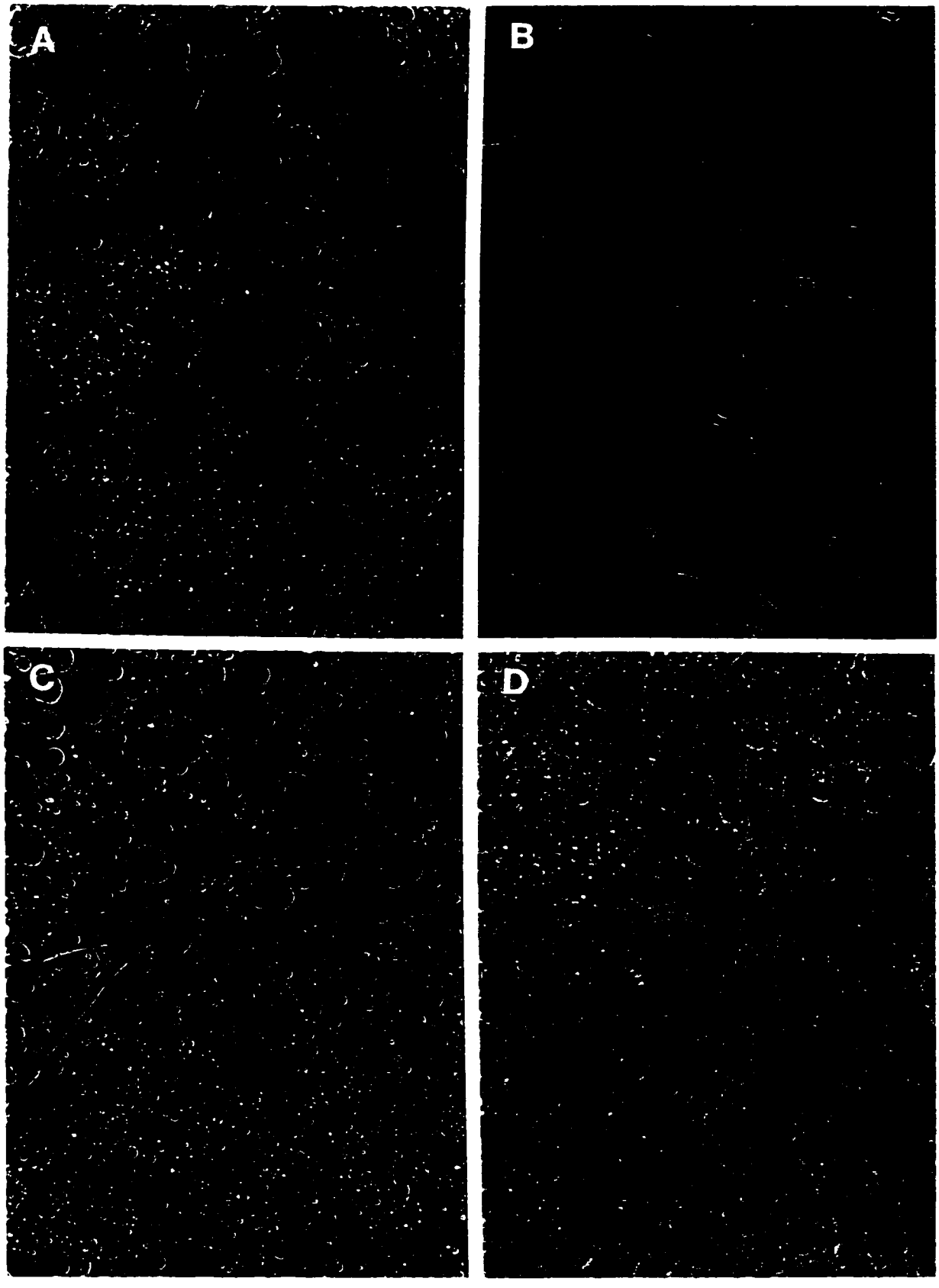
A
B
C
D

Immunohistochemical detection of UCP in INWAT

Figure 7.9: Immunohistochemical detection of UCP in INWAT of: control mice at day zero (A), UCP-DTA mice at day zero (B), control mice acclimated to 14°C for 14 days (C), and UCP-DTA mice acclimated to 14°C for 14 days (D). Magnification x 200. Multilocular brown adipocytes that are positive for UCP present at day zero in control mice (A); only large unilocular cells are seen in UCP-DTA mice (B). Multilocular brown adipocytes staining positively appeared in UCP-DTA mice by day 14 of acclimation (D), and increased in control mice after this time (C). Note that the immunostaining was much darker in brown adipocytes of both groups after 14 days of acclimation (C and D).

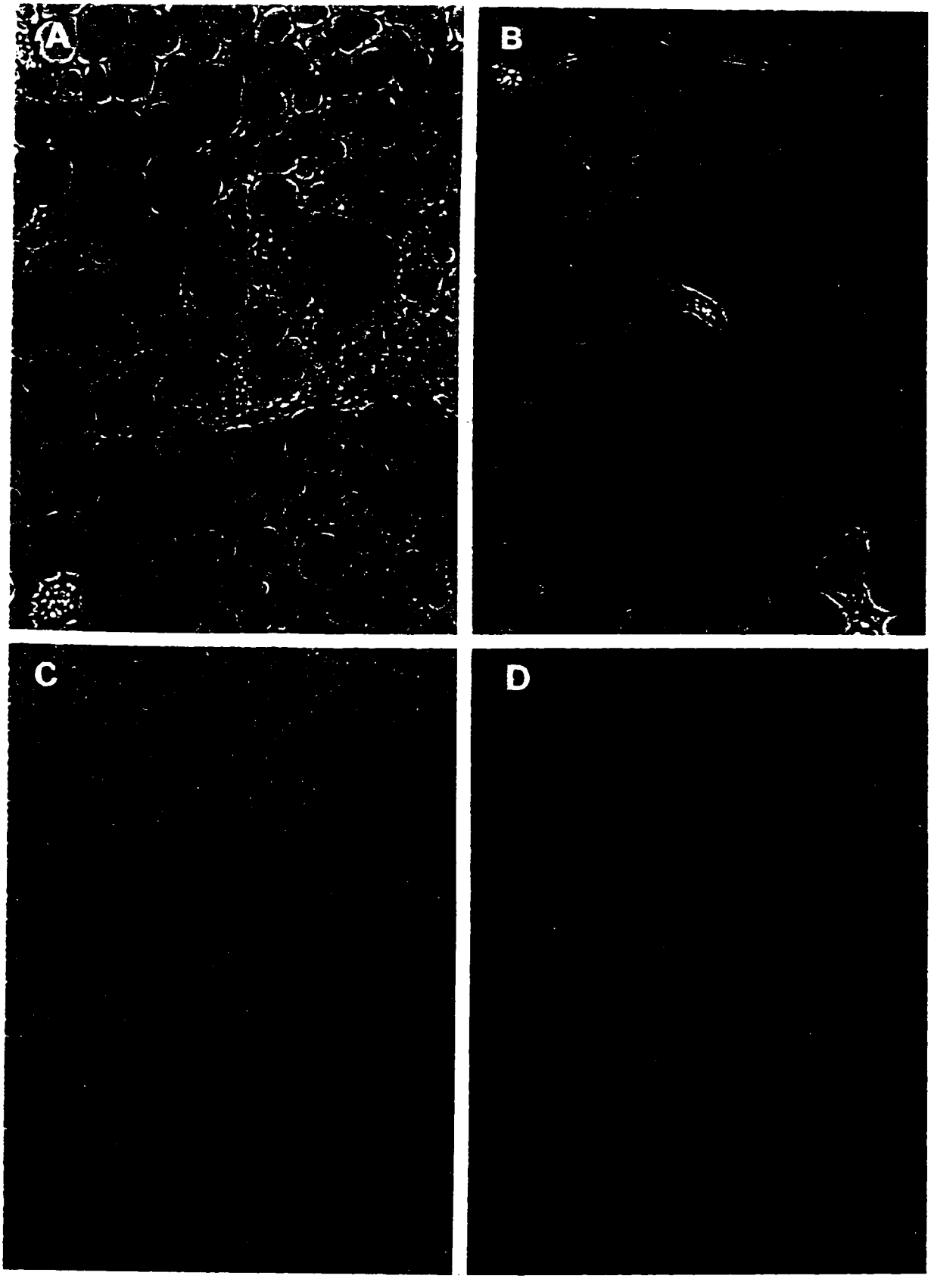
A
B
C
D

Histology of inguinal white adipose tissue

Figure 7.10: Hematoxylin and eosin stained 4μm sections of INWAT of: control mice (A, C, E), and UCP-DTA mice (B, D, F) acclimated to 14°C for 1 day (A, B), 2 days (C, D), and 7 days (E, F). Magnification x 200. Multilocular brown adipocytes appear in INWAT of UCP-DTA mice after 1 day of cold exposure (B). In both groups, there is an increase in brown adipocyte number from day 1 (A, B) to day 7 (C, D), followed by an increased lipid accumulation in these cells from day 7 to day 14 (E, F).

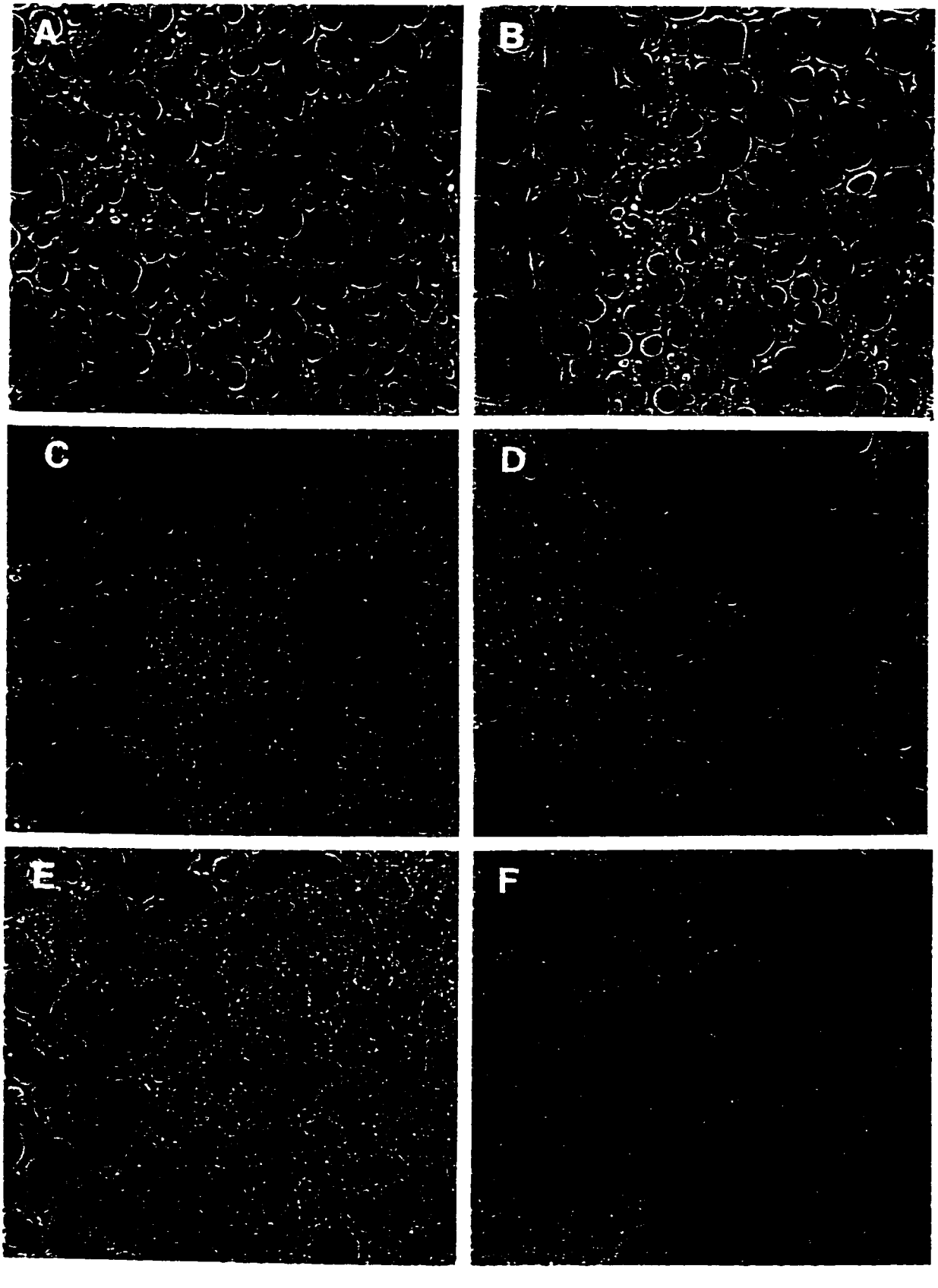
A
B
C
D
E
F

Immunohistochemical detection of UCP in INWAT

Figure 7.11: Immunohistochemical detection of UCP in INWAT of: control mice (A, C, E), and UCP-DTA mice (B, D, F) acclimated to 14 °C for 1 day (A, B), 2 days (C, D), and 7 days (E, F). Magnification x 200. Multilocular brown adipocytes that are positively stained appear in INWAT of UCP-DTA mice after 1 day of cold exposure (B). Note the increase in positively stained brown adipocytes in both groups after 2 days of acclimation (C, D), and the marked patchiness of the immunostaining (C, D), also apparent at 7 days (E, F). In Figure 7.11C, the immunostained tissue has a 'Harlequin' appearance.

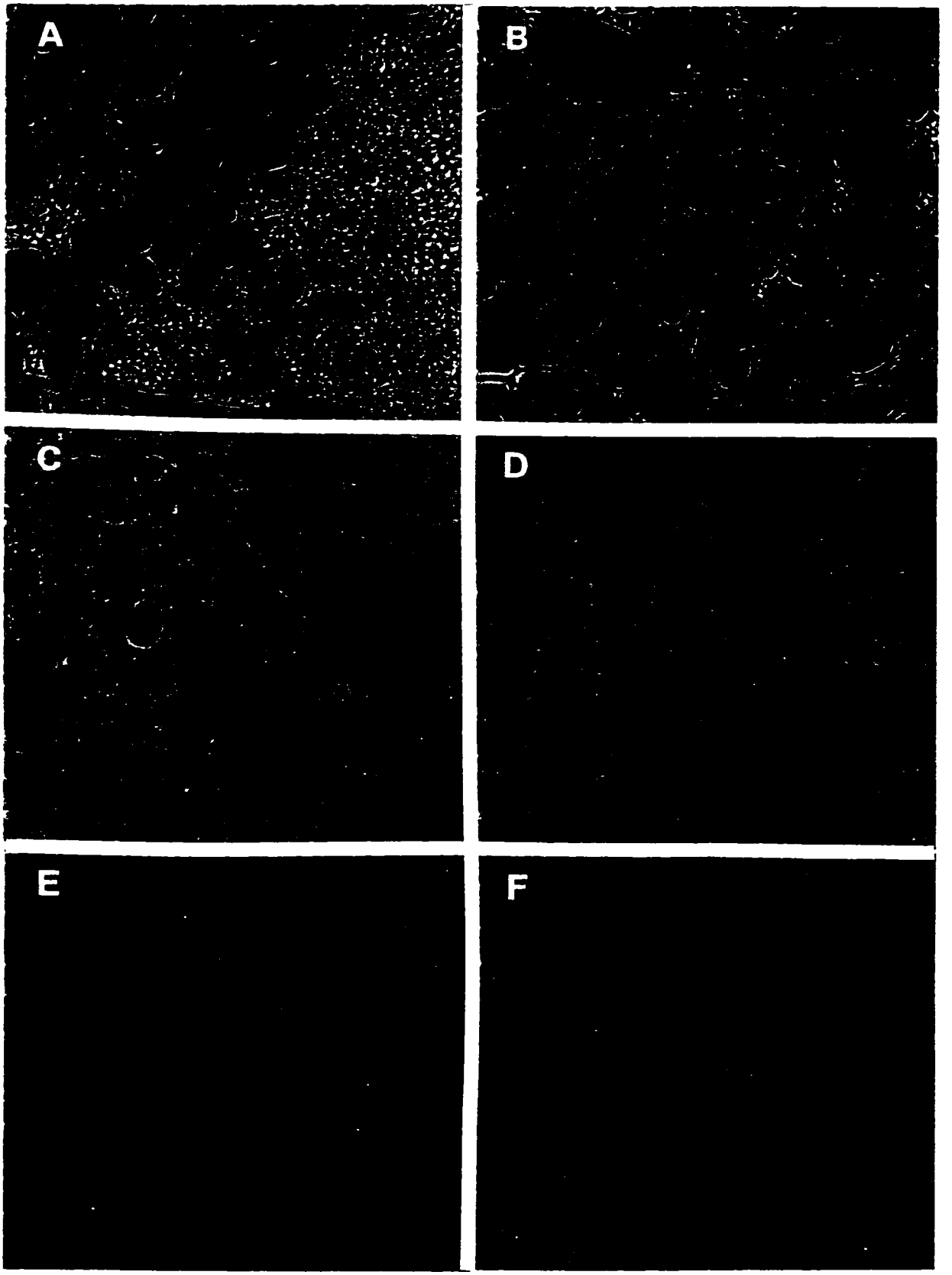
A
B
C
D
E
F

Interscapular brown adipose tissue:

The wet weight of IBAT remained little altered by cold in either type of mouse until 14 days, when it was increased in both groups (Figure 7.12). There was no difference in the weight of IBAT between control and UCP-DTA mice at any of the time points studied.

Protein content of IBAT increased rapidly in control mice, reaching a maximum level by 2 days (Figure 7.13), at which point it was significantly different from that of UCP-DTA mice. Protein content of IBAT of UCP-DTA mice was lower than that of control mice on day zero and increased more slowly than that of control mice. By 7 days of acclimation to cold the IBAT protein content of the UCP-DTA mice had increased significantly from that of UCP-DTA mice at day zero (Figure 7.13).

Cold-induced change in interscapular BAT weight

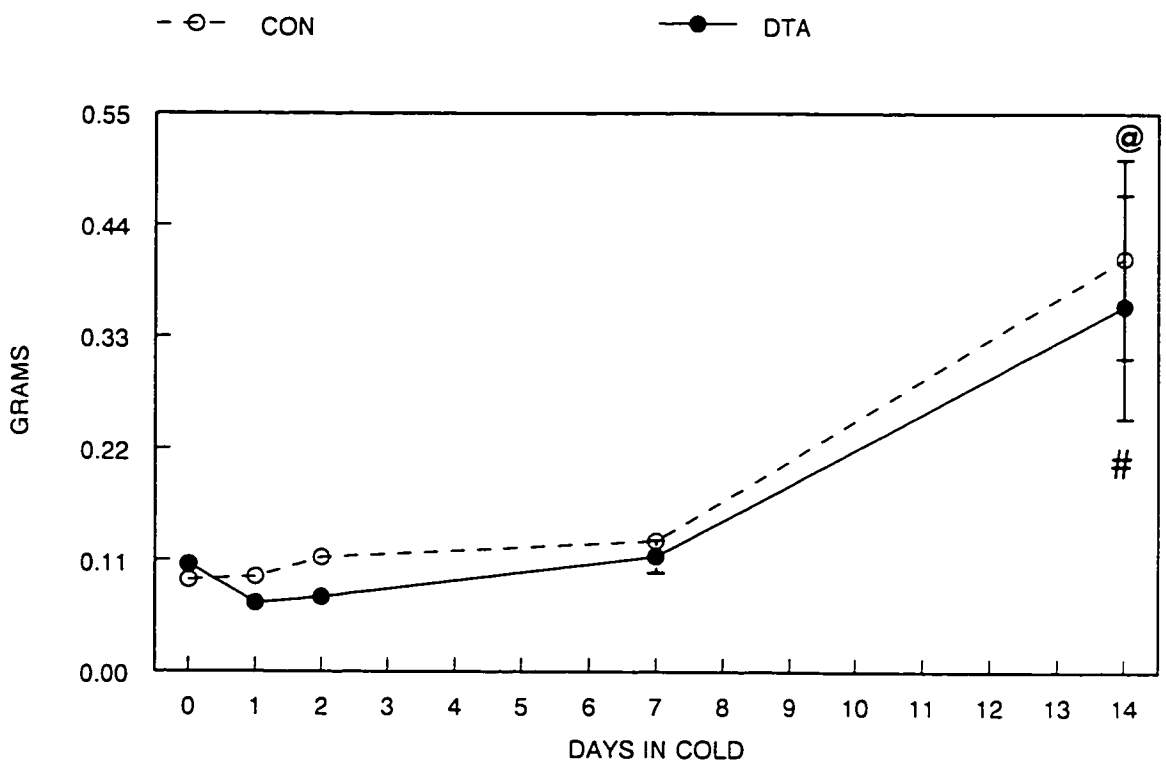

Figure 7.12: Wet weight of IBAT of control and transgenic mice. For numbers of mice see Table 7.1.
@ denotes significant difference from control at day zero; # denotes significant difference from UCP-DTA at day zero.

Cold-induced increase in interscapular BAT protein

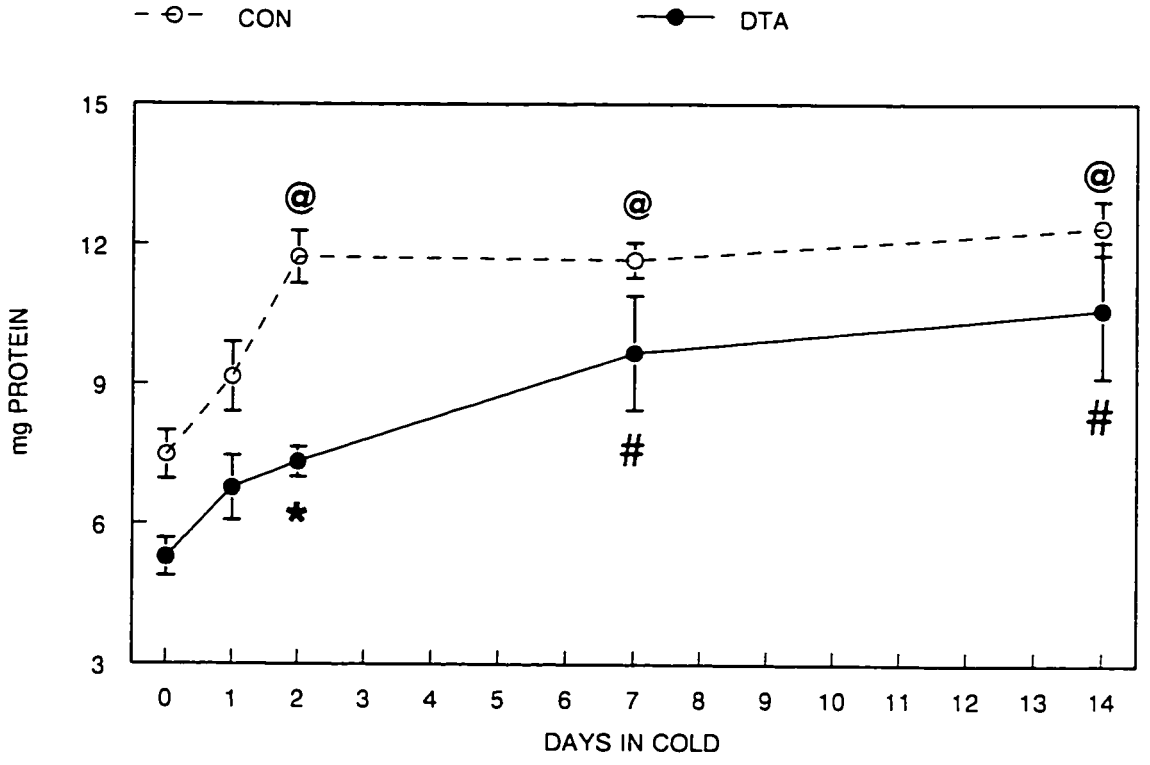

Figure 7.13: Total protein content of IBAT of control and transgenic mice.The only significant difference in protein content seen between UCP-DTA and control mice is at 2 days in the cold. For numbers of mice see Table 7.1.
*denotes significant difference between UCP-DTA and control; @ denotes significant difference from control at day zero; # denotes significant difference from UCP-DTA at day zero.

Histology of interscapular brown adipose tissue:

IBAT of control and UCP-DTA mice at 18 weeks of age has a different appearance (Figures 7.14 and 7.15; A, B). Multilocular adipocytes that are positive for UCP are present in both groups of mice at this time (Figures 7.14, 7.15; A, B). Unilocular adipocytes are present and abundant in the UCP-DTA mice (Figures 7.14, and 7.15; A, B).

When control mice are acclimated to 14°C for two weeks the proportion of multilocular brown adipocytes increases (Figures 7.14 and 7.15; C); the adipocytes also have a much more dense appearance (Figure 7.14), with more UCP staining (Figure 7.15). An increase in the proportion of multilocular cells is also apparent in UCP-DTA mice after 14 days of acclimation (Figures 7.14 and 7.15; D). The difference in the appearance of IBAT between the two groups is still apparent after 14 days of acclimation (Figures 7.14 and 7.15; C, D). Transgenic mice have more lipid in their multilocular brown adipocytes and they are less densely stained than the control mice (Figure 7.14; C, D).

Figures 7.16 and 7.17 show the effects of acclimation to 14°C on IBAT appearance over time. Multilocular brown adipocytes of UCP-DTA mice contain more lipid than those of control mice at all time points (Figures 7.16 and 7.17).

Histology of interscapular brown adipose tissue

Figure 7.14: Hematoxylin and eosin stained 4μm sections of IBAT of: control mice at day zero (A), UCP-DTA mice at day zero (B), control mice acclimated to 14°C for 14 days (C), and UCP-DTA mice acclimated to 14°C for 14 days (D). Magnification x 200. Appearance of IBAT of UCP-DTA mice is different from control mice at time zero (A, B) and after 14 days at 14°C (C, D). UCP-DTA mice have more unilocular adipocytes at day zero (B) and more lipid in their multilocular brown adipocytes at 14 days (D). An increase in the density of staining of brown adipocytes is seen at 14 days (C, D), which is more pronounced in control mice (C).

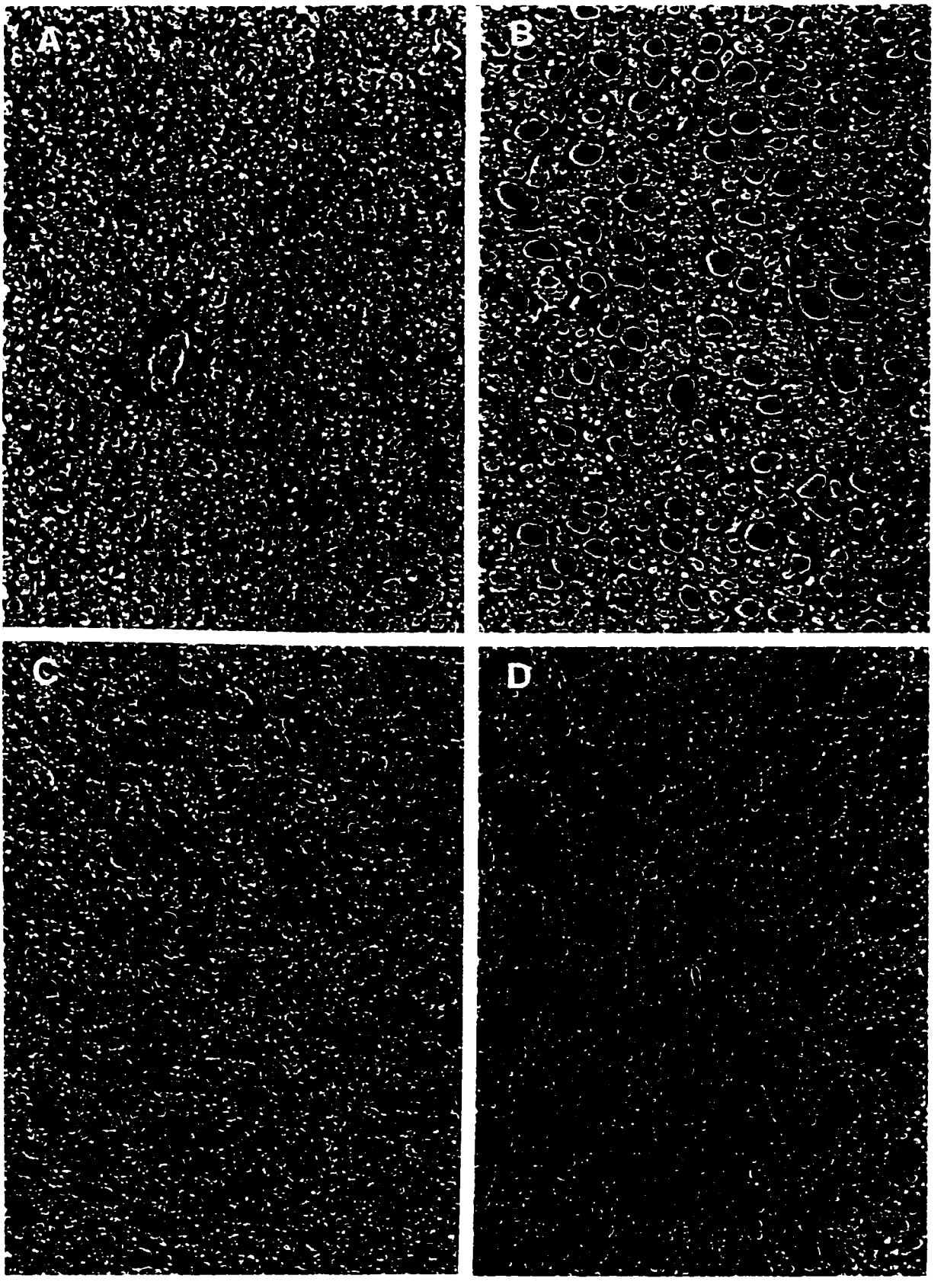
A
B
C
D

Immunohistochemical detection of UCP in IBAT

Figure 7.15: Immunohistochemical detection of UCP counterstained with hematoxylin in IBAT of: control mice at day zero (A), UCP-DTA mice at day zero (B), control mice acclimated to 14°C for 14 days (C), and UCP-DTA mice acclimated to 14°C for 14 days (D). Magnification x 200. Many positive staining multilocular brown adipocytes are present in all groups at all times. UCP-DTA mice have unilocular adipocytes present in their IBAT (B, D).

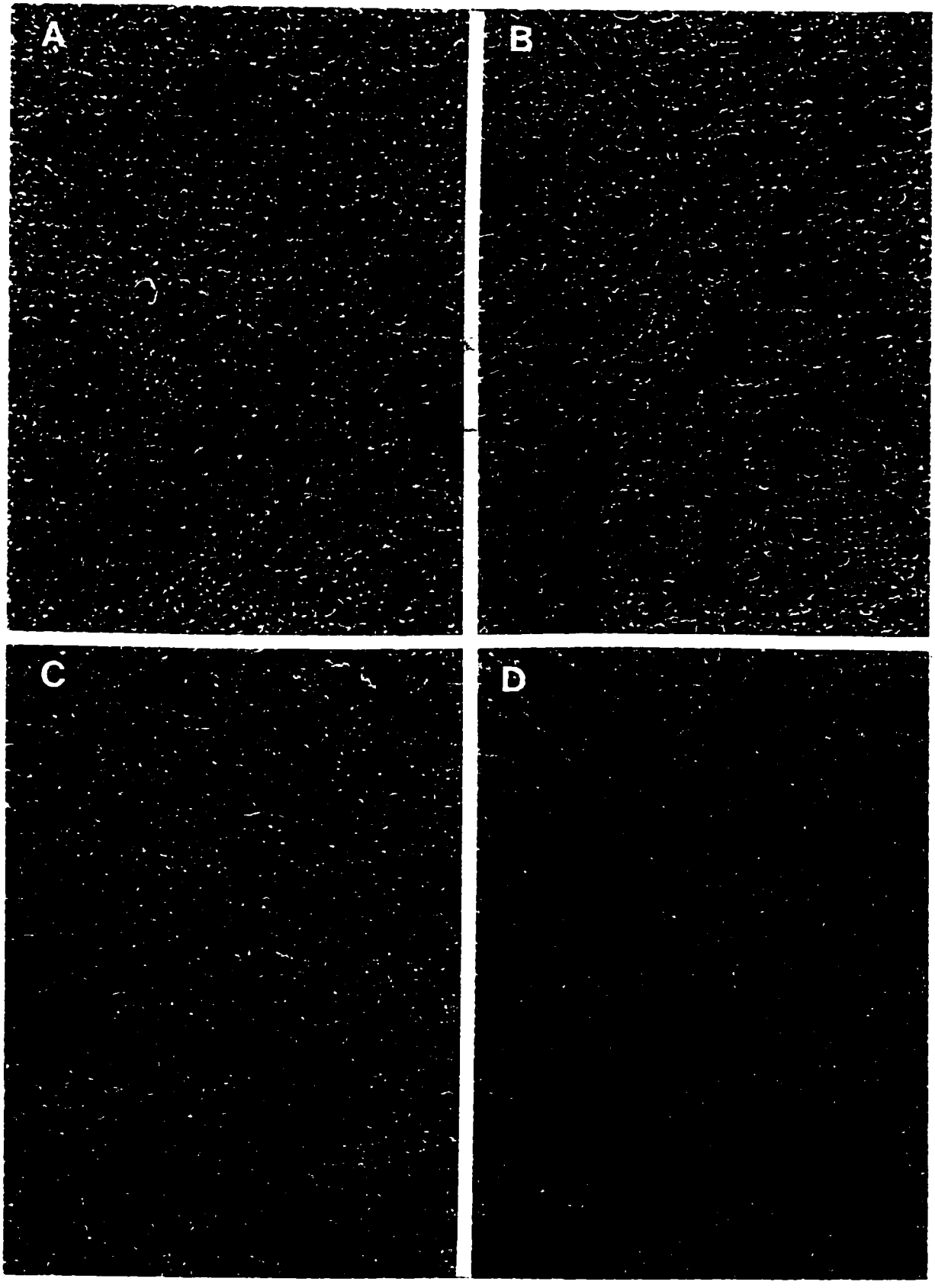
A
B
C
D

Histology of interscapular brown adipose tissue

Figure 7.16: Hematoxylin and eosin stained 4μm sections of IBAT of: control mice (A, C, E), and UCP-DTA mice (B, D, F) acclimated to 14°C for 1 day (A, B), 2 days (C, D), and 7 days (E, F). Magnification x 200. No unilocular adipocytes are seen in IBAT of any groups when acclimated to cold. Multilocular brown adipocytes have a very heterogeneous appearance.

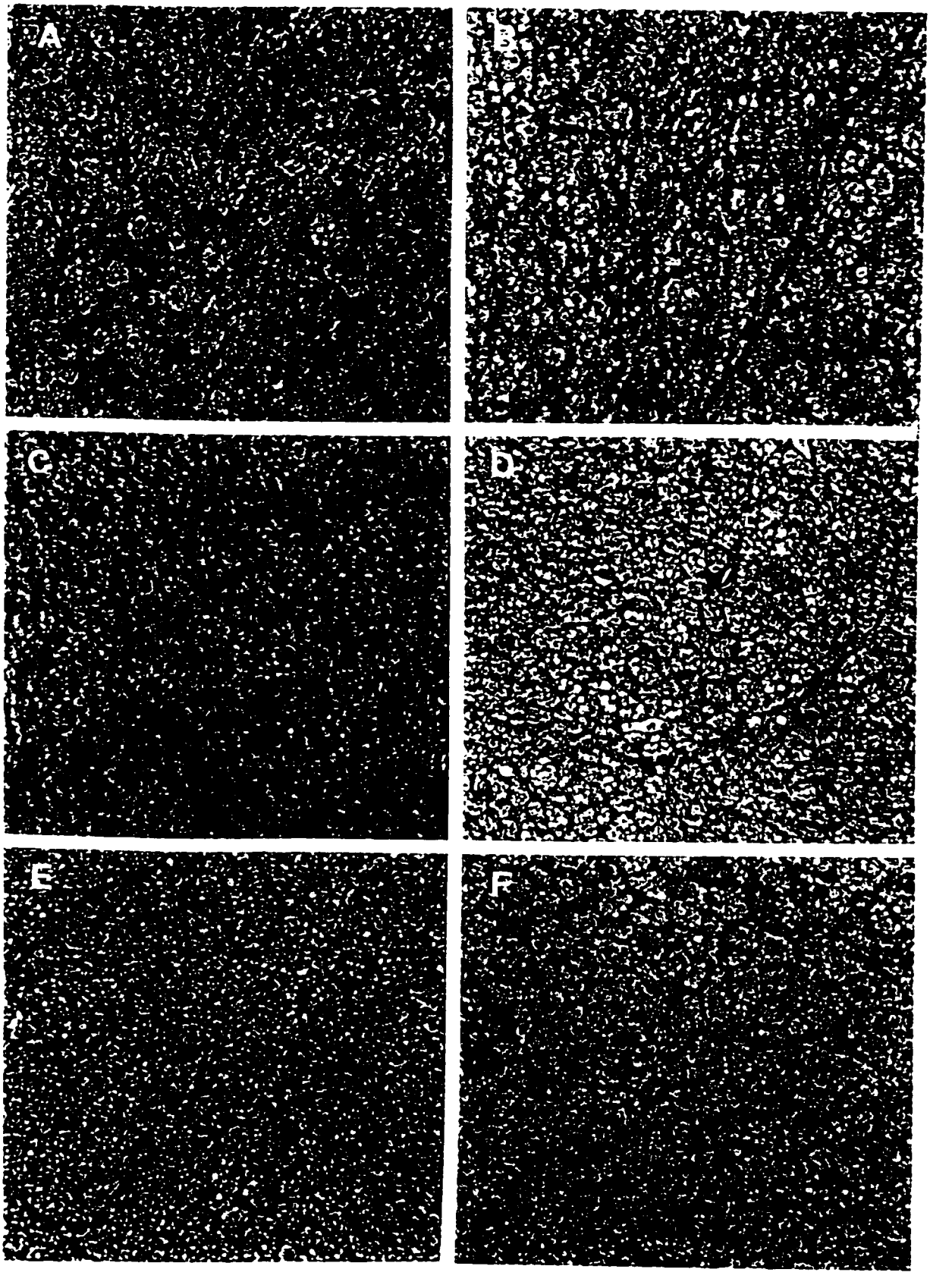
A
B
C
D
E
F

Immunohistochemical detection of UCP in IBAT

Figure 7.17: Immunohistochemical detection of UCP counterstained with hematoxylin in IBAT of: control mice (A, C, E), and UCP-DTA mice (B, D, F) acclimated to 14°C for 1 day (A, B), 2 days (C, D), and 7 days (E, F). Magnification x 200. Positively staining multilocular brown adipocytes are present in all groups always. UCP-DTA mice have unilocular adipocytes present in their IBAT after 7 days acclimation to 14°C (F). Very faint indication of Harlequin effect can be seen in IBAT of both groups with acclimation to cold.

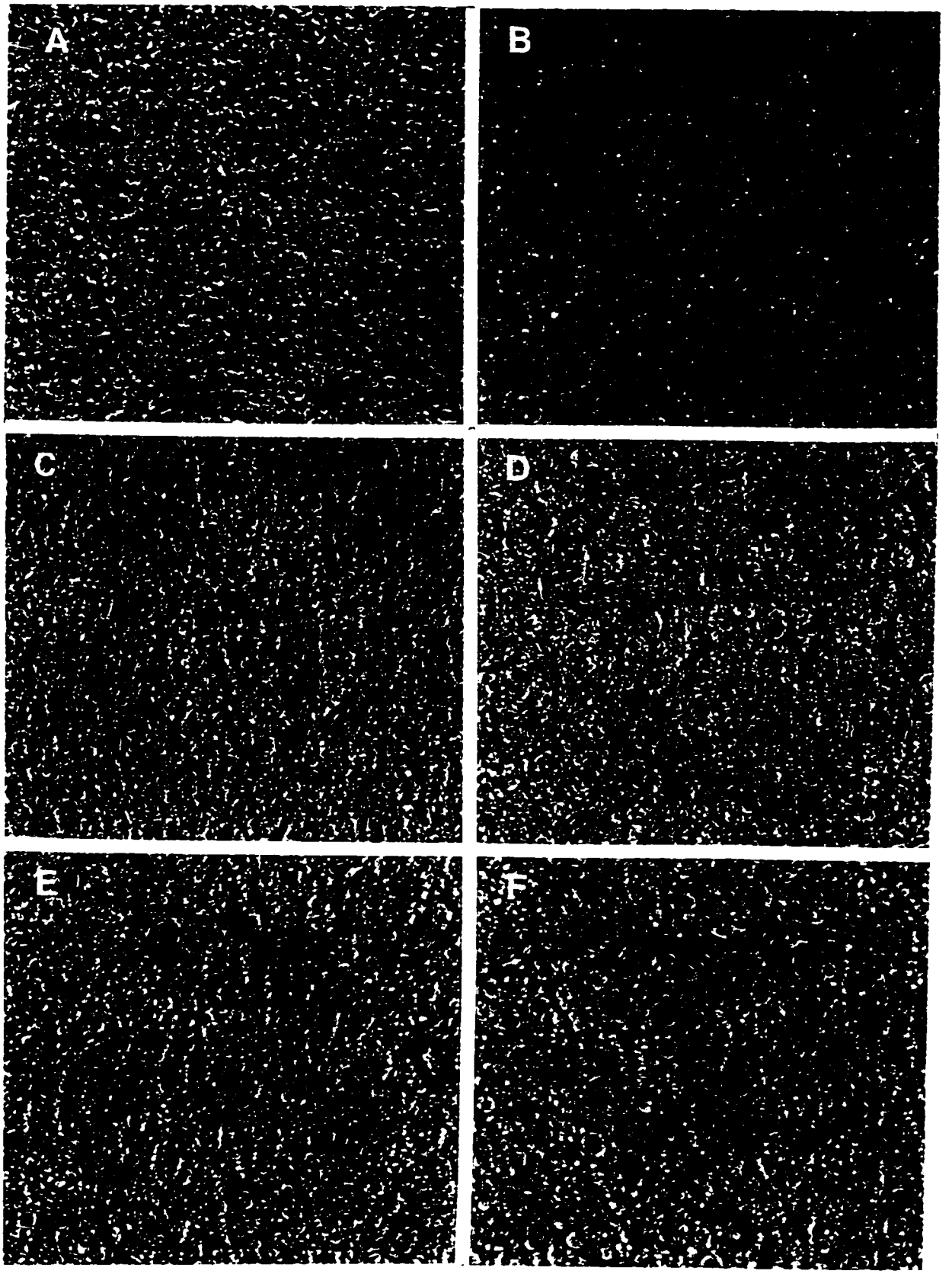
A
B
C
D
E
F

Discussion

One major finding in this study is that the increase in food intake that occurs in normal mice when they are exposed to cold is not correlated with any change in serum leptin levels and that the mechanism controlling this temperature-mediated change in food intake is defective in the UCP-DTA mouse.

Normal mice increase food intake very rapidly in the cold (almost doubled by one day with no further increase after that), during which time there is no change at all in their serum leptin. UCP-DTA mice, already hyperphagic, did not increase their food intake very rapidly in the cold. At 4-7 days of acclimation to cold there is still no change in their food intake, but eventually it reaches the high level seen in control mice by 11-14 days. Leptin levels in the UCP-DTA mice are initially fivefold higher than those in controls (Figure 7.4), at a time when they are eating twice as much as controls. Serum leptin levels in transgenic mice dropped by 50% with one day of exposure to cold, during which time their food intake did not change. Leptin levels did not change significantly during the remainder of the period of cold acclimation in the UCP-DTA mice. Contrary to this, the UCP-DTA mice gradually increased their food intake to a level not significantly different from that of control mice by day 4 (Figure 7.3), at a time when leptin levels did not change. The decrease in leptin level in UCP-DTA mice did however parallel almost exactly the decrease in wet weight of their INWAT and PWAT, which likewise reached a level only slightly greater than that of control mice by day 14 (Figures 7.5, 7.6).

The second major finding of this study was the nature of the compensation in the UCP-DTA mouse when exposed to cold. The UCP-DTA mouse appears to compensate for its lack of UCP1 expressing brown adipocytes, in a manner not available to the UCP1-KO mouse (Enerbäck *et al.* 1997), which is sensitive to cold.

Acclimation to cold induces hypertrophy of BAT that includes massive proliferation of mitochondria. Growth of BAT (increase in protein) was rapid in control mice and slow after a lag in UCP-DTA mice, but the same maximum was reached eventually. Acclimation of the UCP-DTA mouse to cold results in a delayed growth of BAT and in an almost normal BAT histology. This delay in UCP-DTA mice may be due to a lack of hypertrophy of UCP1 adipocytes. The later growth may be due to hypertrophy of adipocytes expressing another isoform of UCP. Acclimation to cold also induces the appearance of abundant multilocular adipocytes in INWAT of both control and UCP-DTA mice. These are identified as brown adipocytes because of their expression of UCP {as recognized by an antiserum that recognizes both UCP1 and UCP2 (Chapter 3, Figure 3.2), and probably UCP3 as well}.

This interpretation of the growth of BAT in the cold-acclimated UCP-DTA mouse is based on recent evidence for the existence of more than one type of brown adipocyte (Cinti *et al.* 1997; Pellet & Lheritier 1975; Vallin 1970); see the discussion of the Harlequin effect (Cinti *et al.* 1997), Chapter 1, and Chapter 6. This Harlequin phenomenon leads to the conclusion that at least two kinds of brown adipocyte exist, one expressing UCP1 and the other expressing a different isoform of UCP. These brown adipocytes would be in both BAT and in the clusters of multilocular adipocytes that appear in WAT during chronic stimulation

of β_3 -ARs by acclimation to cold (Cousin *et al.* 1996; Cousin *et al.* 1992; Loncar 1991; Young *et al.* 1984a) or by administration of a β_3 -AR agonist (Collins *et al.* 1997; Ghorbani *et al.* 1997; Ghorbani & Himms-Hagen 1997; Nagase *et al.* 1996; Umekawa *et al.* 1997). We suggest, therefore, that when the UCP-DTA mouse loses its UCP1-expressing brown adipocytes to DTA at all temperatures below thermoneutrality it compensates by replacing them with a population of brown adipocytes that express a different isoform of UCP. This new population is not normally abundant but it can compensate thermogenically for the population that should express UCP1. We also suggest that this population does not compensate in the UCP1-KO mouse because the population of brown adipocytes that would normally express UCP1 in some way prevents this compensation.

Chapter 8: General discussion

Summary of major findings

Three different models of known atrophy of BAT (Cap-Des rats, UCP-DTA mice) or of predicted atrophy of BAT (NTS-lesioned rats) were studied.

Cap-Des rats are not hyperphagic or obese, despite the persistent relatively atrophied state of their BAT. Cap-desensitization at the age of 1.5 months prevented the aging-associated, hyperplastic obesity that develops in 13.5-month-old Sprague-Dawley rats. No clear relationship exists between the leanness in the Cap-Des rat and any known function of Cap sensitive sensory nerves, neither to their local effector functions in all peripheral tissues nor to the function of their central projections.

The attenuated age-associated increase in circulating CGRP (derived mainly from Cap-sensitive nerves) in the Cap-Des rat (Wimalawansa 1993) was suggested to result in a lower degree of aging-associated insulin-resistance, and thus in a lesser degree of obesity (Melnyk & Himms-Hagen 1995).

Lesions of the NTS did not affect the thermogenic capacity of BAT. IBAT of the NTS-lesioned rats was not different with respect to weight, protein content, cellularity, content of mitochondria or content of UCP. Atrophy of BAT cannot explain the lack of thermogenic response of BAT to catecholamines seen by others in NTS-lesioned rats (Fyda *et al.* 1991) and an NTS lesion cannot explain the atrophy of BAT seen in the Cap-Des rat (Cui & Himms-Hagen 1992a; Cui & Himms-Hagen 1992b; Cui *et al.* 1990; Himms-Hagen & Cui 1991; Himms-Hagen *et al.* 1990), Chapter 4.

The obesity of the UCP-DTA mouse at 8 weeks of age is hypertrophic; the doubling of body fat is achieved by increased adipocyte size with no increase in adipocyte number and is associated with hyperphagia. In WAT, the total number of cells increased, with a concomitant increase in protein content, which is interpreted as an increase in vascularity to support the expanded mass of the tissue.

The development of obesity and hyperphagia in UCP-DTA mice is temperature sensitive. Both were prevented when these mice were raised from weaning to the age of 8 weeks in a thermoneutral environment (35°C). An obligatory link appears to exist between intact BAT and the ability to adjust food intake in accordance with environmental temperatures below thermoneutrality. This study has been published (Melnyk *et al.* 1997).

The increase in food intake that occurs in normal mice when they are acclimated to different temperatures, from 35°C down to 14°C, is not correlated with any change in serum leptin levels. The mechanism controlling this temperature-mediated change in food intake is defective in the UCP-DTA mouse. These mice are normophagic at thermoneutrality, eat the same large amount as control mice at 14°C, but are hyperphagic at 24°C (Figure 8.1). Acclimation to cold (14°C) partially reverses the obesity of UCP-DTA mice because they do not immediately adjust their food intake upwards to meet their increased energy expenditure.

The UCP-DTA mouse appears to compensate for its lack of UCP1 expressing brown adipocytes when exposed to cold, in a manner not available to the UCP1-KO mouse (Enerbäck *et al.* 1997), which lacks UCP1 but possesses brown adipocytes and is cold

intolerant. Acclimation of the UCP-DTA mouse to cold results in a delayed growth of BAT and an almost normal BAT histology. This delay in growth of BAT in UCP-DTA mice is postulated to be due to a lack of hypertrophy of UCP1 adipocytes. Acclimation to cold also induces the appearance of abundant multilocular adipocytes in INWAT of both control and UCP-DTA mice. These are identified as brown adipocytes because of their expression of UCP {as recognized by an antiserum that recognizes both UCP1 and UCP2 (Chapter 3, Figure 3.2), and probably UCP3 as well}.

These findings are further discussed below, in relation to more recent findings in the literature.

Food intake at different temperatures: UCP-DTA mice

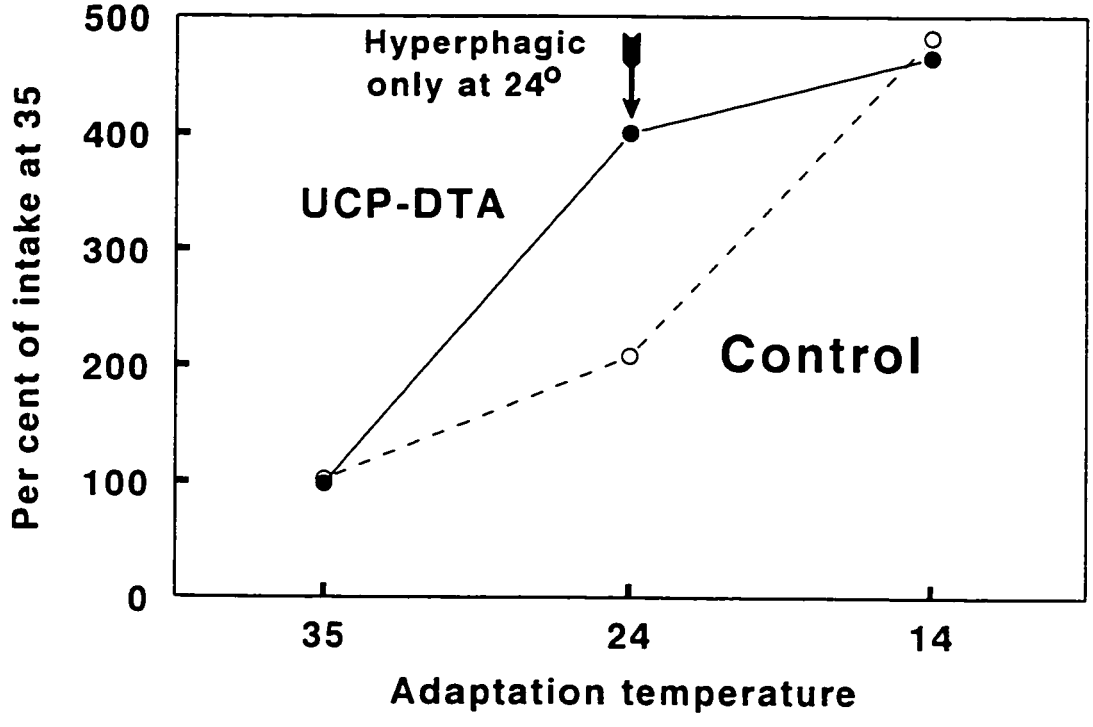

Figure 8.1: Food intake of UCP-DTA mice at different temperatures. Intake is expressed as percent of intake at 35°C for same type of mouse. Data used from experiments outlined in Chapters 6 and 7. UCP-DTA mice are hyperphagic at 24°C, normophagic at 14°C and 35°C.

Perspectives

The most intriguing finding in these studies is that both the hyperphagia and the obesity of UCP-DTA mice are temperature-sensitive. Both are prevented when these mice are raised at thermoneutrality (35°C). Their obesity is reversed and the hyperphagia is the same as that of control mice when these mice become acclimated to cold (14°C). Possible explanations for the relation between this temperature-sensitive abnormality in UCP-DTA mice and the lesion induced by the transgene (the ablation of UCP1 expressing brown adipocytes) are presented here.

In normal mice, the adjustment of food intake over a 4-5 fold range to match energy expenditure and conserve the same level of body fat stores is here shown to be independent of any changes in leptin concentration. The control mechanism that allows this adjustment of food intake in relation to temperature of acclimation is not understood. The mechanism does not need the presence of leptin or any action of leptin since it operates normally in both *ob/ob* and *db/db* mice (Coleman 1982), Figure 8.2. Some clues to the nature of this control mechanism can be obtained from the study of UCP-DTA mice, in which it appears to be defective. Since the lesion in these transgenic mice resides in the ablation of UCP1 expressing brown adipocytes when these cells are stimulated by NA, the question arises "*Is there a role for brown adipocytes in adjustment of food intake in relation to temperature?*"

Food intake at different temperatures: Lean and genetically obese mice

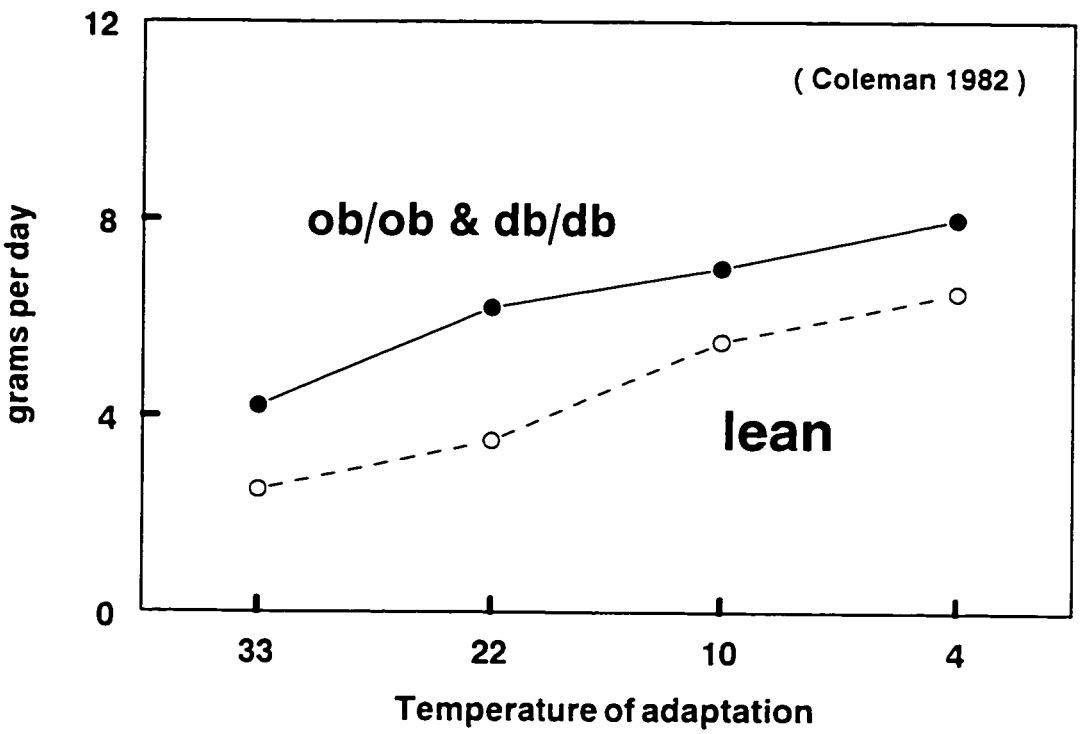

Figure 8.2: Food intake of lean and obese (*ob/ob* & *db/db*) mice. *ob/ob* mice lack leptin and *db/db* mice lack a functioning leptin receptor, and are able to adjust food intake with temperature. Data taken from (Coleman 1982).

Hyperphagia in the UCP-DTA mouse at 24°C was initially thought to be related to a deficit in BAT thermogenesis at this temperature, a deficit not felt by the UCP-DTA mouse at thermoneutrality where thermogenesis is equally suppressed in control and UCP-DTA mice and both eat the same low amount. However, UCP1-KO mice also have a deficit in BAT thermogenesis at 24°C and are cold-intolerant yet these mice are neither hyperphagic nor obese. Thus, there must be another explanation for the hyperphagia of the UCP-DTA mouse at 24°C that is related to the ablation of UCP1 expressing brown adipocytes.

We suggest, therefore, that UCP1 expressing brown adipocytes (BA1s) generate a signal, possibly a satiety factor, in direct relationship to environmental temperature and in an inverse relationship to NA. The generation of this signal would thus be maximal at thermoneutrality, progressively suppressed by NA as temperature of acclimation decreases and sympathetic nervous system activity increases, to reach a minimum in a cold environment where sympathetic nervous system activity reaches a maximum level.

A close direct relationship exists between food intake at different temperatures (35°C down to 14°C), with sympathetic nervous system activity in BAT (Zaror-Behrens & Himms-Hagen 1983), with UCP concentration in BAT mitochondria (Ashwell *et al.* 1983) (which is a direct consequence of NA action on BAT), and with energy expenditure at these different temperatures (Trayhurn & James 1978). It is plausible that the signal that informs the mouse how much to eat at these different temperatures to match its energy expenditure might reside in the tissue that is so exquisitely sensitive to change in the thermal environment, namely, BAT.

UCP-DTA mice are predicted to secrete this factor normally at thermoneutrality, when BA1s survive because DTA expression is not stimulated, so that their food intake is normal and low at this temperature. They are predicted to lose the ability to secrete the factor at 24°C when these cells are lost, so become hyperphagic. They would continue to lack the factor at 14°C, when their hyperphagia becomes appropriate for this temperature.

There is precedence for a satiety factor secreted by BAT and very sensitive to suppression by sympathetic nervous system activity: this factor is leptin itself (Deng *et al.* 1997). We therefore propose the existence of a second, perhaps leptin-like, satiety factor secreted by BA1s in inverse relationship to their heat production, and acting entirely independently of leptin on a different type of receptor.

Leptin can be regarded as a signal of the adequacy of the fat stores in WAT for a variety of purposes; its main function, indicated by a decrease in its concentration, is to permit adaptations for starvation and hunger to take advantage of food supply when it becomes available (Ahima *et al.* 1996). The postulated satiety factor from BA1s is a signal of the need for food intake to support thermoregulatory heat production; its main function, indicated by a decrease in its concentration, is to promote an increase in food intake to match increasing energy expenditure as environmental temperature decreases.

The growth of BAT and the appearance of multilocular brown adipocytes in WAT during acclimation to cold in UCP-DTA mice and the lack of cold-intolerance in these mice suggests that some compensatory mechanism allows for the cold-induced thermogenesis. If we assume that BA1s are indeed ablated, then brown adipocytes expressing other UCP

isoforms must substitute for these cells. This raises the question "*Is there more than one type of brown adipocyte?*" The existence of more than one type, already suggested by the "Harlequin" effect (Cinti *et al.* 1997), is a plausible explanation for our findings.

Since both UCP2 and UCP3 are known to be cold-inducible in BAT (Boss *et al.* 1997a; Boss *et al.* 1997b), the brown adipocytes recognized by our antiserum in BAT and WAT of cold-acclimated UCP-DTA mice could be brown adipocytes that express both UCP2 and UCP3 or two types of brown adipocyte, one expressing UCP2, the other expressing UCP3.

UCP-DTA mice have UCP and multilocular brown adipocytes in their BAT. As BA1s are destroyed in this model, and our antibody is not specific for UCP1, it is likely that there are other brown adipocyte populations present expressing other isoforms of UCP.

UCP3 expression is increased by NA, but the response is less rapid than the increase in UCP1 expression. Brown adipocytes expressing UCP3 (BA3s), are proposed to be under the control of NA. BA3s appear to increase as a compensation for the lack of BA1s in UCP-DTA mice acclimated to cold.

When mice were exposed to 14°C, growth of BAT (increase in protein) was rapid in control mice and slow after a lag in UCP-DTA mice, but the same maximum was reached eventually. Similar unilocular cells appear in both control and UCP-DTA mice. The delay of growth of BAT in UCP-DTA mice is postulated to be due to a lack of hypertrophy of BA1s. BA3s eventually take over, but their response is slower. Note that control of both UCP2 and UCP3 expression seems similar to that of UCP1 (Boss *et al.* 1997a; Boss *et al.*

1997b). Unilocular adipocytes are interpreted as UCP2 expressing adipocytes (BA2s). There appear to be more of these cells in the UCP-DTA mice, but this may be because of loss of the BA1s. Most other adipocytes appear to be larger than those in control mice, and are postulated to be BA3s. For a model of the hypothesis of multiple brown adipocytes see Figure 8.3.

The atrophy of BAT in the Cap-Des rat involves a loss of cells, including brown adipocytes. It is not known whether this is a selective loss of one type of brown adipocyte or not. These rats are not hyperphagic, nor obese, and are able to adjust their food intake with temperature over most of the range (Figure 8.4) (Cormarèche-Leydier 1981). Presumably BA1s are not lost, nor the satiety factor secreted from these brown adipocytes. Cap-Des rats have a delayed growth of BAT in the cold, like UCP-DTA mice, but are presumably compensating in a different way. With age their BAT seems to recover somewhat, perhaps again by compensation. Perhaps they have more of the postulated satiety factor if they compensate by increasing the number of BA1s.

Model: Multiple brown adipocytes

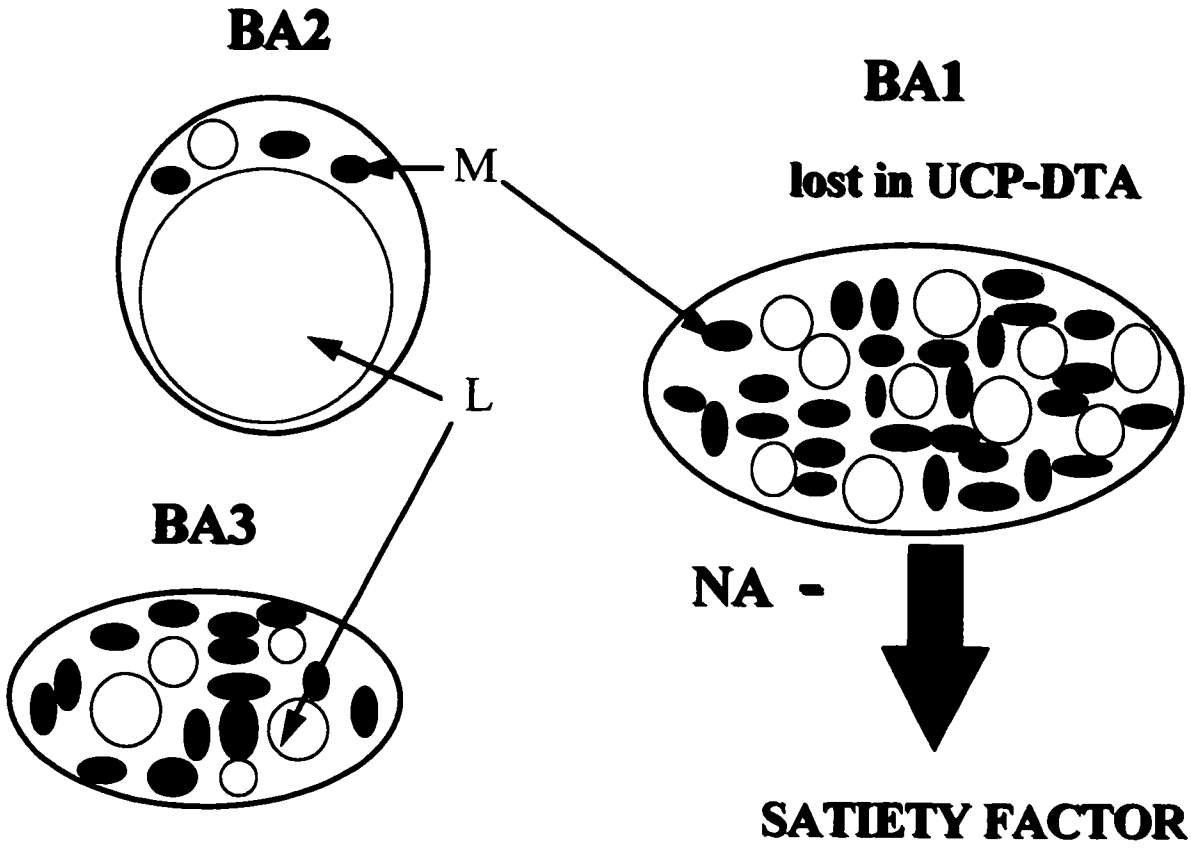

Figure 8.3: Model illustrating the proposed brown adipocyte types. Shown are three distinct brown adipocytes, each expressing a different UCP isoform. We postulate that UCP1 expressing brown adipocytes secrete a satiety factor, the secretion of which is inhibited by NA. See text for details on the proposal of the existence of multiple brown adipocytes, and of a satiety factor secreted by UCP1 expressing brown adipocytes. Abbreviations: BA1, UCP1 expressing brown adipocyte; BA2, UCP2 expressing brown adipocyte; BA3, UCP3 expressing brown adipocyte; M, mitochondrion; L, lipid droplet; NA, noradrenaline.

Food intake at different temperatures: Control and Cap-Des rats

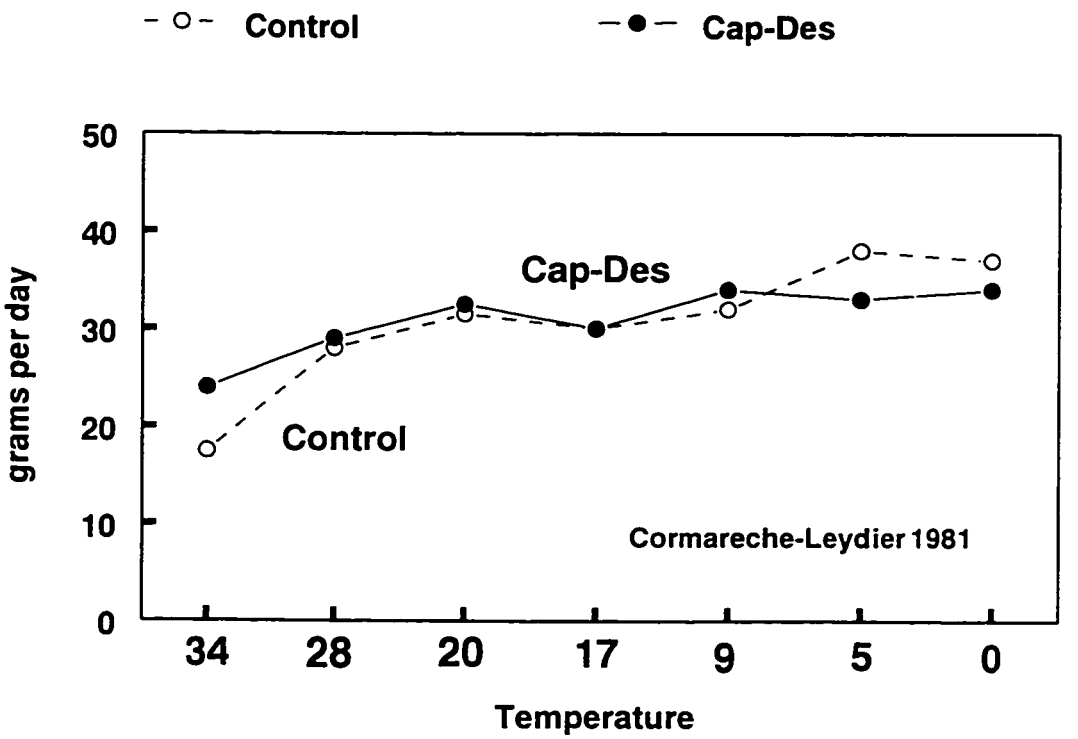

Figure 8.4: Food intake of control and Cap-Des rats. Cap-Des rats have atrophied BAT, with a decrease in cell number of BAT; they are not hyperphagic or obese. Cap-Des rats can adjust their food intake with temperature over most of the range shown. Data from (Cormarèche-Leydier 1981).

Future prospects

Further studies are needed to test the hypotheses outlined in the Perspectives section of this chapter.

Is there more than one type of brown adipocyte ?

Development of specific antibodies for the different UCP isoforms is needed. These antibodies need to be suitable for immunohistochemistry of consecutive sections of BAT and WAT of cold-acclimated control and UCP-DTA mice as well as for Western blotting. Northern blotting to assess mRNA levels for the different isoforms would be feasible but would not identify the cell type(s) in which they were expressed and would not give information about the levels of the proteins.

Application of these same procedures to BAT of Cap-Des rats would help to identify the nature of the brown adipocytes which persist in these animals. A further question relates to the role of CGRP or other sensory neuropeptides in maintenance and function of another type of brown adipocytes (not BA1).

Is there a role for brown adipocytes in the adjustment of food intake in relation to temperature ?

The hypothesis that UCP1 expressing brown adipocytes secrete a satiety factor will probably require cloning of the postulated factor to prove its existence. A possible experimental approach would be differential screening of cDNA libraries prepared from BAT of mice acclimated to 35°C and from BAT of mice acclimated to 14°C. While most

mRNA species expressed in BAT would be upregulated at 14°C, the postulated factor should be upregulated at 35°C.

Generating transgenic mice with the genes of the other UCP isoforms knocked out, as well as mice with specific brown adipocyte ablation, will delineate the roles that these various UCP isoforms and postulated brown adipocytes play in thermogenesis, food intake, and obesity.

Further studies into the various components of energy balance as they relate to obesity will advance the current understanding of this complex disease.

References

Abumrad, N. A. & Perry, P. R. 1985 Stimulation by epinephrine of the membrane transport of long chain fatty acid in the adipocyte. *Journal of Biological Chemistry* **260**, 9969.

Ahima, R. S., Prabakaran, D., Mantzoros, C., Qu, D., Lowell, B., Maratos-Flier, E. & Flier, J. S. 1996 Role of leptin in the neuroendocrine response to fasting. *Nature* **382**, 250-252.

Ailhaud, G. 1991 Cellular and secreted lipoprotein lipase revisited. *Clinical Biochemistry* **23**, 343-347.

Ailhaud, G., Grimaldi, P. & Négrel, R. 1992 A molecular view of adipose tissue. *International Journal of Obesity* **16**, S17-S21.

Allars, J., Holt, S. J. & York, D. A. 1987 Energetic efficiency and brown adipose tissue uncoupling protein of obese Zucker rats faed high-carbohydrate and high-fat diets: the effects of adrenalectomy. *International Journal of Obesity* **11**, 591-601.

Alvarez, R., De Andrés, J., Yubero, P., Viñas, O., Mampel, T., Iglesias, R., Giralt, M. & Villarroya, F. 1995 A novel regulatory pathway of brown fat thermogenesis. Retinoic acid is a transcriptional activator of the mitochondrial uncoupling protein gene. *Journal of Biological Chemistry* **270**, 5666-5673.

Antras, J., Lasnier, F. & Pairault, J. 1991 β-Adrenergic-cyclic AMP signalling pathway modulates cell function at the transcriptional level in 3T3-F442A adipocytes. *Molecular & Cellular Endocrinology* **82**, 183-190.

Arch, J. R. S., Brooks, B. J., Thurlby, P. L. & Wilson, S. 1986 Sympathetic and hormonal regulation of brown adipose tissue thermogenesis. *Biochemical Society Transactions* **14**, 230-233.

Arch, J. R. S. & Kaumann, A. J. 1993 β_3 - and atypical β -adrenoceptors. *Medicinal Research Reviews* **13**, 663-729.

Ashwell, M., Jennings, G., Richard, D., Stirling, M. D. & Trayhurn, P. 1983 Effect of acclimation temperature on the concentration of the mitochondrial 'uncoupling' protein measured by radioimmunoassay in mouse brown adipose tissue. *FEBS Letters* **161**, 108-112.

Auwerx, J., Martin, G., Guerremillo, M. & Staels, B. 1996 Transcription, adipocyte differentiation, and obesity. *Journal of Molecular Medicine* **74**, 347-352.

Banks, W. A., Kastin, A. J., Huang, W., Jaspan, J. B. & Maness, L. M. 1996 Leptin enters the brain by a saturable system independent of insulin. *Peptides* **17**, 305-311.

Barash, I. A., Cheung, C. C., Weigle, D. S., Ren, H., Kabigting, E. B., Kuijper, J. L., Clifton, D. K. & Steiner, R. A. 1996 Leptin is a metabolic signal to the reproductive system. *Endocrinology* **137**, 3144-3147.

Baumann, H., Morella, K. K., White, D. W., Dembski, M., Bailon, P. S., Kim, H., Lai, C.-F. & Tartaglia, L. A. 1996 The full-length leptin receptor has signaling capabilities of interleukin 6-type cytokine receptors. *Proceedings of the National Acadamy of Science* **93**, 8374-8378.

Benjamin, W., Gellhorn, A., Wagner, M. & Kundel, H. 1961 Effect of aging on lipid composition and metabolism in the adipose tissues of the rat. *American Journal of Physiology* **201**, 540-546.

Bennett, B. D., Solar, G. P., Yuan, J. Q., Mathias, J., Thomas, G. R. & Matthews, W. 1996 A role for leptin and its cognate receptor in hematopoiesis. *Current Biology* **6**, 1170-1180.

Beutler, B., Greenwald, D., Hulmes, J. D., Chang, M., Pan, Y. C., Mathison, J., Ulevitch, R. & Cerami, A. 1985 Identity of tumor necrosis factor and the macrophage secreted factor cachectin. *Nature* **316**, 552-555.

Bianco, A. C., Kieffer, J. D. & Silva, J. E. 1992 Adenosine 3',5'-monophosphate and thyroid hormone control of uncoupling protein messener ribonucleic acid in freshly dispersed brown adipocytes. *Endocrinology* **130**, 2625-2633.

Bianco, A. C., Sheng, X. & Silva, J. E. 1988 Triiodothyronine amplifies norepinephrine stimulation of uncoupling protein gene transcription by a mechanism not requiring protein synthesis. *Journal of Biological Chemistry.* **263**, 18168-18175.

Bianco, A. C. & Silva, J. E. 1987 Intracellular conversion of thyroxine to triiodothyronine is required for the optimal thermogenic function of brown adipose tissue. *Journal of Clinical Investigation* **79**, 295-300.

Billington, C. J., Bartness, T. J., Briggs, J., Levine, A. S. & Morley, J. E. 1987 Glucagon stimulation of brown adipose tissue growth and thermogenesis. *American Journal of Physiology* **252**, R160-R165.

Björntorp, P., Karlsson, M., Pertoft, H., Pettersson, P., Sjöström, L. & Smith, U. 1978 Isolation and characterization of cells from rat adipose tissue developing into adipocytes. *Journal of Lipid Research* **19**, 316-324.

Bloom, W. & Fawcett, D. W. 1993 . In *A textbook of histology.*, pp. 170-181. Philadelphia: WB Saunders.

Boss, O., Samec, S., Dulloo, A., Seydoux, J., Muzzin, P. & Giacobino, J.-P. 1997a Tissue-dependent upregulation of rat uncoupling protein-2 expression in response to fasting or cold. *FEBS Letters* **412**, 111-114.

Boss, O., Samec, S., Paoloni-Giacobino, A., Rossier, C., Dulloo, A., Seydoux, J., Muzzin, P. & Giacobino, J.-P. 1997b Uncoupling protein-3: a new member of the mitochondrial carrier family with tissue-specific expression. *FEBS Letters* **408**, 39-42.

Bothwell, A., Yancopoulos, G. D. & Alt, F. W. 1990 *Methods for cloning and analysis of eukaryotic genes.* Boston: Jones and Bartlett Publishers.

Bouillaud, F., Ricquier, D., Thibault, J. & Weissenbach, J. 1985 Molecular approach to thermogenesis in brown adipose tissue: cDNA cloning of the mitochondrial uncoupling protein. *Proceedings of the National Academy of Science* **82**, 445-448.

Bouillaud, F., Villarroya, F., Hentz, E., Raimbault, S., Cassard, A.-M. & Ricquier, D. 1988 Detection of brown adipose tissue uncoupling protein in adult patients by a human genomic probe. *Clinical Science* **75**, 21-27.

Boyer, B. B. & Kozak, L. P. 1991 The mitochondrial uncoupling protein gene in brown fat: correlation between DNase I hypersensitivity and expression in transgenic mice. *Molecular and Cellular Biology* **11**, 4147-4156.

Bray, G. A. 1990 Obesity - a state of reduced sympathetic activity and normal or high adrenal activity (the autonomic and adrenal hypothesis revisited). *International Journal of Obesity* **14**, 77-92.

Bray, G. A. & York, D. A. 1971 Genetically transmitted obesity in rodents. *Physiological Reviews* **51**, 598-646.

Bronnikov, G., Houstek, J. & Nedergaard, J. 1992 β -Adrenergic, cAMP-mediated stimulation of proliferation of brown fat cells in primary culture. Mediation via β_1-but not via β_3 -adrenoceptors. *Journal of Biological Chemistry* **267**, 2006-2013.

Brück, K. 1978 Heat production and temperature regulation. In *Perinatal Physiology* (ed. U. Stave), pp. 455-498. New York: Plenum Press.

Bukowiecki, L. J. 1986 Lipid metabolism in brown adipose tissue. In *Brown adipose tissue* (ed. P. Trayhurn & D. G. Nicholls), pp. 105-121. London: Arnold.

Bukowiecki, L. J., Collet, A. J., Folléa, N., Guay, G. & Jahjah, L. 1982 Brown adipose tissue hyperplasia: a fundamental mechanism of adaptation to cold and hyperphagia. *American Journal of Physiology* **242**, E353-E359.

Bukowiecki, L. J., Gélöen, A. & Collet, A. J. 1986 Proliferation and differentiation of brown adipocytes from interstitial cells during cold acclimation. *American Journal of Physiology* **250**, C880-C887.

Burcelin, R., Kandé, J., Ricquier, D. & Girard, J. 1993 Changes in uncoupling protein and GLUT4 glucose transporter expression in interscapular brown adipose tissue of diabetic rats: relative roles of hyperglycaemia and hypoinsulinaemia. *Biochemical Journal* **291**, 109-113.

Burýsek, L. & Houstek, J. 1997 β -Adrenergic stimulation of interleukin-1α and interleukin-6 expression in mouse brown adipocytes. *FEBS Letters* **411**, 83-86.

Campbell, D. J. & Habener, J. F. 1987 Cellular localization of angiotensinogen gene expression in brown adipose tissue and mesentery: quantification of messenger ribonucleic acid abundance using hybridization in situ. *Endocrinology* **121**, 1616-1626.

Campfield, L. A., Smith, F. J., Guisez, Y., Devos, R. & Burn, P. 1995 Recombinant mouse ob protein-evidence for a peripheral signal linking adiposity and central neural networks. *Science* **269**, 546-549.

Cannon, B., Nedergaard, J., Lundberg, J. M., Hökfelt, T., Terenius, L. & Goldstein, M. 1986 "Neuropeptide tyrosine" (NPY) is co-stored with noradrenaline in vascular but not in parenchymal sympathetic nerves of brown adipose tissue. *Experimental Cell Research* **16f4**, 546-550.

Carneheim, C., Nedergaard, J. & Cannon, B. 1988 Cold-induced β -adrenergic recruitment of lipoprotein lipase in brown fat is due to increased transcription. *American Journal of Physiology* **254**, E155-E161.

Caro, J. F., Kolaczynski, J. W., Nyce, M. R., Ohannesian, J. P., Opentanova, I., Goldman, W. H., Lynn, R. B., Zhang, P.-L., Sinha, M. K. & Considine, R. V. 1996 Decreased cerebrospinal-fluid/serum leptin ratio in obesity: a possible mechanism for leptin resistance. *Lancet* **348**, 159-161.

Carpéné, C., Castan, I., Collon, P., Galitzky, J., Moratinos, J. & Lafontan, M. 1994 Adrenergic lipolysis in guinea pig is not a β_3 -adrenergic response: comparison with human adipocytes. *American Journal of Physiology* **266**, R905-R913.

Cassard-Doulcier, A.-M., Gelly, C., Fox, N., Schrementi, J., Raimbault, S., Klaus, S., Forest, C., Bouillaud, F. & Ricquier, D. 1993 Tissue-specific and β -adrenergic gene regulation of the mitochondrial uncoupling protein gene: control by *cis*-acting elements in the 5'-flanking region. *Molecular Endocrinology* **7**, 497-506.

Cassard-Doulcier, A.-M., Larose, M., Matamala, J. C., Champigny, O., Bouillaud, F. & Ricquier, D. 1994 In vitro interactions between nuclear proteins and uncoupling protein gene promoter reveal several putative transactivating factors including Ets 1, retinoid X receptor, thyroid hormone receptor, and a CACCC box-binding protein. *Journal of Biological Chemistry* **269**, 24335-24342.

Cassis, L. A. 1993 Role of angiotensin II in brown adipose tissue thermogenesis during cold acclimation. *American Journal of Physiology* **265**, E860-E865.

Cassis, L. A. & Dwoskin, L. P. 1991 Presynaptic modulation of neurotransmitter release by endogenous angiotensin II in brown adipose tissue. *Journal of Neural Transmission* **Suppl 34**, 129-137.

Cassis, L. A. & Dwoskin, L. P. 1994 Acute and chronic losartan administration: effect on angiotensin II content and modulation of [^{3}H]norepinephrine release from rat interscapular brown adipose tissue. *Journal of Neural Transmission* **98**, 159-163.

Cassis, L. A., Saye, J. & Peach, M. J. 1988 Location and regulation of rat angiotensinogen messenger RNA. *Hypertension* **11**, 591-596.

Castonguay, T. W. & Bellinger, L. L. 1987 Capsaicin and its effects upon meal patterns, and glucagon and epinephrine suppression of food intake. *Physiology & Behavior* **40**, 337-342.

Cawthorne, M. A., Smith, S. A. & Young, P. 1987 Effect of thermogenic drugs on insulin sensitivity and glucose utilization by brown adipose tissue. In *Recent Advances in Obesity Research*, vol. 5 (ed. E. M. Berry, S. H. Blondheim, H. E. Eliahou & E. Shafrir), pp. 312-318. London: Libbey.

Champigny, O., Holloway, B. R. & Ricquier, D. 1992 Regulation of UCP gene expression in brown adipocytes differentiated in primary culture. Effects of a new β - adrenoceptor agonist. *Molecular and Cellular Endocrinology* **86**, 73-82.

Champigny, O. & Ricquier, D. 1996 Evidence from in vitro differetntiating cells that adrenoceptor agonists can increase uncoupling protein mRNA level in adipocytes of adult humans: an RT-PCR study. *Journal of Lipid Research* **37**, 1907-1914.

Chan, B. L., Lisanti, M. P., Rodriguez-Boulan, E. & Saltiel, A. R. 1988 Insulin-stimulated release of lipoprotein lipase by phophatidylinositol anchor. *Science* **241**, 1670-1672.

Chehab, F. F., Lim, M. E. & Lu, R. 1996 Correction of the sterility defect in homozygous obese female mice by treatment with the human recombinant leptin. *Nature Genetics* **12**, 318-320.

Chen, H., Charlat, O., Tartaglia, L. A., Woolf, E. A., Weng, X., Ellis, S. J., Lakey, N. D., Culpepper, J., Moore, K. J., Breitbart, R. E., Duyk, G. M., Tepper, R. I. & Morgenstern, J. P. 1996 Evidence that the diabetes gene encodes the leptin receptor: identification of a mutation in the leptin receptor in *db/db* mice. *Cell* **84**, 491-495.

Chua, S. C., Jr, Chung, W. K., Wu-Peng, X. S., Zhang, Y., Liu, S.-M., Tartaglia, L. & Leibel, R. L. 1996a Phenotypes of mouse *diabetes* and rat *fatty* due to mutations in the OB (leptin) receptor. *Science* **271**, 994-996.

Chua, S. C., Jr., White, D. W., Wu-Peng, X. S., Liu, S.-M., Okada, N., Kershaw, E. E., Chung, W. K., Power-Kehoe, L., Chua, M., Tartaglia, L. A. & Leibel, R. L. 1996b Phenotype of *fatty* due to Gln269Pro mutation in the leptin receptor (*Lepr*). *Diabetes* **45**, 1141-1143.

Cincotta, A. H., Schiller, B. C., Landry, R. J., Herbert, S. J., Miers, W. R. & Meier, A. H. 1993 Circadian neuroendocrine role in age-related changes in body fat stores and insulin sensitivity of the male Sprague-Dawley rat. *Chronobiology International* **10**, 244-258.

Cinti, S., De Matteis, R., Zingaretti, M. C., Cancello, R., Himms-Hagen, J. & Ricquier, D. 1997 Harlequin secret: UCP-immunostained brown adipose tissue. *International Journal of Obesity* **21**, S47.

Cioffi, J. A., Shafer, A. W., Zupancic, T. J., Smithgbur, J., Mikhail, A., Platika, D. & Snodgrass, H. R. 1996 Novel B219/ob receptor isoforms-possible role of leptin in hematopoiesis and reproduction. *Nature Medicine* **2**, 585-589.

Cleary, M. P., Brasel, J. A. & Greenwood, M. R. C. 1979 Developmental changes in thymidine kinase, DNA, and fat cellularity in Zucker rats. *American Journal of Physiology* **236**, E508-E513.

Closa, D., Gómez-Sierra, J.-M., Latres, E., Alemany, M. & Remesar, X. 1993 Short-term oscillations of aortic core temperature and thermogenic organ blood flow in the rat. *Experimental Physiology* **78**, 243-253.

Cohen, B., Novick, D. & Rubinstein, M. 1996 Modulation of insulin activities by leptin. *Science* **274**, 1185-1188.

Coleman, D. L. 1982 Thermogenesis in diabetes-obesity syndromes in mutant mice. *Diabetologia* **22**, 205-211.

Collins, S., Daniel, K. W., Petro, A. E. & Surwit, R. S. 1997 Strain-specific response to β_3 -adrenergic receptor agonist treatment of diet-induced obesity in mice. *Endocrinology* **138**, 405-413.

Collins, S., Daniel, K. W., Rohlfs, E. M., Ramkumar, V., Taylor, I. L. & Gettys, T. W. 1994 Impaired expression and functional activity of the β_3 - and β_1 -adrenergic receptors in adipose tissue of congenitally obese (C57Bl/6J *ob/ob*) mice. *Molecular Endocrinology* **8**, 518-527.

Considine, R. V., Considine, E. L., Williams, C. J., Hyde, T. M. & Caro, J. F. 1996 The hypothalamic leptin receptor in humans: identification of incidental sequence polymorphisms and absence of the *db/db* mouse and *fa/fa* rat mutations. *Diabetes* **19**, 992-994.

Considine, R. V., Considine, E. L., Williams, C. J., Nyce, M. R., Magosin, S. A., Bauer, T. L., Rosato, E. L., Colberg, J. & Caro, J. F. 1995 Evidence against either a premature stop codon or the absence of obese gene mRNA in human obesity. *Journal of Clinical Investigation* **95**, 2986-2988.

Cooney, G. J., Astbury, L. D., Williams, P. F. & Caterson, I. D. 1987 Insulin response in individual tissues of control and gold thioglucose-obese mice in vivo with [^{14}C] 2-deoxyglucose. *Diabetes* **36**, 152-158.

Cooney, G. J. & Newsholme, E. A. 1984 Does brown adipose tissue have a metabolic role in the rat? *Trends in Biochemical Sciences* **9**, 303-305.

Cooper, G. J. S. 1994 Amylin compared with calcitonin gene-related peptide: structure, biology, and relevance to metabolic disease. *Endocrine Reviews* **15**, 163-201.

Cormarèche-Leydier, M. 1981 The effect of ambient temperature on rectal temperature, food intake and short term body weight in the capsaicin-desensitized rat. *Pflügers Archiv European Journal of Physiology* **389**, 171-174.

Coscina, D. V., Chambers, J. W., Park, I., Hogan, S. & Himms-Hagen, J. 1985 Impaired diet-induced thermogenesis in brown adipose tissue from rats made obese with parasagittal hypothalamic knife cuts. *Brain Research Bulletin* **14**, 585-593.

Cousin, B., Bascands-Viguerie, N., Kassis, N., Nibbelink, M., Ambid, L., Casteilla, L. & Pénicaud, L. 1996 Cellular changes during cold acclimatation in adipose tissues. *Journal of Cellular Physiology* **167**, 285-289.

Cousin, B., Casteilla, L., Dani, C., Muzzin, P., Revelli, J. P. & Pénicaud, L. 1993 Adipose tissues from various anatomical sites are characterized by different patterns of gene expression and regulation. *Biochemical Journal* **292**, 873-876.

Cousin, B., Cinti, S., Morroni, M., Raimbault, S., Ricquier, D., Pénicaud, L. & Casteilla, L. 1992 Occurence of brown adipocytes in rat white adipose tissue: molecular and morphological characterization. *Journal of Cell Science* **103**, 931-942.

Crandall, D. L., Herzlinger, H. E., Saunders, B. D. & Kral, J. B. 1994 Developmental aspects of adipose tissue renin-angiotensin system: therapeutic implications. *Drug Dev Res* **32**, 117-125.

Cui, J. & Himms-Hagen, J. 1992a Rapid but transient atrophy of brown adipose tissue in capsaicin-desensitized rats. *American Journal of Physiology* **262**, R562-R567.

Cui, J. & Himms-Hagen, J. 1992b Long-term decrease in body fat and in brown adipose tissue in capsaicin-desensitized rats. *American Journal of Physiology* **262**, R568-R573.

Cui, J., Zaror-Behrens, G. & Himms-Hagen, J. 1990 Capsaicin desensitization induces atrophy of brown adipose tissue in rats. *American Journal of Physiology* **259**, R324-R332.

D'Allaire, F., Atgie, C., Mauriege, P., Simard, P.-M. & Bukowiecki, L. J. 1995 Characterization of β_1 - and β_3 -adrenoceptors in intact brown adipocytes of the rat. *British Journal of Pharmacology* **114**, 275-282.

Dascombe, M. J., Rothwell, N. J., Sagay, B. O. & Stock, M. J. 1988 *American Journal of Physiology* **256**, E7-E11.

De Vos, P., Lefebvre, A.-M., Miller, S., Guerre-Millo, M., Wong, K., Saladin, R., Hamann, L. G., Staels, B., Briggs, M. R. & Auwerx, J. 1996 Thiazolidinediones repress ob gene expression in rodents via activation of peroxisome proliferator-activated receptor gamma. *Journal of Clinical Investigation* **98**, 1004-1009.

DeMartinis, F. D. & Francendese, A. 1982 Very small fat cell populations: mammalian occurrence and effect of age. *Journal of Lipid Research* **23**, 1107-1120.

Deng, C., Moinat, M., Curtis, L., Nadakal, A., Preitner, F., Boss, O., Assimacopoulos-Jeannet, F., Seydoux, J. & Giacobino, J.-P. 1997 Effects of β -adrenoceptor subtype stimulation of *obese* gene messenger ribonucleic acid and on leptin secretion in mouse brown adipocytes differentiated in culture. *Endocrinology* **138**, 548-552.

Depocas, F., Foster, D. O., Zaror-Behrens, G., Lacelle, S. & Nadeau, B. 1984 Recovery of function in sympathetic nerves of interscapular brown adipose tissue of rats treated with 6-hydroxydopamine. *Canadian Journal of Physiology & Pharmacology* **62**, 1327-1332.

Desautels, M. & Dulos, R. A. 1988 Is adrenergic innervation essential for maintenance of UCP in hamster BAT mitochondria? *American Journal of Physiology* **254**, R1035-R1042.

Dessolin, S., Schalling, M., Champigny, O., Lönnqvist, F., Ailhaud, G., Dani, C. & Ricquier, D. 1997 Leptin gene is expressed in rat brown adipose tissue at birth. *FASEB Journal* **11**, 382-387.

Di Girolamo, M. & Rudman, D. 1968 Variations in glucose metabolism and sensitivity to insulin of the rat's adipose tissue, in relation to age and body weight. *Endocrinology* **82**, 1133-1141.

Diez Guerra, F. J., Zaidi, M., Bevis, P., MacIntyre, I. & Emson, P. C. 1988 Evidence for release of calcitonin gene-related peptide and neurokinin A from sensory nerve endings in vivo. *Neuroscience* **25**, 839-846.

Djazayery, A., Miller, D. S. & Stock, M. J. 1979 Energy balances in obese mice. *Journal of Nutrition & Metabolism* **23**, 357-367.

Downs, T. R. & Wilfinger, W. W. 1983 Fluorometric quantification of DNA in cells and tissue. *Analytical Biochemistry* **131**, 538-547.

Ebner, S., Burnol, A.-F., Ferre, P., De Saintaurin, M.-A. & Girard, J. 1987 Effects of insulin and norepinephrine on glucose transport and metabolism in rat brown adipocytes. Potentiation by insulin of norepinephrine-induced glucose oxidation. *European Journal of Biochemistry* **170**, 469-474.

Edwards, G. L. & Ritter, R. C. 1986 Area postrema lesions: cause of overingestion is not altered visceral nerve function. *American Journal of Physiology* **251**, R575-R581.

Eley, J. & Himms-Hagen, J. 1989 Brown adipose tissue of mice with GTG-induced obesity: altered circadian control. *American Journal of Physiology* **256**, E773-E779.

Emorine, L. J., Marullo, S., Briend-Sutren, M.-M., Patey, G., Tate, K., Delavier-Klutchko, C. & Strosberg, A. D. 1989 Molecular characterization of the human β_3-adrenergic receptor. *Science* **245**, 1118-1121.

Emson, P. C. & Zaidi, M. 1989 Further evidence for the origin of circulating calcitonin gene-related peptide in the rat. *Journal of Physiology* **412**, 297-308.

Enerbäck, S., Jacobsson, A., Simpson, E. M., Guerra, C., Yamashita, H., Harper, M.-E. & Kozak, L. P. 1997 Mice lacking mitochondrial uncoupling protein are cold-sensitive but not obese. *Nature* **387**, 90-94.

Erickson, J. C., Clegg, K. E. & Palmiter, R. D. 1996 Sensitivity to leptin and susceptibility to seizures of mice lacking neuropeptide Y. *Nature* **381**, 415-418.

Fernandez, M., Nicholls, D. G. & Rial, E. 1987 The uncoupling protein from brown adipose tissue mitochondria. Chymotrypsin-induced structural and functional modifications. *European Journal of Biochemistry* **164**, 675-680.

Fishman, R. B. & Dark, J. 1987 Sensory innervation of white adipose tissue. *American Journal of Physiology* **253**, R942-R944.

Fisler, J. S., Yoshida, T. & Bray, G. A. 1984 Catecholamine turnover in S 5B/P1 and Osborne-Mendel rats: response to a high fat diet. *American Journal of Physiology* **247**, R290-R295.

Flaim, K. E., Horowitz, J. M. & Horwitz, B. A. 1976 Functional and anatomical characteristics of the nerve-brown adipose tissue interaction in the rat. *Pflügers Archiv European Journal of Physiology* **365**, 9-14.

Flaim, K. E., Horwitz, B. A. & Horowitz, J. M. 1977 Coupling of signals to brown fat: α - and β -adrenergic responses in intact rats. *American Journal of Physiology* **232**, R101-R109.

Fleury, C., Neverova, M., Collins, S., Raimbault, S., Champigny, O., Levi-Meyrueis, C., Bouillaud, F., Seldin, M. F., Surwit, R. S., Ricquier, D. & Warden, C. H. 1997 Uncoupling protein-2: a novel gene linked to obesity and hyperinsulinemia. *Nature Genetics* **15**, 269-272.

Flier, J. S. 1995 The adipocyte: storage depot or node on the energy information superhighway? *Cell* **80**, 15-18.

Forman, B. M., Tontonoz, P., Chen, J., Brun, R. P., Speigelman, B. M. & Evans, R. M. 1995 15-Deoxy- $\Delta^{12,14}$ -prostaglandin J2 is a ligand for the adipocyte determination factor PPARγ. *Cell* **83**, 803-812.

Foster, D. O. 1985 Participation of α -adrenoceptors in brown adipose tissue thermogenesis in vivo. *International Journal of Obesity.* **9**, 25-29.

Foster, D. O. 1986 Quantitative role of brown adipose tissue in thermogenesis. In *Brown adipose tissue* (ed. P. Trayhurn & D. G. Nicholls), pp. 31-51. London: Arnold.

Foster, D. O., Depocas, F. & Frydman, M. L. 1980 Noradrenaline-induced calorigenesis in warm- and in cold-acclimated rats: relations between concentration of noradrenaline in arterial plasma, blood flow to differently located masses of brown adipose tissue, and calorigenic response. *Canadian Journal of Physiology & Pharmacology* **58**, 915-924.

Foster, D. O., Depocas, F. & Zaror-Behrens, G. 1982 Unilaterality of the sympathetic innervation of each pad of rat interscapular brown adipose tissue. *Canadian Journal of Physiology and Pharmacology* **60**, 107-113.

Foster, D. O. & Frydman, M. L. 1978 Nonshivering thermogenesis in the rat. II. Measurements of blood flow with microspheres point to brown adipose tissue as the dominant site of the calorigenesis induced by noradrenaline. *Canadian Journal of Physiology and Pharmacology.* **56**, 110-122.

Foster, D. O. & Frydman, M. L. 1979 Tissue distribution of cold-induced thermogenenesis in conscious warm- or cold-acclimated rats reevaluated from changes in tissue blood flow: the dominant role of brown adipose tissue in the replacement of shivering by nonshivering thermogenesis. *Canadian Journal of Physiology and Pharmacology.* **57**, 257-270.

Frederich, R. C., Hamann, A., Anderson, S., Löllmann, B., Lowell, B. B. & Flier, J. S. 1995a Leptin levels reflect body lipid content in mice: Evidence for diet-induced resistance to leptin action. *Nature Medicine* **1**, 1311-1314.

Frederich, R. C., Kahn, B. B., Peach, M. J. & Flier, J. S. 1992 Tissue-specific nutritional regulation of angiotensinogen in adipose tissue. *Hypertension* **19**, 339-344.

Frederich, R. C., Lollmann, B., Hamann, A., Napolitano-Rosen, A., Kahn, B. B., Lowell, B. B. & Flier, J. S. 1995b Expression of the ob mRNA and its encoded protein in rodents. Impact of nutrition and obesity. *Journal of Clinical Investigation* **96**, 1658-1663.

Fukushima, M., Lupien, J. & Bray, G. A. 1985 Interaction of light and corticosterone on food intake and brown adipose tissue of the rat. *American Journal of Physiology* **491**, R753-R757.

Fyda, D. M., Cooper, K. E. & Veale, W. L. 1991 Modulation of brown adipose tissue-mediated thermogenesis by lesions to the nucleus tractus solitarius in the rat. *Brain Research* **546**, 203-210.

Fyda, D. M. & Wilson, J. R. 1991 The effects of lesions to the nucleus tractus solitarius on the metabolic and cardiovascular responses to graded warm and cold exposures in rats. *American Journal of Physiology* .

Galitzky, J., Carpéné, C., Bousquet-Mélou, A., Berlan, M. & Lafontan, M. 1995 Differential activation of β_1 -, β_2 -, and β_3 -adrenoceptors by catecholamines in white and brown adipocytes. *Fundamental & Clinical Pharmacology* **9**, 324-331.

Galpin, K. S., Henderson, R. G., James, W. P. T. & Trayhurn, P. 1983 GDP binding to brown-adipose-tissue mitochondria of mice treated chronically with corticosterone. *Biochemical Journal* **214**, 265-268.

Garlid, K. D., Orosz, D. E., Modriansky, M., Vassanelli, S. & Jezek, P. 1996 On the mechanism of fatty acid-induced proton transport by mitochondrial uncoupling protein. *Journal of Biological Chemistry* **271**, 2615-2620.

Garruti, G. & Ricquier, D. 1992 Analysis of uncoupling protein and its mRNA in adipose tissue deposits of adult humans. *International Journal of Obesity* **16**, 383-390.

Géloën, A., Collet, A. J. & Bukowiecki, L. J. 1992 Role of sympathetic innervation in brown adipocyte proliferation. *American Journal of Physiology* **263**, R1176-R1181.

Géloën, A., Collet, A. J., Guay, G. & Bukowiecki, L. J. 1988 β -adrenergic stimulation of brown adipocyte proliferation. *American Journal of Physiology* **254**, C175-C182.

Géloën, A., Collet, A. J., Guay, G. & Bukowiecki, L. J. 1990 In vivo differentiation of brown adipocytes in adult mice: an electron microscopic study. *American Journal of Anatomy* **188**, 366-372.

Géloën, A. & Trayhurn, P. 1990a Regulation of the level of uncoupling protein in brown adipose tissue by insulin requires the mediation of the sympathetic nervous system. *FEBS Letters* **267**, 265-267.

Géloën, A. & Trayhurn, P. 1990b Regulation of the level of uncoupling protein in brown adipose tissue by insulin. *American Journal of Physiology* **258**, R418-R424.

Gettys, T. W., Harkness, P. J. & Watson, P. M. 1996 The β_3 -adrenergic receptor inhibits insulin-stimulated leptin secretion from isolated rat adipocytes. *Endocrinology* **137**, 4054-4057.

Ghilardi, N., Ziegler, S., Wiestner, A., Stoffel, R., Heim, M. H. & Skoda, R. C. 1996 Defective STAT signaling by the leptin receptor in *diabetic* mice. *Proceedings of the National Acadamy of Science* **93**, 6231-6235.

Ghorbani, M., Claus, T. H. & Himms-Hagen, J. 1997 Hypertrophy of brown adipocytes in brown and white adipose tissues and reversal of diet-induced obesity in rats treated with a β_3 -adrenoceptor agonist. *Biochemical Pharmacology* **54**, 121-131.

Ghorbani, M. & Himms-Hagen, J. 1997 Appearance of brown adipocytes in white adipose tissue during CL 316,243-induced reversal of obesity and diabetes in Zucker *fa/fa* rats. *International Journal of Obesity* **21**, 465-475.

Giacobino, J.-P. 1995 β_3 -Adrenoceptor: an update. *European Journal of Endocrinology* **132**, 377-385.

Gimble, J. M., Robinson, C. E., Wu, X. & Kelly, K. A. 1996 The function of adipocytes in the bone marrow stroma: an update. *Bone* **19**, 421-428.

Gimeno, R. E., Dembski, M., Weng, X., Deng, N., Shyjan, A. W., Gimeno, C. J., Iris, F., Ellis, S. J., Woolf, E. A. & Tartaglia, L. A. 1997 Cloning and characterization of an uncoupling protein homolog. A potential molecular mediator of human thermogenesis. *Diabetes* **46**, 900-906.

Girardier, L. & Seydoux, J. 1986 Neural control of brown adipose tissue thermogenesis. In *Brown adipose tissue* (ed. P. Trayhurn & D. G. Nicholls), pp. 122-151. London: Arnold.

Goglia, F., Géloën, A., Lanni, A., Minaire, Y. & Bukowiecki, L. J. 1992 Morphometric-stereologic analysis of brown adipocyte differentiation in adult mice. *American Journal of Physiology* **262**, C1018-C1023.

Granneman, J. G. 1995a Expression of adenylyl cyclase subtypes in brown adipose tissue: neural regulation of type III. *Endocrinology* **136**, 2007-2012.

Granneman, J. G. 1995b Why do adipocytes make the β_3 -adrenergic receptor? *Cell Signal* **7**, 9-15.

Granneman, J. G. & Campbell, R. G. 1984 Effects of sucrose feeding and denervation on lipogenesis in brown adipose tissue. *Metabolism* **33**, 257-261.

Granneman, J. G. & Lahners, K. N. 1992 Differential adrenergic regulation of β_1 - and β_3 - adrenoreceptor messenger ribonucleic acids in adipose tissues. *Endocrinology* **130**, 109-114.

Greco-Perotto, R., Assimacopoulos-Jeannet, F. & Jeanrenaud, B. 1987 Insulin modifies the properties of glucose transporters in rat brown adipose tissue. *Biochemical Journal* **247**, 63-68.

Guerra, C., Porras, A., Roncero, C., Benito, M. & Fernandez, M. 1994 Triiodothyronine induces the expression of the uncoupling protein in long term fetal rat brown adipocyte primary cultures: role of nuclear thyroid hormone receptor expression. *Endocrinology* **134**, 1067-1074.

Guerra, C., Roncero, C., Porras, A., Fernandez, M. & Benito, M. 1996 Triiodothyronine induces the transcription of the uncoupling protein gene and stabilizes its mRNA in fetal rat brown adipocyte primary cultures. *Journal of Biological Chemistry* **271**, 2076-2081.

Gulve, E. A., Henriksen, E. J., Rodnick, K. J., Youn, J. H. & Holloszy, J. O. 1993 Glucose transporters and glucose transport in skeletal muscles of 1- to 25-mo-old rats. *American Journal of Physiology* **264**, E319-E327.

Gurr, M. I. & Kirtland, J. 1978 Adipose tissue cellularity: a review 1. Techniques for studying cellularity. *International Journal of Obesity* **2**, 401-427.

Halaas, J. L., Gajiwala, K. S., Maffei, M., Cohen, S. L., Chait, B. T., Rabinowitz, D., Lallone, R. L., Burley, S. K. & Friedman, J. M. 1995 Weight-reducing effects of the plasma protein encoded by the obese gene. *Science* **269**, 543-546.

Hamann, A., Benecke, H., Le Marchand-Brustel, Y., Susulic, V. S., Lowell, B. B. & Flier, J. S. 1995 Characterization of insulin resistance and NIDDM in transgenic mice with reduced brown fat. *Diabetes* **44**, 1266-1273.

Hamann, A., Büsing, B., Kausch, C., Ertl, J., Preibisch, G., Greten, H. & Matthaei, S. 1997 Chronic leptin treatment does not prevent the development of obesity in transgenic mice with brown fat deficiency. *Diabetologia* **40**, 810-815.

Hamann, A., Flier, J. S. & Lowell, B. B. 1996 Decreased brown fat markedly enhances susceptibility to diet-induced obesity, diabetes, and hyperlipidemia. *Endocrinology* **137**, 21-29.

Hamilton, B. S., Paglia, D., Kwan, A. Y. M. & Deitel, M. 1995 Increased *obese* mRNA expression in omental fat cells from massively obese humans. *Nature Medicine* **1**, 953-956.

Hardie, L. J., Rayner, D. V., Holmes, S. & Trayhurn, P. 1996 Circulating leptin levels are modulated by fasting, cold exposure, and insulin administration in lean but not Zucker (*fa/fa*) rats as measured by ELISA. *Biochemical and Biophysical Research Communications* **223**, 660-665.

Harper, M.-E. & Brand, M. D. 1993 The quantitative contributions of mitochondrial proton leak and ATP turnover reactions to the changed respiration rates of hepatocytes from rats of different thyroid hormone status. *Journal of Biological Chemistry* **268**, 14850-14860.

He, Y., Chen, H., Quon, M. J. & Reitman, M. 1995 The mouse *obese* gene. Genomic organization, promoter acitivity, and activation by CCAAT/enhancer-binding protein α. *Journal of Biological Chemistry* **270**, 28887-28891.

Heim, M. H. 1996 The Jak-STAT pathway: specific signal transduction from the cell membrane to the nucleus. *European Journal of Clinical Investigation* **26**, 1-12.

Himms-Hagen, J. 1979 Obesity may be due to a malfunctioning of brown fat. *Canadian Medical Association Journal* **121**, 1361-1364.

Himms-Hagen, J. 1989a Brown adipose tissue thermogenesis and obesity. *Progress in Lipid Research* **28**, 67-115.

Himms-Hagen, J. 1989b Role of thermogenesis in the regulation of energy balance in relation to obesity. *Canadian Journal of Physiology and Pharmacology* **67**, 394-401.

Himms-Hagen, J. 1990a Brown adipose tissue thermogenesis: a role in thermoregulation, energy regulation and obesity. In *Thermoregulation: Physiology and Biochemistry* (ed. E. Schönbaum & P. Lomax), pp. 327-414. New York: Pergamon Press, Inc.

Himms-Hagen, J. 1990b Brown adipose tissue thermogenesis: interdisciplinary studies. *FASEB Journal* **4**, 2890-2898.

Himms-Hagen, J. 1991 Neural control of brown adipose tissue thermogenesis, hypertrophy, and atrophy. *Frontiers in Neuroendocrinology* **12**, 38-93.

Himms-Hagen, J. 1995 Does thermoregulatory feeding occur in newborn infants? A novel view of the role of brown adipose tissue thermogenesis in control of food intake. *Obesity Research* **3**, 361-369.

Himms-Hagen, J. & Cui, J. 1991 Diet-induced obesity and brown adipose tissue. In *Obesity: Dietary Factors and Control.* (ed. D. Romsos, J. Himms-Hagen & M. Suzuki), pp. 81-95. Basel: Karger.

Himms-Hagen, J., Cui, J., Danforth, E., Jr, Taatjes, D. J., Lang, S. S., Waters, B. L. & Claus, T. H. 1994 Effect of CL-316,243, a thermogenic β_3 -agonist, on energy balance and brown and white adipose tissues in rats. *American Journal of Physiology* **266**, R1371-R1382.

Himms-Hagen, J., Cui, J. & Sigurdson, S. L. 1990 Sympathetic and sensory nerves in control of growth of brown adipose tissue: effects of denervation and of capsaicin. *Neurochemistry International* **17**, 271-279.

Himms-Hagen, J. & Danforth, E., Jr. 1996 The potential role of β_3 adrenoceptor agonists in the treatment of obesity and diabetes. *Current Opinion in Endocrinology and Diabetes* **3**, 59-65.

Himms-Hagen, J. & Ghorbani, M. 1995 Reversal of obesity in *fa/fa* rats by treatment with a β_3 -adrenoceptor agonist, CL 316,243: cellularity and biochemical characteristics of white and brown adipose tissues. *Obesity Research* **3**, 406a.

Himms-Hagen, J. & Ricquier, D. 1997 Brown adipose tissue. In *Handbook of obesity* (ed. G. A. Bray, C. Bouchard & W. P. T. James), pp. in press. New York: Marcel Dekker, Inc.

Himms-Hagen, J., Triandafillou, J., Bégin-Heick, N., Ghorbani, M. & Kates, A.-L. 1995 Apparent lack of β_3 -adrenoceptors and of insulin regulation of glucose transport in brown adipose tissue of guinea pigs. *American Journal of Physiology* **268**, R98-R104.

Hirsch, J. & Gallian, E. 1968 Methods for the determination of adipose cell size in man and animals. *Journal of Lipid Research* **9**, 110-119.

Hogan, S. & Himms-Hagen, J. 1980 Abnormal brown adipose tissue in obese mice (*ob/ob*): response to acclimation to cold. *American Journal of Physiology* **239**, E301-E309.

Hogan, S. & Himms-Hagen, J. 1983 Brown adipose tissue of mice with gold thioglucose-induced obesity: effect of cold and diet. *American Journal of Physiology* **244**, E581-E588.

Holt, S. J., York, D. A. & Fitzsimons, J. T. R. 1983 The effects of corticosterone, cold exposure and overfeeding with sucrose on brown adipose tissue of obese Zucker rats (*fa/fa*). *Biochemical Journal* **214**, 215-223.

Holzer, P. 1988 Local effector functions of capsaicin-sensitive sensory nerve endings: involvement of tachykinins, calcitonin gene-related peptide and other neuropeptides. *Neuroscience* **24**, 739-768.

Holzer, P. 1991a Capsaicin as a tool for studying sensory neuron functions. *Advances in Experimental Medicine & Biology* **298**, 3-16.

Holzer, P. 1991b Capsaicin: cellular targets, mechanisms of action, and selectivity for thin sensory neurons. *Pharmacological Reviews* **43**, 143-201.

Horwitz, B. A. & Hamilton, J. 1984 α adrenergic-induced changes in hamster (mesocricetus) brown adipocyte respiration and membrane potential. *Comparative Biochemistry & Physiology* **78C**, 99-104.

Hotamisligil, G. S., Shargill, N. S. & Spiegelman, B. M. 1993 Adipose expression of tumor necrosis factor-α: direct role in obesity linked insulin resistance. *Science* **259**, 87-91.

Hotamisligil, G. S. & Spiegelman, B. M. 1994 Tumor necrosis factor α: A key component of the obesity-diabetes link. *Diabetes* **43**, 1271-1278.

Hotta, K., Gustafson, T. A., Ortmeyer, H. K., Bodkin, N. L., Nicolson, M. A. & Hansen, B. C. 1996 Regulation of obese (*ob*) mRNA and plasma leptin levels in rhesus monkeys: effects of insulin, body weight, and non-insulin-dependent diabetes mellitus. *Journal of Biological Chemistry* **271**, 25327-25331.

Hu, E. D., Tontonoz, P. & Spiegelman, B. M. 1995 Transdifferentiation of myoblasts by the adipogenic transcription factors PPARγ and C/EBPα. *Proceedings of the National Academy of Science* **92**, 9856-9860.

Huttunen, P., Hirvonen, J. & Kinnula, V. 1981 The occurrence of brown adipose tissue in outdoor workers. *European Journal of Applied Physiology & Occupational Physiology* **46**, 339-345.

Hyde, T. M. & Miselis, R. R. 1983 Effects of area postrema/caudal medial nucleus of solitary tract lesions on food intake and body weight. *American Journal of Physiology* **244**, R577-R587.

Isler, D., Hill, H.-P. & Meier, M. K. 1987 Glucose metabolism in isolated brown adipocytes under β -adrenergic stimulation. Quantitative contribution of glucose to total thermogenesis. *Biochemical Journal* **245**, 789-793.

Johnson, P. R., Greenwood, M. R. C., Horwitz, B. A. & Stern, J. S. 1991 Animal models of obesity: Genetic aspects. *Annual Review of Nutrition* **11**, 325-353.

Kallen, C. B. & Lazar, M. A. 1996 Antidiabetic thiazolidinediones inhibit leptin (*ob*) gene expression in 3T3-L1 adipocytes. *Proceedings of the National Academy of Sciences* **93**, 5793-5796.

Karlsson, S., Scheurink, A. J. W., Steffens, A. B. & Ahrén, B. 1994 Involvement of capsaicin-sensitive nerves in regulation of insulin secretion and glucose tolerance in conscious mice. *American Journal of Physiology* **267**, R1071-R1077.

Kashiwagi, A., Huecksteadt, T. P. & Foley, J. E. 1983 The regulation of glucose transport by cAMP stimulators via three different mechanisms in rat and human adipocytes. *Journal of Biological Chemistry* **258**, 13685-13692.

Kieffer, T. J., Heller, R. S. & Habener, J. F. 1996 Leptin receptors expressed on pancreatic β-cells. *Biochemical and Biophysical Research Communications* **224**, 522-527.

Kirkland, J. L., Hollenberg, C. H. & Gillon, W. S. 1993 Ageing, differentiation, and gene expression in rat epididymal preadipocytes. *Biochemistry & Cell Biology* **71**, 556-561.

Klaus, S., Cassard-Doulcier, A.-M. & Ricquier, D. 1991 Development of Phodopus sungorus brown preadipocytes in primary cell culture: effect of an atypical β -adrenergic agonist, insulin, and triiodothyronin on differentiation, mitochondrial development, and expression of the uncoupling protein UCP. *Journal of Cell Biology* **115**, 1783-1790.

Klaus, S., Choy, L., Champigny, O., Cassard-Doulcier, A. M., Ross, S., Spiegelman, B. & Ricquier, D. 1994 Characterization of the novel brown adipocyte cell line HIB 1B. Adrenergic pathways involved in regulation of uncoupling protein gene expression. *Journal of Cell Science* **107**, 313-319.

Klaus, S., Muzzin, P., Revelli, J.-P., Cawthorne, M. A., Giacobino, J.-P. & Ricquier, D. 1995 Control of β_3 -adrenergic receptor gene expression in brown adipocytes in culture. *Molecular & Cellular Endocrinology* **109**, 189-195.

Kliewer, S. A., Lenhard, J. M., Willson, T. M., Patel, I., Morris, D. C. & Lehmann, J. M. 1995 A prostaglandin J2 metabolite binds peroxisome proliferator-activated receptorγ and promotes adipocyte differentiation. *Cell* **83**, 813-819.

Klingenberg, M. 1984 Characteristics of the uncoupling protein from brown-fat mitochondria. *Biochemical Society Transactions* **12**, 390-393.

Klingenberg, M. 1988 Nucleotide binding to uncoupling protein. Mechanism of control by protonation. *Biochemistry* **27**, 781-791.

Kopecký, J., Baudysová, M., Zanotti, F., Janíková, D., Pavelka, S. & Houstek, J. 1990 Synthesis of mitochondrial uncoupling protein in brown adipocytes differentiated in cell culture. *Journal of Biological Chemistry* **265**, 22204-22209.

Kortelainen, M.-L., Pelletier, G., Ricquier, D. & Bukowiecki, L. J. 1993 Immunohistochemical detection of human brown adipose tissue uncoupling protein in an autopsy series. *Journal of Histochemistry & Cytochemistry* **41**, 759-764.

Kott, J. N., Ganfield, C. L. & Kenney, N. J. 1984 Area postrema/nucleus of the solitary tract ablations: analysis of the effects of hypophagia. *Physiology & Behavior* **32**, 429-435.

Kozak, U. C., Kopecky, J., Teisinger, J., Enerbäck, S., Boyer, B. B. & Kozak, L. P. 1994 An upstream enhancer regulating brown-fat-specific expression of the mitochondrial uncoupling protein gene. *Molecular & Cellular Biology* **14**, 59-67.

Kreutter, D. K., Orena, S. J., Torchia, A. J., Contillo, L. G., Andrews, G. C. & Stevenson, R. W. 1993 Amylin and CGRP induce insulin resistance via a receptor distinct from cAMP-coupled CGRP receptor. *American Journal of Physiology* **264**, E606-E613.

Kuroshima, A., Yahata, T. & Habara, Y. 1984 Hormonal regulation of brown adipose tissue with special reference to the participation of endocrine pancreas. *Journal of Thermal Biology* **9**, 81-86.

Lafontan, M. 1994 Differential recruitment and differential regulation by physiological amines of fat cell β -1, β -2 and β -3 adrenergic receptors expressed in native fat cells and in transfected cells. *Cell Signalling* **6**, 363-392.

Lafontan, M. & Berlan, M. 1993 Fat cell adrenergic receptors and the control of white and brown fat cells function. *Journal of Lipid Research* **34**, 1057-1091.

Lambe, K. G. & Tugwood, J. D. 1996 A human peroxisome-proliferator-activated receptor-γ is activated by inducers of adipogenesis, including thiazolidinedione drugs. *European Journal of Biochemistry* **239**, 1-7.

Lanoue, K. F., Koch, C. D. & Meditz, R. B. 1982 Mechanism of action of norepinephrine in hamster brown adipocytes. *Journal of Biological Chemistry* **257**, 13740-13748.

Largis, E. E., Burns, M. G., Muenkel, H. A., Dolan, J. A. & Claus, T. H. 1994 Antidiabetic and antiobesity effects of a highly selective β_3 -adrenoceptor agonist (CL 316,243). *Drug Dev Res* **32**, 69-76.

Larose, M., Cassard-Doulcier, A. M., Fleury, C., Serra, F., Champigny, O., Bouillaud, F. & Ricquier, D. 1996 Essential cis-acting elements in rat uncoupling protein gene are in an enhancer containing a complex retinoic acid response domain. *Journal of Biological Chemistry* **271**, 31533-31542.

Larrouy, D., Laharrague, P., Carrera, G., Viguerie-Bascands, N., Levi-Meyrueis, C., Fleury, C., Pecqueur, C., Nibbelink, M., André, M., Casteilla, L. & Ricquier, D. 1997 Kupffer cells are a dominant site of uncoupling protein 2 expression in rat liver. *Biochemical and Biophysical Research Communications* **235**, 760-764.

Lean, M. E. J. 1992a Brown adipose tissue and obesity. In *Obesity: Basic Concepts and Clinical Aspects.* (ed. F. Belfiore, B. Jeanrenaud & D. Papalia), pp. 37-49. Basel: Karger.

Lean, M. E. J. 1992b Evidence for brown adipose tissue in humans. In *Obesity* (ed. P. Bjorntorp & B. Brodoff), pp. 117-129. Philadelphia: Lippincott.

Lean, M. E. J., Branch, W. J., James, W. P. T., Jennings, G. & Ashwell, M. 1983 Measurement of rat brown-adipose-tissue mitochondrial uncoupling protein by radioimmunoassay: increased concentration after cold acclimation. *Bioscience Reports* **3**, 61-71.

Lean, M. E. J. & James, W. P. T. 1986 Brown adipose tissue in humans. In *Brown adipose tissue* (ed. P. Trayhurn & D. G. Nicholls), pp. 339-365. London: Arnold.

Lean, M. E. J., James, W. P. T., Jennings, G. & Trayhurn, P. 1986 Brown adipose tissue uncoupling protein content in infants, children and adult humans. *Clinical Science* **71**, 291-297.

Lee, G.-H., Proenca, R., Montez, J. M., Carroll, K. M., Darvishzadeh, J. G., Lee, J. I. & Friedman, J. M. 1996 Abnormal splicing of the leptin receptor in *diabetic* mice. *Nature* **379**, 632-635.

Lehmann, J. M., Moore, L. B., Smith-Oliver, T. A., Wilkison, W. O., Willson, T. M. & Kliewer, S. A. 1995 An antidiabetic thiazolidinedione is a high affinity ligand for peroxisome proliferator-activated receptor γ (PPAR γ). *Journal of Biological Chemistry* **270**, 12953-12956.

Lehninger, A. L. 1982 *Principles of biochemistry*. New York: Worth Publishers, Inc.

Leibowitz, S. F. 1988 Hypothalamic paraventricular nucleus: interaction between α2 - noradrenergic system and circulating hormones and nutrients in relation to energy balance. *Neuroscience & Biobehavioral Reviews* **12**, 101-109.

Leighton, B. & Cooper, G. S. 1990 The role of amylin in the insulin resistance of non-insulin-dependent diabetes mellitus. *Trends in Biochemical Sciences* **15**, 295-299.

Leighton, B. & Foot, E. A. 1995 The role of the sensory peptide calcitonin-gene-related peptide(s) in skeletal muscle carbohydrate metabolism: effects of capsaicin and resiniferatoxin. *Biochemical Journal* **307**, 707-712.

Leonard, J. L., Mellen, S. A. & Larsen, P. R. 1983 Thyroxine 5'-deiodinase activity in brown adipose tissue. *Endocrinology* **112**, 1153-1155.

Lever, J. D., Mukherjee, S., Norman, D., Symons, D. & Jung, R. T. 1988 Neuropeptide and noradrenaline distributions in rat interscapular brown fat and in its intact and obstructed nerves of supply. *Journal of the Autonomic Nervous System* **25**, 15-25.

Lever, J. D., Mukherjee, S., Norman, D., Symons, D., Wheeler, M. H., Connacher, A. & Jung, R. T. 1989 Catecholaminergic and peptidergic nerves in naturally occurring and pheochromocytoma-associated human brown adipose tissue. *Clinical Anatomy* **2**, 157-166.

Lin, C.-s. & Klingenberg, M. 1982 Characteristics of the isolated purine nucleotide binding protein from brown fat mitochondria. *Biochemistry* **21**, 2950-2956.

Loncar, D. 1991 Convertible adipose tissue in mice. *Cell & Tissue Research* **266**, 149-161.

Lönnroth, P. & Smith, U. 1992 Intermediary metabolism with an emphasis on lipid metabolism, adipose tissue, and fat cell metabolism: a review. In *Obesity* (ed. P. Björntorp & B. N. Brodoff), pp. 3-15. Philadelphia: J. P. Lippincott Company.

Lopez-Soriano, F. J. & Alemany, M. 1986 Activities of enzymes of amino acid metabolism in rat brown adipose tissue. *Biochemistry International* **12**, 471-478.

Lowell, B. B. & Flier, J. S. 1995 The potential significance of β(3) adrenergic receptors. *Journal of Clinical Investigation* **95**, 923-924.

Lowell, B. B., S-Susulic, V., Hamann, A., Lawitts, J. A., Himms-Hagen, J., Boyer, B. B., Kozak, L. P. & Flier, J. S. 1993 Development of obesity in transgenic mice after genetic ablation of brown adipose tissue. *Nature* **366**, 740-742.

Lowell, B. B., Susulic, V. S., Hamaan, A., Lawitts, J. A., Himms-Hagen, J., Boyer, B. B., Kozak, L. P. & Flier, J. S. 1996 Transgenic ablation of brown adipose tissue. In *Molecular and Genetic Aspects of Obesity.* (ed. G. A. Bray & D. H. Ryan), pp. 593-608. Baton Rouge: Louisiana State University Press.

Lowry, O. H., Rosenbrough, N. J., Farr, A. L. & Randal, R. J. 1951 Protein measurement with Folin phenol reagent. *Journal of Biological Chemistry* **193**, 265-275.

Ludvigsen, C., Jarett, L. & McDonald, J. M. 1980 The characterization of catecholamine stimulation of glucose transport by rat adipocytes and isolated plasma membranes. *Endocrinology* **106**, 786-790.

Lupien, J. R., Hirshman, M. F. & Horton, E. S. 1990 Effects of norepinephrine infusion on *in vivo* insulin sensitivity and responsiveness. *American Journal of Physiology* **259**, E210-E215.

Ma, S. W. Y. & Foster, D. O. 1984 Potentiation of in vivo thermogenesis in rat brown adipose tissue by stimulation of α_1 -adrenoceptors is associated with increased release of cyclic AMP. *Canadian Journal of Physiology & Pharmacology* **62**, 943-948.

Ma, S. W. Y. & Foster, D. O. 1986 Uptake of glucose and release of fatty acids and glycerol by rat brown adipose tissue in vivo. *Canadian Journal of Physiology and Pharmacology* **64**, 609-614.

MacDougald, O. A., Hwang, C.-S., Fan, H. Y. & Lane, M. D. 1995 Regulated expression of the obese gene product (leptin) in white adipose tissue and 3T3-L1 adipocytes. *Proceedings of the National Acadamy of Science* **92**, 9034-9037.

Madej, T., Boguski, M. S. & Bryant, S. H. 1995 Threading analysis suggests that the obese gene product may be a helical cytokine. *FEBS Letters* **373**, 13-18.

Maffei, M., Fei, H., Lee, G. H., Dani, C., Leroy, P., Zhang, Y. Y., Proenca, R., Negrel, R., Ailhaud, G. & Friedman, J. M. 1995a Increased expression in adipocytes of ob RNA in mice with lesions of the hypothalamus and with mutations at the *db* locus. *Proceedings of the National Acadamy of Science* **92**, 6957-6960.

Maffei, M., Halaas, J., Ravussin, E., Pratley, R. E., Lee, G. H., Zhang, Y., Fei, H., Kim, S., Lallone, R., Ranganathan, S., Kern, P. A. & Friedman, J. M. 1995b Leptin levels in human and rodent-measurement of plasma leptin and ob RNA in obese and weight-reduced subjects. *Nature Medicine* **1**, 1155-1161.

Maggi, C. A. 1991 The pharmacology of the efferent function of sensory nerves. *Journal of Autonomic Pharmacology* **11**, 173-208.

Maggi, C. A. & Meli, A. 1988 The sensory-efferent function of capsaicin-sensitive sensory neurons. *General Pharmacology* **19**, 1-43.

Maniatis, T., Fritsch, E. F. & Sambrook, J. 1982 *Molecular cloning. A laboratory manual.* Cold Spring Harbour: Cold Spring Harbour Laboratory.

Mantzoros, C. S., Qu, D., Frederich, R. C., Susulic, V. S., Lowell, B. B., Maratos-Flier, E. & Flier, J. S. 1996 Activation of β_3 adrenergic receptors suppresses leptin expression and mediates a leptin-independent inhibition of food intake in mice. *Diabetes* **45**, 909-914.

Marchington, D., Rothwell, N. J., Stock, M. J. & York, D. A. 1986 Thermogenesis and sympathetic activity in BAT of overfed rats after adrenalectomy. *American Journal of Physiology* **250**, E362-E366.

Marette, A. & Bukowiecki, L. J. 1989 Stimulation of glucose transport by insulin and norepinephrine in isolated rat brown adipocytes. *American Journal of Physiology* **257**, C714-C721.

Masuzaki, H., Ogawa, Y., Isse, N., Satoh, N., Okazaki, T., Shigemoto, M., Mori, K., Tamura, N., Hosoda, K., Yoshimasa, Y., Jingami, H., Kawada, T. & Nakao, K. 1995a Human obese gene expression - adipocyte-specific expression and regional differences in the adipose tissue. *Diabetes* **44**, 855-858.

Masuzaki, H., Ogawa, Y., Shigemoto, M., Satoh, N., Mori, K., Tamura, N., Hosoda, K., Yoshimasa, Y., Jingami, H. & Nakao, K. 1995b Adipose tissue-specific expression of the *obese (ob)* gene in rats and its marked augmentation in genetically obese-hyperglycemic Wistar fatty rats. *Proceedings of the Japan Academy Series* **71**, 148-152.

McIntyre, J., Hull, D., Nedergaard, J. & Cannon, B. 1993 Thermoregulation. In *Perinatal and Pediatric Pathophysiology: a clinical perspective.* (ed. P. D. Gluckman & M. A. Heymann), pp. 357-368. London: Arnold.

Melicow, M. M. 1957 Hibernating fat and pheochromocytoma. *AMA Arch Pathol* **63**, 367.

Melnyk, A., Harper, M.-E. & Himms-Hagen, J. 1997 Raising at thermoneutrality prevents both obesity and hyperphagia in BAT-ablated transgenic mice. *American Journal of Physiology* **272**, R1088-R1093.

Melnyk, A. & Himms-Hagen, J. 1995 Resistance to aging-associated obesity in capsaicin-desensitized rats one year after treatment. *Obesity Research* **3**, 337-344.

Mercer, J. G., Hoggard, N., Williams, L. M., Lawrence, C. B., Hannah, L. T., Morgan, P. J. & Trayhurn, P. 1996a Coexpression of leptin receptor and preproneuropeptide Y mRNA in arcuate nucleus of mouse hypothalamus. *Journal of Neuroendocrinology* **8**, 733-735.

Mercer, J. G., Hoggard, N., Williams, L. M., Lawrence, C. B., Hannah, L. T. & Trayhurn, P. 1996b Localization of leptin receptor mRNA and the long form splice variant (Ob-Rb) in mouse hypothalamus and adjacent brain regions by in situ hybridization. *FEBS Letters* **387**, 113-116.

Mills, I., Barge, R. M., Silva, J. E. & Larsen, P. R. 1987 Insulin stimulation of iodothyronine 5'-deiodinase in rat brown adipocytes. *Biochemical and Biophysical Research Communications* **143**, 81-86.

Minokoshi, Y., Saito, M. & Shimazu, T. 1986 Sympathetic denervation impairs responses of brown adipose tissue to VMH stimulation. *American Journal of Physiology* **251**, R1005-R1008.

Minokoshi, Y., Saito, M. & Shimazu, T. 1988 Sympathetic activation of lipid synthesis in brown adipose tissue of the rat. *Journal of Physiology (London)* **398**, 361-370.

Minokoshi, Y., Saito, M. & Shimazu, T. 1990 Adrenergic blockade paradoxically increases lipogenic response of brown adipose tissue to sympathetic nerve stimulation. *Neuroscience Letters* **109**, 341-346.

Mohell, N., Connolly, E. & Nedergaard, J. 1987 Distinction between mechanisms underlying α1 - and β -adrenergic respiratory stimulation in brown fat cells. *American Journal of Physiology* **253**, C301-C308.

Moinat, M., Deng, C., Muzzin, P., Assimacopoulos-Jeannet, F., Seydoux, J., Dulloo, A. G. & Giacobino, J. P. 1995 Modulation of obese gene expression in rat brown and white adipose tissues. *FEBS Letters* **373**, 131-134.

Montague, C. T., Farooqi, I. S., Whitehead, J. P., Soos, M. A., Rau, H., Wareham, N. J., Sewter, C. P., Digby, J. E., Mohammed, S. N., Hurst, J. A., Cheetham, C. H., Earley, A. R., Barnett, A. H., Prins, J. B. & O'Rahilly, S. 1997 Congenital leptin deficiency is associated with severe early-onset obesity in humans. *Nature* **387**, 903-908.

Moriscot, A., Rabelo, R. & Bianco, A. C. 1993 Corticosterone inhibits uncoupling protein gene expression in brown adipose tissue. *American Journal of Physiology* **265**, E81-E87.

Morroni, M., Barbatelli, G., Zingaretti, M. C. & Cinti, S. 1995 Immunohistochemical, ultrastructural and morphometric evidence for brown adipose tissue recruitment due to cold acclimation in old rats. *International Journal of Obesity* **19**, 126-131.

Mory, G., Ricquier, D., Pesquies, P. & Hemon, P. 1981 Effects of hypothyroidism on the brown adipose tissue of adult rats: comparison with the effects of adaptation to cold. *Journal of Endocrinology* **91**, 515-524.

Moss, D., Ma, A. & Cameron, D. P. 1985a Cafeteria feeding promotes diet-induced thermogenesis in monosodium glutamate-treated mice. *Metabolism* **34**, 1094-1099.

Moss, D., Ma, A. & Cameron, D. P. 1985b Defective thermoregulatory thermogenesis in monosodium glutamate-induced obesity in mice. *Metabolism* **34**, 626-630.

Mukherjee, S., Lever, J. D., Norman, D., Symons, D., Spriggs, T. L. B. & Jung, R. T. 1989 A comparison of the effects of 6-hydroxydopamine and reserpine on noradrenergic and peptidergic nerves in rat brown adipose tissue. *Journal of Anatomy* **167**, 189-193.

Murakami, T., Iida, M. & Shima, K. 1995 Dexamethasone regulates *obese* expression in isolated rat adipocytes. *Biochemical & Biophysical Research Communications.* **214**, 1260-1267.

Murakami, T. & Shima, K. 1995 Cloning of the rat obese cDNA and its expression in obese rats. *Biochemical & Biophysical Research Communications* **209**, 944-952.

Muscelli, E., Camastra, S., Masoni, A., Baldi, S., Sironi, A. M., Natali, A. & Ferrannini, E. 1996 Acute insulin administration does not affect plasma leptin levels in lean or obese subjects. *European Journal of Clinical Investigation* **26**, 940-943.

Muzzin, P., Revelli, J.-P., Fraser, C. M. & Giacobino, J.-P. 1992 Radioligand binding studies of the atypical β_3 -adrenoceptor in rat brown adipose tissue using [^{3}H]CGP 12177. *FEBS Letters* **298**, 162-164.

Muzzin, P., Revelli, J.-P., Ricquier, D. & Meier, M. K. 1989 The novel thermogenic β -adrenergic agonist Ro 16-8714 increases the interscapular brown-fat β -receptor-adenylate cyclase and the uncoupling-protein mRNA level in obese (*fa/fa*) Zucker rats. *Biochemical Journal* **261**, 721-724.

Nagasaka, T., Shibata, H., Nunomura, T. & Ohmae, O. 1984 Baroflex suppression of non-shivering thermogenesis in restrained and non-restrained rats. *Journal of Thermal Biology* **9**, 93-96.

Nagase, I., Yoshida, T., Kumamoto, K., Umekawa, T., Sakane, N., Nikami, H., Kawada, T. & Saito, M. 1996 Expression of uncoupling protein in skeletal muscle and white fat of obeses mice treated with thermogenic β3 -adrenergic agonist. *Journal of Clinical Investigation* **97**, 2898-2904.

Narimiya, M., Azhar, S., Dolkas, C. B., Mondon, C. E., Sims, C., Wright, D. W. & Reaven, G. M. 1984 Insulin resistance in older rats. *American Journal of Physiology* **246**, E397-E404.

Néchad, M. 1986 Structure and development of brown adipose tissue. In *Brown adipose tissue* (ed. P. Trayhurn & D. G. Nicholls), pp. 1-30. London: Arnold.

Nedergaard, J., Bronnikov, G., Golozoubova, V., Rehnmark, S., Bengtsson, T., Thonberg, H., Jacobsson, A. & Cannon, B. 1994 Brown adipocyte differentiation: an innate switch in adrenergic receptor endowment and in adrenergic response. In *Obesity in Europe.* (ed. H. Ditschuneit, F. A. Gries, H. Hauner, V. Schusdziarra & J. G. Wechsler), pp. 73-80. London: John Libbey.

Nedergaard, J. & Cannon, B. 1992 Brown adipose tissue: development and function. In *Fetal and Neonatal Physiology*, vol. 1 (ed. R. A. Polin & W. W. Fox), pp. 314-325. Philadelphia: W B Saunders.

Newby, F. D., DiGirolamo, M., Cotsonis, G. A. & Kutner, M. H. 1990 Model of spontaneous obesity in aging male Wistar rats. *American Journal of Physiology* **259**, R1117-R1125.

Nicholls, D. G., Cunningham, S. A. & Rial, E. 1986 The bioenergetic mechanisms of brown adipose tissue thermogenesis. In *Brown adipose tissue* (ed. P. Trayhurn & D. G. Nicholls), pp. 52-85. London: Arnold.

Nicholls, D. G. & Rial, E. 1984 Brown fat mitochondria. *Trends in Biochemical Sciences* **9**, 489-491.

Nishimura, H., Kuzuya, H., Okamoto, M., Yoshimasa, Y., Yamada, K., Ida, T., Kakehi, T. & Imura, H. 1988 Change of insulin action with aging in conscious rats determined by euglycemic clamp. *American Journal of Physiology* **254**, E92-E98.

Nnodim, J O & Lever, J. D. 1988 Neural and vascular provisions of rat interscapular brown adipose tissue. *American Journal of Anatomy* **182**, 283-293.

Nobes, C. D., Brown, G. C., Olive, P. N. & Brand, M. D. 1990 Non-ohmic proton conductance of the mitochondrial inner membrane in hepatocytes. *Journal of Biological Chemistry* **265**, 12903-12909.

Nolan, J. J., Olefsky, J. M., Nyce, M. R., Considine, R. V. & Caro, J. F. 1996 Effect of troglitazone on leptin production: studies in vitro and in human subjects. *Diabetes* **45**, 1276-1278.

Norman, D., Mukherjee, S., Symons, D., Jung, R. T. & Lever, J. D. 1988 Neuropeptides in interscapular and perirenal brown adipose tissue in the rat: a plurality of innervation. *Journal of Neurocytology* **17**, 305-311.

O'Brien, S. N., Mantzke, K. A., Kilgore, M. W. & Price, T. M. 1996 Relationship between adipose stromal-vascular cells and adipocytes in human adipose tissue. *Analytical and Quantitative Cytology and Histology* **18**, 137-143.

Ogawa, Y., Masuzaki, H., Isse, N., Okazaki, T., Mori, K., Shigemoto, M., Satoh, N., Tamura, N., Hosoda, K., Yoshimasa, Y., Jingami, H., Kawada, T. & Nakao, K. 1995 Molecular cloning of rat obese cDNA and augmented gene expression in genetically obese zucker fatty (*fa/fa*) rats. *Journal of Clinical Investigation* **96**, 1647-1652.

Ong, J. M., Kirchgessner, T. G., Schotz, M. C. & Kern, P. A. 1988 Insulin increases the synthetic rate and messenger RNA level of lipoprotein lipase in isolated rat adipocytes. *Journal of Biological Chemistry* **263**, 12933-12938.

Park, I. R. A. & Himms-Hagen, J. 1988 Neural influences on trophic changes in brown adipose tissue during cold acclimation. *American Journal of Physiology* **255**, R874-R881.

Pavelka, S., Hermanská, J., Baudysová, M. & Houstek, J. 1993 Adrenergic control of type II iodothyronine 5'-deiodinase activity in cultured mouse brown adipocytes. *Biochemical Journal* **292**, 303-308.

Paxinos, G. & Watson, C. 1982 *The rat brain in stereotaxic coordinates.* New York: Academic Press.

Pellet, H. & Lheritier, M. 1975 Mise en évidence de deux types cellulaires dans le tissue adipeux brun du rat. Étude en microscopie électronique. *Comptes Rendus Société de Biologie.* **168**, 1221-1223.

Pelleymounter, M. A., Cullen, M. J., Baker, M. B., Hecht, R., Winters, D., Boone, T. & Collins, F. 1995 Effects of the obese gene product on body weight regulation in ob/ob mice. *Science* **269**, 540-543.

Phillips, M. S., Liu, Q. Y., Hammond, H. A., Dugan, V., Hey, P. J., Caskey, C. T. & Hess, J. F. 1996 Leptin receptor missense mutation in the fatty Zucker rat. *Nature Genetics* **13**, 18-19.

Picó, C., Herron, D., Palou, A., Jacobsson, A., Cannon, B. & Nedergaard, J. 1994 Stabilization of the mRNA for the uncoupling protein thermogenin by transcriptional/translational blockade and by noradrenaline in brown adipocytes differentiated in culture: a degradation factor induced by cessation of stimulation? *Biochemical Journal* **302**, 81-86.

Porter, R. & Brand, M. D. 1993 Body mass dependence of H^+ leak in mitochondria and its relevance to metabolic rate. *Nature* **362**, 628-630.

Pradines-Figueres, A., Vannier, C. & Ailhaud, G. 1988 Short-term stimulation by insulin of lipoprotein lipase secretion in adipose cells. *Biochemical & Biophysical Research Communications* **154**, 982-990.

Raasmaja, A. & Larsen, P. R. 1989 α_1 - and β -adrenergic agents cause synergistic stimulation of the iodothyronine deiodinase in rat brown adipocytes. *Endocrinology* **125**, 2502-2509.

Rabelo, R., Reyes, C., Schifman, A. & Silva, J. E. 1996a A complex retinoic acid response element in the uncoupling protein gene difines a novel role for retinoids in thermogenesis. *Endocrinology* **137**, 3488-3496.

Rabelo, R., Reyes, C., Schifman, A. & Silva, J. E. 1996b Interactions among receptors, thyroid hormone response elements, and ligands in the regulation of the rat uncoupling protein gene expression by thyroid hormone. *Endocrinology* **137**, 3478-3487.

Rabelo, R., Schifman, A., Rubio, A., Sheng, X. & Silva, J. E. 1995 Delineation of thyroid hormone-responsive sequences within a critical enhancer in the rat uncoupling protein gene. *Endocrinology* **136**, 1003-1013.

Rappaport, E. B., Young, J. B. & Landsberg, L. 1982 Initiation, duration and dissipation of diet-induced changes insympathetic nervous system activity in the rat. *Metabolism* **31**, 143-146.

Raynolds, M. V., Awald, P. D., Gordon, D. F., Gutierrez-Hartmann, A., Rule, D. C., Wood, W. H. & Eckel, R. H. 1991 Lipoprotein lipase gene expression in rat adipocytes is regulated by isoproterenol and insulin through different mechanisms. *Molecular Endocrinology* **4**, 1416-1422.

Rehnmark, S., Bianco, A. C., Kieffer, J. D. & Silva, J. E. 1992 Transcriptional and posttranscriptional mechanisms in uncoupling protein mRNA response to cold. *American Journal of Physiology* **262**, E58-E67.

Rehnmark, S., Néchad, M., Herron, D., Cannon, B. & Nedergaard, J. 1990 α - and β -adrenergic induction of the expression of the uncoupling protein thermogenin in brown adipocytes differentiated in culture. *Journal of Biological Chemistry* **265**, 16464-16471.

Ricquier, D., Bouillaud, F., Toumelin, P., Mory, G., Bazin, R., Arch, J. & Pénicaud, L. 1986 Expression of uncoupling protein mRNA in thermogenic or weakly thermogenic brown adipose tissue. Evidence for a rapid β -adrenoceptor-mediated and transcriptionally regulated step during activation of thermogenesis. *Journal of Biological Chemistry* **261**, 13905-13910.

Ricquier, D. & Cassard-Doulcier, A.-M. 1993 The biochemistry of white and brown adipocytes analysed form a selection of proteins. *European Journal of Biochemistry* **218**, 785-796.

Ritter, R. C. & Edwards, G. L. 1984 Area postrema lesions cause overconsumption of palatable foods but not calories. *Physiology & Behavior* **32**, 923-927.

Ritter, S. & Dinh, T. T. 1988 Capsaicin-induced neuronal degeneration: silver impregnation of cell bodies, axons, and terminals in the central nervous system of the adult rat. *Journal of Comparative Neurology* **271**, 79-90.

Ritter, S. & Dinh, T. T. 1990 Capsaicin-induced neuronal degeneration in the brain and retina of preweanling rats. *Journal of Comparative Neurology* **296**, 447-461.

Ritter, S. & Dinh, T. T. 1992 Age-related changes in capsaicin-induced degeneration in rat brain. *Journal of Comparative Neurology* **318**, 103-116.

Ritter, S. & Taylor, J. S. 1989 Capsaicin abolishes lipoprivic but not glucoprivic feeding in rats. *American Journal of Physiology* **256**, R1232-R1239.

Ritter, S. & Taylor, J. S. 1990 Vagal sensory neurons are required for lipoprivic but not glucoprivic feeding in rats. *American Journal of Physiology* **258**, R1395-R1401.

Roberts, S. B. & Greenberg, A. S. 1996 The new obesity genes. *Nutrition Reviews* **54**, 41-49.

Rohlfs, E. M., Daniel, K. W., Premont, R. T., Kozak, L. P. & Collins, S. 1995 Regulation of the uncoupling protein gene (UCP) by β1, β2, and β -adrenergic receptor subtypes in immortalized brown adipose cell lines. *Journal of Biological Chemistry* **270**, 10723-10732.

Romsos, D. R., Ferguson, D. & Vander Tuig, J. G. 1985 Effects of a warm environment on energy balance in obese (ob/ob) mice. *Metabolism* **34**, 931-937.

Romsos, D. R., Vander Tuig, J. G., Kerner, J. & Grogan, C. K. 1987 Energy balance in rats with obesity-producing hypothalamic knife cuts: effects of adrenalectomy. *Journal of Nutrition* **117**, 1121-1128.

Rosenblum, C. I., Tota, M., Cully, D., Smith, T., Collum, R., Qureshi, S., Hess, J. F., Phillips, M. S., Hey, P. J., Vongs, A., Fong, T. M., Xu, L., Chen, H. Y., Smith, R. G., Schindler, C. & Van der Ploeg, L. H. T. 1996 Functional STAT 1 and 3 signaling by the leptin receptor (OB-R); reduced expression of the rat *fatty* leptin receptor in transfected cells. *Endocrinology* **137**, 5178-5181.

Rossetti, L., Farrace, S., Choi, S. B., Giaccari, A., Sloan, L., Frontoni, S. & Katz, M. S. 1993 Multiple metabolic effects of CGRP in conscious rats: role of glycogen synthase and phosphorylase. *American Journal of Physiology* **264**, E1-E10.

Rothwell, N. J., Busbridge, N. J., Humphray, H. & Hissey, P. 1990 . In *The Physiological and Pathalogical Effects of Cytokines.*, pp. 307-311. New York: Wiley-Liss Inc.

Rothwell, N. J. & Stock, M. J. 1984 Effects of denervating brown adipose tissue on the responses to cold, hyperphagia, and noradrenaline treatment in the rat. *Journal of Physiology (London)* **355**, 457-463.

Rudman, D. & Di Girolamo, M. 1967 Comparative studies on the physiology of adipose tissue. *Advances in Lipid Research* **5**, 35-117.

Ruffolo, R. R. J. 1991 Molecular structure and genetics of adrenoceptors: Chairman's comments. In *Adrenoceptors: Structure, Mechanisms, Function* (ed. Birkhäuser), pp. 111-114. Basel: Verlag.

Saggerson, E. D., McAllister, T. W. J. & Baht, H. S. 1988 Lipogenesis in rat brown adipocytes. Effects of insulin and noradrenaline, contributions from glucose and lactate as precursors and comparisons with white adipocytes. *Biochemical Journal* **251**, 701-709.

Saito, M. & Bray, G. A. 1984 Adrenalectomy and food restriction in the genetically obese (*ob/ob*) mouse. *American Journal of Physiology* **246**, R20-R25.

Saito, M., Minokoshi, Y. & Shimazu, T. 1985 Brown adipose tissue after ventromedial hypothalamic lesions in the rat. *American Journal of Physiology* **248**, E20-E25.

Sbarbati, A., Morroni, M., Zancanaro, C. & Cinti, S. 1991 Rat interscapular brown adipose tissue at different ages: a morphometric study. *International Journal of Obesity* **15**, 581-588.

Schacterle, G. & Pollack, R. 1973 A simplified method for the quantitative assay of small amounts of protein in biological material. *Analytical Biochemistry* **51**, 654-655.

Scheidegger, K., Robbins, D. C. & Danforth, E. 1984 Effects of chronic beta receptor stimulation on glucose metabolism. *Diabetes* **33**, 1144-1149.

Schimmel, R. J., McCarthy, L. & McMahon, K. K. 1986 Effects of insulin, adenosine, and prostaglandin on α-adrenergic-stimulated respiration in brown adipocytes. *American Journal of Physiology* **250**, C738-C743.

Schneider-Picard, G., Carpentier, J.-L. & Girardier, L. 1984 Quantitative evaluation of gap junctions in rat brown adipose tissue after cold acclimation. *Journal of Membrane Biology* **78**, 85-89.

Schneider-Picard, G., Carpentier, J.-L. & Orci, L. 1980 Quantitative evaluation of gap junctions during development of the brown adipose tissue. *Journal of Lipid Research* **21**, 600-607.

Schwartz, M. W., Seeley, R. J., Campfield, L. A., Burn, P. & Baskin, D. G. 1996 Identification of targets of leptin action in rat hypothalamus. *Journal of Clinical Investigation.* **98**, 1101-1106.

Sears, I. B., MacGinnitie, M. A., Kovacs, L. G. & Graves, R. A. 1996 Differentiation-dependent expression of the brown adipocyte uncoupling protein gene: regulation by peroxisome proliferator-activated receptor γ. *Molecular & Cellular Biology* **16**, 3410-3419.

Seitz, P. K. & Cooper, C. W. 1987 Calcitonin, calcitonin gene-related peptide and renal calcitonin receptors in the Zucker rat. *Bone and Mineral* **2**, 53-62.

Shalev, A. & Meier, C. A. 1996 Peroxisome proliferator-activated receptors: a nuclear hormone receptor involved in adipocyte differentiation and lipid homeostasis. *European Journal of Endocrinology* **134**, 541-545.

Shibata, H. 1982 Baroreflex suppression of nonshivering thermogenesis in rats. *Japanese Journal of Physiology* **32**, 937-944.

Shibata, H., Pérusse, F., Vallerand, A. & Bukowiecki, L. J. 1989 Cold exposure reverses inhibitory effects of fasting on peripheral glucose uptake in rats. *American Journal of Physiology* **257**, R96-R101.

Shimazu, T. 1981 Central nervous system regulation of liver and adipose tissue metabolism. *Diabetologia* **20**, 343-356.

Shimomura, Y., Bray, G. A. & Lee, M. 1987 Adrenalectomy and steroid treatment in obese (*ob/ob*) and diabetic (*db/db*) mice. *Hormone & Metabolic Research* **19**, 295-299.

Silva, J. E. 1988 Full expression of uncoupling protein gene requires the concurrence of norepinephrine and triiodothyronine. *Molecular Endocrinology* **2**, 706-713.

Silva, J. E. 1993 Hormonal control of thermogenesis and energy dissipation. *Trends in Endocrinology and Metabolism* **4**, 25-32.

Silva, J. E. & Larsen, P. R. 1985 Adrenergic activation of triiodothyronine production in brown adipose tissue. *Nature* **305**, 712-713.

Silva, J. E. & Larsen, P. R. 1986 Hormonal regulation of iodothyronine 5'-deiodinase in rat brown adipose tissue. *American Journal of Physiology* **251**, E639-E643.

Silva, J. E. & Rabelo, R. 1997 Regulation of the uncoupling protein gene expression. *European Journal of Endocrinology* **136**, 251-264.

Slinde, E., Pederson, J. I. & Flatmark, T. 1975 Sedimentation coefficient and buoyant density of brown adipose tissue mitochondria from guinea pig. *Analytical Biochemistry* **65**, 581-585.

Slot, J. W., Geuze, H. J., Gigengack, S., Lienhard, G. E. & James, D. E. 1991 Immuno-localization of the insulin regulatable glucose transporter in brown adipose tissue of the rat. *Journal of Cell Biology* **113**, 123-135.

Smith, S. A., Young, P. & Cawthorne, M. A. 1986 Quantification in vivo of the effects of insulin on glucose utilization in individual tissues of warm- and cold-acclimated rats. *Biochemical Journal* **237**, 789-795.

Sober, H. A. (ed.) 1968 *CRC Handbook of Biochemistry*. Cleveland: The Chemical Rubber Co.

Speake, B. K., Parkinson, C. & Robinson, D. S. 1985 The effect of insulin on the synthesis of lipoprotein lipase in rat adipose tissue. *Hormone & Metabolic Research* **17**, 637-640.

Spiegelman, B. M., Choy, L., Hotamisligil, G. S., Graves, R. A. & Tontonoz, P. 1993 Regulation of adipocyte gene expression in differentiation and syndromes of obesity/diabetes. *Journal of Biological Chemistry* **268**, 6823-6826.

Spooner, P. M., Chernick, S. S., Garrison, M. M. & Scow, R. O. 1979 *Journal of Biological Chemistry* **254**, 10021-10029.

Strålfors, P., Björsell, P. & Belfrage, P. 1984 Hormonal regulation of hormone-sensitive lipase in intact adipocytes: Identification of phosphorylated sites and effects on the phosphorylation by lipolytic hormones and insulin. *Proceedings of the National Acadamy of Science* **81**, 3317-3321.

Strosberg, A. D. & Pietri-Rouxel, F. 1996 Function and regulation of the β_3 -adrenoceptor. *Trends in Pharmacological Sciences* **17**, 373-381.

Szekely, M. & Szelenyi, Z. 1979 Endotoxin fever in the rat. *Acta Physiologica Academiae Scientarium Hungaricae* **53**, 265-277.

Szekely, M. & Szolcsanyi, J. 1979 Endotoxin fever in capsaicin treated rats. *Acta Physiologica Academiae Scientarium Hungaricae* **53**, 469-477.

Takahashi, A., Shimazu, T. & Maruyama, Y. 1992 Importance of sympathetic nerves for the stimulatory effect of cold exposure on glucose utilization in brown adipose tissue. *Japanese Journal of Physiology* **42**, 653-664.

Takano, Y., Nagashima, A., Kamiya, H., Kurosawa, M. & Sato, A. 1988 Well-maintained reflex responses of sympathetic nerve activity to stimulation of baroreceptor, chemoreceptor and cutaneous mechanoreceptors in neonatal capsaicin-treated rats. *Brain Research* **445**, 188-192.

Takaya, K., Ogawa, Y., Hiraoka, J., Hosoda, K., Yamori, Y., Nakao, K. & Koletsky, R. J. 1996 Nonsense mutations of leptin receptor in the obese spontaneously hypertensive Koletsky rat. *Nature Genetics* **14**, 130-131.

Taniguchi, T. 1995 Cytokine signaling through nonreceptor protein tyrosine kinases. *Science* **268**, 251-255.

Tartaglia, L. A., Dembski, M., Weng, X., Deng, N., Culpepper, J., Devos, R., Richards, G. J., Campfield, L. A., Clark, F. T., Deeds, J., Muir, C., Sanker, S., Moriarty, A., Moore, K. J., Smutko, J. S., Mays, G. G., Woolf, E. A., Monroe, C. A. & Tepper, R. I. 1995 Identification and expression cloning of a leptin receptor, OB-R. *Cell* **83**, 1263-1271.

Thomas, S. A. & Palmiter, R. D. 1997 Thermoregulatory and metabolic phenotypes of mice lacking noradrenaline and adrenaline. *Nature* **387**, 94-97.

Thonberg, H., Zhang, S.-J., Tvrdik, P., Jacobsson, A. & Nedergaard, J. 1994 Norepinephrine utilizes α_1 - and β -adrenoceptors synergistically to maximally induce c-*fos* expression in brown adipocytes. *Journal of Biological Chemistry* **269**, 33179-33186.

Thurlby, P. L. & Ellis, R. D. M. 1986 Differences between the effects of noradrenaline and the β -adrenoceptor agonist BRL 28410 in brown adipose tissue and hind limb of the anesthetized rat. *Canadian Journal of Physiology & Pharmacology* **64**, 1111-1114.

Tokuyama, K. & Himms-Hagen, J. 1986 Brown adipose tissue thermogenesis, torpor, and obesity of glutamate-treated mice. *American Journal of Physiology* **251**, E407-E415.

Tokuyama, K. & Himms-Hagen, J. 1987 Increased sensitivity of the genetically obese mouse to corticosterone. *American Journal of Physiology* **252**, E202-E208.

Tokuyama, K. & Himms-Hagen, J. 1989 Adrenalectomy prevents obesity in glutamate-treated mice. *American Journal of Physiology* **257**, E139-E144.

Tontonoz, P., Graves, R. A., Budavari, A. I., Erdjument-Bromage, H., Lui, M., Hu, E., Tempst, P. & Spiegelman, B. M. 1994a Adipocyte-specific transcription factor ARF6 is a heterodimeric complex of two nuclear hormone receptors, PPARγ and RXRα. *Nucleic Acids Research* **22**, 5628-5634.

Tontonoz, P., Hu, E., Devine, J., Beale, E. G. & Spiegelman, B. M. 1995 PPARγ2 regulates adipose expression of the phosphoenolpyruvate carboxykinase gene. *Molecular & Cellular Biology* **15**, 351-357.

Tontonoz, P., Hu, E., Graves, R. A., Budavari, A. I. & Spiegelman, B. M. 1994b mPPARγ2: tissue-specific regulator of an adipocyte enhancer. *Genes & Development* **8**, 1224-1234.

Tontonoz, P., Hu, E. & Spiegelman, B. M. 1994c Stimulation of adipogenesis in fibroblasts by PPARγ2, a lipid-activated transcription factor. *Cell* **79**, 1147-1156.

Tontonoz, P., Kim, J. B., Graves, R. A. & Spiegelman, B. M. 1993 ADD1: a novel helix-loop-helix transcription factor associated with adipocyte determination and differentiation. *Molecular & Cellular Biochemistry* **13**, 4753-4759.

Trayhurn, P. & James, W. P. T. 1978 Thermoregulation and non-shivering thermogenesis in the genetically obese (*ob/ob*) mouse. *Pflügers Archiv European Journal of Physiology* **373**, 189-193.

Trayhurn, P. & Milner, R. E. 1989 A commentary on the interpretation of *in vitro* biochemical measures of brown adipose tissue thermogenesis. *Canadian Journal of Physiology and Pharmacology* **67**, 811-819.

Trayhurn, P., Thomas, M. E. A., Duncan, J. S. & Rayner, D. V. 1995 Effects of fasting and refeeding on *ob* gene expression in white adipose tissue of lean and obese (*ob/ob*) mice. *FEBS Letters* **368**, 488-490.

Triandafillou, J., Gwilliam, C. & Himms-Hagen, J. 1982 Role of thyroid hormone in cold-induced changes in rat brown adipose tissue mitochondria. *Canadian Journal of Biochemistry* **60**, 53-537.

Umekawa, T., Yoshida, T., Sakane, N., Saito, M., Kumamoto, K. & Kondo, M. 1997 Anti-obesity and anti-diabetic effects of CL316,243, a highly specific β3 -adrenoceptor agonist, in Ostuka Long-Evans Tokushima Fatty rats: induction of uncoupling protein and activation of glucose transporter 4 in white fat. *European Journal of Endocrinology* **136**, 429-437.

Utriainen, T., Malmstrom, R., Makimattila, S. & Ykijarvinen, H. 1996 Supraphysiological hyperinsulinemia increases plasma leptin concentrations after 4 H in normal subjects. *Diabetes* **45**, 1364-1366.

Vaisse, C., Halaas, J. L., Horvath, C. M., Darnell, J. E., Jr., Stoffel, M. & Friedman, J. M. 1996 Leptin activation of Stat3 in the hypothalamus of wild-type and *ob/ob* mice but not *db/db* mice. *Nature Genetics* **14**, 95-97.

Vallerand, A. L., Pérusse, F. & Bukowiecki, L. J. 1987 Cold exposure potentiates the effect of insulin on in vivo glucose uptake. *American Journal of Physiology* **253**, E179-E186.

Vallerand, A. L., Pérusse, F. & Bukowiecki, L. J. 1990 Stimulatory effects of cold exposure and cold acclimation on glucose uptake in rat peripheral tissues. *American Journal of Physiology* **259**, R1043-R1049.

Vallin, I. 1970 Norepinephrine response in brown adipose tissue from newborn rats. *Acta Zoologica* **51**, 129-139.

Vander Tuig, J. G., Kerner, J. & Romsos, D. R. 1985 Hypothalamic obesity, brown adipose tissue, and sympathoadrenal acitivity in rats. *American Journal of Physiology* **248**, E607-E617.

Vander Tuig, J. G. & Romsos, D. R. 1984 Effect of dietary carbohydrate, fat and protein on norepinephrine turnover in rats. *Metabolism* **33**, 26-33.

Vidal-Puig, A., Jimenez-Liñan, M., Lowell, B. B., Hamann, A., Hu, E., Spiegelman, B., Flier, J. S. & Moller, D. E. 1996 Regulation of PPARγ gene expression by nutrition and obesity in rodents. *Journal of Clinical Investigation* **97**, 2553-2561.

Vidal-Puig, A., Solanes, G., Grujic, D., Flier, J. S. & Lowell, B. B. 1997 UCP3: An uncoupling protein homologue expressed preferentially and abundantly in skeletal muscle and brown adipose tissue. *Biochemical and Biophysical Research Communications* **235**, 79-82.

Vilberg, T. R. & Keesey, R. E. 1984 Reduced energy expenditure after ventromedial hypothalamic lesions in female rats. *American Journal of Physiology* **247**, R183-R188.

Vydelingum, S., Shillabeer, G., Hatch, G., Russell, J. C. & Lau, D. C. W. 1995 Overexpression of the obese gene in the JCR-LA-corpulent rat. *Biochemical & Biophysical Research Communications* **216**, 148-153.

Wabitsch, M., Jensen, P. B., Blum, W. F., Christoffersen, C. T., Englaro, P., Heinze, E., Rascher, W., Teller, W., Tornqvist, H. & Hauner, H. 1996 Insulin and cortisol promote leptin production in cultured human fat cells. *Diabetes* **45**, 1435-1438.

Walgren, M. C. & Powley, T. L. 1985 Effects of intragastric hyperalimentation on pair-fed rats with ventromedial hyothalamic lesions. *American Journal of Physiology* **248**, R172-R180.

Walgren, M. C., Young, J. B., Kaufman, L. N. & Landsberg, L. 1987 The effects of various carbohydrates on sympathetic activity in heart and interscapular brown adipose tissue of the rat. *Metabolism* **36**, 585-594.

Watanabe, J., Mishiro, K., Amatsu, T. & Kanamura, S. 1994 Absence of paravascular nerve projection and cross-innervation in interscapular brown adipose tissues of mice. *Journal of the Autonomic Nervous System* **49**, 269-276.

Weingarten, H. P., Chang, P. & McDonald, T. J. 1985 Comparison of the metabolic and behavioural disturbances following paraventricular- and ventromedial-hypothalamic lesions. *Brain Research Bulletin* **14**, 551-559.

Wilkison, W. O. & Spiegelman, B. M. 1993 Biosynthesis of the vasoactive lipid monobutyrin. Central role of diacylglycerol. *Journal of Biological Chemistry* **268**, 2844-2849.

Wilson, S., Thurlby, P. L. & Arch, J. R. S. 1987 Substrate supply for thermogenesis induced by beta-adrenoceptor agonist BRL 26830A. *Canadian Journal of Physiology & Pharmacology* **65**, 113-119.

Wimalawansa, S. J. 1991 Age-related increase of calcitonin gene-related peptide in rat thyroid and circulation. *Peptides* **12**, 1143-1147.

Wimalawansa, S. J. 1993 The effects of neonatal capsaicin on plasma levels and tissue contents of CGRP. *Peptides* **14**, 247-252.

Woods, A. J. & Stock, M. J. 1994 Biphasic brown fat temperature responses to hypothalamic stimulation in rats. *American Journal of Physiology* **266**, R328-R337.

Woods, A. J. & Stock, M. J. 1996a Inhibition of brown fat activity during hypothalamic stimulation in the rat. *American Journal of Physiology* **270**, R605-R613.

Woods, A. J. & Stock, M. J. 1996b Leptin activation in hypothalamus. *Nature* **381**, 745.

Yamaguchi, A., Chiba, T., Morishita, T., Nakamura, A., Inui, T., Yamatani, T., Kadowaki, S., Chihara, K., Fukase, M. & Fujita, T. 1990 Calcitonin gene-related peptide and induction of hyperglycemia in conscious rats in vivo. *Diabetes* **39**, 168-174.

Yang, Y. T. & McElligott, M. A. 1989 Multiple actions of β -adrenergic agonists on skeletal muscle and adipose tissue. *Biochemical Journal* **261**, 1-10.

Yonetani, T. & Ray, G. S. 1965 Studies on cytochrome oxidase. *Journal of Biological Chemistry* **240**, 3392-3398.

York, D. A., Holt, S. J. & Marchington, D. 1985a Regulation of brown adipose tissue thermogenesis by corticosterone in obese *fa/fa* rats. *International Journal of Obesity* **9**, 89-95.

York, D. A., Marchington, D., Holt, S. J. & Allars, J. 1985b Regulation of sympathetic activity in lean and obese Zucker (*fa/fa*) rats. *American Journal of Physioloy* **249**, E299-E305.

Yoshida, T., Nishioka, H., Nakamura, Y. & Kondo, M. 1984 Reduced noradrenaline turnover in streptozotocin-induced diabetic rats. *Diabetologia* **28**, 692-696.

Yoshida, T., Sakane, N., Wakabayashi, Y., Umekawa, T. & Kondo, M. 1994a Anti-obesity and anti-diabetic effects of CL 316,243, a highly specific β_3 -adrenoceptor agonist, in yellow KK mice. *Life Sciences* **54**, 491-498.

Yoshida, T., Sakane, N., Wakabayashi, Y., Umekawa, T. & Kondo, M. 1994b Anti-obesity effect of CL 316,243, a highly specific β_3 -adrenoceptor agonist, in mice with monosodium-L-glutamate-induced obesity. *European Journal of Endocrinology* **131**, 97-102.

Yoshioka, K., Yoshida, T., Wakabyashi, Y., Nishioka, H. & Kondo, M. 1989 The role of insulin in norepinephrine turnover and thermogenesis in brown adipose tissue after acute cold-exposure. *Endocrinologia Japonica* **36**, 491-499.

Young, J. B., Saville, E., Rothwell, N. J. & Stock, M. J. 1982 Effect of diet and cold exposure on norepinephrine turnover in brown adipose tissue of the rat. *Journal of Clinical Investigation* **69**, 1061-1071.

Young, P., Arch, J. R. S. & Ashwell, M. 1984a Brown adipose tissue in the parametrial fat pad of the mouse. *FEBS Letters* **167**, 10-14.

Young, P., Cawthorne, M. A., Levy, A. L. & Wilson, K. 1984b Reduced maximum capacity of glycolysis in brown adipose tissue of genetically obese, diabetic (*db/db*) mice and its restoration following treatment with a thermogenic β -adrenoceptor agonist. *FEBS Letters* **176**, 16-20.

Young, P., Cawthorne, M. A. & Smith, S. A. 1985 Brown adipose tissue is a major site of glucose utilization in C57Bl/6 *ob/ob* mice treated with a thermogenic β -adrenoceptor agonist. *Biochemical and Biophysical Research Communications* **130**, 241-248.

Yubero, P., Manchado, C., Cassard-Doulcier, A. M., Mampel, T., Viñas, O., Iglesias, R., Giralt, M. & Villarroya, F. 1994a CCAAT/enhancer binding proteins α and β are transcriptional activators of the brown fat uncoupling protein gene promoter. *Biochemical & Biophysical Research Communications* **198**, 653-659.

Yubero, P., Viñas, O., Iglesias, R., Mampel, T., Villarroya, F. & Giralt, M. 1994b Identification of tissue-specific binding domains in the 5'-proximal regulatory region of the rat mitochondrial brown fat uncoupling protein gene. *Biochemical & Biophysical Research Communications* **204**, 867-873.

Zaidi, M., Bevis, P. J. R., Abeyasekera, G., Girgis, S. I., Wimalawansa, S. J., Morris, H. R. & MacIntyre, I. 1986 The origin of circulating calcitonin gene-related peptide in the rat. *Journal of Endocrinology* **110**, 185-190.

Zaror-Behrens, G. & Himms-Hagen, J. 1983 Cold-stimulated sympathetic activity in brown adipose tissue of obese (*ob/ob*) mice. *American Journal of Physiology* **244**, E361-E366.

Zelissen, P. M. J., Koppeschaar, H. P. F., Lips, C. J. M. & Hackeng, W. H. L. 1991 Calcitonin gene-related peptide in human obesity. *Peptides* **12**, 861-863.

Zhang, Y., Proenca, R., Maffei, M., Barone, M., Leopold, L. & Friedman, J. M. 1994 Positional cloning of the mouse obese gene and its human homologue. *Nature* **372**, 425-431.

Zhang, Y., Proenca, R., Maffei, M., Barone, M., Leopold, L. & Friedman, J. M. 1995 Positional cloning of the mouse obese gene and its human homologue (correction). *Nature* **374**, 479.

Zhao, J., Unelius, L., Bengtsson, T., Cannon, B. & Nedergaard, J. 1994 Coexisting β - adrenoceptors subtypes: significance for thermogenic process in brown fat cells. *American Journal of Physiology* **267**, C969-C979.

Zhou, X.-F., Jhamandas, K. H. & Livett, B. G. 1990 Capsaicin-sensitive nerves are required for glucostasis but not for catecholamine output during hypoglycemia in rats. *American Journal of Physiology* **258**, E212-E219.

CURRICULUM VITAE

NAME:	**ANNA MELNYK**	
	WORK	**HOME**
ADDRESS:	Department of Biochemistry Health Sciences Building University of Ottawa 451 Smyth Road Ottawa, Ontario K1H 8M5	19A Varley Drive Kanata, Ontario K2K 1E9
TELEPHONE:	(613) 562-5800 x8217	(613) 592-1610
FAX:	(613) 562-5440	
E-mail:	g491449@labsun1.med.uottawa.ca	
DATE OF BIRTH:	October 7, 1969	**CITIZENSHIP:** Canadian

EDUCATION

Ph.D.	Department of Biochemistry, University of Ottawa Projected completion date: September 1997
B.Sc.1991	Department of Biochemistry, University of Ottawa

ACADEMIC AWARDS

1996-1997	Ontario Graduate Scholarship
1995-1996	Ontario Graduate Scholarship
1994-1995	University of Ottawa Entrance Scholarship
1991-1992	University of Ottawa Entrance Scholarship
1987	Ontario Scholar, Earl of March Secondary School, Kanata, Ontario

SOCIETIES

NAASO: North American Association for the Study of Obesity

VOLUNTEER ACADEMIC SERVICE

1991-1992	Secretary for the Biochemistry Department on the Graduate Student Association Council

WORK EXPERIENCE

1991 FOURTH YEAR HONOURS STUDENT in the lab of Dr. Jean Himms-Hagen. The title of my thesis was **"Atrophied brown adipose tissue in capsaicin-desensitized rats: influence on regulation of body weight and fat content"**.

1991-1997 GRADUATE STUDENT in the Ph.D. program in the Department of Biochemistry at the University of Ottawa under the supervision of Dr. Jean Himms-Hagen. The title of my thesis is **"Brown adipose tissue atrophy: effects on energy expenditure and body composition"**.

1990-1995 LABORATORY DEMONSTRATOR for third year undergraduate students in the Biochemistry program at the University of Ottawa. The courses were: BCH 3140 and BCH 3946 (now BCH 3046) Metabolism, Physical Biochemistry, and Molecular Biology lab courses.

PUBLICATIONS

PAPERS:

Melnyk A, and Himms-Hagen J (1998) Temperature-dependent feeding: lack of role for leptin and defect in brown adipose tissue-ablated obese mice. *American Journal of Physiology (Regulatory Integrative Comp. Physiol.) in press*

Melnyk A, Harper M-E, and Himms-Hagen J (1997) Raising at thermoneutrality prevents both obesity and hyperphagia in BAT-ablated transgenic mice. *American Journal of Physiology (Regulatory Integrative Comp. Physiol.)* **272**:R1088-R1093.

Melnyk A, and Himms-Hagen J (1995) Resistance to aging-associated obesity in capsaicin-desensitized rats one year after treatment. *Obesity Research* **3**:337-344.

ABSTRACTS:

Melnyk A, and Himms-Hagen J (1997) Influence of temperature on leptin concentration and food intake in control and BAT-ablated (UCP-DTA) mice.
Obesity Research in press
North American Association for the Study of Obesity: Cancun, Mexico; Nov. 1997.

Himms-Hagen J, Melnyk A, and Harper M-E (1997) Leptin-independent regulation of food intake in relation to temperature of adaptation in control and UCP-DTA transgenic mice: what is the role of brown adipocytes ?
The Brain and the Adipocyte: Integrating Diverse Signalling Pathways. NIDDK Workshop, Bethesda MD; Sept. 1997.

Melnyk A, Harper M-E, Triandafillou J, and Himms-Hagen J (1995) Raising at thermoneutrality prevents obesity in brown adipose tissue (BAT)-ablated transgenic mice.
Obesity Research **3** (Suppl. 3):407S
North American Association for the Study of Obesity: Baton Rouge, LA; Oct. 1995.

Melnyk A, and Himms-Hagen J (1994) Leanness in capsaicin-desensitized rats one year after treatment. *Int J Obesity* **18** (Suppl. 2):130
7th International Congress for the Study of Obesity: Toronto, ON; Aug. 1994.

Melnyk A, and Himms-Hagen J (1993) White adipose tissue of capsaicin-desensitized (Cap-Des) rats one year after treatment. *Obesity Research* **1** (Suppl. 2):103S
North American Association for the Study of Obesity: Milwaukee, WI; Oct. 1993.

Melnyk A, Himms-Hagen J, Dihn T, and Ritter S (1993) Effects of lesions to the nucleus tractus solitarius (NTS) on brown adipose tissue of rats. *FASEB J.* 7:A606
Experimental Biology: New Orleans, LA; March 1993.

IMAGE EVALUATION TEST TARGET (QA-3)

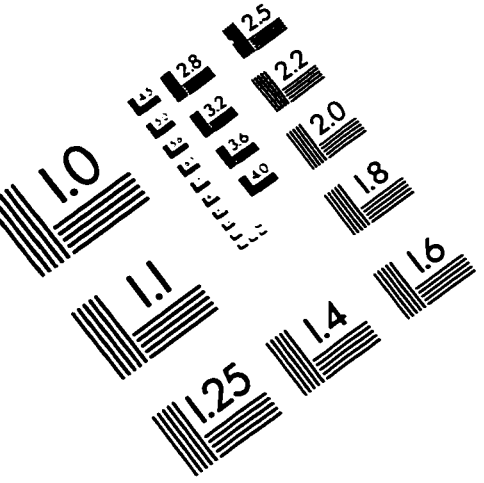

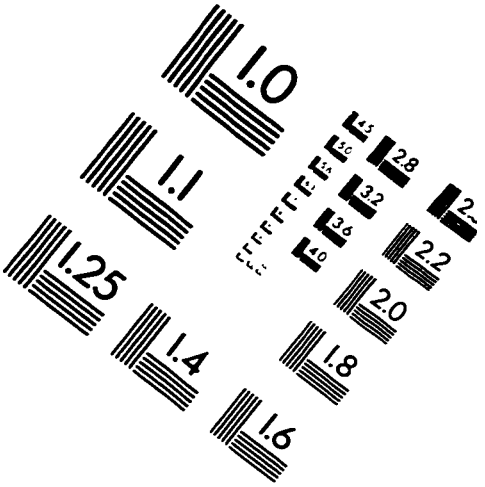

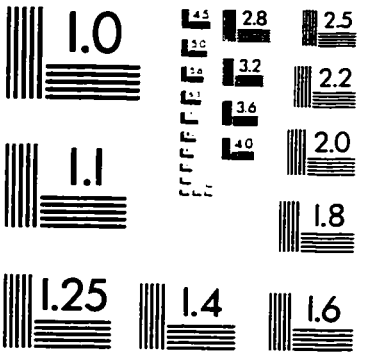

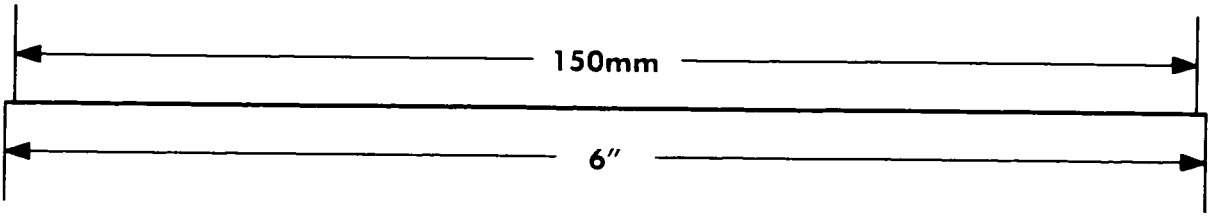

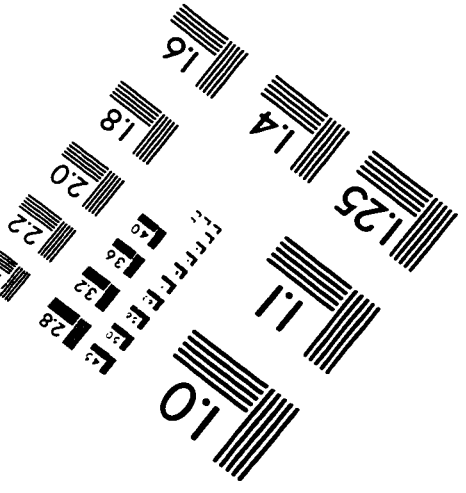

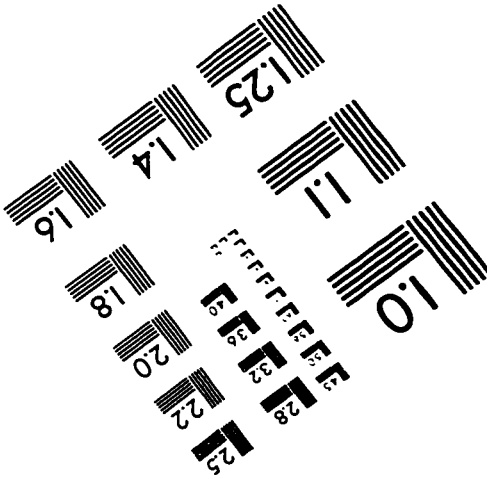

APPLIED IMAGE, Inc
1653 East Main Street
Rochester, NY 14609 USA
Phone: 716/482-0300
Fax: 716/288-5989